ENHANCING THE BIOAVAILABILITY OF BCS CLASS IV DRUGS USING POLYMERIC NANOPARTICLES

Ramesh Soundararajan

PhD Drug Delivery

Department of Pharmaceutics

Supervisors:

Professor Ijeoma Uchegbu

Professor Andreas Schatzlein

A dissertation submitted in part fulfillment of the requirements for the Doctor of Philosophy degree at

THE SCHOOL OF PHARMACY

UNIVERSITY COLLEGE LONDON

2016

DECLARATION

I, Ramesh Soundararajan confirm that the work presented in this thesis is my own. Where information has been derived from other sources, I confirm that this has been indicated in the thesis.

Signature:

Date:

Abstract

Hydrophobic drugs that are P-gp substrates (BCS Class IV) such as paclitaxel, CUDC-101 etc. pose a serious challenge for oral drug delivery. Polymeric amphiphiles such as N-palmitoyl-N-monomethyl-N,N-dimethyl-N,N,N-trimethyl-6-O-glycolchitosan (GCPQ) are capable of enhancing the bioavailability of hydrophobic drugs by forming nanoparticles. The general hypothesis is that the physicochemical properties of the polymer will affect the colloidal stability, encapsulation efficiency and absorption of hydrophobic drugs. The main aims of the project are as follows: a) to examine the feasibility of using GCPQ with different characteristics, for the oral and subcutaneous delivery of CUDC-101 and b) to examine the effect of N-(2-phenoxyacetamide)-6-O-glycolchitosan (GCPh) on the P-gp efflux of paclitaxel.

GCPh, a new polymeric amphiphile was synthesized by conjugating glycol chitosan to phenoxy acetic acid. Paclitaxel and CUDC-101 were encapsulated with GCPh and GCPQ of different molecular weights and hydrophobicity. The *in vivo* oral drug absorption profile for paclitaxel-GCPh nanoparticles and paclitaxel-Taxol® nanoparticles were determined in mice with and without verapamil, a P-gp inhibitor. In another study, the oral and subcutaneous drug absorption profile for CUDC-101 – GCPQ nanoparticles were conducted in mice and rat models respectively.

Results indicated that GCPh improved the oral absorption of paclitaxel by improving the dissolution and promoting particle uptake through enterocytes. Experiments with Taxol® suggested that it is possible to saturate the P-gp pumps by improving the drug's dissolution. Oral absorption of CUDC-101 was poor due to the drug's extremely poor water solubility. The subcutaneous absorption of CUDC-101 – GCPQ nanoparticles were excellent. The colloidal stability and absorption of these nanoparticles can be improved by increasing polymer concentration and its hydrophobicity. These nanoparticles also prolonged the life span of human A431 tumour bearing mice by 28 days ($p < 0.001$).

To conclude, the new polymeric amphiphile (GCPh), capable of improving the oral absorption of BCS Class IV P-gp substrates was developed. A new strategy to nullify the P-gp efflux was developed. A clinically relevant subcutaneous dosage form for CUDC-101 was also successfully developed.

Acknowledgements

There are so many people that I would like to thank for helping me during the course of my PhD at the UCL School of Pharmacy. I will try my best to acknowledge all their good deeds, which made my life easier at UCL.

First and foremost, I would like to thank my supervisor, Prof. Ijeoma Uchegbu for entrusting me with this project and for sponsoring my studies. Your knowledge and guidance were fundamental for the success of my PhD. Be it your encouragement, applause or criticism; it all helped me to strive towards achieving the perfection in my research and also helped me develop self-confidence. I would also like to thank my second supervisor Prof. Andreas Schatzlein, whose keen analysis helped me resolve few hidden messages from my data heap. I thank both my supervisors for their tremendous support and I could not have completed the project if not for such support.

Next, I would like to thank the senior members of the 'Nanomedicine' laboratory for their help and guidance in my day-to-day laboratory experiments. Dr. Katerina Lalatsa, you taught me the basics of the pharmaceutics and helped me to stand on my own in the lab. Dr. Lisa Godfrey, Dr. Antonio Ianitelli, Dr. Lorenzo Capretto and Dr. George Wang, you all helped me through various phases of my project. I also learnt how to think critically, analyze results in different dimension, lab work organization etc. from all you guys, which I believe are essential research skills.

I would also like to thank the technical staffs of our school, for helping me generate publication quality data. I thank Dr. David McCarthy for helping me get excellent TEM results, Dr. Colin James and Dr. Mire Zloh for maintaining NMR, and Dr. David Gathercole for helping with the confocal microscopy. I thank Mr. Steve Coppard and his staffs at the Biological Safety Unit for helping me on number of occasions with animal studies. I also thank Ms. Isabel Goncalves, Ms. Kate Keen, Mr. John Frost and Ms. Catherine Baumber for helping me with the day-to-day activities in the department. Special thanks to Dr. Anna Caldwell of the Mass Spectrometry facility at King's College London, for helping me with the LC-MS at the initial stages of my PhD.

I would also like to thank my fellow PhD students and friends for dealing with my silliness in a friendly manner. I thank Loli, Mankhood, Funmi, Abdullah, and Margarida for being supportive at the beginning of my PhD. I also thank, Sunish, Xian, Nick, Era and Uche for making my life easier during the final stages of my PhD. I would like to thank my friends from other labs for providing timely help as and when I requested. Zahra, Isa Cruz, Brenda, Rita, Vipul and Nithin, I thank you guys for your moral and technical support at various stages of my project.

I thank Miss. Preethi Marimuthu, who was a huge pillar of support throughout my PhD. Thank you Preethi for being there from the start, which itself was a great moral support. I would also like to thank Miss. Vanessa Breuer for encouraging me at the final stages of my PhD.

Last but not least, my sincere love and gratitude for my Family and relatives for always being there for me. Thank you ‘Appa’ and ‘Amma’ for all your love and support, which is the driving factor for my success. I also thank my little sister for taking care of our family in my absence. I dedicate this thesis to my family.

Table of content

List of Figures

List of Tables

List of abbreviations

%	Percentage
° C	Degree Celsius
^{13}C NMR	Carbon Nuclear Magnetic Resonance
^{1}HNMR	Proton Nuclear Magnetic Resonance
Ac-H3	Acetylated – Histone H3 protein
ACN	Acetonitrile
ANOVA	Analysis of Variance
API	Active Pharmaceutical Ingredients
AUC	Area Under the Curve
BBB	Blood Brain Barrier
BCA	Bicinchoninic Acid assay

BCS	Biopharmaceutics Classification System
BMI	Body Mass Index
CARS	Coherent anti-Stokes Raman Spectroscopy
CD	Cyclodextrin
CFU	Colony Forming Units
C_{max}	Concentration maximum
CMC	Critical Micellar Concentration
CsA	Cyclosporine A
DLS	Dynamic Light Scattering
DMF	Dimethylformamide
DMSO	Dimethyl sulfoxide
EDTA	Ethylenediaminetetraacetic acid
ELISA	Enzyme-Linked Immunosorbent Assay
EPO	Erythropoietin
EPR	Enhanced Permeation and Retention
FA	Formic Acid
FBS	Fetal Bovine Serum
FDA	Food and Drug Administration
FTIR	Fourier Transform Infra-red Spectroscopy
GAGs	Glycosaminoglycans
GC	Glycol Chitosan
GCPh	Phenoxylated Glycol Chitosan
GCPQ	Quartenary ammonium Palmitoyl Glycol Chitosan
GI	Gastro Intestine
Glc	α-D-glucopyranose
GPC	Gel Permeation Chromatography

h	Hour
HA	Hyaluronic Acid
HAse	Hyaluronidase enzyme
HDAC	Histone deacetylase
HER2	Human Epidermal Growth Factor Receptor 2
hGH	Human Growth Hormone
HPMA	Hydroxy propyl methacrylamide
HRP	Horse Radish Peroxidase
IC	Inhibitory Concentration
IM	Intra Muscular
ITC	Isothermal Calorimetry
IV	Intra Venous
IW	Intestinal Wash
LC-MS	Liquid Chromatography – Mass Spectroscopy
MALLS	Multi-Angle Laser Light Scattering
mg	Milli Gram
min	Minute
mL	Milli Litre
mmol	Milli Molar
mOsm	Milli Osmole
MRM	Multiple Reaction Monitoring
mV	Milli Volt
MWCO	Molecular Weight Cutoff
NCE	New Chemical Entity
ng	Nano Gram
NIR	Near Infra Red

NMP	N-Methyl-2-Pyrrolidone
P-gp	P-glycoprotein pump
P%	Mole % Palmitoylation
PBS	Phosphate Buffer Saline
PD	Pharmacodynamic
PD	Polydispersity
PEG	Polyethylene Glycol
pEGFR	Phosphorylated Epidermal Growth Factor Receptor
PEO	Polyethylene oxide
Ph%	Mole % Phenoxylation
PK	Pharmacokinetic
PLGA	Poly(lactic-co-glycolic acid)
PO	Peroral
PTX	Paclitaxel
PVP	Poly vinyl pyrrolidone
Q%	Mole % Quaternisation
rHuPH20	Human recombinant hyaluronidase enzyme
RP-HPLC	Reverse Phase – High Pressure Liquid Choromatography
rpm	Rotations per minute
SC	Subcutaneous
SCF	Supercritical Fluid processing
SEDDS	Self-emulsifying Drug Delivery Systems
SGF	Simulated Gastric Fluid
SIF	Simulated Intestinal Fluid
TEM	Transmission Electron Microscopy
T_{max}	Time taken to reach C_{max}

TR	Texas Red
UV	Ultraviolet
UWL	Unstirred Water Layer
v/v	Volume by volume
VEGF	Vascular Endothelial Growth Factor
w/v	Weight by volume
XRD	X-ray Diffraction spectroscopy
µL	Microliter
µm	Micrometer
µM	Micro Molar

1 Introduction:

This chapter of the thesis is a review on oral and subcutaneous drug delivery. The physiology of drug absorption sites, factors affecting the drug uptake and strategies used to enhance the drug uptake suggested in the literature are presented in this chapter.

1.1 Oral drug delivery:

Oral drug delivery systems are clear favorites in pharmaceutical research because of their patient compliance and cost effective nature[1,2]. The oral route for drug delivery doesn't require any special skills to administer the dose, multiple doses are possible and more importantly the oral route is non-invasive, which favors patient adherence. From an industrial point of view, the oral formulations are easy to mass-produce, do not require sterile production conditions and have a longer shelf life, all of which contribute to cheaper cost of production[2]. The oral route also has its limitations such as low drug levels in the blood and limited bioavailability when compared with the intravenous route, unconscious patients cannot take oral medication and more importantly the presence of various physicochemical and physiological barriers may hinder oral drug absorption. Even with all these limitations pharmaceutical companies prefer oral route, and this is evident from the high level of research in oral drug delivery[3–5].

Hydrophobic drug delivery is the prime focus of this project because a number of water insoluble NCEs (New Chemical Entities) are discovered each year[6]. Oral delivery of these hydrophobic NCEs is limited mainly due to their poor bioavailability, which in turn is dependent on their solubility, uptake and metabolism[7]. A large portion of these hydrophobic NCEs do not reach the clinical trials due to the lack of proper delivery systems[2], which means development of an efficient oral delivery system might help some of these NCEs reach the market and thus benefit the society. In order to enhance the oral bioavailability of a drug, the drug formulation must overcome the physicochemical and physiological barriers of the digestive system, details of which and methods employed to overcome these barriers are discussed in this section.

1.1.1 Barriers to oral drug delivery:

The barriers that hinder the oral drug delivery can be classified into two; they are physiological and physicochemical barriers. The physiological barriers are the conditions that exist in the digestive tract whereas the physicochemical barriers are due to the intrinsic properties of the drug and its formulation. The nature and properties of these barriers are as follows.

1.1.1.1 Physicochemical barriers:

1.1.1.1.1 Solubility and Dissolution

Solubility is the major factor in determining the bioavailability. Only the substances that are soluble in the digestive fluids can be absorbed from the intestine[8]. The gastric medium is 100% aqueous, which means if the drug is insoluble in water then there is no chance that it will be absorbed from the gut. However, if the hydrophobic drug dissolves to some extent, it will be absorbed as the dissolved fraction will cross the gut epithelium, provided it can traverse the mucus barrier. Thus aqueous solubility is the biggest challenge for hydrophobic drugs, which limits their use orally. The hydrophobic drug formulations must be capable of maintaining the drug in solution while in the gut in order to get absorbed[8].

Dissolution is the process through which a drug dissolves in a solvent from the solid or semi-solid dosage form. Dissolution is directly dependent on a drug's solubility and the speed at which a drug dissolves is called the dissolution rate[9]. The dissolution rate, solubility and drug absorption are directly proportional as in, the higher the solubility the faster the dissolution and more readily the drug is absorbed, provided it has good intestinal permeability. The equation for dissolution rate was first given by Noyes-Whitney[10,11] as follows,

$$\frac{\partial C}{\partial t} = kS(C_s - C) \qquad \text{Equation 1.1}$$

where $'k'$ is a constant, 'C' is concentration at a given time 't', $'C_s'$ is the saturation solubility and 'S' is the surface area. A higher rate of dissolution in the small intestine is preferred than in the stomach, because of the large surface area in the gut, which facilitates better absorption. Hence,

hydrophobic drugs have poor oral bioavailability due to their poor aqueous solubility, which affects their dissolution rate[12] and almost 40 % of the NCEs are practically insoluble in water[5,13], which highlights the importance of solubility and dissolution in drug delivery.

1.1.1.1.2 Particle size

The particle size of a molecule affects its solubility and dissolution and thus influences the absorption[14]. As from Equation 1.1, the surface area and dissolution rate are directly proportional to each other. This means that the smaller the drug's particle size the larger the surface area and higher the dissolution rate and ultimately the bioavailability.

1.1.1.1.3 Ionisation

The aqueous solubility of a drug depends on the extent of its ionisation and in general the drugs in an ionic state are more readily soluble than the unionised drugs[15]. Most of the drugs are either weak acids or weak bases that cannot undergo complete ionisation in aqueous media. The degree of ionisation at a particular pH can be determined from its pKa value and it is given by Henderson-Hasselbalch[16] equation:

For weak acid,

$$\%\ unionised = {}^{100}/_{1 + antilog\ (pH - pKa)} \qquad \text{(Equation 1.2)}$$

For weak base,

$$\%\ unionised = {}^{100}/_{1 + antilog\ (pKa - pH)} \qquad \text{(Equation 1.3)}$$

The knowledge on ionisation is particularly important to predict a drug's absorption. Cell membranes are made of lipid bilayers and are only permeable to unionised solutes[17]. By using Henderson-Hasselbalch equation, it is easy to determine if a drug will ionise at physiological conditions, just by the knowledge of the drug's pKa. For example, aspirin is a weak acid with a pKa of 3.5. By using Equation 1.2, the percentage of unionised aspirin in the stomach (pH 1.2) is calculated to be 99.5 %. This means the majority of the aspirin molecules will be absorbed from the stomach. Whereas when the drug reaches small intestine, the pH increases to 6.8, which means 99.9 % of the aspirin molecules will be ionized and thus

no drug absorption takes place. Hence the drug should not only be in solution but also should be unionized in order to be absorbed through the gut.

1.1.1.1.4 Permeability

Permeability is the process through which a drug molecule penetrates the intestinal epithelium and reaches the systemic circulation. A molecule can pass through the epithelium in three different ways; a) active transport, which is carrier mediated, b) passive diffusion, which is concentration dependent and c) specialized routes like endocytosis, paracellular transport. The majority of drug absorption occurs through passive diffusion[18,19]. In order to permeate the epithelial membrane, a molecule must possess a certain degree of lipophilicity because the epithelial plasma membrane is made of phospholipids. The LogP (the octanol/water partition coefficient) is a measure of lipophilicity and LogP value has a non-linear relation with permeability. Both low and high LogP values result in poor permeation and mid LogP values generally result in high permeability[20]. Apart from LogP, factors like molecular size, hydrogen bonding ability, molecular weight and ionisation have a profound effect on permeability[21].

The permeability of a molecule can be predicted using Lipinski's rule of five, which states that a NCEs might be orally active, if it has not more than five hydrogen bond donors, not more than 10 hydrogen bond acceptors, a molecular mass lower than 500 Daltons and a LogP not greater than five. These four parameters determine a molecule's permeability and any NCEs that does not obey these rules pose a serious challenge for oral delivery [3–5].

1.1.1.1.5 Polymorphism and amorphism

Some solid compounds exist in different physical states such as, crystalline and amorphous states[22]. When the molecules of a compound are arranged in a definite order then it is in crystalline form and if the molecules are in random order then the compound is in the amorphous form (Figure 1.1). Often, there also exists a different pattern in the crystalline molecular arrangement leading to polymorphism. For example, ice has fifteen known naturally occurring crystalline structures, which have different physical properties from one another[23]. The crystalline structure of a solid is considered to be thermodynamically more stable than the amorphous form

and some of the polymorphic forms can be metastable[22]. From a solubility point of view, amorphous forms of a solid are more soluble than the crystalline state (Solubility of amorphous > metastable polymorphs > crystalline). This is due to the fact that molecules are loosely packed in random order and have a low surface free energy in amorphous form, which enables the molecules to dissociate easily[24]. Thus the amorphous form of a drug has higher dissolution and hence better absorption than its crystalline counterpart[24,25].

1.1.1.2 Physiological barriers

The morphology of the digestive tract and its secretions limit the absorption of many toxic substances along with that of useful therapeutics. Understanding the nature of these barriers is necessary to design an efficient oral formulation and the components of the gastrointestinal barrier are discussed below. Please refer to Figure 1.2 for an illustration of human digestive tract highlighting some of the physiological barriers for oral drug absorption.

1.1.1.2.1 pH of the Gastrointestinal fluids

Upon ingestion, the first barrier the drug molecule encounters is the extreme acidic conditions in the stomach (pH 1 - 2). These extreme acidic conditions might drastically affect the chemical stability of the drug where the drug may be degraded and lose its activity. Penicillin is a classic example of a drug losing its activity due to acid hydrolysis[26]. If the drug escapes the acidic conditions, it enters the small intestine, where the pH is around 5 – 7. This change in pH might affect the drug's degree of ionisation, which might in turn affect its absorption.

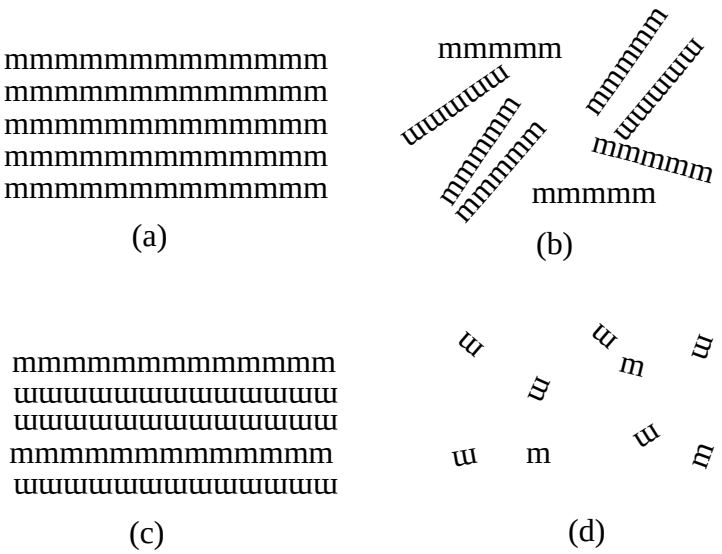

Figure 1.1 Polymorphism in materials.

(a) Crystalline structure – molecular arrangements in crystalline solids follow a definite long-range order; (b) Amorphism – molecules in amorphous solid lacks a long range order; (c) Polymorphism – molecular arrangement in polymorphism is definite and follows a long range order but differ from the original crystal; (d) gas – molecules in gaseous state are loosely packed.

1.1.1.2.2 Gastric emptying

The stomach, after thoroughly mixing the bolus of ingested food, periodically empties its content (chyme) into the duodenum of the small intestine for further digestion and absorption. This process is called gastric emptying and the rate at which it happens varies among individuals[27]. Hunger, anxiety and liquid intake hastens gastric emptying while a fatty diet, gastric ulcers and depression delay the gastric emptying[28]. The small intestine is the major site for drug absorption so a faster gastric emptying is preferred in particular for drugs that undergo acid hydrolysis. Variations in gastric emptying rate may play a significant role in determining a drug's absorption.

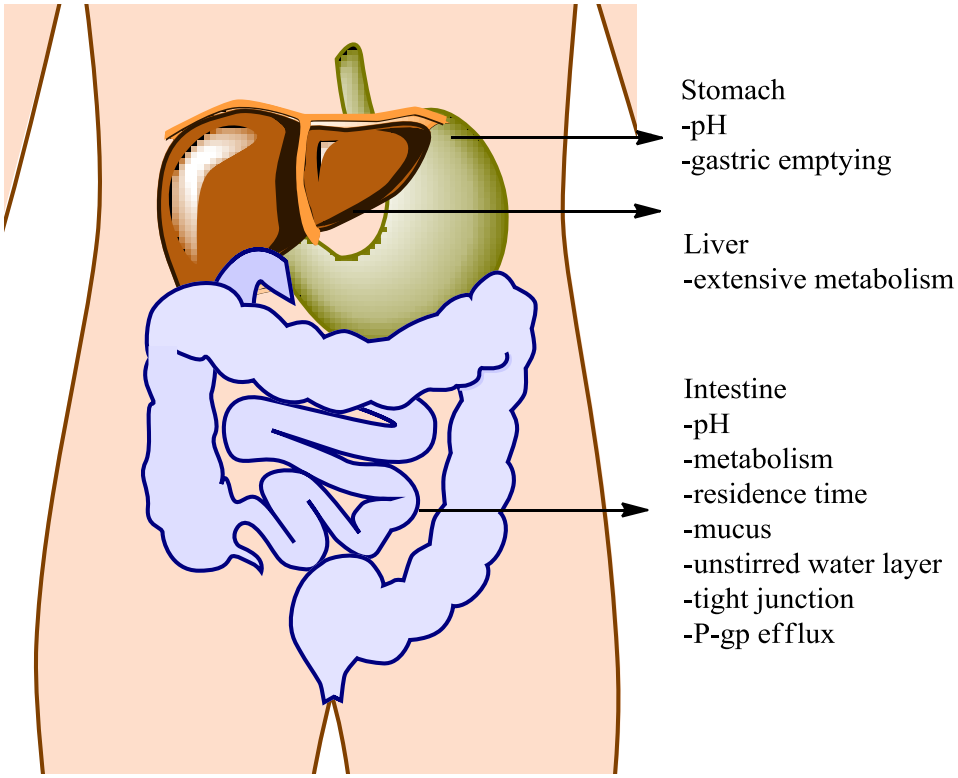

Figure 1.2 Physiological barriers in the gastro-intestinal tract

1.1.1.2.3 Influence of food in stomach

Drug absorption from the intestine may be different in the fed and fasted state[28]. Food increases the viscosity of luminal fluids, which might affect the drug's dissolution[29]. The intake of a fatty meal will also reduce gastric emptying, delaying the absorption[30]. Some drugs might not be compatible with some diets; for example, tetracyclines are poorly absorbed in the presence of dairy products[31]. Sometimes, food also enhances the dissolution of drugs, for example intake of a fatty meal triggers the secretion of bile salts, which improves dissolution of hydrophobic drugs through the formation of micelles[32]. Bile salts along with the breakdown products of fat metabolism form micelles, which can solubilise the hydrophobic drugs in their core, thereby enhancing the dissolution[29]. The presence of bile also reduces the interfacial tension between the luminal fluid and the drug particle, which improves the drug's wettability and eventually its dissolution[33].

1.1.1.2.4 Metabolism by intestinal enzymes

The intestinal lumen is rich in enzymatic activity, where the majority of digestion takes place[34]. Cytochrome P450 (CYP450), a class of metabolising enzymes are present in the intestinal lumen and liver, which poses a huge barrier for oral drug delivery[35]. The bioavailability of drugs such as verapamil[36], cyclosporine[37] and midazolam[38] are hugely reduced due to the activity of CYP450 enzymes. The enzyme oxidises the bound substrates by the addition of hydroxyl group and converts the substrates into metabolites that are easily eliminated from the body[39]. CYP450 family of enzymes have a wide range of substrate specificity because the enzyme's binding pocket operates under the principle of induced fit, i.e. when a substrate binds to the CYP450 active site, conformational changes in the enzyme ensures a tighter binding[35]. Hence, a wide class of compounds such as steroids, alkaloids, fatty acids, prostanoids and several small molecules are all metabolized by CYP450[39].

1.1.1.2.5 Mucus layer

The whole of the alimentary canal is coated with the mucus layer, which is produced by the specialised cells in the underlying epithelium. The thickness of the mucus varies from 50-450 μm in the intestine and this mucus layer protects the epithelial cells from harsh stomach acids and microbial colonisation[19]. Apart from the mechanical protection, the mucus also hinders the diffusion of solutes depending on the thickness of mucus layer, size of the drug molecule and any possible interaction with components of the mucus[40,41]. Due to the lipophilic nature of the mucus, hydrophobic molecules cross the mucus with relative ease when compared to the hydrophilic molecules[42].

1.1.1.2.6 Unstirred water layer

Between the mucus and the epithelial cells, there is a thin lining known as the Unstirred Water Layer (UWL) with a mean thickness of 40 μm. The UWL is made up of water, glycoproteins, proteins and ions, which are capable of binding with solutes. The drug molecules must diffuse through this layer in order to get absorbed into the systemic circulation, which is harder for hydrophobic drugs in particular[43–45].

1.1.1.2.7 Tight junctions

The epithelial wall of the intestine provides a vast surface for absorption but is only permeable for compounds which some degree of lipophilicity[21]. The intercellular spaces in the epithelium are encircled with tight junctions making them virtually impermeable. However, active transport of certain ions are facilitated through intercellular tight junctions but hinder the paracellular diffusion of many hydrophilic solutes [46].

1.1.1.2.8 Efflux pumps

The drugs that enter the epithelium through passive diffusion may be expelled back into the lumen if they are substrates of the P-glycoprotein (P-gp)[47,48] efflux pump. The P-gp efflux pumps belong to a class of efflux pumps found in the villi and they have a huge potential to limit the bioavailability of drugs such as verapamil[47], cyclosporine[49] and midazolam[38]. P-gp also has broad substrate specificity and most drugs, which are substrates of P-gp, are also substrates for cytochrome P-450 and this combined effect drastically reduces a drug's bioavailability[37].

1.1.1.2.9 First pass effect

The solutes, after crossing the entire gastrointestinal barrier, are absorbed via intestinal epithelium from where they are transported to liver, which is a locus for enzymatic activity[50]. Once in the liver, the solutes are extensively metabolised by various classes of enzymes including cytochrome P-450[36]. These enzymatic activities degrade any potential toxins to prevent them from entering the systemic circulation but also render therapeutics ineffective[36,37,51]. This is called hepatic first pass metabolism and this plays a significant role in reducing the bioavailability of many drugs including, lidocaine[52], alprenolol[53] and pethidine[54].

1.1.2 Poorly soluble drugs

Of all the above-mentioned barriers, poor solubility is the major hindrance for low bioavailability for a large portion of lipophilic drugs[55]. As a matter of fact,

a certain degree of lipophilicity is necessary for a molecule to permeate the intestinal barrier but that should not be at the expense of poor aqueous solubility, which might greatly limit the absorption[21]. A drug is considered to be poorly soluble[56] if its aqueous solubility is below 1 mg ml^{-1}. With 40 % of NCEs being hydrophobic, poor aqueous solubility is of major concern for pharmaceutical industries, which is evident from the magnitude of research carried out to screen poorly soluble compounds at the initial stage of the drug development processes[57]. These poorly soluble NCEs can be delivered as parenteral formulations but their use is limited due to tolerability and patient compliance issues[58]. Developing oral formulations for these therapeutically important poorly aqueous soluble drugs will be of great benefit for not only the pharmaceutical industries but also for the consumers due to patient acceptability of these dosage forms[1,2]. Thus the following section is a brief review on methods to enhance the oral bioavailability of poorly soluble drugs.

1.1.2.1 Methods to overcome the poor aqueous solubility:

1.1.2.1.1 Chemical modification:

Chemically modifying the existing drug species to improve the solubility and permeability is the most effective technique to improve oral bioavailability. The new chemical species formed might dissociate into its active state after metabolism (e.g. pro-drug) or be active on its own, based on the type of modifications carried out (salt forms). Table 1.1 gives an overview on different methods employed to overcome the poor aqueous solubility.

Salt formation is the most common technique employed to improve the solubility of drug. Many scientists have reported increase in dissolution kinetics of the salt form of a drug, than the free drug itself[59,60]. Almost all new chemical entities (NCEs) that are poorly soluble will be tested for salt formation in order to improve the solubility. Tolbutamide is a classic example for improving the drug absorption kinetics using salt forms, where salts of tolbutamide showed faster dissolution than its acidic form. Following the oral administration of tolbutamide salts, the blood glucose levels dropped by 20 – 30 %, whereas the acidic form of the drug lowered the glucose by just 5 %. This difference is attributed to increased oral absorption of tolbutamide salts

and the mono-sodium salt of tolbutamide is currently in the market for the treatment of diabetes[61].

Table 1.1 Methods to overcome poor aqueous solubility

Techniques		Principle	Disadvantages	Examples
Chemical modification	Salt form[60]	1) Converts the insoluble compounds into stable soluble salts. 2) Effectively enhances solubility and dissolution.	1) Requires an ionisable group in the compound. 2) The Salt form should be ionisable at physiological pH. 3) Common ion effect	Mono-sodium salt of tolbutamide[61]
	Prodrugs[62]	1) Insoluble compound is covalently linked to a chemical species. 2) This soluble inactive precursor is activated by metabolism.	1) Structural feasibility of the drug. 2) Creates a new NCE.	PEGylated Paclitaxel[62] activated by endogenous esterases.
Physical modification	Solid state polymorphs[22]	1) Amorphous state of a solid is highly soluble because of its thermodynamic properties. 2) Solubility of amorphous > metastable polymorphs > crystalline	1) Short shelf life due to high reactivity. 2) Might revert back to stable crystalline condition upon exposure to solvents/moisture.	Amorphous Cefuroxime axetil[63]
	Particle size reduction[14]	1) Reduced particle size, increases the surface area which improves the solubility and dissolution (Noyes-Whitney equation)[10].	1) Mechanical stress might degrade the compound as seen with Cryogrinding of Furosemide[64].	Micronized megastrol acetate[65]
Co-administration with soluble excipients[66]		1) The combined effect of mixture water miscible solvents/surfactants might improve the solubility.	1) Might precipitate upon dilution with water. 2) Toxicity issues with various solvents	Nifedipine marketed as Procardia[67].

Techniques	Principle	Disadvantages	Examples
Cyclodextrin(CD) inclusion complexes[68]	1) CDs are a class of cyclic oligosaccharides with hydrophilic outer surface and a hydrophobic cavity capable of forming inclusion complexes with hydrophobic drugs.	1) Can only form complexes with the molecules that fit their pore size. 2) Nephrotoxicity issues with repeated use[69,70].	Artemisin[71]
Lipid based drug delivery systems[72]	1) Lipophilic drugs can be solubilised in GRAS approved oils or liposomes. Micro-emulsions and SEDDS are highly advantageous[73]	1) Limited drug loading capacity. 2) Use of surfactants to stabilise the formulation might compromise the drug's safety.	Ampothericin B[72]
Polymeric nanoparticles[74]	1) Encapsulation of drugs in dendrimers or polymeric amphiphiles helps to suspend the drug in an aqueous environment.	1) Physicochemical property of the drug makes it hard to develop a universal carrier.	CyclosporinA, Griseofulvin by polymeric GCPQ amphiphiles[75].

Pro-drug administration is also a choice of interest to improve the bioavailability. The idea is to administer a chemically inactive form (pro-drug) of the drug, which is then converted into an active metabolite *in situ,* before reaching the target tissue. The pro-drug often displays a superior pharmacokinetic profile than its active form and relies on an endogenous enzyme for its activation[76]. The bioavailability of orally delivered PEGylated Paclitaxel (pro-drug) increased four folds when compared with paclitaxel alone[62]. The PEGylated pro-drug is activated by endogenous esterases to form active paclitaxel. The pro-drug enhanced the water solubility, improved the gut permeability and also protected the active drug from liver metabolism by the cytochrome P450 enzyme family, which ultimately increased the mean absolute bioavailability by 4 folds when compared to that of normal paclitaxel[62]. The structural feasibility of the drug for chemical modification remains a major constraint for drug delivery through this approach [77].

1.1.2.1.2 Physical modification:

Modifying the physical properties of a drug such as particle size[14] and solid polymorphic forms[22] might also improve the drug's bioavailability. Changing the crystalline form of a drug into its amorphous form, improves the pharmacokinetic parameters of the drug[25]. This is because the amorphous form of a solid has the highest internal energy among the different polymorphic forms which means the molecules are loosely packed in a random order with a low surface free energy[25]. This makes the molecule highly reactive which in turn improves the drugs solubility, dissolution and ultimately the bioavailability. The amorphous form of cefuroxime axetil[63] (antibiotic), improved the survival of mice infected with *E. coli* by approximately 20 %, when compared to the mice that received the normal drug, which is currently marketed. Most of the compounds are crystalline in their natural state, which is the lowest energy state and amorphous forms are obtained from the crystals using procedures like milling and compaction of crystals, lyophilisation, precipitation from solution, super-cooling of the melt or vapour condensation[78,79]. But the high reactivity of the amorphous state means they tend to recrystallize upon exposure to solvents or moisture, which might affect the shelf life of the drug and result in poor dissolution[24]. Thus, careful considerations should be made while selecting the excipients to stabilize the formulation.

Particle size reduction is also another kind of physical modification, which reduces the particles into fine powder[14]. This increases the surface area of the drug that is in contact with the solvent and thus promotes solubility and dissolution. Bruner and Tolloczko in 1900[10] established the relation between the particle size and dissolution by elaborating the Noyes and Whitney equation as shown below.

Noyes and Whitney initially stated:

$$\frac{\partial C}{\partial t} = k(C_s - C) \qquad \text{(Equation 1.4)}$$

Where $'k'$ is a constant, 'C' is the drug's concentration at a given time 't' and $'C_s'$ is the saturation solubility. Bruner and Tolloczko demonstrated through a

series of experiments that the dissolution is also related to the surface area, temperature, stirring and thus the equation 1.4. becomes,

$$\frac{\partial C}{\partial t} = kS(C_s - C) \qquad \text{(Equation 1.1)}$$

where 'S' is the surface area, which means surface area is directly proportional to dissolution. So reducing the particle size increases the surface area thereby improving dissolution[80]. Micronized megestrol acetate tablets showed improved dissolution when compared with the conventional solid dosage form[65]. The mean AUC of human volunteers orally dosed with the micronized drug was twice higher than that of the conventional megestrol acetate tablets, which explains the usefulness of this strategy to improve the oral drug absorption.

Milling, grinding, spray drying, homogenization etc. are the traditionally used methods used to reduce the particle size and improve the bioavailability. But the main disadvantage of these technique is that the compounds experience a huge amount of mechanical stress, which might degrade the compound and reduce its activity[65]. Cryogrinding mechanically induced the degradation of furosemide[64], a diuretic, in a study, where high amounts of degraded furosemide residues were identified in the formulation. This resulted in chemical instability of the drug and illustrates the negative effect that these mechanical forces can impose on a drug, rendering it inactive. To overcome these difficulties novel techniques such as supercritical fluid processes (SCF), piston gap homogenizer, etc. have been developed which have their own advantages and limitations[81].

1.1.2.1.3 Co-administration with soluble excipients:

Lipophilic drugs are often co-administered with a mixture of miscible solvents, in order to enhance their solubility[66,82]. Water miscible solvents like ethanol, PEG400, propylene glycol, glycerol and water insoluble solvents like vegetable oils, vitamin E, oleic acid etc. are used for this purpose. Nifedipine, a calcium channel blocker is marketed as Procardia, which is a solubilized in a soft gel capsule by excipients like PEG400, glycerine, peppermint oil and sodium saccharin[67]. In cases where the poor bioavailability is due to poor intestinal penetration, the drugs are often co-administered with mucolytic

agents or surfactants such as N-acetylcysteine (a mucolytic agent) and TX-100 (a non-ionic surfactant)[82]. Mucolytic agents, dissolve the mucus barrier by breaking the disulphide bonds between the mucoproteins, which eventually reduces the viscosity of mucus facilitating easy diffusion of the drug[82]. Surfactants affect the fluidity of the epithelial cell membranes by solubilising the membrane components, which improves the drug's permeability[83].

1.1.2.1.4 Cyclodextrin inclusion complexes:

Cyclodextrins (CD) display amphoteric properties and possess a unique structure with an internal hydrophobic core; the internal hydrophobic core enables the cyclodextrins to form inclusion complexes with the hydrophobic drugs, solubilising these with aqueous media. CDs are cyclic oligomers of α-D-glucopyranose (Glc) units linked through α(1-4) glycosidic bonds. This gives CDs their unique structure and based on the number of Glc units, the CDs are divided into α, β and γ which have 6, 7 and 8 Glc units respectively. The increase in Glc units increases the size of the hydrophobic cavity and thus they can accommodate different sizes of hydrophobic molecules[68,84]. The drug-CD complexes are easy to form, by just supersaturating the CD solution with drug under mild agitation. The complex formation is mainly due to hydrophobic and van der Waals interactions and the complexes dissociate easily upon dilution thereby releasing the drugs for intestinal absorption. The problem with these complexes is the high ratio of CDs to drug that is required to form a complex with the given drug. This limits their use due to toxicity issues[69]. CDs are fermented by intestinal microflora, so they are considered as safe for enteral delivery at limited doses but are found to cause irreversible nephrotoxicity and haemolytic activity on repeated use via parenteral route[85]. Various modifications of natural CDs have been carried out to overcome their nephrotoxicity and the presence of a primary alcohol group on the Glc unit facilitates these modifications[70]. Artemisin[71] and tolbutamide[86] are some of the examples of drugs exhibiting improved bioavailability upon complexion with cyclodextrins.

1.1.2.1.5 Drug nanoparticles:

A recent trend in drug delivery is to associate drugs with specially engineered vectors to form nano carriers such as nanoparticles[14], polymeric micelles[87] or vesicles[88], which increase the therapeutic index through a variety of different mechanisms. Briefly, reducing the particle size increases the surface area, which favours better dissolution, which in turn enhances the absorption. Nanoparticles also have other advantages such as prolonging the drug absorption, evading phagocytes and targeted delivery, which are few of the mechanisms that help in improving the efficacy of the drugs[74].

Hydrophobic drugs are conjugated[89], solubilised[90] or encapsulated[91] with their nano carriers in order to achieve an enhanced therapeutic index. Chemical conjugation of drugs with a water-soluble polymer will improve the solubility of the drug and eventually its absorption. Paclitaxel was covalently linked to N-(2-hydroxypropyl)-methacryla-mide (HPMA) copolymer, which not only increased the water solubility of paclitaxel but also improved its cytotoxicity against tumour tissue due to the site-specific targeting of the HPMA copolymer[92]. Amphiphilic and hydrophobic drugs solubilised in liposomal vesicles offers an efficient method for drug delivery, mainly via intravenous route[93]. A poorly water-soluble drug fenofibrate was solubilized in liposomes made up of soybean phosphatidylcholine and sodium deoxycholate and the bioavailability of these liposomes was 5 folds higher than that of the micronized finofibrate[94]. The liposomes are made of lipid bilayers with an aqueous core and thus can be used to solubilise both hydrophobic and hydrophilic drugs. Liposomes have versatile functions in the field of drug delivery and currently researched extensively for the delivery of small molecules, proteins, antibiotics, and vaccines and also for diagnostic purposes[95,96]. Encapsulation of amphiphilic and hydrophobic drugs in an amphiphilic polymer matrix result in drug-loaded micelles that are capable of enhancing the oral bioavailability to a significant level[97]. The amphiphilic polymers in an aqueous environment form micelles with an outer hydrophilic shell, which helps to suspend the drug in an aqueous environment while the inner hydrophobic core acts as a reservoir for poorly water soluble drugs. Bioavailability of gresiofulvin and cyclosporine A were enhanced by 6 folds

and 5 folds respectively, by using GCPQ, an amphiphilic modification of glycol chitosan. The mechanism of action is through improved dissolution, mucoadhesion and transcellular drug uptake[75]. The potential of drug nano carriers have been well understood by scientific world and ever since a variety of polymers like block-polymers, dendrimers, amphiphilic polymers etc. have been developed and researched for their potential as delivery vehicles[75,98–100].

1.1.2.1.6 Emulsions:

Emulsions are colloidal suspensions of two or more immiscible liquids i.e. dispersion of oil droplets in water or water droplets in oil. These emulsions are more often stabilised by a surfactant, which reduces surface tension between the two liquid phases there by decreasing the kinetic interactions, thus increasing the stability[73]. Based on the size of the colloidal liquid phase, the emulsions may be classified as nano emulsions or micro emulsions. A new class of delivery system called self-emulsifying drug delivery systems (SEDDS) have been recently exploited for drug delivery[101]. In SEDDS an isotropic mixture of oil, surfactant, solvents and co-solvent of a hydrophobic drug are used to improve the solubility of the drug and upon ingestion, the mixture forms emulsions due to the gastric motility. A concept of non-aqueous emulsions also prevails, where other polar solvents such as glycerol, PEG400 etc, replace the aqueous phase[102]. These systems possess unique properties different from traditional emulsions and may be useful to deliver the drugs that are neither soluble in water or in oil, which might aid in oral delivery of certain hydrophobic drugs, while scarcity of information and narrow choice of polar phase pose limitations on use of these non-aqueous emulsions[102–104].

The idea of using oils for drug delivery stems from the way the fats are metabolised in the digestive tract. Fats upon ingestion, form crude emulsions due to the action of gastric lipases and gastric motility. When these crude emulsions enters the duodenum, it stimulates the secretion of bile salts, cholesterol, and phosphatidylcholine from gall bladder and pancreatic lipases/co-lipase from pancreas[105]. The action of bile salts promotes micronisation of oil droplets and the action of pancreatic lipases along with

the breakdown products promotes the formation of stable micellar and vesicular species, which are readily absorbed by the intestinal epithelium. Based on this principle various hydrophobic drugs were dissolved in lipid-based delivery systems and the oral bioavailability of amphotericin B was successfully enhanced using a lipid based drug delivery system[106]. When the amphotericin B SEDDS formulation was orally administered to the rats infected with *Aspergillus fumigatus*, it reduced the total CFU count for the fungus by >80 % when compared to the non-treated controls[107]. This superior pharmacodynamic activity is attributed to the improved drug solubility, better *in vitro* stability and reduced renal toxicity of amphotericin B SEDDS formulation[107].

1.1.2.1.7 Gastro-retentive dosage forms:

Prolonging the gastric retention time of the dosage form is another strategy used to improve the absorption of drugs with a narrow absorption window. The absorption of certain drugs occurs only at certain segments of the gastro-intestinal tract due to high variations in the pH of the gastro-intestinal tract. So prolonging the residence time of the dosage form in the stomach serves as an excellent strategy to improve the absorption of the drugs that are predominantly absorbed at low pH conditions.

Different approaches are available to increase the gastric residence time such as floating systems, mucoadhesive systems, swelling systems and expanding systems. The idea behind these techniques is to increase the gastric residence time by escaping gastric emptying by using physical principles[108,109]. For example, floating dosage forms do not sink in the gastric medium due to their low density in comparison with the gastric fluid. Swelling or expanding devices increase their size by several folds so that they cannot pass through the pylorus during the gastric emptying. Mucoadhesive systems adhere to the mucous lining in the stomach thus prolonging its gastric retention time. Using a floatation device, the bioavailability of atorvastatin calcium, a hydrophobic drug was enhanced up to 1.6 folds when compared to that of the conventional tablets[110]. A floatation device for ciprofloxacin is also currently marketed under the brand name Cifran O.D by Ranbaxy[111].

1.1.3 Competent oral formulation strategies:

Although there are different options available to enhance the bioavailability of a hydrophobic drug, each strategy has its own advantage and disadvantage as shown in Table 1.1. Also, the feasibility of using a technique is mainly limited by the physicochemical properties of the drug. For example, it may not be possible at all to develop a pro-drug form of a drug due to its structural constraints. Thus while choosing a formulation strategy one has to make a rational approach by assessing the physicochemical properties of the drug along with other considerations related to the desired release profile, manufacturing limitations etc.

Of all the strategies to enhance the oral absorption of hydrophobic drugs, developing a salt form of a drug is by far the most successful strategy amongst the pharmaceutical industries[112]. According to a study more than 50 % of the drugs listed in the US Orange Book Database are formulated with the salt forms of the drug[113]. The popularity of this technique lies in the fact that a) it is an old concept, which means the technique is well understood; b) no expensive excipients are used and c) it is relatively easier to generate a stable salt form of a drug[114]. The success of this technique also lies in the fact that a salt form of a drug is also compatible with other formulation strategies. For example, calcium salt of atorvastatin was used to develop an amorphous form of the drug as the combined effect of solubility and amorphous nature improved the dissolution by a factor of 2 when compared to that of the crystalline atorvastatin calcium[115].

Physical modifications of the drug such as alternative polymorphic forms and particle size reduction are also successful strategies to enhance the dissolution of the hydrophobic drugs. But the formulation strategies such as salt forms or polymorphic forms only focuses on improving the concentration of the API in the blood stream after oral administration. The drug molecules are then left on their own to find their target and in this pursuit most of the molecules end up in tissues where they are not meant to be. This seems to be like a strategy of previous era due to the advent of ‘smart drug delivery systems’ that are capable of targeting the right tissues, reducing the toxicity,

enhancing the absorption, reducing the dosing frequency etc. all of which improves the therapeutic outcome. New drug delivery systems such as liposomes, polymeric nanocarriers, gastro-retention devices etc. have made these changes possible.

Polymers that are capable of forming micelles or nanoparticles with the API have found novel uses in drug delivery. They are used to orally deliver a variety of therapeutics such as small molecules, proteins, peptides, anti-bodies, nucleic acids and vaccines to hard to reach targets such as central nervous system or a tumour[116]. The polymeric carriers are capable improving the aqueous solubility of the drug, protect them from harsh environment in the GI tract, improve the drug absorption and can also deliver their drug load to the pathological site[117,118]. The surfaces of these polymeric nanoparticles can be functionalized with target ligands due to the presence of reactive functional groups. This has led to the development of a variety of applications for polymeric nanoparticles, such as stimuli-responsive drug release, target recognition, disease diagnosis and intracellular drug delivery[119]. Gastro-retention is another smart strategy to improve the absorption of drugs that have a narrow absorption window. Releasing the drug specifically at the absorption site ensures complete uptake of the drug, which eventually enhances the treatment efficiency.

Due to increase in the global awareness on drug safety and efficacy, use of smart drug delivery systems is the current trend in drug delivery[120]. Polymeric nanoparticles in particular are gaining popularity due to their tremendous potential for versatile applications[118–124]. Even though the salt forms of the API dominate the current market, the future drug delivery strategies will revolve around exploiting the polymer technology for the delivery of API in an efficient way.

1.2 Subcutaneous drug delivery:

Parenteral dosage forms are the first choice delivery option for a hard-to-formulate poorly soluble drug, for which the bioavailability following the oral delivery is negligible. Other advantages of parenteral delivery include, drug delivery to unconscious patients, easy access to systemic circulation and

rapid drug action, while the disadvantages are poor patient compliance and the high cost of production[125]. Of all the parenteral routes, subcutaneous injections are by far less painful and has better patient adherance[126]. Also controlled or prolonged release of the active ingredient is possible leading to less frequent injections. Thus the subcutaneous route for drug administration is one of the desired routes for drug delivery and this section gives an overview of subcutaneous drug absorption.

1.2.1 Factors affecting the subcutaneous drug absorption

1.2.1.1 Physiological Factors

Unlike oral absorption, subcutaneous absorption is fairly straightforward and has fewer barriers hindering the drug absorption. Both the nature of the subcutaneous tissue as well as the physiochemical property of the drug would affect the rate, duration and the extent of drug absorption. The main factors affecting the subcutaneous drug absorption are as follows.

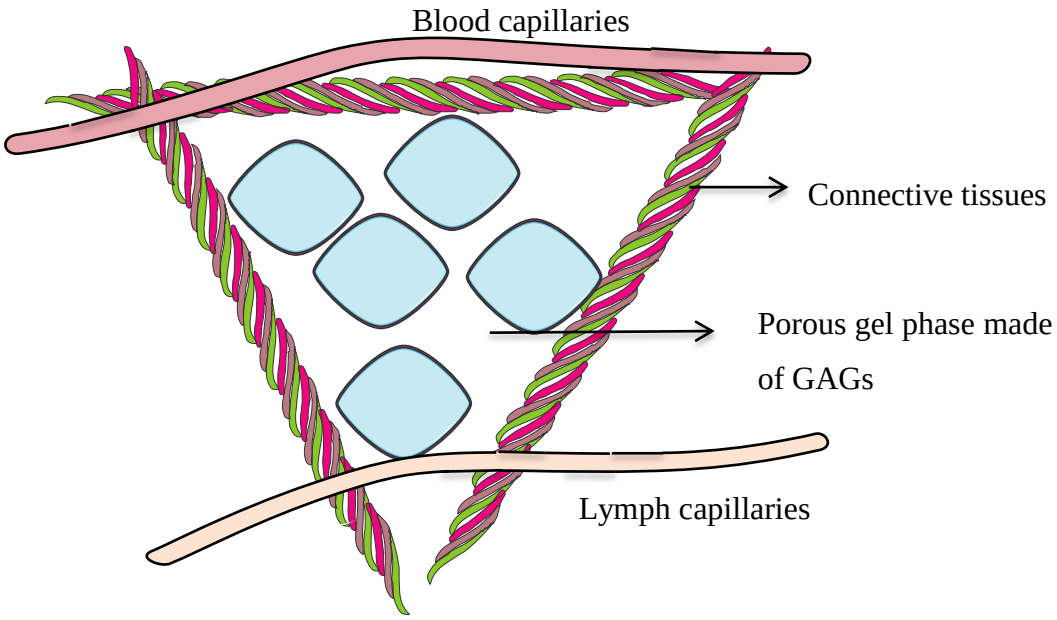

Figure 1.3 Structure of interstitium

1.2.1.1.1 The interstitial space:

The subcutaneous layer forms the hypodermis of the skin and is the last layer of the integumentary system. The main components of the

subcutaneous layer in respect to drug absorption are the interstitial space, fat cells (adipocytes), salts, plasma proteins, blood and lymph vessels[127]. The interstitial space is made up of loose connective tissue, which consists of elastin, collagen, glycosaminoglycans such as hyaluronan along with salts and proteins (Figure 1.3). The presence of collagen provides a structural framework to the connective tissue and anchors the hypodermis to the deep fascia of muscle skeleton, elastin contributes towards elasticity while the glycosaminoglycans (GAGs) form a gelatinous network, providing firmness to the tissue[127].

Hyaluronan (hyaluronic acid) that makes the bulk of GAGs is a high molecular weight (10^5 - 10^7 Da) polymer made of repeating disaccharide units. It forms an entangled network in an aqueous environment, which under physiological conditions forms a porous gel. The gel phase provides a barrier to the bulk fluid flow, while the porous matrix acts as a filter by impeding the flow of macromolecules[127]. Hyaluronan is negatively charged and this strong negative charge of the GAG limits the interstitial fluid content and hydraulic conductivity. The negative charges of GAGs attract the counter ions to establish electro neutrality, which in turn increases the interstitial osmotic pressure that maintains fluid balance[128]. Hydraulic conductivity describes the ease with which a fluid passes through a porous matrix and it depends on the fluid's density and viscosity[129]. Since the GAGs make up the porous gelatinous matrix of the interstitium, the contents of the GAGs determines the hydraulic conductivity and thereby interstitial fluid flow[129].

The passage of injected fluids in the subcutaneous space is facilitated by either by convection or diffusion. The driving forces for the convection are the hydrostatic and osmotic pressure differences that occur among the blood capillaries, interstitium and the lymphatics[129]. The rate of convection of a molecule is limited by steric hindrance and the charge of the molecule while the rate of diffusion of a molecule is inversely proportional to its molecular weight. Thus the absorption of hydrophilic small molecules such as glucose is rapid from subcutaneous injections while large molecular weight proteins have slower absorption rates[127,129].

The other factor hindering the diffusion of particles in the interstitial fluid is the net negative charge of GAGs. This might affect the diffusion of charged solutes due to electrostatic attractions or repulsions. Ionic interactions with salts, interstitial protein binding, hydration status of the interstitial space, are the other factors affecting the subcutaneous absorption of the drugs[130].

1.2.1.1.2 Blood and lymphatic vessels:

The plasma proteins and other components of the interstitial space are constantly replenished by the drainage through blood and lymph vessels. The same applies for xenobiotics injected into the subcutaneous tissue. The xenobiotic travels through the interstitial space and reaches either the blood or lymphatic vessels, from where it reaches the systemic circulation. The molecular weight and permeability of a molecule determines if it is absorbed through blood capillaries or lymphatic vessels, where a molecule of molecular weight less than 16 kDa gets predominantly absorbed from the blood capillaries, while a large molecular weight compound gets absorbed through lymph. The difference is mainly due to the structural differences between the blood and lymph vessels[127].

The blood capillaries contribute to the bulk of fluid volume exchange between the tissues (20 – 40 L/day against 2 – 4 L/day of fluids drained by lymphatic vessels) and thus a major transporter for injected xenobiotics[131]. The arteries in the subcutaneous layer form highly branched network of capillaries called the cutaneous plexus, which eventually combines together to form post-capillary veinule. The capillary walls are made of single layer of endothelial cells lined by basal lamina but characterised by the presence of nano pores (Figure 1.4a). The presence of tight junctions in these endothelial cells forms a virtually impermeable barrier to the fluid flow[132]. But there is continuous exchange of plasma contents between the vascular capillaries and the interstitium due to convective fluid flow and diffusion through the nanopores[129,132]. The convective fluid flow is due to the hydrostatic and osmotic pressure differences between the vasculature and the interstitial space. For example the absorption of glucose, a hydrophilic small molecule is rapid following the subcutaneous administration, which is mainly due to the capillary uptake mechanism.

On the other hand, the absorption of high molecular weight solutes such as proteins and colloidal particles are facilitated through the lymphatic system. The lymph capillaries are made of endothelial cells with a discontinuous basal layer (Figure 1.4b). Also the endothelial cells in the lymph capillaries are loosely bound and overlapping to form a 'cleft-like' junction. These clefts open and close due to changes in the interstitial pressure, which also allows the passage of large molecular weight solutes and colloidal particles of size around 100 nm as the molecules above the size 100 nm are usually found to be trapped in the interstitium. The interstitial fluid pressure is affected by blood pressure, composition of the interstitium, cell density, tissue hydration, metabolism and exercise[131,132].

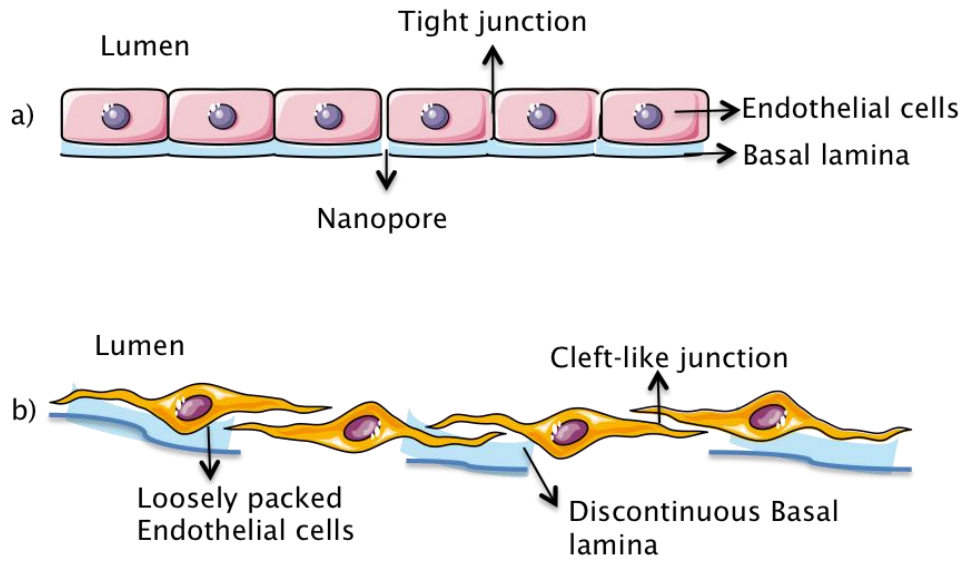

Figure 1.4 Structure of a) Blood capillaries and b) Lymph capillaries

1.2.1.1.3 Site of administration

The rate and extent of the absorption of therapeutics depends on the site of subcutaneous injection. This is because the thickness and composition of the subcutaneous tissue varies throughout the body and also varies from person to person. For example, the amount of muscular activity, BMI of a person, gender can all contribute towards the composition and thickness of the SC[127]. The relationship between the subcutaneous pharmacokinetics and the site of injection has been reported for insulin and several other proteins in humans[133,134]. In a study, the absorption of insulin was monitored following

the subcutaneous administration at three different injection sites, abdominal, deltoid and femoral[133]. Abdominal injections produced greater C_{max} values for insulin when compared with deltoid and femoral injections. The T_{max} value also varied among the injection sites but the AUC values were not greatly influenced by the injection site. The delayed absorption from femoral and deltoid sites resulted in prolonged duration of action for insulin, which means more potential sites for subcutaneous injections should be studied in order to achieve desired PK and PD properties[133]. The variation is mainly due to the regional differences in the blood pressure, which affects the interstitial fluid flow and lymph flow influencing the drug uptake[127].

1.2.1.1.4 Catabolism

The bioavailability of the therapeutics, particularly proteins, might be affected by proteolysis at the subcutaneous injection site. The endogenous protein content of the interstitium is totally derived from that of plasma but the concentration of these proteins is usually around 40 % of what is found in the plasma[135]. Thus endogenous proteases and peptidases might be a problem for protein and hormone therapeutics such as insulin[136], hGH[137] etc. In a study, PEGylated erythropoietin (EPO) was used to demonstrate the effect of catabolism in reducing the bioavailability following its subcutaneous administration[138]. Radioactively labelled EPO and lymph duct cannulised rat models were used in this study. After various experimental observations, the bioavailability of EPO was reduced by 60 – 70 %, which is mainly attributed to catabolic activities at the subcutaneous injection site and also at the lymph nodes[138].

1.2.1.2 Physicochemical properties of the drug

1.2.1.2.1 Water solubility:

The interstitial space is a highly hydrated environment and thus the water solubility of the drug will affect its subcutaneous absorption. Precipitation of the drug would result in the dosage being physically trapped in the interstitial matrix and thus unavailable for absorption. However, some degree of lipophilicity is required to cross the epithelial barrier of the capillaries due to the nature of the plasma membrane[132]. The ideal logP to cross the cellular barriers in the gut[3] and blood brain barrier (BBB)[139] is logP < 5 and logP 1.5

– 2.7 respectively. Given the similarities in the structure of endothelial cells[140] in BBB and subcutaneous capillaries (Figure 1.4a), an ideal logP to penetrate the blood capillaries following the subcutaneous injection could be assumed to be similar to that of the BBB (logP 1.5 – 2.7), although there could be exceptions to this generalisation.

1.2.1.2.2 Molecular size

As discussed earlier molecular weight and molecular size plays an important role in determining the subcutaneous absorption of injected molecules. Molecules that are 10 nm in diameter are absorbed via blood capillaries while larger molecules are taken up via the lymph. In terms of molecular weight, therapeutics that are less than 16 kDa are predominantly taken up via the blood capillaries while larger molecules are taken up via the lymph. In general the absorption of small molecules are rapid, which is mainly due their rapid movement through the interstitial space, while large particles (> 100 nm) are trapped in the interstitial space. A linear relationship between the size of the molecule and lymphatic absorption was observed on different occasions in animal models[141] and sometimes the dosage forms are specifically designed to target lymphatic absorption by increasing the molecule's size[142]. For example, several researchers have used liposomes of different sizes and have demonstrated enhanced lymphatic absorption of drug-loaded liposomes[143–145]. This phenomenon could be potentially used to treat diseases that affect the lymph node[146].

1.2.1.2.3 Charge of the molecule:

As previously mentioned, the interstitial space is negatively charged due to the presence of glycosaminoglycans. Thus the movement of positively charged molecules will be impaired due to electrostatic attraction. In a study, involving liposomes the lymphatic absorption of the liposomes was rapid for negatively charged liposomes, followed by positively charged and neutral liposomes[147]. This is because the negative charges in the liposomes move with ease due to electrostatic repulsion in the interstitial space. There are several other publications that have reported a rapid uptake rate for negatively charged particles when compared to the positively charged ones[148–150]. This charge-based discrepancy in the rate of subcutaneous

absorption could be potentially used to prolong the drug absorption by formulating the drug in a positively charged delivery vehicle.

1.2.2 Considerations while designing for subcutaneous injections

One advantage of subcutaneous injection is that, manipulation of the dosage form to meet the therapeutic requirement is possible unlike other parenteral routes; example, the dosage form can be designed for lymphatic uptake or controlled release. While the intramuscular (IM) route is also used for controlled release depot formulations, the IM routes are more invasive and cause tissue damage, which limits the patient adherence. The following section is about the factors to consider, while designing subcutaneous dosage forms for human use.

1.2.2.1 Carrier selection:

A hydrophilic or amphiphilic carrier often facilitates the subcutaneous absorption of hydrophobic drugs or unstable proteins. The carrier could be of synthetic, semisynthetic or inorganic origin. An ideal carrier should a) be biocompatible and biodegradable – the carrier should be toxicologically safe and get eliminated by normal metabolic pathways; b) deliver the drug at clinically effective doses and c) be amenable for modifications to achieve desired drug release profile. Due to diversity in diseases, dosage range and special requirements, a multitude of vehicles are available for subcutaneous injections. Polymeric materials such as α – hydroxyacids (PLGA)[151], polysaccharides (hyaluronic acid, chitosan etc.)[152], nanoparticle systems such as liposomes[153] and inorganic materials such as hydroxylapatite[154] are some of the commonly used carriers for subcutaneous drug delivery.

1.2.2.2 Pharmacokinetic (PK) profile:

The main factor to consider while designing a subcutaneous dosage form is the desired pharmacokinetic profile of the drug. For example, for some treatments, slow and steady release of the active ingredient would be desirable and for some a rapid release rate might be desirable. The dosage form should be carefully designed to meet these PK requirements in order to achieve a clinical effect. Advances in polymer technology have led to the

development of subcutaneous dosage forms with a variety of drug release profile. By modifying the molecular weight and the hydrophobicty, Poly lactic-co-glycolic acid (PLGA) was tuned to achieve different drug release profile[155]. In one particular study[156], PLGA microspheres of three different molecular weights (10, 20 and 30 kDa) were used to encapsulate exenatide, a peptide used to treat type II diabetes. When given subcutaneously to humans, the 10-kDa PLGA microspheres had a severe initial burst release, while the release of exenatide from the 30-kDa PLGA microspheres was prolonged for a period of 30 days[156].

Controlled drug release is also possible, where a polymer matrix can be engineered to respond to an external or internal stimulus such as heat, pH changes, electrical field or radiation. Extensive research is being carried out to explore the control drug release behaviour of polymeric matrices. A thermo-sensitive *in situ* forming hydrogel was developed by conjugating Paclitaxel to poly(ε-caprolactone)-poly(ethylene glycol)-poly(ε-caprolactone) (PCEC/PTX), which remains liquid at room temperature but solidfies to form a gel at body temperatures when injected[157]. This thermosensitive gel sustained the release of paclitaxel for a period of 28 days in animal models and the release of the drug was due to gradual erosion of the polymer matrix. In another study, on/off release of the drug load was achieved by using Near Infra red (NIR) waves as a trigger for *N*-isopropylacrylamide-*co*-acrylamide (NIPAAm-*co*-AAm) hydrogels loaded with silica-gold nanoshells[158]. The nanoshells when irradiated with NIR achieve their peak extinction coefficient, which converts light radiations into heat energy, which heats the surrounding microenvironment. NIPAAm-*co*-AAm forms hydrogels at body temperature but collapses at temperatures around 50 °C. When the hydrogels containing silica-gold nanoshells are irradiated with NIR laser, a local rise in temperature destabilizes the hydrogel with reversible effects. When this hydrogel - nanoshell matrix is loaded with a drug, switching on or off the NIR laser source can control its release.

1.2.2.3 Targeting lymphatic system:

Lymph vessels form an important unidirectional circulation route for extravasated plasma proteins, excess fluid and cell debris[130]. It also plays an

important role in the transport of dietary lipids and highly lipophilic compounds from the site of absorption to the circulatory system bypassing liver metabolism. In addition to this, the lymphatic system plays a key role in the maintenance of an effective immune system and dissemination of the metastases from solid tumours[159]. It is also established that the bacterial and viral pathogens might use the lymphatic system to gain access to the systemic circulation. Thus, targeting the lymphatic system serves as a formulation strategy when the drug undergoes high first-pass metabolism or the drug's desired site of action is lymph nodes such as in case of treating tumour metastasis[146].

As previously discussed, macromolecules with molecular weights greater than 16 kDa and particulates that are larger than 10 nm in diameter are preferentially absorbed via lymph capillaries following subcutaneous injections. Hence, by nature, the bio therapeutics such as proteins and other macromolecules are selectively absorbed via the lymph due to their high molecular weight. For small molecules that are less 16 kDa, colloidal particles larger than 10 nm in diameter offer an easy way to facilitate lymphatic absorption. Liposomes are widely used for lymphatic delivery and in one particular study, LyP-1, a cyclic peptide for tumour targeting was conjugated to PEGylated liposomes loaded with fluorescein or doxorubicin[160]. These liposomes selectively accumulated in lymphatic nodes, following the subcutaneous injection of these liposomes in tumour bearing mice. Thus by specifically designing the formulation, the subcutaneous route can be effectively used to selectively target the lymphatics.

1.2.2.4 Formulation parameters:

Other formulation parameters to consider while designing a subcutaneous formulation are, the dosage volume, viscosity, pH and osmolality of the formulation[132]. The viscosity of the formulation shouldn't be too high as this will restrict interstitial flow or would be difficult to inject causing discomfort to the patients. Similarly, extreme pH in the formulation might give rise to local irritation at the injection site. The formulation should also be isotonic, which is determined by the ionic strength or osmolality of the formulation. Also factors like, massage, exercise, heat can also affect subcutaneous drug

absorption[127]. As described previously, the interstitial fluid flow is regulated by the oncotic and hydrostatic pressure difference in the blood capillaries, interstitium and the lymph[129]. This pressure gradient would be disrupted when hyperosmolar solutions are injected in the interstitium, resulting in excess extravasation leading to necrosis.

Also there are restrictions on the total volume of formulation that could be administered subcutaneously. Unlike furry mammals, humans have fibrous bands that run deep into the fascia, which reduces the compliance of tissue space to injected fluids. This limits the subcutaneous injection volume in humans to less than 2 mL[161]. One strategy to overcome this restriction is to reduce the viscosity of the interstitial space by depolymerizing the hyaluronan component of the interstitial matrix. The hyaluronan has a half-life of just 15 – 20 h and hence the degraded polymer would be quickly restored allowing sufficient time for the absorption of the injected liquid. Traditionally, hyaluronidase enzyme from the bovine and ovine sources were used for this purpose. But the use of hyaluronidase obtained from animal sources will lead to potential immunogenic reactions in humans[162]. Thus the Human recombinant hyaluronidase (rHuPH20) enzyme was synthesized using genetic engineering technology, which offers a safe and highly specific method for the degradation of the hyaluronan in humans[162]. Experiments revealed that the depolymerized hyaluronan layer was restored to its former self within 24 hours following the injection of rHuPH20 and importantly, the subcutaneous injection volume could be increased up to 5 – 10 mL per injection. Co-administration with rHuPH20 also affects the pharmacokinetics of the therapeutics, where the bioavailability of the peginterferon and infliximab were dramatically increased when injected with rHuPH20[162]. rHuPH20 is currently marketed under the brand name Hylenex®, by Halozyme® therapeutics and is approved by FDA for cancer treatment in combination with Herceptin.

1.2.3 Competent subcutaneous formulation strategies

As mentioned earlier, drug delivery is advancing towards the development of ‘smart drug delivery systems’[120]. Advances in polymer technology has

enabled these progress in smart drug delivery possible[99,119,163]. The biggest advantage of subcutaneous drug delivery is that the smart drug delivery systems could be easily deployed via this route of adminstration[127]. This is due to the nature of the subcutaneous site, which facilitates easy drug absorption while reducing the pain and discomfort for the patients. Polymeric systems that are capable of prolonging the absorption, controlling the drug release, targeting the lymph nodes etc. have been recently developed and the ultimate goal of these smart drug delivery systems is to reduce the dosing frequency while maximising its therapeutic efficacy[119].

While targeting the lymphatic system via subcutaneous route is a good strategy, it is particularly useful only if the pathological site is the lymph node[146]. If the disease target is elsewhere then there is no particular advantage in delivering therapeutics via the lymphatic route in the context of subcutaneous administration. But on the other hand, controlled drug delivery has many exciting applications for the delivery of therapeutics. For example, drug delivery systems are engineered to respond to a stimulus, which triggers the drug release only when the stimulus is present[164]. The stimulus could be internal, such as pH, an indigenous chemical or external, such as heat, radiation etc. Various small molecule drugs such as docetaxel, ethosuxcimide, leuprolide etc. are formulated in stimuli-responsive polymers for disease treatments[163]. Self-propelled polymeric ‘nanomotors’ that are capable of delivering hydrophobic drugs such as doxorubicin are also recently developed[165]. These locomotive structures loaded with anticancer agent were designed to sense the hydrogen peroxide released by cancer cells, utilise it as their fuel and self-propel their motion towards them, where they release their cargo and eventually kill the cancer cells[166]. The nanomotors could be potentially used to treat and diagnose cancer, wound healing and tissue regeneration.

The advantages of using these controlled drug delivery systems include, prolonged drug release, targeted drug release to the site of pathology, improved treatment efficacy, reduced side effects and reduced dosing frequency[163]. With these novel and versatile applications, ‘polymeric

controlled drug delivery systems' are gaining popularity[120,158,163,167] and thus serves as a competent strategy for subcutaneous drug delivery.

1.3 Aim:

The aim of the project is divided into two main categories. First, is to enhance the oral absorption of hydrophobic drugs that are P-gp substrates (BCS Class IV) such as paclitaxel, CUDC-101 by the use of new and existing polymeric amphiphiles as excipients. The absorption of hydrophobic drugs that are P-gp substrates are hampered by poor solubility and P-gp efflux. Use of the new amphiphilic polymers might enhance the drug absorption by forming colloidal particles that behave differently when compared to the free drug. While more NCEs are discovered each year due to the advances in combinatorial chemistry, there is always a growing demand for more and more efficient excipients for oral drug delivery[57]. Thus this project might lead to the development of an efficient oral drug delivery system for BCS class IV drugs.

The other aim of this project is to develop a subcutaneous dosage form for CUDC-101, an anti-cancer agent to be taken into clinical trials. The dosage form has to be optimized for drug content, tonicity and should be easily injectable. The main challenge lies in achieving therapeutically effective levels of the CUDC-101, particularly due to the extremely hydrophobic nature of the drug and limitations on subcutaneous dosage volume in humans.

1.4 Model drugs:

1.4.1 CUDC-101:

CUDC-101 is a clinical stage multi-target anti-cancer drug developed by Curis Inc., USA and is currently in Phase1b clinical trial as an intravenous dosage form[168]. CUDC-101 targets epidermal growth factor receptor (EGFR), epidermal growth factor 2 (Her2) and histone deacetylase (HDAC) with very low IC50 values of 2.4nM, 15.7nM and 4.4nM respectively[168,169].

Though CUDC-101 (Figure 1.5) is a potent anti-cancer drug, its chemical properties make it highly hydrophobic (Table 1.2). CUDC-101 is classified as

a Class IV drug under Biopharmaceutical Classification System (BCS), which means a drug has poor permeability and poor solubility. While the LogP of the drug is 4, the poor permeability is due to the fact that the drug is P-glycoprotein substrate (Curis's internal data). This makes CUDC-101 an ideal candidate for our experiments to develop a drug delivery system for poorly soluble drugs.

1.4.2 Paclitaxel

Paclitaxel (Figure 1.5) was first isolated from the bark of Pacific Yew tree, *Taxus brevifolia* and is currently marketed under the trade name Taxol® for the treatment of various types of cancer. Paclitaxel interferes with normal breakdown of microtubules during cell division by binding to beta-tubule subunits of the microtubule[170]. This blocks the progression of mitosis and triggers apoptotic pathways leading to cancer cell death. Paclitaxel is extremely hydrophobic and is a substrate of P-gp efflux, thus has very low oral bioavailability (6.5 %)[170,171].

Table 1.2 Physicochemical properties of the model drugs

Common name	**CUDC-101**	**Paclitaxel**
Chemical name	7-(4-(3-ethynylphenylamino)-7-methoxyquinazolin-6-yloxy)-N-hydroxyheptanamide	(1S,2S,3R,4S,7R,9S,10S,12R,15S)-4,12-Diacetoxy-15-{[(2R,3S)-3-(benzoylamino)-2-hydroxy-3-phenylpropanoyl]oxy}-1,9-dihydroxy-10,14,17,17-tetramethyl-11-oxo-6-oxatetracyclo [11.3.1.0~3,10~.0~4,7~] heptadec-13-en-2-yl rel-benzoate
Appearance	White crystalline powder	White crystalline powder
Molecular Formula	$C_{24}H_{26}N_4O_4$	$C_{47}H_{51}NO_{14}$
Molecular weight	434.49 g mol^{-1}	853.9 g mol^{-1}

Common name	**CUDC-101**	**Paclitaxel**
Water solubility	29 ± 10 µg ml^{-1} (calculated value)	5 µg ml^{-1} (predicted value)
Cal LogP	4	3

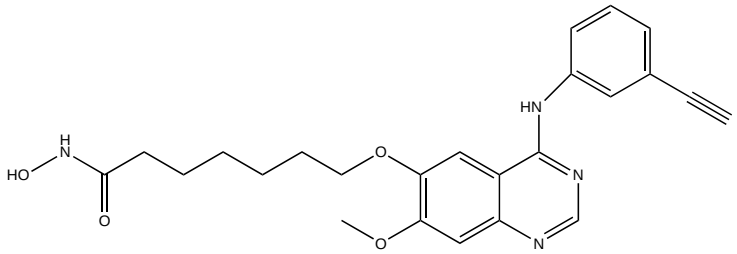

(a)

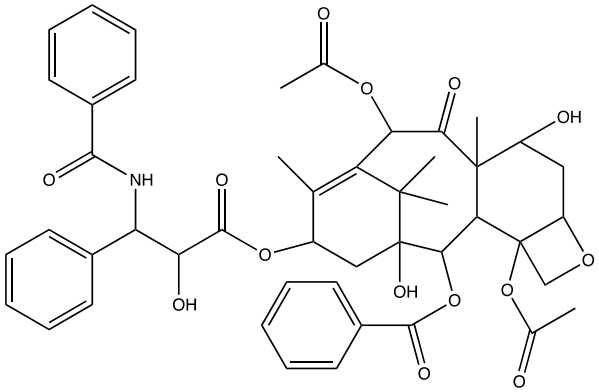

(b)

Figure 1.5 Chemical structures of a) CUDC-101 and b) Paclitaxel

2 Amphiphile synthesis and characterisation

2.1 Introduction:

Amphiphilic molecules are those with both hydrophilic and hydrophobic functional groups in their structure. This gives amphiphiles a unique property of self-assembly in aqueous environment, where the hydrophobic units of the amphiphiles are oriented in such a way to reduce their contact with water. This phenomenon forms colloidal particles called micelles and the driving force for micelle formation in aqueous environment is the entropy gain enjoyed by the water molecules when they are liberated from a hydrophobic environment. The amphiphiles have surface-active properties and have a wide range of applications in the field of drug delivery[172].

The use of polymeric amphiphiles for oral drug delivery has gained attention in recent times and the potential for these systems to aid in drug delivery has been researched extensively[173]. Polymeric amphiphiles are those with repeating units of hydrophilic and hydrophobic units that self-assemble in aqueous environment and are capable of forming nanoparticles with hydrophobic molecules, which improves drug absorption. This chapter covers the synthesis and characterisation of polymeric amphiphiles, namely N-palmitoyl-N-monomethyl-N,N-dimethyl-N,N,N-trimethyl-6-O-glycolchitosan (GCPQ) and N-(2-phenoxyacetamide)-6-O-glycolchitosan (GCPh).

2.1.1 Glycol Chitosan based amphiphiles:

2.1.1.1 GCPQ:

GCPQ is a chitosan based amphiphilic polymer, with hydrophobic palmitic acid molecules covalently linked to hydrophilic sugar backbone[174]. This comb shaped amphiphile (Figure 2.1) has positively charged quaternary ammonium groups, which increase the water dispersibility of the molecule and also aids in mucoadhesion[75]. GCPQ form micelles when suspended in aqueous environments and has been shown to encapsulate hydrophobic drugs and peptides[75,175]. The micelles are formed at a low critical micellar concentration (CMC) of ~20 μM[75]. It has been previously shown that the GCPQ nanoparticles enhanced the bioavailability of the therapeutics through

ocular[176] and the oral route[75]. It was also established through CARS (Coherent Anti-Stokes Raman Spectroscopy) imaging that the drug loaded GCPQ nanoparticles are taken up as a whole through enterocytes[175,177]. The mechanism of action of GCPQ is to increase the aqueous solubility of the drugs, mucoadhesion, protecting the therapeutic from degradation and enhancing its transcellular transport [75,175].

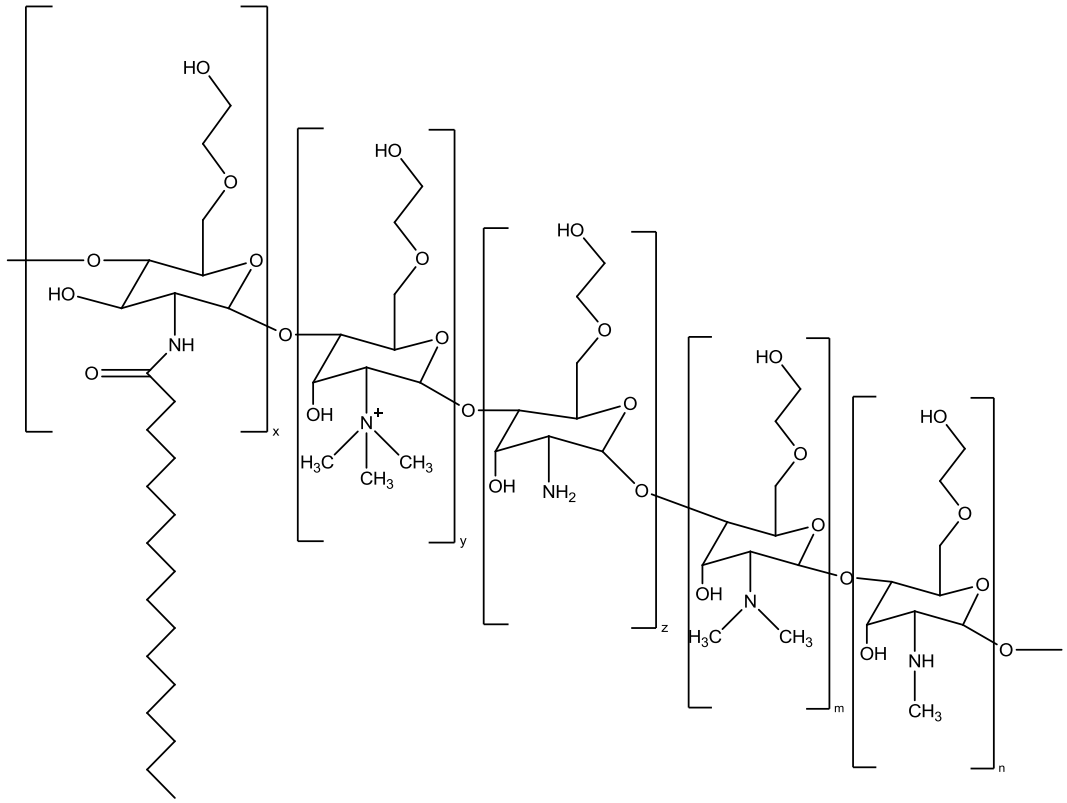

Figure 2.1 Chemical structure of GCPQ

Structure of GCPQ, x = GC units with hydrophobic palmitoyl group, y = GC units with trimethyl ammonium group (Quarternized ammomium), z = unmodified GC units, m and n = dimethyl and monomethyl ammonium groups formed during quaternization.

2.1.1.2 GCPh

GCPh is a new chitosan based amphiphile, in which the phenoxyacetamide ring contributes to the hydrophobicity of the polymer (Figure 2.2). Amphiphilic polymer forms self-assemblies in aqueous environment, with its hydrophobic group forming the core of the assembly. When a hydrophobic drug is added to this dispersion, the drug will either precipitate or aggregate within the core of the amphiphilic self-assembly forming colloidal particles of sizes in nanometer range. The principle behind the polymer self-assembly and the formation of hydrophobic nanoparticles can be explained as follows. When a hydrophobic moiety is dropped in an aqueous medium, the hydrogen bonds of the surrounding water molecules are broken to accommodate the hydrophobe[178]. This is an endothermic reaction as the water molecules do not interact with the hydrophobe and heat energy is used to break the hydrogen bonding of water molecules. The distorted water molecules form new hydrogen bonds surrounding the hydrophobe like a cage. But this affects the entropy of a system (ΔS), which becomes negative. According to the Gibbs free energy equation,

$$\Delta G = \Delta H - T\Delta S \qquad \text{(Equation 2.1)}$$

where ΔG is change in Gibbs free energy, ΔH is change in enthalpy, T is temperature and ΔS is change in entropy. A negative ΔS value means that the ΔG is positive, which means that the mixing of water molecules and the hydrophobe is thermodynamically unstable. To overcome this instability, the hydrophobic molecules start to interact among themselves, which results in the breakage of water cage formed around the hydrophobe. These liberated water molecules increase the entropy of the system and thus ΔS becomes positive. A positive ΔS ensures a negative ΔG, which means the system is now thermodynamically stable. Thus the liberation of water molecules during hydrophobic interactions is the key driver for polymer self-assembly and also the formation of drug – polymer nanoparticles[75,178].

The idea behind using a phenoxy ring is to exploit the aromatic interactions between the polymer's side chain and that of the drug, forming stable

nanoparticles. Aromatic interactions are considered to be the strongest of all hydrophobic interactions[179], which is due to the π-π stacking of the electrons in the π orbital. The interaction is further strengthened by the delocalisation of the electronic charge in an aromatic ring, which contributes towards London dispersion forces. Thus the hydrophobic interaction between two aromatic molecules would be stronger than the interaction between an aliphatic and aromatic molecule. Given that the most of the drug molecules contain aromatic ring in their structure, GCPh might form stable nanoparticles with those molecules.

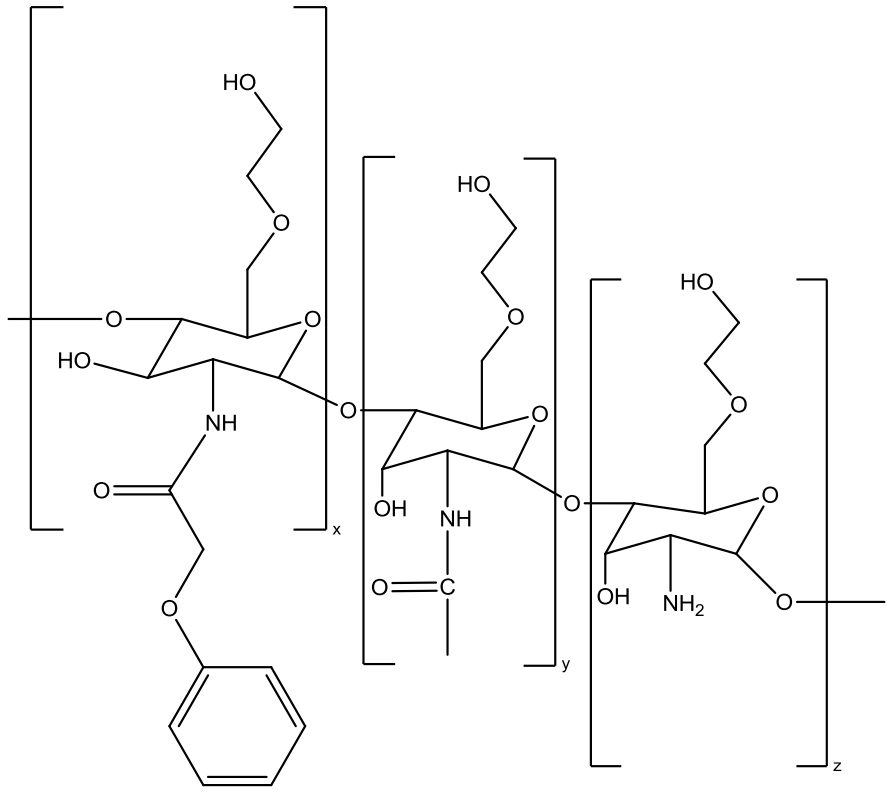

Figure 2.2 Chemical structure of GCPh

Structure of GCPh, x = GC units with hydrophobic phenoxy acetamide group, y = naturally acetylated GC units, z = unmodified GC units.

2.1.2 Characterisation methods

2.1.2.1 Nuclear Magnetic resonance:

Nuclear Magnetic Resonance (NMR) is a structure prediction tool, based on the observation that atomic nuclei behave like bar magnets when placed in a magnetic field. The atoms with an odd number of protons or neutrons have a

non-zero nuclear spin whereas atoms with an even number of protons and neutrons have a zero spin and NMR relies on non-zero nuclear spin (I) for structural prediction. ^{1}H and ^{12}C being the most common elements in organic molecules, studying their spin behaviour will help us to predict a molecule's structure[180]. But ^{12}C has a zero nuclear spin and hence its naturally occurring isotope ^{13}C is studied for structural prediction. Both ^{1}H and ^{13}C have a spin I = ½ and can align in 2I+1 ways or just in 2 ways when applied a magnetic field, a low energy orientation aligned with applied field or higher energy orientation opposed to the applied field (Figure 2.3).

So, the nucleus of an atom aligns when in a magnetic field and at a particular frequency they change their orientation from lower energy to higher energy, which is called as resonance frequency for that atom. Once the resonance pulse is over, the nuclei return to their low energy state with a release of energy and a receiver coil picks up these minute energy responses, which are documented for structural determination. The resonance frequency is dependent on both the nature of the nuclei and applied field strength, which means an independent nucleus, will always have the same resonance frequency. But in a complex molecule there are many neighbouring atoms, whose nuclear magnetic field will influence the alignment of other nearby nuclei causing them to resonate at a different frequency. The influence of one atom over another has been extensively studied and it is this information that is particularly valuable for structural determination[180,181].

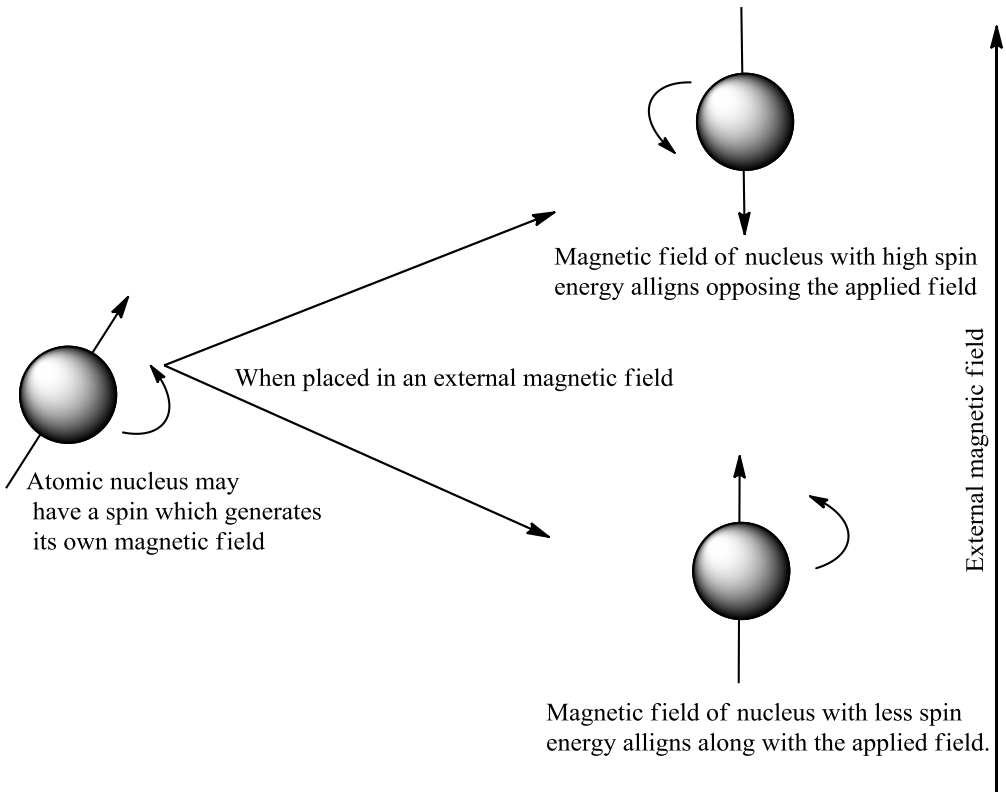

Figure 2.3 Nuclear magnetic spin (I=1/2) pattern with an external magnetic field.

The presence of electron withdrawing atoms (O, N), π bonds and high electron density, will all have an impact on the resonance frequency and will result in different chemical shifts (δ). The chemical shift of an atom is the difference between the resonance frequency of the atom in analysis and that of a reference standard, usually tetramethylsilane (TMS), which has an arbitrary assigned shift of $\delta=0$[181]. These chemical shifts are generally recorded, as peaks in the NMR spectrum and the relative area under these peaks are directly proportional to the number of protons giving rise to the signal. The test samples are dissolved in a solvent that does not give rise to the signals on its own. Deuterated solvents such as D_2O, $CDOD_3$, C_6D_6, d_6-DMSO etc. are usually used for this purpose.

For complex organic molecules, complete spectrum assignment is not possible with one-dimensional NMR alone, so two-dimensional techniques like Correlation Spectroscopy (COSY), Nuclear Over Hauser Effect Spectroscopy (NOESY), etc. are developed. In COSY, the connectivity of a molecule is probed by determining which protons are spin-spin coupled. These complex NMR techniques provide scope for accurate prediction of a molecule's structure.

2.1.2.2 Fourier Transform Infrared Spectroscopy (FTIR)

Infrared spectroscopy is a rapid, convenient and non-destructive method for characterisation of a molecule. When a range of infrared frequencies is passed through a molecule, some of the frequencies get absorbed and the rest are transmitted unchanged. The absorption is because of the energy transfer between the covalent bonds in a molecule and the infrared (IR) frequencies and this energy transfer changes the vibrational status of the chemical bonds involved. The energy transfer occurs only at a certain frequency called the resonance frequency, where the frequencies of the natural vibration of the molecule and the infrared radiation match. As a result of this the vibration of the chemical bonds are amplified and this generates an IR spectrum unique for the molecule. An important criterion for molecules to absorb infrared frequencies is that there should be a net change in its dipole moment. A dipole moment arises when there is a difference in electron densities around the atoms involved in the bonding. As the bond vibrates, the atomic charge differences in the dipole create an electrical field. This field will interact with the electrical field associated with the IR radiation and if the resonance frequency is matched the molecular vibration is amplified. When the molecules lacks a dipole moment, there will be no interaction with the electrical field of IR radiation and thus the molecule will be IR inactive[180].

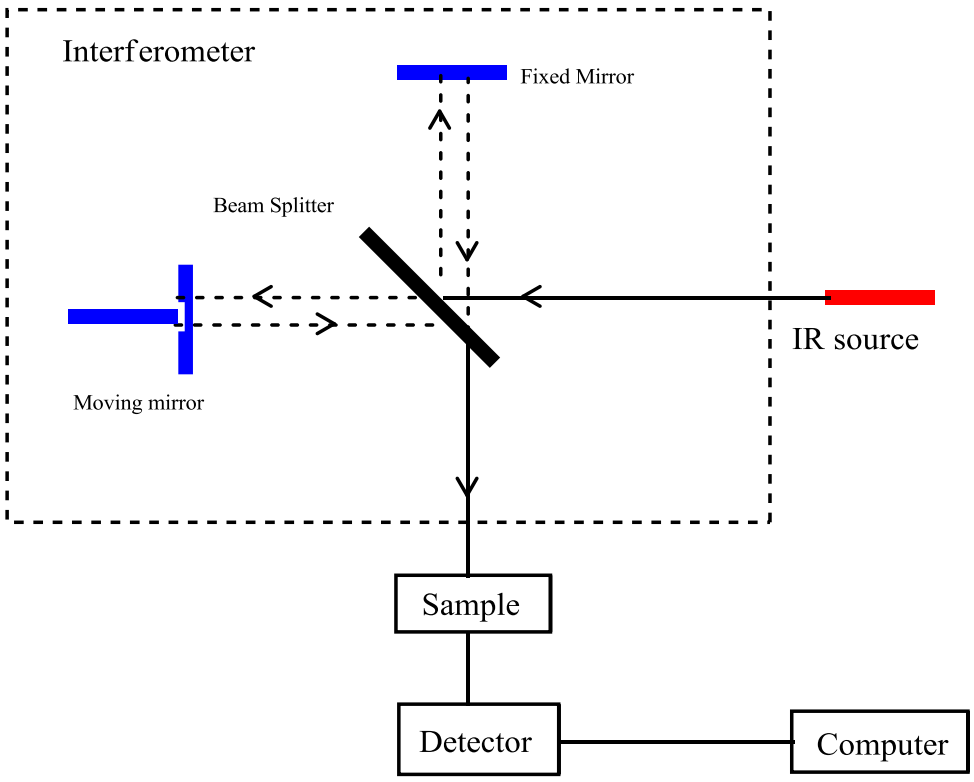

Figure 2.4 Instrumentation of FTIR

In FTIR, the sample of interest is placed on a dais and the IR beam is shone on it (Figure 2.4). The IR beam is initially split into two in an interferometer using a beam splitter and a fixed mirror reflects one of the beams while the other beam is reflected in a movable mirror. By adjusting the position of the movable mirror, a path difference is created between the two laser beams, which are later combined together in the interferometer and shone on a sample. The intensity differences in the IR radiation before and after striking the sample were monitored using a suitable detector within the interferometer and the signal is Fourier transformed to yield the IR spectrum.

2.1.2.3 Gel Permeation Chromatography-Multi-angle Laser Light Scattering (GPC-MALLS)

Gel Permeation Chromatography (GPC) is a size exclusion chromatographic technique, which separates molecules based on size (molecular mass and hydrodynamic radius). The GPC columns are packed with porous beads of

different pore sizes and molecules with large hydrodynamic radii can't pass through these pores and thus elute quickly. Whereas molecules with radii that fit the pores pass through these pores, which hinders their movement and they elute later. So molecules with high molecular weight (M_w) elute first followed by molecules with lower molecular weights in a descending order[182].

The eluted molecules are monitored using a Multi-Angle Laser Light Scattering (MALLS) detector, which works on the principle of Rayleigh scattering. When a monochromatic light of certain intensity is incident on a solution, the solute molecules scatter some portion of light elastically (same intensity as that of incident light) in different directions according to the concentration, size and shape of the solute molecules. The scattered light is monitored using various detectors set at different angle and this information is used to calculate the M_w[183]. But the light scattering information alone will not give us accurate molecular weight.

Absolute measurements of molecular weight are possible when the concentration, refractive index (η) and differential refractive index increment $d\eta/dc$ values are known[184]. For this purpose, a differential Refractive Index (dRI) detector is connected in line with the GPC-MALLS. If the concentrations of solutes in a solution are known, it is possible to calculate the values for η and $d\eta/dc$ from which the exact M_w can be calculated from the following equations.

$$K_c/R_\theta = 1/M_w + 1/M_w \left(16\pi^2/3\lambda^2\right) \sin^2(\theta/2) (< r >_z)^2 + A_2 c \qquad \text{(Equation 2.2)}$$

where, c is solute concentration; R_θ is the Rayleigh ratio; M_w, the weight-averaged molecular weight; λ, the wavelength of incident light; θ, π, the scattering angle; $<r>_z$, the z-averaged mean radius of gyration and A_2, the second virial coefficient, which quantifies the interaction between the macromolecule and the solvent. K_c is given by equation

$$K_c = \frac{2\pi^2\eta^2 \left(\frac{d\eta}{dc}\right)}{N_0\lambda^4} \quad \text{(Equation 2.3)}$$

where, N_o is the Avogadro's number; η, the refractive index and $d\eta/dc$, the change in refractive index per unit change in solute concentration.

2.2 Aims and objectives:

The aim of this chapter is to synthesize amphiphilic polymers by hydrophobic modification of glycol chitosan for drug delivery. One of the main objectives is to synthesise and characterise a new amphiphilic polymer with phenoxyacetamide group as the hydrophobic moiety.

2.3 Materials and methods:

2.3.1 Materials

Chemical	Purity	Supplier
1-Methyl-2-pyrrolidone	99%	Sigma-Aldrich (Gillingham, UK)
Acetic acid		VWR BDH Prolabo (Fontenay-sous-Bois, France)
Acetonitrile HPLC grade	≥ 99.5%	Fisher Scientific (Loughborough, UK)
Amberlite IRA-96, free base, 20-50 mesh		Sigma-Aldrich (Gillingham, UK)
Deutrium oxide		Sigma-Aldrich (Gillingham, UK)
Diethyl ether	≥ 99.5%	Sigma-Aldrich (Gillingham, UK)

Chemical	Purity	Supplier
DMTMM	≥ 96%	Sigma-Aldrich (Gillingham, UK)
Ethanol (absolute)	99.7-100%	UCL School of Pharmacy
Glycol chitosan	≥ 60%	Sigma-Aldrich (Gillingham, UK)
Hydrochloric acid	36.5-38%	VWR BDH Prolabo (Fontenay-sous-Bois, France)
Iodomethane, reagent plus	99%	Sigma-Aldrich (Gillingham, UK)
Methanol-D4	99.80%	Cambridge Isotope Laboratories, Goss Scientific Instruments Ltd. (Worleston, Nantwich, UK)
N-Methylmorpholine	≥ 99.5%	Sigma-Aldrich (Gillingham, UK)
Palmitic acid N-hydroxy succinamide ester	98%	Sigma-Aldrich (Gillingham, UK)
Phenoxyacetic acid	98%	Sigma-Aldrich (Gillingham, UK)
Sodium acetate anhydrous	≥ 99%	Sigma-Aldrich (Gillingham, UK)
Sodium bicarbonate	≥ 99.5%	Sigma-Aldrich

Chemical	Purity	Supplier
		(Gillingham, UK)
Sodium hydroxide	99.13%	Sigma-Aldrich (Gillingham, UK)
Sodium iodide	≥ 99.5%	Sigma-Aldrich (Gillingham, UK)
Visking dialysis membranes with a cut-off of 3.5, 7, 12-14 kDa		Medicell International LTD (London, UK)
Water deionised		Millipore Elix-Progaard 2
Water double deionised	<18 ohm	Millipore Synergy-Simpak1

2.3.2 Methods

2.3.2.1 Synthesis of Quaternary Ammonium Palmitoyl Glycol Chitosan (GCPQ)

GCPQ was synthesized as previously described[174] and a brief outline of the protocol is as follows. Please refer to Figure 2.5 for schematic representation of GCPQ synthesis.

Acid Degradation of Glycol Chitosan

Glycol chitosan (10 g) was degraded by dissolving it in hydrochloric acid (4 M, 760 ml) and incubated on a pre-heated water bath at 50°C. Separate batches of degradation were set, where the batches were degraded for 2 hours, 24 hours and 48 hours to get GC2, GC24 and GC48 respectively. Variations in degradation time will give rise to degraded glycol chitosan with different molecular weights (approximate estimation) as shown in Table 2.1. After the reaction time, the product was isolated by exhaustive dialysis

against water using dialysis membrane with a molecular weight cut-off (MWCO) of 3500 Da. The degraded glycol chitosan was recovered as cream-coloured cotton-wool-like solid.

Table 2.1 Relationship between degradation time and molecular weight of GC

Final (GC) molecular weight (Da)	GC degradation time (h)
80000 – 120000	0 (undegraded GC)
35000 – 45000	2
10500 – 12000	24
6500 – 8500	48

Palmitoylation of degraded Glycol Chitosan

N-palmitoyl-6-O-glycol chitosan (PGC) was synthesized by dissolving degraded GC (6 g) and Sodium bicarbonate (4.585 g) in a mixture of water (912 mL) and absolute ethanol (288 mL), to which was added drop-wise a solution of Palmitic acid N-hydroxysuccinamide ester (PNS, 9.65 g) dissolved in absolute ethanol (1830 mL) over a period of 1 hour. PGC with different degrees of palmitoylation could be obtained by modifying the GC to PNS molar ratio and drop-rate of PNS (Table 2.2). The mixture was stirred for a period of 72 hours and the product was isolated by removing the excess of ethanol by evaporation and the remaining aqueous phase was extracted with thrice the volume of diethyl ether. The aqueous mixture of PGC was the exhaustively dialysed (MWCO = 12-14 kDa) against water (5 L) for a period of 24 hours with six changes of water. The resultant product was freeze - dried and the PGC was recovered as white cotton-like solid.

Table 2.2 Relationship between molar ratio and drop-rate on palmitoylation of GC

GC48 (mg)	PNS (mg)	Ethanol (mL)	Drop rate (mL min^{-1})	Temperature (°C)	Expected %P (%)
500	792	150	8 – 11	20	16 – 18
	792		12 – 15		24 – 28
	1984		12 – 15		35 – 50
	396		6 – 8		9 – 12
	198		2 – 4		3 – 5

Quarternisation of PGC

GCPQ was synthesized from PGC (7 g) by dispersing it in N-Methyl-2-Pyrrolidone (590 mL) for minimum of 2 hours. An ethanolic suspension (5 mL) of sodium hydroxide (944 mg), sodium iodide (1062 mg) and methyl iodide (10.38 mL) were added and the reaction mixture was stirred under a stream of nitrogen at 36°C. GCPQ with varying degrees of quarternisation can be obtained by varying the reaction time and also by altering the methyl iodide volume. The GCPQ was recovered by adding excess of diethyl ether and the precipitate was washed with copious amount of absolute ethanol. The resulting brown hygroscopic precipitate was dissolved in 100 mL of water and the solution was dialysed exhaustively (MWCO 7000 Da) against water (5 L) for 24 hours with six changes of water. The quaternary ammonium iodide salt was passed through a column (Amberlite IRA, 10 cm in length) and the straw coloured, fibrous, cotton wool like GCPQ is recovered from the resultant filtrate by freeze-drying.

Deprotonation of GCPQ:

GCPQ was deprotonated by dialysis of an aqueous suspension of GCPQ (3.5 g in 100 mL of water) against a dialysate (5 L) containing sodium chloride (0.1 M) and sodium bicarbonate (0.01 M) for 4.5 hours with three changes of the salt solution. The GCPQ solution was then exhaustively

dialysed against water (5 L) for 24 hours with six changes of water and the deprotonated GCPQ was collected by freeze-drying.

2.3.2.2 Storage stability of GCPQ

Samples of GCPQ were stored dry in sealed amber bottles at room temperature for 36 months. At various time intervals, samples were withdrawn and analysed by ^{1}H NMR and GPC-MALLS, to monitor any changes in polymer characteristics during storage.

2.3.2.3 Synthesis of Phenoxy Glycol Chitosan (GCPh):

High molecular weight Palmitoylated Glycol Chitosan (GCPh) was synthesized from GC2 by dissolving GC2 (500 mg) in a mixture of water and absolute ethanol (1:1, 50 mL). Phenoxyacetic acid (125 mg) was dissolved in absolute ethanol (100 mL) and added drop-wise at the rate of 5 mL min^{-1} to the GC2 solution, followed by N-Methylmorpholine (100 µL) and 4-(4,6-Dimethoxy-1,3,5-triazin-2-yl)-4-methylmorpholinium chloride (DMTMM, 1660.32 mg). The reaction was carried out at room temperature for 5 hours in an uncapped vessel and the product was isolated by evaporating most of the ethanol and extracting the remaining aqueous phase with diethyl ether (3x100 ml). The aqueous mixture of the polymer was exhaustively dialyzed against water (MWCO 12-14 kDa) and the resultant product was freeze-dried to get Phenoxyacetic glycol chitosan (GCPh) as a fibrous solid.

2.3.2.4 Characterisation of the amphiphiles

2.3.2.4.1 ^{1}H and COSY NMR spectroscopy

In a vial, the polymer (2 mg for proton NMR, 20 mg for Carbon NMR) was dissolved in of suitable solvent (0.6 mL, dissolve DGC in D_2O; PGC, GCPQ and GCPh in CD_3OD). A drop of deuterated acetic acid may be added to solubilise the polymer if necessary. Then the solution was transferred to a clean NMR tube and analysed for ^{1}H NMR proton shifts using the Bruker AMX 400 MHz spectrometer, Bruker instruments, UK.

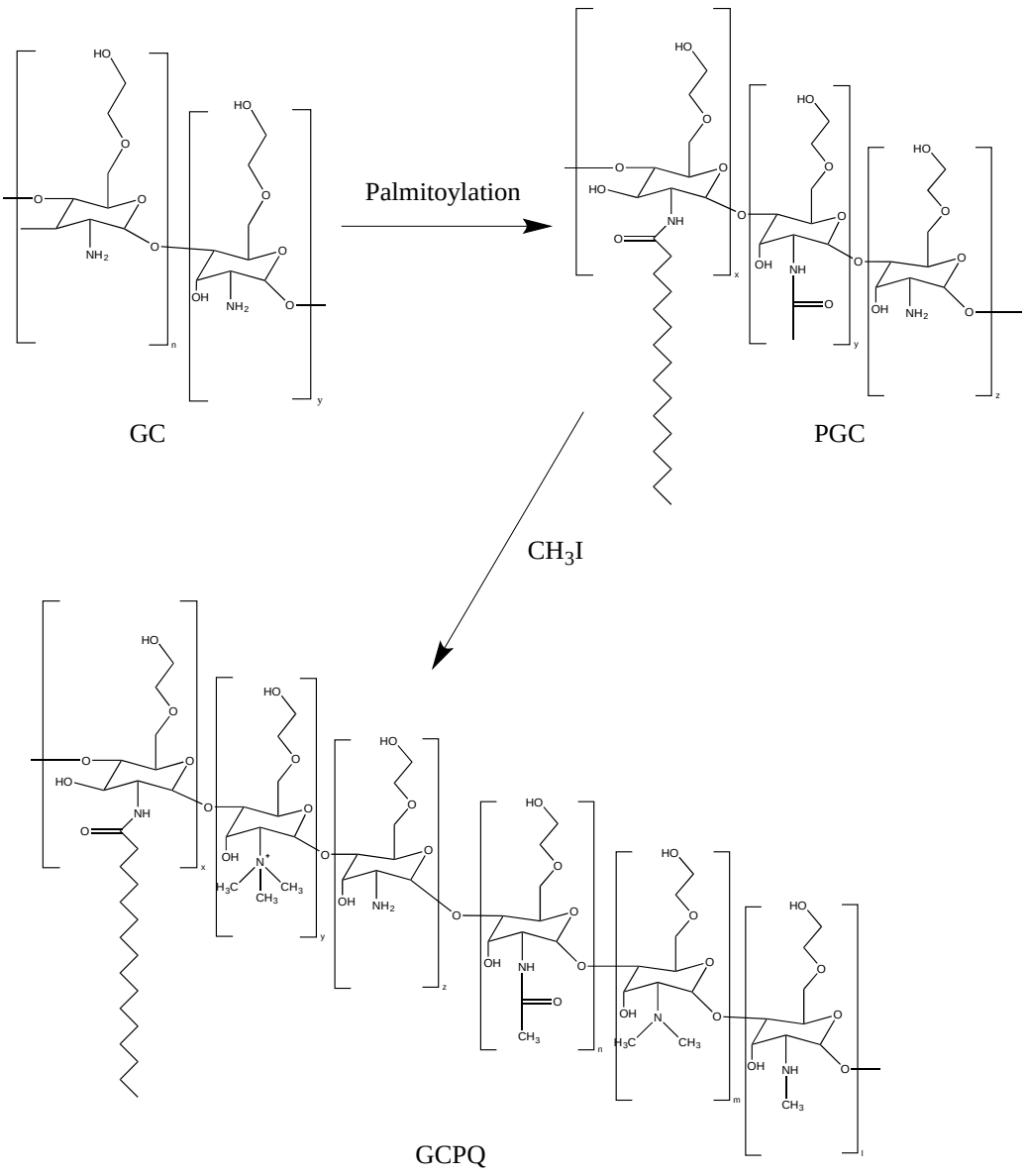

Figure 2.5 Schematic representation of synthesis of GCPQ

The spectra obtained were processed and analysed using the Topspin software for windows. Phenoxylation, Palmitoylation and quarternisation percentages were calculated from the spectrum by taking the ratio of respective peaks against sugar proton peaks and multiplying the quotient by 100.

$$\%\, modification = \frac{area\ of\ modified\ peak/number\ of\ protons}{area\ of\ sugar\ protons\ /number\ of\ sugar\ protons} \times 100 \qquad \text{(Equation 2.4)}$$

2.3.2.4.2 Gel Permeation Chromatography - Multi-angle Laser Light Scattering (GPC-MALLS)

Gel Permeation Chromatography (GPC) coupled with Multi Angle Laser Light Scattering (MALLS) detector and a differential Refractive Index (dRI) detector enables us to accurately measure the molecular weight of the polymer produced. The detectors used were 120 mW solid-state laser (wave length, λ_{658} nm) DAWN® HELEOSTM II MALLS detector and Optilab rEX Interferometric Refractometer (dRI) detector, which were supplied by Wyatt Technology Corporation, USA. MALLS detector was also coupled to Quasi Elastic Light Scattering (QELS) detector supplied by Wyatt Technology Corporation. GPC was performed using POLYSEPTM-GFC-P 4000 column (300 x 7.8 mm) protected by a POLYSEPTM-GFG-P guard column (35 x 7.8 mm) as stationary phase. The columns were from Phenomenex, Cheshire, UK and the mobile phase was fed to the column using a HPLC system assembled with Agilent Series Isocratic pump coupled with Agilent 1200 series degasser and auto sampler that are all supplied by Agilent Technologies, Berkshire, UK.

The mobile phase (500 mM, Acetate buffer) was prepared by dissolving anhydrous sodium acetate (24.6 g) and glacial acetic acid (11.4 mL) in double deionised milli-Q water (1 L). The buffer was filtered using a 0.2 μm PES filter (Millex-HA, Millipore) before passing it in the HPLC system. To determine the molecular weight of GC and DGC, acetate buffer is used, whereas for GCPQ and GCPh, 35:65 volume-by-volume ratios of acetate buffer and methanol were used. This is to prevent the self-aggregation of GCPh/GCPQ micelles in the aqueous media.

Specific refractive index increments over concentration ($d\eta/dC$) were measured by, manually injecting a series of standard solutions of the polymer at different concentrations (0.1 to 0.6 mg mL^{-1}), dissolved in an appropriate mobile phase, through the dRI detector set at 25°C and a wave length of 658 nm and a pump flow rate of 0.3 mL min^{-1}.

GPC-MALLS experiments were performed by injecting a known concentration of the polymer (5 mg mL^{-1}) in an appropriate solvent through the GPC column and analysing the eluent using MALLS detector and dRI detector at a flow rate of 0.7 mL min^{-1} and a run time of 20 minutes. The data obtained from both $d\eta/dC$ and GPC-MALLS experiment were analysed using the ASTRA software for Windows, version 5.3.4.14 supplied by Wyatt Technologies.

2.3.2.4.3 CMC measurements:

The heats of demicellization of GCPh were measured using an ITC200 MicroCalorimeter (MicroCal, LLC, Northampton, MA USA). The sample cell was filled with degassed ultrapure water. Concentrated polymer samples were loaded into a syringe (17.35 µM / 1 mg mL^{-1}, 40 µL), and at 120 s intervals, polymer samples (2 µL) were injected into the sample cell and the heat flow was measured as a function of time. The syringe was rotated at 1000 rpm to enable even mixing throughout the experiment. Data analysis was carried out using the MicroCal Origin version 7.0 Software. Each titration experiment was carried out at room temperature (25 °C).

2.4 Results

2.4.1 Degradation and characterisation of GC:

Different batches of GC were degraded and characteristics documented as shown in Table 2.3. The 48 hours-degraded GC was designed as GC48, where the suffix ‘48’ represents the time duration in hours for which the degradation was carried out, while the 24 hours and 2 hours degraded GC was labelled GC24 and GC2 respectively. The degraded GC was then characterised using NMR and GPC-MALLS. From the table, it can be seen that the molecular weight of the GC is inversely proportional to the duration of degradation. Thus the GC of required molecular weight can be obtained by adjusting the degradation time accordingly.

From the NMR (Figure 2.6), the proton spectrum was assigned to DGC as follows[180]: ^{1}H NMR [D_2O], $\delta_{2.02}$ = [$C\boldsymbol{H_3}$−CO−NH−, acetylated glycol chitosan], $\delta_{2.6}$ = (−CH(OH)−C***H***(NH_2)−, glycol chitosan), $\delta_{2.7}$ = (−CH−C***H***−NH−CO−,

glycol chitosan), $\delta_{3.4-4.2}$ = [−C***H***(OH)− and −C***H***$_2$−OH, glycol chitosan], $\delta_{4.4}$ = water, $\delta_{5.2\text{-}5.5}$ = (O−C***H***−O anomeric proton). Yield of GC48 ~ 6.2 g (62 %); GC2 ~ 8.1 g (81 %).

2.4.2 Characterisation of Palmitoyl GC (PGC):

The proton NMR characterisation of PGC (Figure 2.7) is as follows; ^{1}H NMR [CD_3OD]: $\delta_{0.9}$ [t, C***H*****$_3$**−$(CH_2)_{14}$−CO−, palmitoyl], $\delta_{1.25}$ [m, CH_3−(C***H*****$_2$)$_{12}$**−CH_2−CH_2−CO−, palmitoyl], $\delta_{1.50}$ [CH_3−$(CH_2)_{12}$−C***H*****$_2$**−CH_2−CO−, palmitoyl], $\delta_{2.00}$ [C***H*****$_3$**−CO−NH−, acetyl glycol chitosan], $\delta_{2.20}$ [CH_3−$(CH_2)_{12}$−CH_2−C***H*****$_2$**−CO−, pamitoyl], $\delta_{3.1}$ (−CH−C***H***−NH−CO−, glycol chitosan), $\delta_{3.3}$ = methanol, $\delta_{3.6-4.2}$ = [−C***H***(OH)− and −C***H***$_2$−OH, glycol chitosan], $\delta_{4.4\text{-}5.5}$ = water and (O−C***H***−O anomeric proton) (Figure 2.3.1.2). Percentage of Palmitoylation (P %) was calculated from Equation 3 and found to be 27.35 %. Yield ~ 7.19 g (45.9 %).

Table 2.3 Characteristics of degraded GC

	M_n (Da)	**M_w (Da)**	**M_w/M_n (polydispersity)**
GC	87630	129800	1.481
GC2	40260	102600	2.548
GC2	47780	58090	1.216
GC24	11740	16050	1.368
GC48	5526	6618	1.198

2.4.3 Characterisation of GCPQ:

The GCPQ was synthesized from PGC and labelled along with their manufacturing dates and the initials of chemist who synthesized it. For example, Q48 101111SR means, the GCPQ is from 48 hours degraded GC and was synthesised on 10th of November 2011 by a chemist with initials 'SR'. This type of nomenclature was followed to label all the polymers for identification purposes.

Table 2.4 summarizes the characteristics of different batches of GCPQ synthesized. Protonated and deprotonated GCPQ with varying degrees of palmitoylations and molecular weights were successfully synthesized and characterized. The proton NMR characterization of GCPQ (Figure 2.8) is as follows;

^{1}H NMR [CD3OD]: $\delta_{0.9}$ = [C***H***$_3$−$(CH_2)_{14}$−CO−, palmitoyl], $\delta_{1.3}$ = [CH_3−(C***H***$_2)_{12}$−CH_2−CH_2−CO−, palmitoyl], $\delta_{1.60}$ = [CH_3−$(CH_2)_{12}$−C***H***$_2$−CH_2−CO−, palmitoyl], $\delta_{2.02}$ = [C***H***$_3$−CO−NH−, acetylated glycol chitosan], $\delta_{2.20\text{-}2.40}$ = [CH_3−$(CH_2)_{12}$−CH_2−C***H***$_2$−CO−, palmitoyl], $\delta_{2.7-3.2}$ = [−CH−CH−NH−C***H***$_3$− and −CH−CH−N(C***H***$_3)_2$, monomethylamino and dimethylamino glycol chitosan], $\delta_{3.3}$ = methanol, $\delta_{3.4}$ = [−CH−CH−N(C***H***$_3)_3$, trimethylamino glycol chitosan], $\delta_{3.6-4.4}$ = [−C***H***(OH)− and −C***H***$_2$−OH, glycol chitosan], $\delta_{4.8}$ = water, $\delta_{5.20}$ = (O−C***H***−O anomeric proton) (Fig 2.3.1.3). For the main batch of polymer, the Palmitoylation percentage (P%) and quarternisation percentage (Q%) were calculated to be 18.23 % and 8.94 % respectively. Yield = 4.82 g (68.8 %).

Table 2.4 Characteristics of GCPQ batches

Polymer name	Palmitoylation (P %)	Quarternisation (Q %)	M_n (Da)	M_w (Da)	PD
Q48 100413SR*	18	5	8710	10830	1.24
Q24 050213 SR	18	6	14060	16440	1.17
Q2 090313 SR	11	11	44140	48130	1.09
Q2 220213 SR	19	13	63830	70130	1.1
Q48 091111SR*	35	11	6500	7058	1.08

Polymer name	Palmitoylation (P %)	Quarternisation (Q %)	M_n (Da)	M_w (Da)	PD
Q48 080612 SR	31	7	5950	8630	1.45
Q48 150812 SR	6	11	9200	9750	1.06
Q48 070313 SR	14	26	9180	9210	1.01
Q48 101111 SR	18	9	8670	9470	1.091
Q48 240114 SR	5	5	9420	10040	1.065
Q48 290110 KS	20	9	8710	10830	1.24

*deprotonated polymer; PD = polydispersity

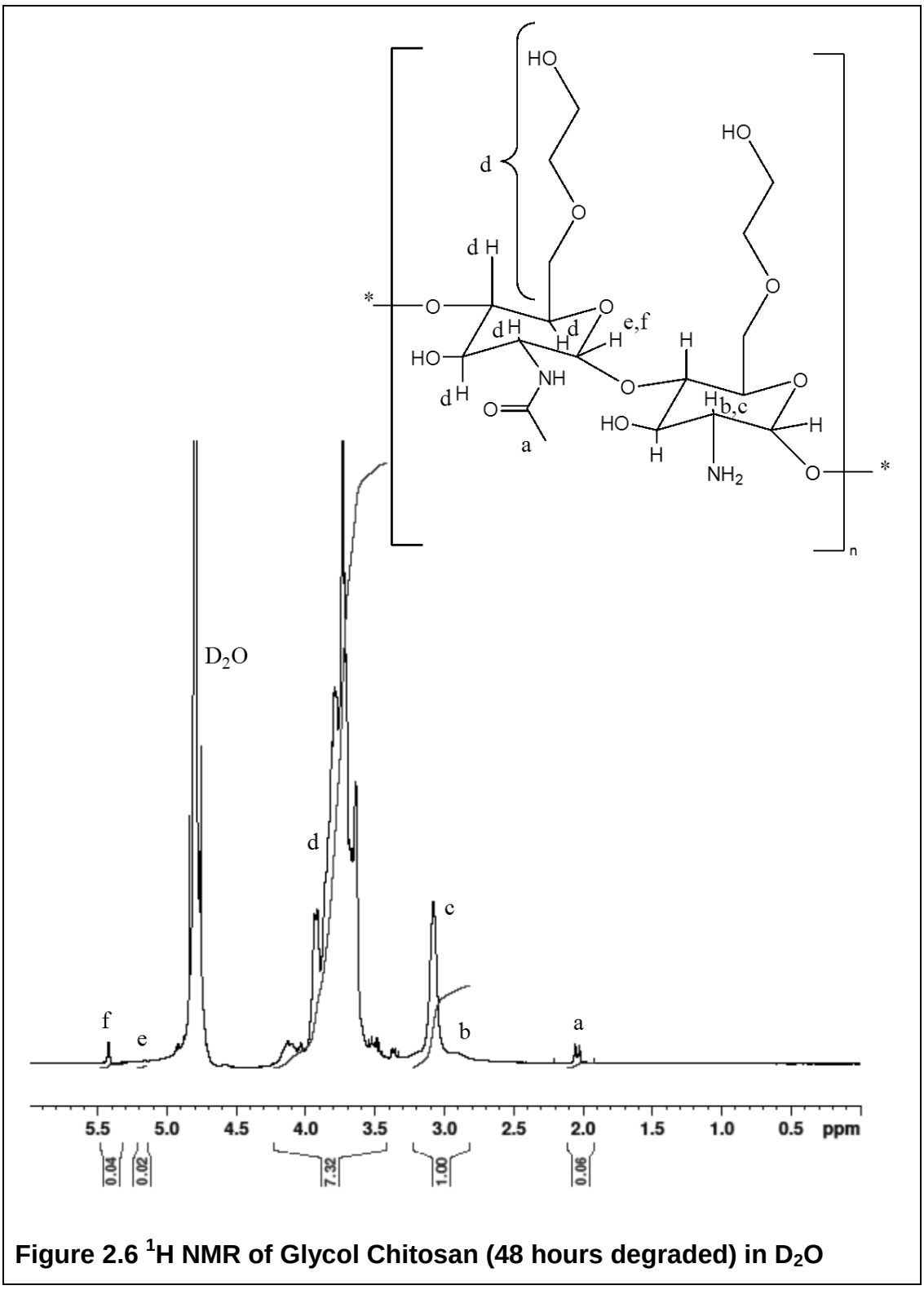

Figure 2.6 ^{1}H NMR of Glycol Chitosan (48 hours degraded) in D_2O

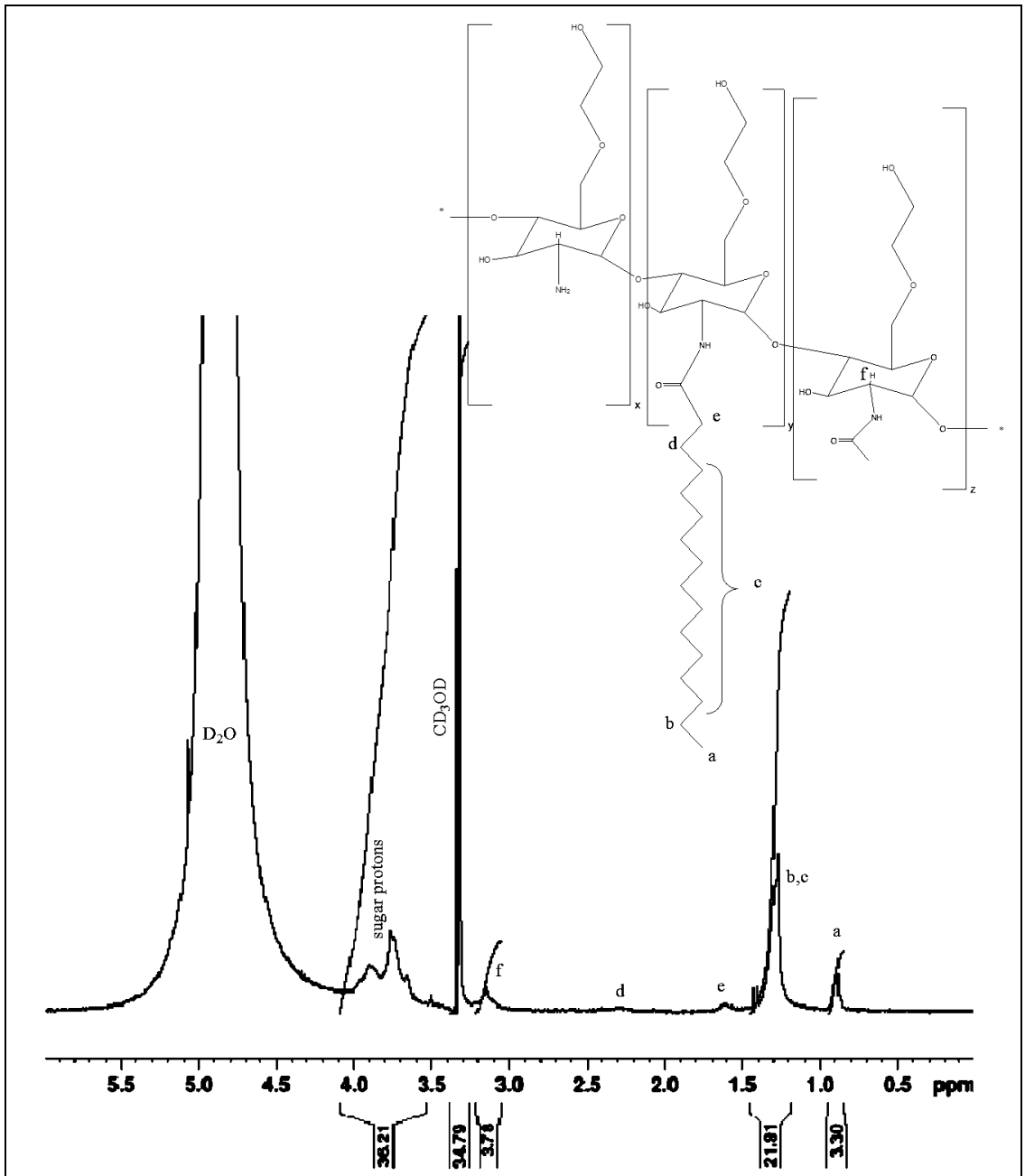

Figure 2.7 ^{1}H NMR spectrum of Palmitoylated Glycol Chitosan (PGC) in CD_3OD

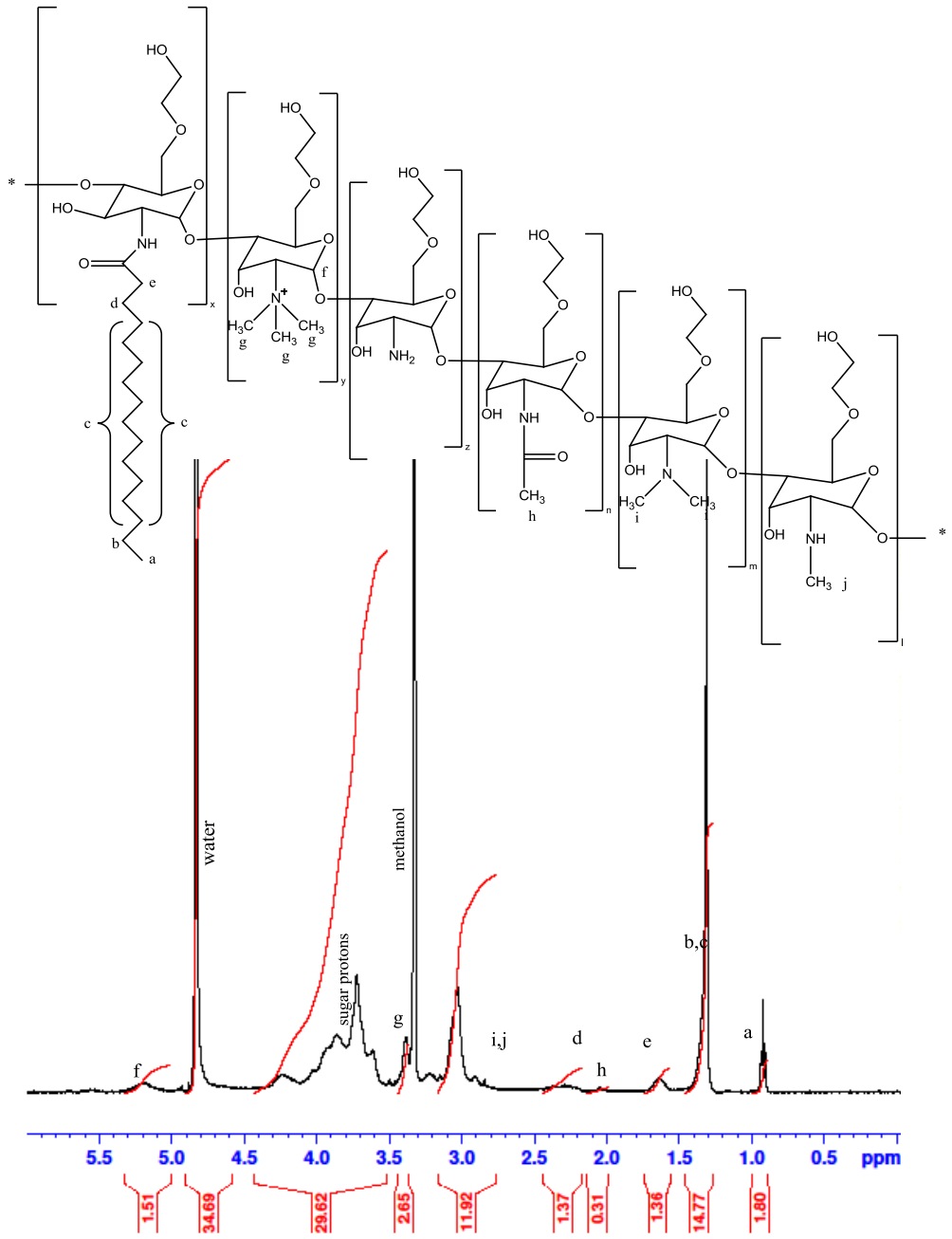

Figure 2.8 ^{1}H NMR spectrum of Quaternary Ammonium Palmitoyl Glycol Chitosan (GCPQ) in CD_3OD.

2.4.4 Stability studies on GCPQ:

GCPQ when stored at room temperature is stable for 18 months (Table 2.5). At month 24 there is a notable change in the M_w data with the M_w doubling, although the M_n data remains unchanged. This data provides evidence of chain cross-linking. The reason for the change in M_w is not clear and warrants further study. It should also be noted that the experiments were done on only one batch of GCPQ (n = 1). Hence, a detailed study should be carried out on different batches of GCPQ with more replicates.

Table 2.5 Long-term storage stability of GCPQ (Q48 101111 SR)

Months	M_w (Da)	M_n (Da)	PD	Q%	P%
0	9400	8680	1.091	8.94	18.23
3	9670	7400	1.306	9.44	19.33
6	9250	9230	1.003	9.54	18.32
9	11020	9960	1.107	8.33	18.76
12	9220	8500	1.085	10.11	17.9
18	10500	10210	1.032	11.25	17.4
24	22030	10800	2.041	10.93	19.41
36	28290	8743	3.236	10.51	18.65

P% = palmitoylation percentage; Q% = quaternization percentage

2.4.5 Characterisation of Phenoxyacetic GC (GCPh 2):

The covalent conjugation of phenoxy acetic acid to glycol chitosan chain was confirmed by the presence of signals for the carboxamide functional group in both FTIR spectrum (Figure 2.9) and ^{13}C NMR spectrum (Figure 2.11). The primary amines in the sugar unit react with the carboxylic acid group of phenoxyacetic acid in th

e presence of the coupling agent DMTMM in basic conditions to form the carboxamide functional group, which covalently links phenoxy acetic acid to glycol chitosan. Additionally, the fingerprint signals for the aromatic ring were also found on ^{1}H NMR spectrum (Figure 2.10) further confirming the

synthesis of Phenoxyacetic glycol chitosan. Yield of the reaction was approximately 0.521 ± 0.046 g (~84 %). The GCPh thus synthesized was thoroughly characterized as follows (Table 4).

^{1}H NMR (CD_3OD): $\delta_{2.05}$ = [s, C***H*****$_3$**−CO−NH−], $\delta_{2.7-3.2}$ = [b, −CH−C***H***−NH^{+}_3], $\delta_{3.30}$ = solvent, $\delta_{3.50-4.40}$ = (−C***H***−O), $\delta_{4.50-5.00}$ = (solvent, O−C***H***−O anomeric carbon), $\delta_{7.05}$ = [m, O-C-C***H***-CH-CH-CH-C***H***- (ortho protons in the phenoxyacetamide ring)], $\delta_{7.4}$ = [m, O-C-CH-C***H***-C***H***-C***H***-CH- (meta and para protons in the phenoxyacetamide ring)]. The level of Phenoxylation was calculated by comparing the ratio of phenyl protons ($\delta_{7.05}$) to sugar methine/methylene protons ($\delta_{3.5 - 4.4}$). Phenoxylation levels of 18-22 % were consistently achieved.

^{13}C NMR – δ_{50} = solvent (methanol), $\delta_{60 - 80}$ = [R_3***C***H in sugar unit], $\delta_{110 - 130}$ = [aromatic carbons], δ_{158} = (−***C***O−NR). The presence of peak at δ_{158} corresponds to the amide group that was formed due to the reaction of phenoxyacetic group with the primary amines in the glycol chitosan.

FTIR spectrum of GCPh was assigned as follows[180]. ν (cm^{-1}) = 3364 (O-H stretch), 2918 and 2851 (C-H stretch), 1648 (C=O amide stretch), 1599, 1547, 1493 (C-C aromatic stretch).

Table 2.6 Characteristics of GCPh batches

Polymer batches	**Phenoxylation (%)**	**M_n (Da)**	**M_w (Da)**	**PD**
GCPh 110513 SR	23	44280	49070	1.108
GCPh 021013 SR	18	39810	51650	1.298
GCPh 020314 SR	21	56330	67030	1.19

PD = Polydispersity

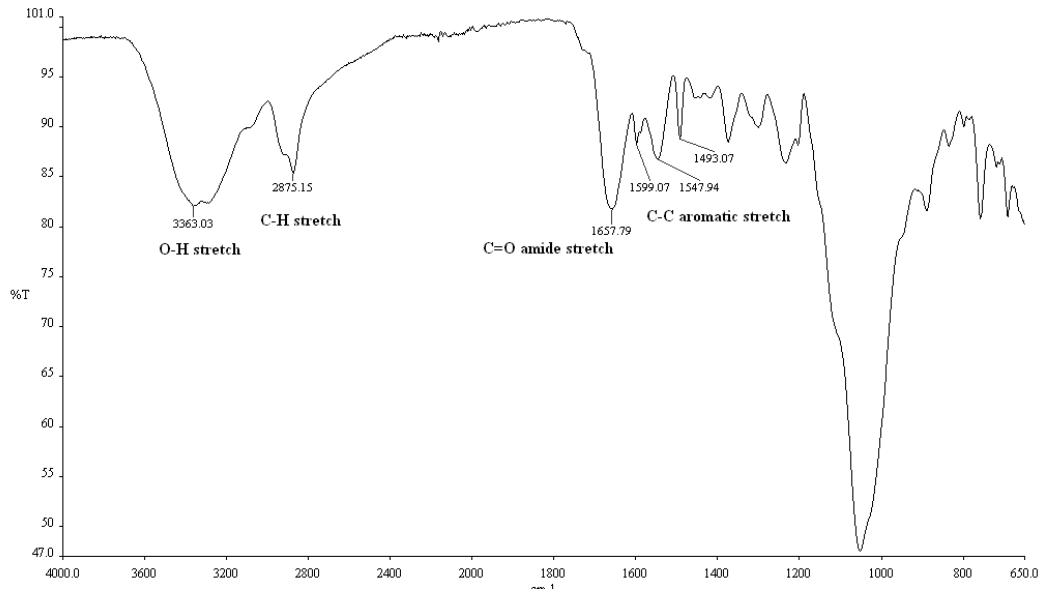

Figure 2.9 FTIR spectrum of GCPh

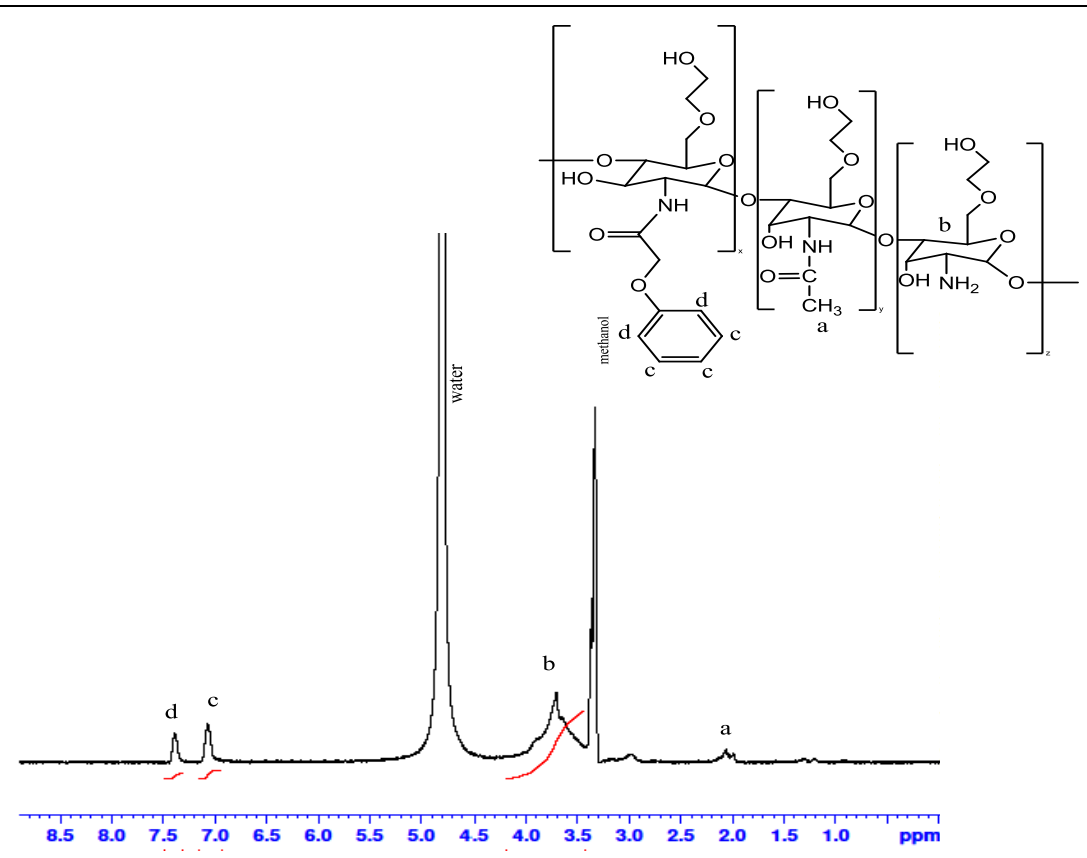

Figure 2.10 ^{1}H NMR of Phenoxyacetic glycol chitosan in CD_3OD.

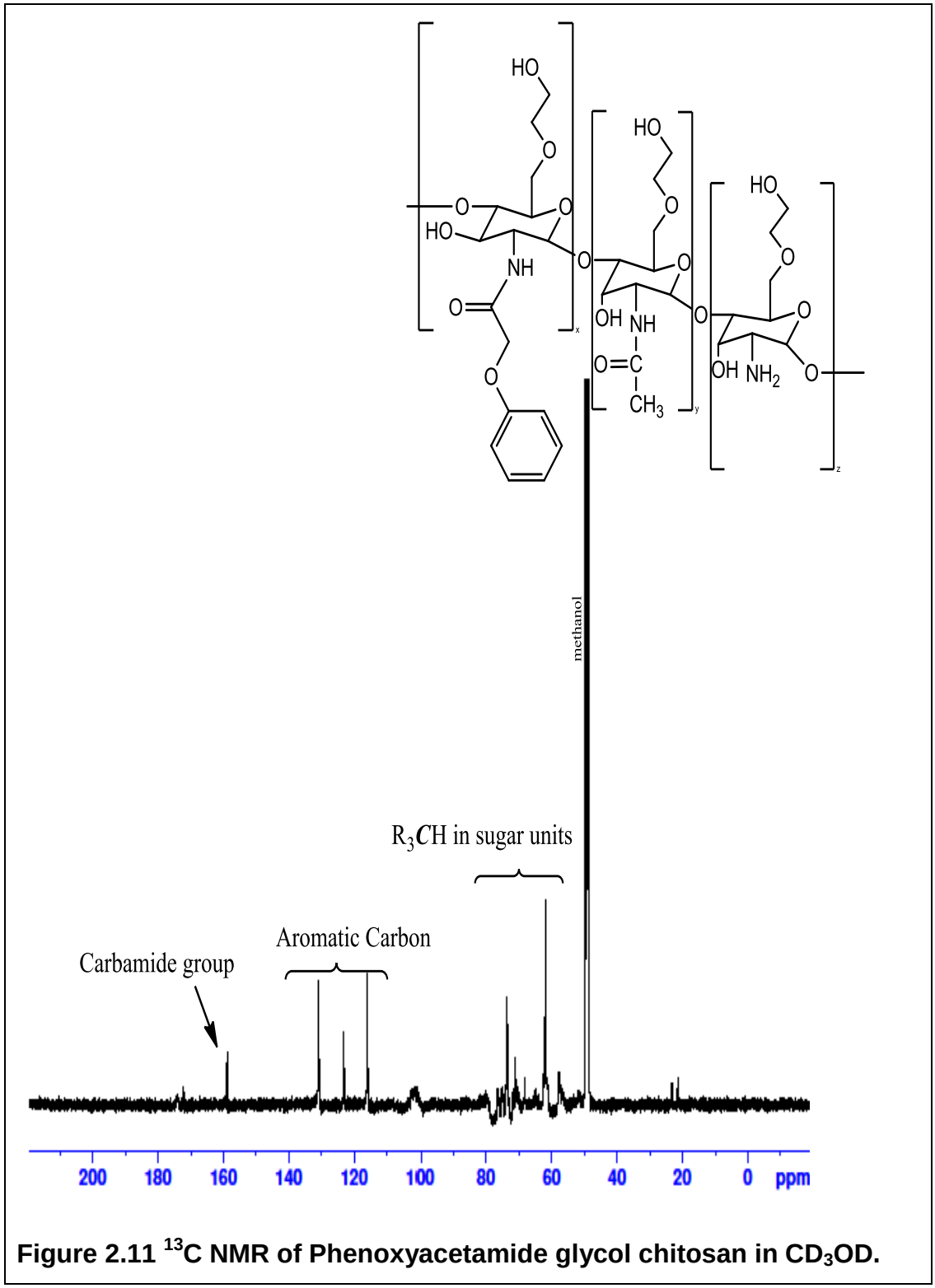

Figure 2.11 ^{13}C NMR of Phenoxyacetamide glycol chitosan in CD_3OD.

2.4.6 CMC measurements

The CMC of the GCPh polymer was measured using Isothermal Calorimetry (ITC) and was found to be 0.3 ± 0.025 µM (Table 2.7 and Figure 2.12). ITC is a probe free method to estimate the CMC and has been previously shown to be the most reliable method for CMC measurements[185]. This extremely low CMC value would facilitate the formation extremely stable self-assemblies in aqueous environment, which would enable the formulation to resist disintegration upon dilution in the gastro-intestinal tract. The low CMC value of GCPh is due to the presence of hydrophobic pendant group, which presents a large hydrophobic surface to the aqueous medium. The self-assembly is driven by the entropy gain enjoyed by the liberated water molecules on contact with hydrophobic surfaces of the polymer. The entropy gain on micellization experienced by GCPh polymer ($T\Delta S_{mic}$ = + 314 kJ mol^{-1}) exceeds that of GCPQ ($T\Delta S_{mic}$ = + 37 kJ mol^{-1})[75] and DAB – GCPQ claw shaped amphiphile of similar molecular weight ($T\Delta S_{mic}$ = + 280 kJ mol^{-1})[186]. This exceptionally high $T\Delta S$ value would result in extremely stable self-assembly. The CMC values of GCPh are at least 100 folds lesser than that of GCPQ (6 – 100 µM) and at least 10 folds higher than DAB-GCPQ, which is mainly due the differences in the molecular weight and the hydrophobicity of the polymer[186].

Table 2.7 Critical Micellar Concentration and thermodynamics of GCPh

Polymer	M_w (Da)	CMC (mM)	ΔG_{mic} (kJ mol^{-1})	ΔH_{mic} (kJ mol^{-1})	$T\Delta S_{mic}$ (kJ mol^{-1})
GCPQ[75]	12,195	1.9 x 10^{-2}	- 36.9	+ 0.96	+ 37.9
GCPh*	49,070	3.2 ± 0.25 x 10^{-4}	- 43.5 ± 0.68	+ 272 ± 32	+ 315 ± 31
DAB-GCPQ[186]	33,000	1.3 x 10^{-5}	- 55	+ 225	+ 280

*Values expressed as mean ± Standard deviation. n = 3.

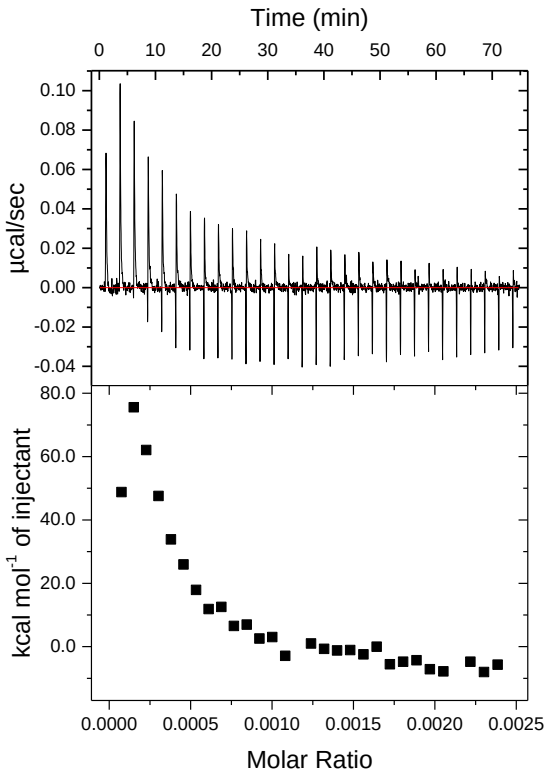

Figure 2.12 Dilution enthalpogram for an aqueous dispersion of GCPh

2.5 Discussion:

Chitosan has been extensively studied in recent years as a drug carrier because the polymer is more amenable to chemical modification, apart from being cheap, non-toxic and mucoadhesive, all of which makes it an ideal candidate for drug delivery research[187]. Chitosan itself is poorly water-soluble and the addition of glycol moiety to the sugar units, overcame the poor aqueous solubility of chitosan polymer. This modified chitosan (Glycol Chitosan) is hydrophilic and the presence of free primary amines provides scope for further chemical modifications[188]. Various amphiphilic chitosan derivatives were synthesized out of chitosan by hydrophobically modifying the polymer[189] and GCPQ is one such polymer with pendent palmitic acid groups attached to the GC chain. The palmitoyl chain provides certain degree of hydrophobicity, the presence of charged quaternary ammonium rendered high aqueous dispersibility, while low acetylation levels and low

molecular weight accounts for less toxicity[174]. GCPQ has been previously shown to self-assemble at low CMC values and also facilitated absorption for hydrophilic and hydrophobic drugs through, oral and ocular routes[75].

A variety of GCPQ molecules were synthesized with different palmitoylation and quaternisation percentages. The characteristics were conformed using ^{1}H NMR experiments and the palmitoylation levels varied between 5 – 35 %, while the quaternisation levels were 9 – 26 % for different batched of GCPQ. The molecular weight of the GCPQ ranged between 7 – 70 kDa, which was measured using GPC-MALLS. It was possible to synthesis GCPQ with different characteristics by altering the molar ratio of the reactants and other reaction parameters as mentioned in Table 2.1 and Table 2.2. Long-term storage stability studies suggested that the GCPQ synthesized is has a shelf life of 18 months after which the M_w of the polymer doubled. The synthesis and characterization of GCPQ has been previously reported on a number of occasions but this is the first instance where the storage stability of dry polymer has been reported.

Phenoxyacetic glycol chitosan (GCPh) is an amphiphilic polymer, where the hydrophobic phenoxyacetamide moiety is attached to a hydrophilic GC backbone. The presence of phenoxy ring will facilitate stronger π-π interactions with hydrophobic drugs containing aromatic ring thus forming stable nanoparticles. While most of the chitosan-based amphiphiles have linear hydrophobic units, GCPh has a phenolic ring, which might be advantageous with certain hydrophobic drugs[189,190]. The synthesis of GCPh molecule was confirmed using ^{1}H, ^{13}C NMR and FTIR spectroscopy. The presence of carboxamide signals in the spectrum is a strong indication for the chemical conjugation. The phenoxylation levels of the polymers ranged from 18 – 22 % and molecular weight ranged between 50 – 70 kDa. The CMC of GCPh was calculated using the ITC and was found to be around 0.3 μM.

In the literature different synthetic routes are mentioned to synthesise amphiphiles from chitosan as summarised in Table 2.8. Most of the synthetic steps involve the use of toxic solvents such as methanol, toluene, pyridine and DMF. Care should be taken to ensure the complete removal of solvent

residue from the final product to reduce the toxicity issues. It is to be noted that the synthesis of GCPh involves only the use of ethanol, which is relatively safe and can be easily evaporated from the reaction mixture. Also, the synthesis of GCPh is a one step reaction and altering the molar ratio of the reactants involved could control the degree of hydrophobic substitution, as observed with GCPQ and other chitosan amphiphiles.

The CMC of GCPQ and GCPh are 6 – 100 µM and 0.3 µM respectively. The CMC values of these amphiphiles are within the range of CMC values reported for other chitosan amphiphiles of similar molecular weight. While the method for CMC calculation in Table 2.8 is predominantly done by pyrene probe based fluorescent spectroscopy, our method of CMC calculation is done by probe-free ITC, which measures the changes in the enthalpy on demicellization (ΔH_{mic}) and other basic thermodynamic parameters such as binding affinity and binding stoichiometry. These measurements are then used to calculate the change in Gibbs free energy (ΔG_{mic}) and the change in entropy (ΔS_{mic}), from which the critical micellar concentration is calculated. Thus CMC calculations from ITC are considered to be more accurate and reliable[185] as basic thermodynamic parameters are used to calculate the CMC, without any interference from a fluorescent probe (pyrene).

Table 2.8 List of chitosan amphipihiles as mentioned in the literature

Name of the Amphiphile	Reaction steps	Solvents used	Reactants	Degree of substitution (%)	CMC (μM)	Molecular weight (kDa)
N-octyl-O-sulphate chitosan[191,192]	N-octylation of chitosan	Methanol	Octaldehyde	0.38	0.45	1000*
	O-Sulfonation of chitisan	DMF	Chlorosulfonic acid	2.56		
PpIX – conjugated GC[193]	Coupling of PpIX to GC	DMSO	Protoporphyrin IX, N-hydroxysuccinamide (NHS), EDC	4.24 ± 0.23	Not available	250#
O-carboxymethyl chitosan[194]	O-carboxymethylation of chitosan	Isopropanol	Monochloroacetic acid	100	0.096	520*

Name of the Amphiphile	**Reaction steps**	**Solvents used**	**Reactants**	**Degree of substitution (%)**	**CMC (μM)**	**Molecular weight (kDa)**
GCPQ[75,176]	N-Palmitoylation	Ethanol	PNS	1.2 – 23	6 – 100	4 – 19
	N-methylation	NMP	Methyl iodide	2.7 – 13.8		
GCPh	N-phenoxylation of GC	Ethanol	Phenoxyacetic acid, NMM, DMTMM	18 – 23	0.318	49 – 67
Anacardoylated chitosan[195]	N-anacardoylation of chitosan	DMF, thionyl chloride, Pyridine	Anacordic acid, acetic anhydride	Not available	Not available	196*
O-carboxymethylated chitosan – deoxycholic acid[196]	N-deoxycholation of O-carboxymethyl chitosan	DMSO, methanol	Deoxycholic acid	3.6 – 6.9	0.31 – 0.76	85*

Name of the Amphiphile	**Reaction steps**	**Solvents used**	**Reactants**	**Degree of substitution (%)**	**CMC (µM)**	**Molecular weight (kDa)**
N-deoxycholic acid – N,O-hydroxyethyl chitosan[197]	N,O-hydroxyethylation	Acetic acid	Ethylene oxide	89.5 – 114	1.6 – 2.6	100*
	N-deoxycholate grafting	DMF	Deoxycholic acid	1.1 – 8.1		
Chitosan – arachidic acid conjugate[198]	Coupling of arachidic acid to chitosan	DMSO	Arachidic acid, EDC, NHS	~ 5	0.28	5
3-diethyl aminopropyl bearing GC[199]	Grafting of 3-diethyl aminopropyl isothiocyanate	DMSO, pyridine, triethylamine	3-diethyl aminopropyl isothiocyanate	95	0.024	250#
Lauroyl sulfated chitosan[200]	N-Sulfonation	Methanol	Sulfobenzoic acid	1.12	Not available	270*
	N-Lauroylation	Acetic acid	Lauryl chloride	23.07		

Name of the Amphiphile	**Reaction steps**	**Solvents used**	**Reactants**	**Degree of substitution (%)**	**CMC (µM)**	**Molecular weight (kDa)**
N-octyl-O-glycol chitosan[201]	N-octylation	Hexane	Octaldehyde	24.2 – 58.7	0.06 – 0.36	87[#]
	O-glycolation	Acetic acid	Ethylene oxide	102 – 105		
Oleoyl - Chitosan[202]	N-acylation of oleoyl chloride	Pyridine, chloroform	Oleoyl chloride	5 – 27	0.28 – 2.8	35[*]
Linolenic acid - chitosan[203]	Coupling reaction	Methanol	Linolenic acid, EDC	1.8	0.33	150[*]
N-cholanoyl-6-O glycol chitosan[204]	Coupling reaction	Methanol	5β-cholanic acid, EDC, NHS	1.1 – 11.5	0.2 – 0.8	250[#]
Deoxycholate chitosan[205]	Coupling reaction	Methanol	Deoxycholic acid, EDC	2.8 – 5.1	0.37 – 0.58	70[*]

Name of the Amphiphile	**Reaction steps**	**Solvents used**	**Reactants**	**Degree of substitution (%)**	**CMC (µM)**	**Molecular weight (kDa)**
Stearic acid grafted chitosan[206]	Coupling reaction	Ethanol	Stearic acid, EDC	9.79 – 63.4	1.33 – 5	3 – 18
N-succinyl-N'-octyl chitosan[207]	N-octlylation	Acetic acid	Octaldehyde	28.6 – 52.5	0.06 – 0.3	100*
	N-succinylation	Methanol	Succinic anhydride	14.7 – 39.1		

*Molecular weight of the chitosan starting material. #Molecular weight of the glycol chitosan starting material.

2.6 Conclusion

The amphiphilic polymers such as GCPQ and GCPh were synthesised and characterised. GCPQ with different molecular weight, palmitoylation and quaternisation levels were synthesized as previously mentioned by altering the reaction parameters. GCPh, a new polymeric amphiphile was also successfully synthesized and the covalent attachment of the phenoxyacetamide moiety was confirmed using NMR and FTIR. The following chapters focus on using these polymeric amphiphiles for the oral delivery of BCS Class IV drugs such as Paclitaxel and CUDC-101.

3 Oral delivery of paclitaxel

3.1 Introduction

Paclitaxel (PTX) is a BCS Class IV anticancer agent with poor aqueous solubility and poor gut permeability due to the drug being a substrate for P-gp efflux pump[171]. The oral bioavailability of paclitaxel is generally low and there are numerous publications on improving the bioavailability of paclitaxel through various strategies such as prodrugs[62], micelles[191,208], modulation of P-gp activity[209] etc. In this section, the use of GCPh, a new polymeric amphiphile to enhance the oral absorption of paclitaxel is discussed. The research was specially focused on deducing the link between the *in vivo* dissolution and the impact of P-gp efflux on the oral absorption of paclitaxel, as the activity of P-gp efflux pump and poor dissolution are the main reasons for poor absorption of paclitaxel[47].

3.1.1 Transmission Electron Microscope (TEM):

The principle of Transmission Electron Microscope (TEM) imaging relies on the ability of atoms to scatter a beam of electrons, which are focussed on a photographic film or phosphorescent screen to form an image[210]. The resolving power of TEM is 1000 times higher than that of an optical microscope and with modern technology it is possible to image even a particle of 0.5 nm in size[211]. The image contrast is higher when the electrons are scattered more and the electrons are scattered more if the atomic number of an atom is large. But since the majority of atoms in biological samples are of small atomic number (carbon, hydrogen, oxygen, nitrogen, phosphorous and sulphur), the samples are negatively stained with heavy metal salts such as lead acetate, uranyl acetate and osmium tetroxide, in order to improve the image contrast[210]. This means, the sample will appear as pale spots because of their poor electron scattering while the electron dense stained background will appear dark due to high electron scattering[210,211].

3.1.2 Reverse Phase-High Performance Liquid Chromatography (RP-HPLC):

High Performance Liquid Chromatography (HPLC) coupled with a UV detection is a commonly used analytical technique to quantify the concentration of a particular solute in a sample[212]. The various solutes are separated based on their polarity, i.e. hydrophilicity. There are two phases in HPLC; the stationary phase (column), where the solute binds and the mobile phase (fed by pump), which elutes the solutes from the column. In Reverse Phase-HPLC (RP-HPLC), the stationary phase is more hydrophobic and a gradient mixture of polar and organic (apolar) solvents make up the mobile phase[212,213]. The solutes effectively bind to the column and when a gradient of mobile phase is passed through the column, the polar compounds elute first. When the organic solvent content in the gradient increases the hydrophobic compounds start to elute with the most hydrophobic solute eluting later. If the solute has a UV chromophore, it can easily be detected using a UV detector attached inline. The intensity of the UV signal increases linearly with the concentration of the solute, which makes the quantification straightforward with the help of a standard curve.

3.2 Aims and Objectives

The aim of this chapter is to enhance the oral uptake of paclitaxel using GCPh nanoparticles. The objectives are as follows:

- Understand the role of dissolution in improving the absorption of paclitaxel.
- Understand the mechanism of action of GCPh nanoparticles.

The criteria of success for this project was established based on the objectives as follows:

1. To get GCPh-Paclitaxel nanoparticles that is as good as Taxol® in terms of absorption, if not better.
2. To improve the oral absorption of paclitaxel without using a P-gp inhibitor to an AUC value of 1000 ng.h mL^{-1} approx..

3.3 Materials and Methods

3.3.1 Materials

Chemical	**Purity**	**Supplier**
Acetonitrile HPLC grade	≥ 99.5%	Fisher Scientific (Loughborough, UK)
Pancreatin	~100%	Sigma-Aldrich (Gillingham, UK)
Texas Red - X succinimidyl ester		Invitrogen (Paisley, UK)
Paclitaxel		LC laboratories (MA, USA)
Verapamil		Sigma-Aldrich (Gillingham, UK)
Pepsin		Sigma-Aldrich (Gillingham, UK)
Phosphate buffer saline		Sigma-Aldrich (Gillingham, UK)
Potassium dihydrogen phosphate	99.5	Sigma-Aldrich (Gillingham, UK)
Sodium chloride	99.50%	Sigma-Aldrich (Gillingham, UK)
Sodium hydroxide	98.90%	Sigma-Aldrich (Gillingham, UK)
Trifluoro acetic acid	≥ 99.5%	Fluka Chemicals (Gillingham, UK)
Water double deionised	<18 ohm	Millipore Synergy-Simpak1

3.3.2 Methods

3.3.2.1 Preparation of paclitaxel formulations:

Paclitaxel GCPh nanoparticles: GCPh (40 mg, GCPh 110513SR) was dispersed in water (1.9 mL) and probe sonicated (QSonica, USA) for 10 minutes. Paclitaxel ethanol solution (0.1 mL, 40 mg mL^{-1}) was added to the pre-sonicated polymer dispersion (final concentration of 5% v/v ethanol) while probe sonicating the mixture on an ice bath for 10 minutes at an amplitude intensity of 10%.

Paclitaxel Taxol® nanoparticles: Commercial paclitaxel formulation, Taxol® was prepared by dissolving paclitaxel (6 mg) in a mixture of ethanol and cremophor EL (1:1, v/v, 1 mL). This solution was diluted to 2 mg mL^{-1} with water before administration. This formulation was used as a positive control to compare the performance of Paclitaxel GCPh nanoparticles.

RP-HPLC was performed using Agilent Technologies 1200 series chromatographic system, which consisted of a vacuum degasser, a quaternary pump, a standard and preparative auto-sampler, a column compartment with a thermostat and a variable wavelength UV detector. The flow rate was set at 1.5 mL min^{-1}, samples (10 μL) were chromatographed over a reverse phase column (Onyx Monolithic C18 column, 100 x 4.6 mm) fitted with a guard column maintained at 40 °C, and monitored for absorption at 227 nm wavelength. Samples were diluted in mobile phase [acetonitrile:water, 1:1] and analysed using a standard curve (y = 36.79x - 0.0857, r^2 = 0.998) with a concentration range of 0.1 - 1.0 μg mL^{-1}.

3.3.2.2 Characterization of paclitaxel formulations:

Photon Correlation Spectroscopy was used to measure the particle size and particle size distribution of the formulations. The instrument (Malvern Zetasizer 3000HSA, Malvern Instruments, UK.) was set at 25 ˚C at a wavelength of 633 nm and the data analyzed using the Contin method. Measurements were performed in triplicate. Transmission electron microscopy was performed using Philips/FEI CM120 Bio Twin (Philips, Netherlands). A drop of the formulation was dried on a copper TEM grid (300 mesh- Fomvar/ carbon coated) and stained with a drop of uranyl acetate (1% w/v, negative staining). Once dried, the samples were analysed under the TEM and the representative images were photographed and documented.

3.3.2.3 Dissolution testing of oral formulations

The paclitaxel formulations were diluted with water to a final concentration of 0.01 mg mL^{-1} paclitaxel. The diluted formulation (1.5 mL) was then placed in a dialysis bag (MWCO: 7000) and the whole bag was placed into 48.5 mL of simulated gastric fluid (SGF, pH 2) or simulated intestinal fluid (SIF, pH 6.8) and shaken at 125 rpm at 37 ˚C. Samples (0.5 mL) were withdrawn at specific time points and measured for drug content using Reverse Phase – High Performance Liquid Chromatography (RP-HPLC) as mentioned above.

3.3.2.4 Oral absorption studies:

The paclitaxel formulations were prepared as mentioned above. Prior to oral administration, all formulations were analysed by HPLC to determine the exact drug concentration for dose calculations. Male MF-1 mice weighing 22-35 g were fasted for 12 h prior to dosing and for a further 4 h thereafter. The mice had free access to water throughout the study. Paclitaxel formulations were administered at low (6.66 mg kg^{-1}), medium (10 mg kg^{-1}) and high doses (20 mg kg^{-1}) by oral gavage in the form of high dissolving formulations (GCPh paclitaxel nanoparticles or Taxol®). The doses were selected based on the literature references on Taxol® as suggested by other researchers[191]. Paclitaxel was administered in the absence or presence of the P-gp efflux pump inhibitor verapamil (40 mg kg^{-1}). Verapamil was chosen, as it is a well-known P-gp inhibitor used to enhance the bioavailability of Paclitaxel[47]. Blood samples were taken at various time intervals by cardiac puncture following the euthanasia of the mouse. Blood samples were centrifuged for 10 minutes at 1000 g and the isolated plasma (100 µL) was then mixed with internal standard solution (10 µL, 10 µg mL^{-1} 4-hydroxybenzoic acid n-hexyl ester in 50% acetonitrile) and ethyl acetate (1 mL). Standard solutions (10 µL, 0.1 – 20 µg mL^{-1} paclitaxel in 50% v/v acetonitrile in water) were added to the plasma in case of standard curve preparations. After vortex mixing for 1 minute, the mixture was centrifuged for 15 minutes at 10,000 g and then the organic layer (900 µL) was transferred to a clean tube and evaporated until dry. The residue was dissolved in 50% acetonitrile (90 µL) by vortex mixing for 1 minute, and centrifuged for 15 minutes at 10,000 g to obtain the supernatant, which was analyzed for paclitaxel content using RP-HPLC.

RP-HPLC was performed using an Agilent Technologies 1200 series chromatographic system, as mentioned above. The flow rate was set at 2 mL min^{-1}, samples (50 µL) were chromatographed over a reverse phase column (Onyx Monolithic C18 column, 200 x 4.6 mm) fitted with a guard column maintained at 40 °C, and monitored for absorption at 227 nm wavelength. Samples were diluted in mobile phase [36% v/v acetonitrile in water] and analysed using a standard curve (y = 36.79x - 0.0857, r^2 = 0.998) with a concentration range of 0.02 - 10.0 µg mL^{-1}.

3.3.2.5 Ex-vivo confocal laser scanning imaging:

GCPh was labeled with Texas Red (Invitrogen, U.K.) using the protocol supplied by the manufacturer. Texas red is a fluorescent marker used in histology but can also be used to study the cellular uptake of nanoparticles[75]. Briefly GCPh 110513SR (100 mg) was dissolved in sodium bicarbonate buffer (0.1 M, 10 mL). Texas Red-X succinimidyl ester (5 mg) was dissolved in DMSO (0.1 mL) and was slowly added to the GCPh solution with continuous stirring. The reaction mixture was incubated for 1 h at room temperature, and the reaction was stopped by adding freshly prepared hydroxylamine (1.5M, 0.1 mL) to the mixture. The hydroxylamine containing reaction mixture was incubated for a further 1 h at room temperature, exhaustively dialyzed (5 L with 6 changes over a period of 24 h, MWCO = 12−14 kDa) and purified using Amicon Ultra15 centrifugal filters (Millipore, UK) as follows. The GCPh-Texas red conjugate (50 mg) was dissolved in 60 % Methanol (50 mL). The solution was then acidified with HCl (1.5 mL, 4M) and centrifuged at 5000 g (Hermle, Germany) for 1 h using Amicon spin filter columns (MWCO = 10 kDa). This step was repeated twice with the retentate and the final retentate containing purified GCPh-TR conjugate was isolated by freeze-drying. The reaction and purification mixtures were protected from light throughout the whole process. A GPC−MALLS analysis was used to confirm the attachment of the fluorescent probe (Texas Red) to GCPh as well as to ensure complete removal of unreacted dye from the labelled polymer.

GCPh – Texas red (20 mg mL^{-1}, ~1 mL, 100 mg kg^{-1}) in distilled water was dosed to male Wistar rats (weight = 200−250 g) by oral gavage and after two hours animals were euthanized and their small intestines harvested. The small

intestine was divided into three sections, the duodenum (up to ~8 cm from the stomach), jejunum (the next ~30 cm) and ileum (the next ~20 cm). The jejunum was flushed with phosphate buffered saline (PBS, 50 mL, 10 mM) and then sealed at one end with a knot, filled with OCT and then sealed at the other end with a knot. The samples were frozen by placing it in an eppendorf tube and dipping in iso-pentane dry ice mixture. This procedure was carried out as quickly as possible (i.e. within 10 min) to avoid the tissue deterioration. The frozen intestinal samples were then cut to remove the knotty ends and prepared for sectioning. The tissues were sectioned into thin slices (30 *μ*m) using a cryostat (LeicaCM1850) set at −25 °C. The slices were placed on poly-Lysine microscope adhesion slides and fixed with freshly prepared paraformaldehyde (4% w/v) in PBS (pH = 7.4). The slides were soaked in PBS for 10 min and a drop of Vectashield® Hardset™ mounting medium with DAPI stain (10 µL) was added on to tissue slices and sealed with a cover slip. Slides were imaged using a Zeiss LSM 710 laser scanning confocal microscopy imaging system, equipped with an argon ion laser and HeNe laser (LASOS Laserteknik GmbH, Carl Zeiss, UK) and linked to a Fujitsu Siemens computer with the Zen 2009 version 5.5.0.451 software (Carl Zeiss, UK). (Red fluorescence excitation wavelength= 561 nm, blue fluorescence excitation wavelength = 405 nm).

3.3.2.6 Statistical Analysis:

Statistical significance was tested with one-way and two-way analysis of variance (ANOVA) using GraphPad Prism 5 statistical software. For multiple comparisons, Post-Hoc tests such as Bonferroni's or Tukey's were used.

3.4 Results

3.4.1 Preparation of paclitaxel formulation

Paclitaxel – GCPh nanoparticles were formed by probe sonicating an ethanolic solution of paclitaxel with GCPh dispersed in water (Figure 3.1). GCPh self-assembles to form micelles in an aqueous environment. The encapsulation of paclitaxel within the GCPh is facilitated due to hydrophobic interactions between the drug and the polymer self-assembly. The phenyl group of GCPh will interact with the aromatic rings of paclitaxel through π-π stacking, which is the strongest of the hydrophobic interactions and thus forms stable

nanoparticles with the drug. These polymeric nanoparticles will have the drug encapsulated in its molecular form, which might facilitate high dissolution rate and enhanced absorption. The sizes of these nanoparticles are in the range of 183 ± 36 nm. Similarly, commercially available Taxol® formulation was prepared by dissolving paclitaxel in a mixture of ethanol and Cremaphor EL, a surfactant. The paclitaxel – Taxol® nanoparticles are formed when this solution is diluted with water, as the cremaphor EL molecules form self-assemblies in water, encapsulating paclitaxel in the process. But the size of the Taxol® nanoparticles (~ 10 nm) are very much smaller than the GCPh nanoparticles because the small molecular weight, amphiphilic cremaphor EL forms micelles while the GCPh forms amorphous drug loaded nanoparticles.

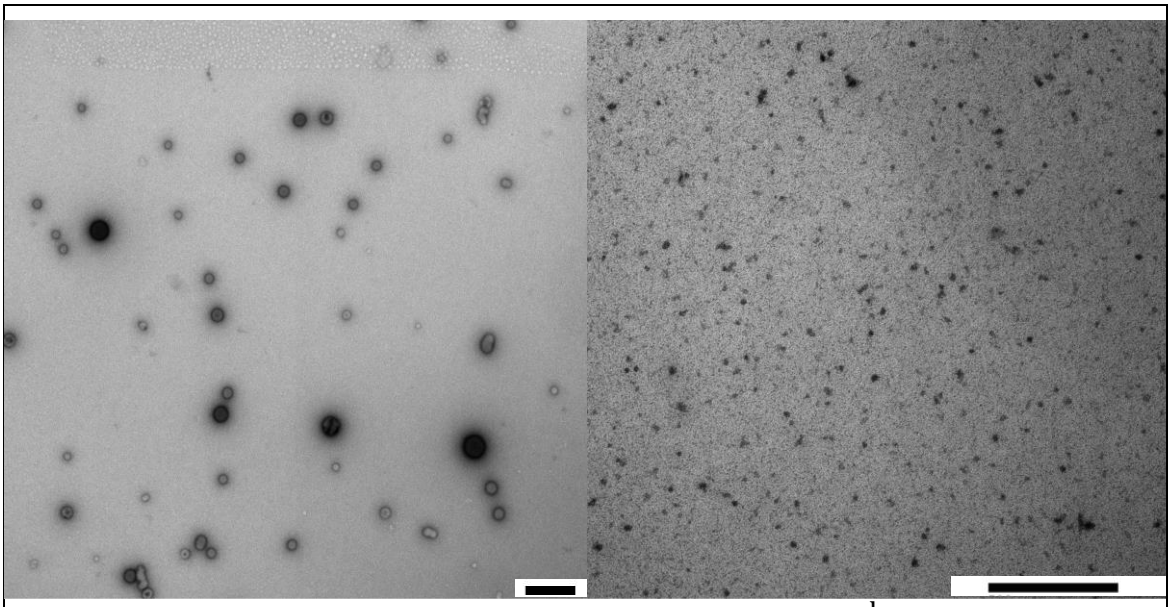

a b

Figure 3.1 TEM images of Paclitaxel formulations

a) GCPh nanoparticles and b) Taxol nanoparticles. Scale bar = 500 nm.

3.4.2 Dissolution testing of oral formulations

Dissolution of the paclitaxel formulations in SGF and SIF are given in Figure 3.2. The dissolution of paclitaxel GCPh nanoparticles and Taxol® nanoparticles is very rapid in SGF owing to the small particle size and molecular form of the drug inside the nanoparticle. The dissolution of Taxol® nanoparticles is significantly slow in SIF when compared to that of the GCPh nanoparticles. The

rapid dissolution of GCPh nanoparticles in both the simulated fluids might improve the *in vivo* absorption of the paclitaxel.

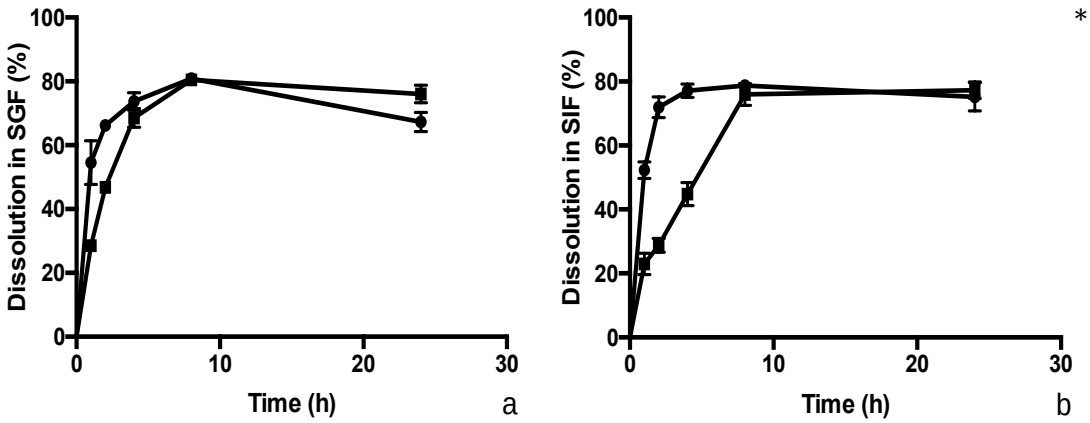

Figure 3.2 Dissolution of Paclitaxel formulations

a) SGF and b) SIF; Paclitaxel formulated as (●) GCPh nanoparticles; (■) Taxol® formulation. * Dissolution of Paclitaxel from Taxol® significantly different from that of GCPh nanoparticles in SIF (Two-way ANOVA, $p < 0.001$, $n = 3$).

3.4.3 Pharmacokinetic studies of oral formulations

Preliminary pharmacokinetic studies were carried out for both the formulations at three different doses; high (20 mg kg^{-1}), medium (10 mg kg^{-1}), and low (6.66 mg kg^{-1}). The formulations were also administered with and without verapamil for all the doses (Figure 3.3). These results highlight the importance of dissolution in the oral absorption of hydrophobic drugs, where dissolution of the drug in the physiological medium is the rate-limiting step for the absorption of these drugs. The absorption of paclitaxel from Taxol® and GCPh nanoparticles are similar which is strongly attributed to the rapid dissolution and molecular form of the drug being encapsulated within these nanoparticles (Figure 3.3a).

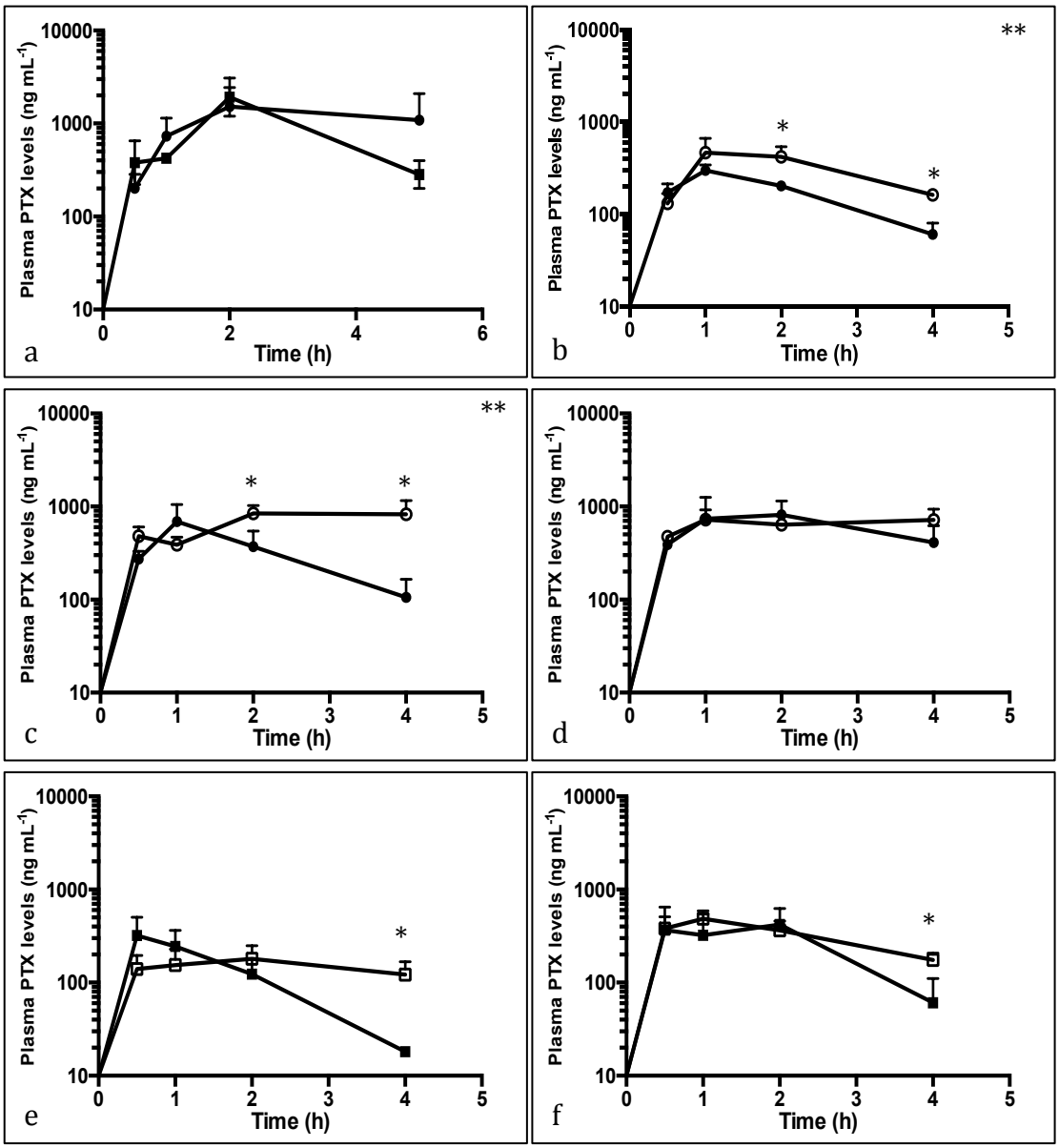

Figure 3.3 Plasma paclitaxel levels following the oral administration of paclitaxel formulations

Paclitaxel dosed as (■) GCPh nanoparticles (-) verapamil; (❑) GCPh nanoparticles (+) verapamil; (●) Taxol® formulation (-) verapamil; (○) Taxol® formulation (+) verapamil at different doses of paclitaxel. (a) Taxol® and GCPh nanoparticles without verapamil at 20 mg kg^{-1}. (b – f) Plasma paclitaxel levels following the oral administration of paclitaxel formulations with and without verapamil at various doses of paclitaxel as Taxol® at (b) 6.66 mg kg^{-1}; (c) 10 mg kg^{-1}; (d) 20 mg kg^{-1}; GCPh nanoparticles at (e) 6.66 mg kg^{-1} and (f) 10 mg kg^{-1}; Verapamil dose = 40 mg kg^{-1}. ** PTX plasma levels of formulation with verapamil significantly different from the formulation without verapamil. * PTX plasma levels significantly different at that time point. (Two-way ANOVA with Tukey's test $p < 0.05$, n = 4, error bars represent standard deviation).

Table 3.1 AUC of paclitaxel formulations at different doses

Formulation	Dose (mg kg^{-1})	$AUC_{0-4\ h}$ (ng h mL^{-1})	
		without verapamil	with verapamil
Taxol® formulation	6.66	633	1176
	10	1246	2502
	20	2284	2333
GCPh nanoparticles	6.66	467	544
	10	1023	1181

* These values are calculated from Figure 3.3

To further explore the relationship between the dissolution and P-gp efflux of the Class IV drugs, different doses of paclitaxel were orally administered to mice in the presence and absence of Verapamil either as Taxol® (6.66 mg kg^{-1}, 10 mg kg^{-1} and 20 mg kg^{-1}) or as GCPh nanoparticles (6.66 mg kg^{-1} and 10 mg kg^{-1}). There was a dose dependent increase in the plasma concentration of paclitaxel when administered as nanoparticles.

The presence of verapamil improved the paclitaxel absorption at the low and medium dose, while the verapamil had no effect on paclitaxel absorption at the highest dose of Taxol® (Figure 3.3 b-d, Table 3.1). This is due to the fact that the energy driven P-gp pumps are saturated when high concentrations of substrates are available for absorption. Hence the presence of a P-gp inhibitor had virtually no effect on the absorption of the drug, as the P-gp is already saturated with excess drug in solution. This saturation of P-gp by excess drug in solution has been previously reported *in vitro*[18,171], but to our knowledge this is the first time that this phenomenon has been reported with mice models through oral route. Our findings stress the fact that, *in vivo* dissolution of the Class IV drug is the main factor affecting the absorption and enhancing the dissolution using suitable excipients would automatically increase the absorption by saturating the P-gp with excess drug in solution.

Interestingly, the paclitaxel plasma levels show no significant difference with and without verapamil, when they are administered as GCPh nanoparticles at

all doses (Figure 3.3 e-f). This suggests that there is an alternative pathway for the absorption for Paclitaxel GCPh nanoparticles that do not involve the P-gp pump. To further explore this phenomenon, GCPh was covalently conjugated to Texas red, a fluorescent dye, orally administered to rats and the sections of small intestine were imaged using confocal microscopy. The confocal images show the presence of GCPh – Texas red (TR) conjugates in the vili (Figure 3.4). From the images, it can also be seen that the GCPh nanoparticles are mucoadhesive and are also transported to the basolateral side of the intestine to reach the systemic circulation via hepatic portal vein as indicated by the arrows. It is due to this particle uptake that the GCPh paclitaxel nanoparticles are able to bypass the P-gp efflux and thus no P-gp inhibitors are necessary. The GCPh nanoparticles are also mucoadhesive, which will further contribute to the enhanced/prolonged oral uptake of the encapsulated drugs. Thus, the new amphiphilic polymer GCPh, not only enhanced the oral absorption of paclitaxel but also by-passed the P-gp efflux due to alternative absorption mechanism, which needs to be clearly understood. Experiments were done to ensure the complete removal of free Texas red from the GCPh-Texas red conjugate (Figure 3.5) and thus the fluorescent signals seen on confocal microscope are those of the conjugate and not that of the free Texas red.

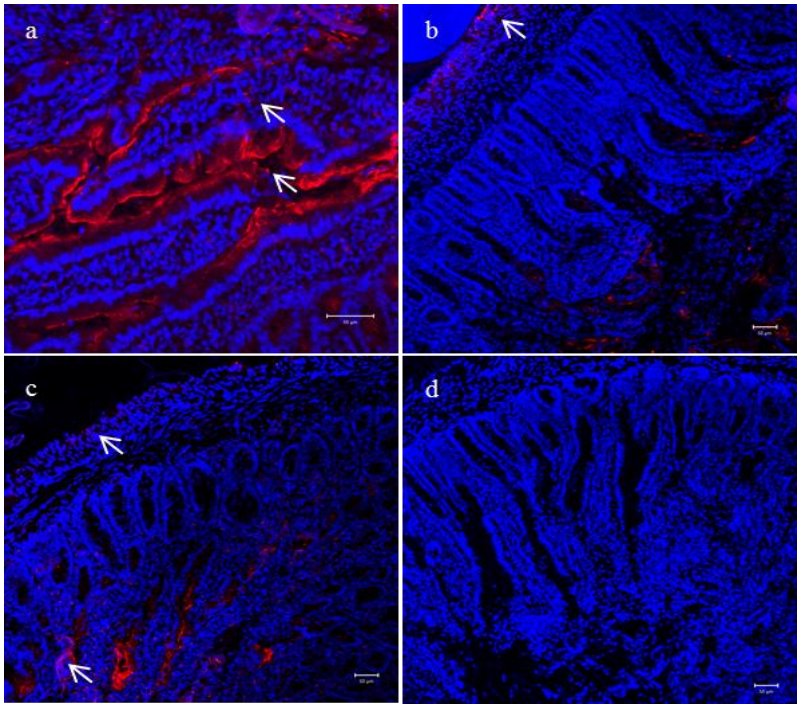

Figure 3.4 Confocal laser-scanning micrographs of rat intestinal tissue.

The images were taken 2 hours after dosing with GCPh-Texas red conjugate (100 mg mL^{-1}). The Texas red signal (red dots) can be seen lining the villi (a), inside the vili and also in the basolateral side of the villi (b,c) as indicated by the arrows. (d) Blank rat intestine for comparison. (scale bars = 10 µm).

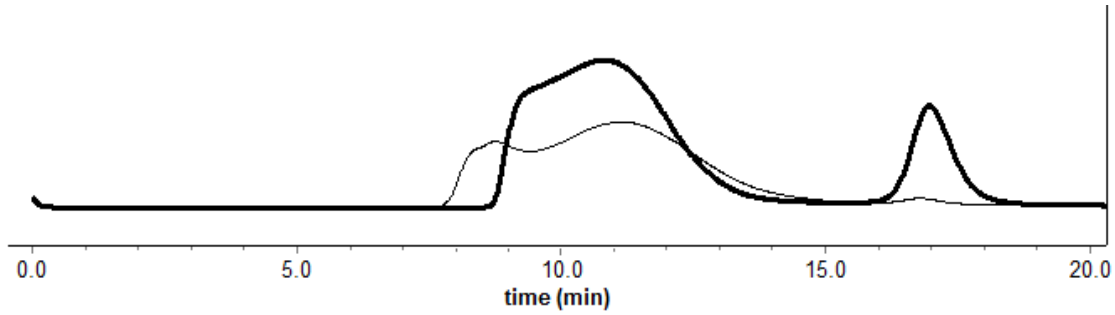

Figure 3.5 GPC-MALLS chromatograms to ensure purification of GCPh-TR

The image shows the GPC-MALLS chromatogram of GCPh-TR conjugate before (thick line) and after (thin line) purification. The free Texas red peak at 17 minutes disappears after the purification steps.

3.5 Discussion:

The oral absorption of certain BCS Class IV drugs is hampered by the activity of the P-gp efflux pumps in addition to poor solubility. Due to this fact, the BCS Class IV drugs are rarely administered orally. One strategy to overcome this obstacle is to enhance the dissolution of the drug to such an extent that the P-gp pumps are saturated, which renders them ineffective. We have demonstrated this phenomenon using paclitaxel as a model drug, where paclitaxel was formulated as Taxol® or polymeric nanoparticles. *In vitro* the formulations displayed good dissolution in both SGF and SIF. Also, both the formulations had similar *in vivo* paclitaxel absorption profiles following oral administration in mice. Co-administering the drug with a P-gp inhibitor increased the absorption of Taxol® at lower doses but made no difference at the highest dose. Poorly soluble paclitaxel formulations were also dosed (20 mg mL^{-1}) with and with out verapamil but the absorption of the drug following the oral administration of these formulations were very poor (data not shown). This suggests that dissolution is the key factor dictating the absorption of

hydrophobic drugs and when the dissolution is poor, co-administration with a P-gp inhibitor is not effective. Our results also suggests that the P-gp pumps may be saturated when higher levels of the drug are in solution, highlighting the importance of enhancing the dissolution for the oral delivery of BCS class IV drugs that are P-gp substrates. This is the first instance, where the dissolution dependent saturation of P-gp efflux for BCS Class IV drugs has been demonstrated *in vivo*.

The saturation of P-gp efflux pump by excess substrate is a well-known phenomenon. *In vitro* saturation of the P-gp efflux pump has been reported for different substrates such as paclitaxel[171], vinblastine[214] and *ex vivo* saturation of the P-gp efflux pump was also demonstrated for digoxin using Ussing chamber techniques[215]. Even though dose dependent saturation of P-gp efflux by paclitaxel was reported *in vivo*, no correlation was made with the dissolution of the hydrophobic drug and the activity of the P-gp efflux pump. Our study emphasizes the fact that merely increasing the dose wouldn't saturate the P-gp pump or increase drug absorption, if the dissolution of the drug is poor in the intestine. On the other hand we have proven that, using a dissolution enhancer and simultaneously increasing the dose would lead to P-gp saturation and maximize the drug absorption.

We also developed a new polymeric amphiphile GCPh, which improved the oral absorption of paclitaxel. The CMC of this polymer was in the nanomolar range (Chapter 2), which is in the range for chitosan based amphiphiles[123,186]. This amphiphile formed nanoparticles when formulated with paclitaxel and the oral plasma levels of paclitaxel from these nanoparticles were similar to that of Taxol® nanoparticles with similar AUC values (Table 3.1), thus meeting our first criterion for success established earlier. However, co-administration with verapamil did not enhance the absorption of paclitaxel when given as GCPh nanoparticles. *Ex vivo* intestinal tissue imaging using fluorescent labels revealed that the GCPh nanoparticles are present within the villi, which might explain why P-gp efflux pump inhibitors have no effect when paclitaxel GCPh nanoparticles are administered orally. Verapamil only has an effect at a later time point (4 hours), which is when the GCPh nanoparticles are destabilized

and free paclitaxel is released in the intestinal lumen making the drug susceptible to P-gp efflux (Figure 3.3 e, f).

The mechanism of action of GCPh nanoparticles include, improving drug solubility by stabilizing a molecular form of the drug, enhanced dissolution due to small size of the nanoparticles, mucoadhesion and nanoparticle uptake via transcellular and/or paracellular routes as demonstrated by *ex-vivo* fluorescent imaging studies (Figure 3.6). Additionally, nanoparticles are also transported to the basolateral side of the villi, which means the paclitaxel nanoparticles might reach the systemic circulation (provided the particles stay intact after first-pass liver metabolism), improving the efficacy of cancer treatment through selective tumour uptake due to EPR effect[216]. A combination of all these factors improved the absorption of paclitaxel and also by-passed the P-gp efflux, making GCPh an ideal vehicle for oral delivery of paclitaxel. The particle uptake of paclitaxel nanoparticles were previously reported by Mo et al.[191] using N-octyl-O-sulphate chitosan (NOSC) micelles, which enhanced the oral uptake of paclitaxel by inhibiting its P-gp efflux and also by promoting the particulate absorption of paclitaxel loaded micelles. In this study, amphiphilic chitosan was prepared with octanol and sulphate pendent groups, which was then used to encapsulate paclitaxel. The oral absorption of paclitaxel was studies in the presence and absence of verapamil and compared to that of Taxol®. The bioavailability of paclitaxel was improved by 6-folds following the oral administration of N-octyl-O-sulphate chitosan micelles when compared to that of Taxol® formulation. The enhanced oral bioavailability was mainly attributed to the absorption of drug loaded NOSC micelles, which inhibited the activity of the P-gp efflux pumps. While the absorption N-octly-O-sulphate chitosan micelles are facilitated by clathrin-mediated transcytosis, more work is needed to determine the nature of uptake of GCPh nanoparticles.

Thus we were also able to meet our second criterion for success, which is to enhance the absorption of paclitaxel without the help of a P-gp efflux pump inhibitor to an AUC value of above 1000 ng.h mL^{-1}. This was achieved in two different ways; either to improve the dissolution in order to saturate the energy driven P-gp efflux pumps or to use polymeric nanoparticles to exploit alternate drug absorption pathways by-passing the P-gp efflux pumps.

3.6 Conclusion:

Dissolution is the key factor controlling the oral absorption of most of the hydrophobic drugs. Improving the dissolution of P-gp substrate BCS Class IV drugs using suitable dissolution enhancers might enhance its oral absorption by saturating the P-gp as demonstrated with paclitaxel. A new polymeric amphiphile, GCPh enhanced the oral absorption of paclitaxel using a variety of mechanisms such as dissolution enhancement through particle size reduction, mucoadhesion, uptake of drug-loaded nanoparticles bypassing the P-gp efflux and transportation of these nanoparticles into the systemic circulation.

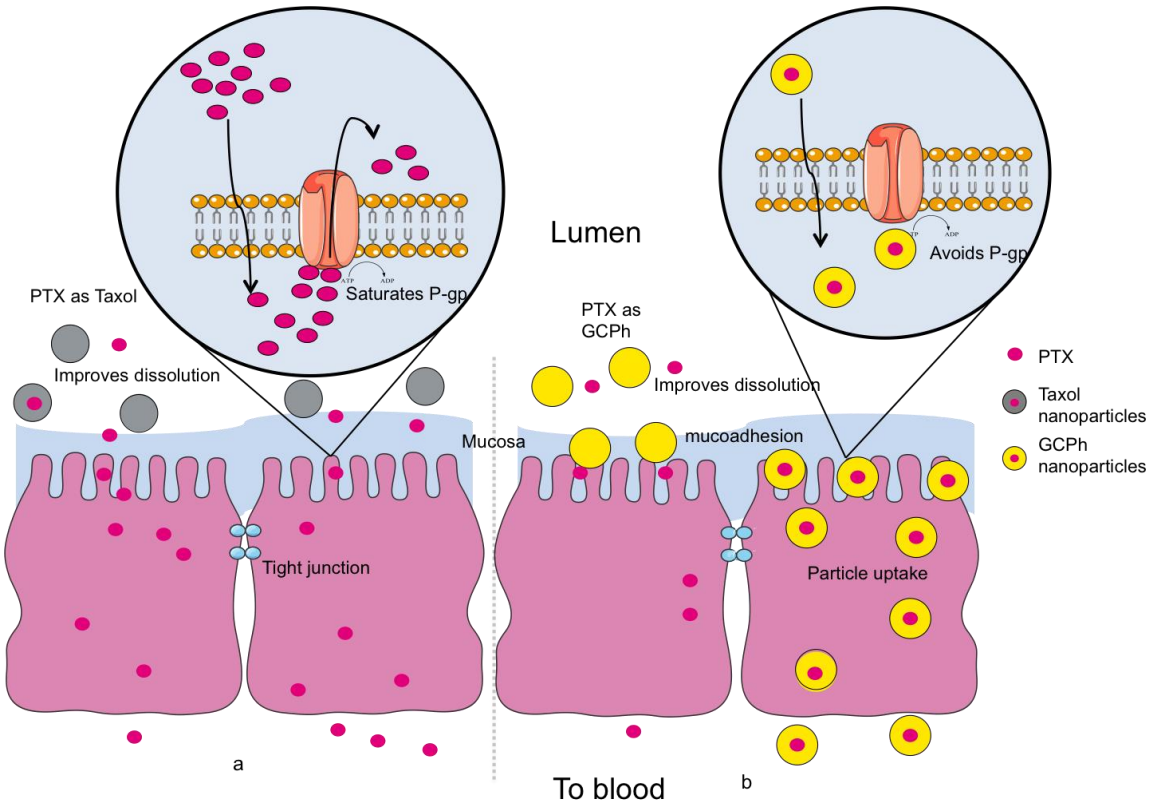

Figure 3.6 The mechanism of uptake of paclitaxel nanoparticles as a) Taxol and b) GCPh

4 Oral delivery of CUDC-101

4.1 Introduction

CUDC-101 is a potent multi-target tumour inhibitor[168,169] but it is a BCS class IV molecule and hence it is hard to deliver orally. Oral absorption of the drug is hampered by the physicochemical properties of the drug and physiology of the alimentary canal, as described in Section 1. Various strategies are proposed in the literature to overcome these barriers and the choice of these techniques mainly depends on the nature of the therapeutic in the study. This section covers the preliminary experiments carried out on CUDC-101 to identify the delivery issues associated with the oral delivery of this molecule. Results from these experiments, were used to design various strategies to address the identified delivery issues and a number of CUDC-101 formulations were developed based on this, which are all explained in detail in this section.

4.1.1 CUDC - 101 polymeric nanoparticles

Polymeric amphiphiles have both hydrophilic and hydrophobic moieties in their structure, which helps to encapsulate hydrophobic drugs and improve its aqueous solubility. GCPQ is a polymeric amphiphile that self-assembles into micelles in aqueous environment[100]. It has previously been shown to form nanoparticles with hydrophobic drugs, presumably by solubilizing the drug in its hydrophobic core and forming a colloidal suspension in water. This improves the aqueous dissolution of the drug and eventually enhances its oral uptake[75]. GCPQ nanoparticles have also been shown to be mucoadhesive and are also taken up by phagocytosis, which all contributes to the enhanced absorption of the drug[217]. Thus, it might be advantageous to formulate CUDC-101 as GCPQ nanoparticles. GCPh, a new polymeric amphiphile similar to GCPQ was also synthesized, which will also be tested with CUDC-101 to enhance its absorption.

There are different ways to form nanoparticles with preformed polymeric amphiphiles[218], such as co-solvent evaporation, solvent displacement, solvent diffusion, salting out etc. All these techniques require the use of organic solvents, which limits their application due to limited availability of safe organic

solvents. Also, preliminary experiments indicated that CUDC-101 has limited solubility in organic solvents, making it hard to form GCPQ – CUDC-101 nanoparticles using conventional techniques. Two different approaches were proposed to make these nanoparticles; 1) to probe sonicate the drug with GCPQ and adding surfactants to stabilise the drug GCPQ colloidal suspension and 2) to add a solution of drug to an aqueous suspension of GCPQ.

The idea behind adding a solution of drug to an aqueous suspension of GCPQ is similar to solvent displacement technique. The drug is poorly soluble in water and when a solution of drug is diluted with water it will precipitate (as observed during preliminary experiments). But a dispersion of amphiphilic polymer in water provides an opportunity for the precipitating drug molecules to partition inside the hydrophobic core of the amphiphile, as the core will have a favourable thermodynamic environment for the hydrophobic drug. This might create a suspension of drug in an aqueous environment, or in other words form the GCPQ-CUDC-101 nanoparticle. Similarly, probe sonication provides sheer and cavitation forces, which reduces the size of the drug crystals to nanoscale and provides an opportunity for GCPQ to encapsulate the hydrophobic drug due to hydrophobic interactions. The presence of a surfactant might reduce the interfacial tension between the drug nanocrystal and the surrounding medium thereby enhancing the diffusion of drug molecules that is important for particle size reduction.

Preliminary experiments were done to narrow down on the choices of solvents, the characteristics of GCPQ and choices of surfactants to make nanoparticles. There are few variants of GCPQ, differing in the molecular weight of the polymer, hydrophobicity of the polymer dictated by percentage of palmitoylation; the protonated or deprotonated state of the primary amines in the polymer backbone. Experiments were done to determine which of these polymers were able to suspend high concentrations of the drug in water, and then surfactants were added to check if that affected the drug recovery. If any formulations were satisfactory then they were promoted for *in vitro* and *in vivo* experiments.

4.1.2 Gastro-retentive dosage form:

Gastro-retentive dosage forms are those where the oral dosage forms are physically designed to escape or delay the gastric emptying, so that the formulation is retained in the stomach for longer period of time than usual[108]. This means, the majority of drug release will happen in the stomach, which will be the desired site of action for most gastro-retentive dosage forms. From the preliminary experiments, the absorption of CUDC-101 was shown to be predominantly from stomach when administered as PEG400 solution or as Captisol inclusion complex. This absorption was observed only for 30 minutes, after which the formulation gradually percolated into the intestine where it precipitates and the absorption terminates. Based on this observation it was hypothesized that, if we can maintain the formulation in the stomach for a longer time frame then it is possible to maximize the absorption of CUDC-101. And hence possible ways of developing a gastro-retentive dosage form for CUDC-101 was explored.

4.1.2.1 PEG/PEO gastro-retentive formulation:

There are different types of gastro-retention mechanisms such as floating devices, sinking devices etc., but since CUDC-101 was soluble in high molecular weight PEG, which is capable of forming gels, it was decided to pursue with swelling dosage forms. Swelling dosage forms are those which increases in size upon contact with gastric fluid such that they cannot pass through the pylorus and thus remain in the stomach until they are eroded to a size small enough to pass through the pylorus[108]. High molecular weight PEG (> 20,000 Da) is called polyethylene oxide (PEO) and PEO (5,000,000 Da) exists as free flowing powder at room temperature. These PEO powder forms a gel in water and it was observed that when these powdery PEO are tightly packed, they swell to form a gelatinous solid. This would make an ideal depot, where the drug is solubilized within this gelatinous matrix that stays in the stomach for a longer duration and slowly releases the drug upon erosion.

But the PEOs have high meting point, which makes it hard to solubilize CUDC-101. Hence it was decided to use waxy 1000 – 3350 Da PEGs for solubilizing

the drug and to mix this solid drug solution in different proportions to PEO to form a swelling dosage form. PEG of 1000 – 3350 Da exist as waxy solids, which is also free flowing at room temperatures. Particularly, PEG 3350 Da melts around 70°C and also solubilize CUDC-101 at around 100 mg mL^{-1} concentration, which makes it ideal for our purpose. Thus, a swelling dosage form was developed using these excipients and they were tested *in vitro* and *in vivo* to prove our hypothesis that it is possible to increase the absorption of CUDC-101 by prolonging the retention of the dosage form in the stomach.

4.1.3 Liquid Chromatography-Mass Spectroscopy (LC-MS):

Liquid Chromatography-Mass Spectrometry (LC-MS) is an analytical tool for quantification of very low concentration solutes[180]. The solutes are separated using a chromatographic column and fed into a Mass Spectrometer (MS), using a high-pressure pump. The solutes are then ionised in the MS from which they are separated based on their mass to charge ratio (m/z). These molecular ions are further subjected to ionisation (MS/MS) in order to produces daughter ions, which are monitored using Multiple Reaction Monitoring (MRM) channels and recorded as chromatograms. The area under the curve for a particular solute in the chromatogram is directly proportional to the concentration of the solute, which makes the quantification straightforward[180]. The main advantage of LC-MS over RP-HPLC is the specificity and sensitivity of MS, which enables the detection of picogram concentrations of solute. The main limitations of LC-MS is that solutes of higher molecular weight are hard to quantify[180].

4.2 Aims and objectives

The main of this chapter is to enhance the oral absorption of CUDC-101 using polymeric nanoparticles. The objectives are as follows:

- Improve the dissolution of the drug in the gastro-intestinal tract.
- Saturate the activity of P-gp efflux pumps by increasing the dissolution as observed with paclitaxel.
- Form nanoparticles with GCPQ and GCPh, to achieve better absorption.
- Explore other strategies to improve oral absorption, e.g. gastro-retention.

The criteria of success for this project was established based on the objectives as follows:

1. To develop a formulation that is stable in the at intestinal pH conditions.
2. To achieve target dose of at least 50 mg kg^{-1}.

3. To achieve a C_{max} of 500 ng mL^{-1} CUDC-101 in plasma following the oral administration of the developed formulations.

4.3 Materials and Methods

4.3.1 Materials

Chemical	Purity	Supplier
Acetonitrile HPLC grade	≥ 99.5%	Fisher Scientific (Loughborough, UK)
Ethyl acetate		Fluka Chemicals (Gillingham, UK)
Hydrochloric acid	36.5-38%	VWR BDH Prolabo (Fontenay-sous-Bois, France)
Pancreatin	~100%	Sigma-Aldrich (Gillingham, UK)
Pepsin		Sigma-Aldrich (Gillingham, UK)
Phosphate buffer saline		Sigma-Aldrich (Gillingham, UK)
Potassium dihydrogen phosphate	99.5	Sigma-Aldrich (Gillingham, UK)
Sodium chloride	99.50%	Sigma-Aldrich (Gillingham, UK)
Sodium hydroxide	98.90%	Sigma-Aldrich (Gillingham, UK)
Trifluoro acetic acid	≥ 99.5%	Fluka Chemicals (Gillingham, UK)
Water double deionised	<18 ohm	Millipore Synergy-Simpak1

Chemical	Purity	Supplier
N-methyl-2-pyrrolidone		Sigma-Aldrich (Gillingham, UK)
Dimethyl sulfoxide		Sigma-Aldrich (Gillingham, UK)
CUDC-101	Batch no. 87889-08	Curis Inc. (MA, USA)

Details of the GCPQ batches used in this chapter

Batch name	Pamitoylation (%)	Quarternisation (%)	M_w (Da)
Q48 100413 KC*	18	5	10830
Q48 101111 SR	18	9	9470
Q24 050213 SR	18	6	16440
Q2 090313 SR	11	11	48130
Q2 150909 AL*	21	11	55460
Q2 220213 SR	19	13	70130
Q48 111111 SR	18	9	9640

***GCPQ with deprotonated primary amines

4.3.2 Methods used in preliminary experiments

4.3.2.1 Dissolution studies in Simulated Gastric and Intestinal fluids:

The Simulated Gastric Fluid (SGF) was prepared following the method described in European Pharmacopeia, 6th edition, 2008. Sodium chloride (2.0 g) and pepsin (3.2 g) were dissolved in hydrochloric acid (1 M, 80 mL) and volume made up to 1 L using distilled water (pH 1.2). Simulated Intestinal Fluid (SIF) was prepared following the method described in European Pharmacopeia, 6th edition, 2008. In distilled water (800 mL), Potassium dihydrogen phosphate (6.8 g) and a solution of sodium hydroxide (0.2 M, 77 mL) were added. Once dissolved, the pH of the solution was adjusted to 6.8 with NaOH (0.2 M) and the volume of the solution was made up to 1 L with distilled water.

The freeze-dried formulations containing CUDC-101 (5 mg mL^{-1}) were placed in SGF/SIF (50 mL, preheated to 37°C) and incubated on a water bath maintained at 37°C with shaking (125 rpm). Samples (150 µL) were withdrawn at specific time points (0, 5, 10, 30, 60, 120 min) and replaced with the same volume of fresh dissolution medium. The withdrawn samples were centrifuged at 1000 g for 10 minutes and the supernatant was extracted as outlined below.

Extraction was carried out by diluting the sample with thrice the volume of acetonitrile (HPLC grade), vortexing for 10 min and centrifuging at 10000 g at room temperature for 10 min (MSE Microcentaur, UK). The supernatant was then collected and analysed as such under RP-HPLC, using the method stated in section 4.3.6. All the experiments were carried out in triplicate and results are calculated by comparing the peak area of the drug with a standard curve.

4.3.2.2 Stability in Simulated Gastric Fluid

SGF aliquots (100 µl) were pipetted in an eppendorf tube. The formulations (10 µl) were spiked in SGF to give a final concentration of 1 mg mL^{-1} drug (approx.) and were incubated on water bath set at 37°C with shaking (125 rpm). Sample tubes were withdrawn at specific time points (0, 10, 30, 60, 120 min) and were extracted as follows.

The samples were extracted with 900 µL of methanol, vortexed for 10 minutes and centrifuged at 10,000 g for 10 minutes at room temperature (MSE Microcentaur, UK). The supernatant was carefully collected and analysed using RP-HPLC. The results were compared with a standard curve prepared and concentration of drug at each time point was calculated. If there is a decrease in concentration over time (compared with conc. at time 0), this was interpreted as drug degradation. All the experiments were done in triplicate.

4.3.2.3 Stability in Rat Intestinal wash (IW)

Four adult male Wistar rats (200 g in wt. approx.) were fasted for 12-16 h and euthanized by CO_2 overdose. The portion of the small intestine from duodenum to ileum was excised and cut into small segments of 10 cm (approx.) length. With the help of a syringe, 10 mL of ice cold PBS (pH 6.8) was flushed through each of these segments. The whole volume thus collected were pooled together

and centrifuged at 1000 g for 10 minutes at 10°C. The supernatant collected after this step is the Rat Intestinal Wash, which is stored at -20°C and thawed at 37°C before use.

IW aliquots (100 μl) were pipetted in an eppendorf tube. The formulations (10 μl) were spiked in IW to give a final concentration of 1mg mL^{-1} drug (approx.) and were incubated on water bath set at 37°C with shaking (125 rpm). Sample tubes were withdrawn at specific time points (0, 10, 30, 60, 120 min) and were extracted as follows.

The samples were extracted with 900 μL of methanol, vortexed for 10 minutes and centrifuged at 10000 g for 10 minutes at room temperature (MSE Microcentaur, UK). The supernatant was carefully collected and analysed using RP-HPLC. The results were compared with a standard curve prepared and concentration of drug at each time point was calculated. If there is a decrease in concentration over time (compared with conc. at time 0), this was interpreted as drug degradation. All the experiments were done in triplicate.

4.3.2.4 Stability in Liver homogenate

Adult male CD-1 mice (approx. 20 g in wt.) were euthanized by overdose of carbon dioxide. The liver of the animal was carefully excised and weighed. For 100 mg of liver tissue, 150 μL of 50 mM sucrose solution was added and the liver macerated thoroughly. This homogenate was stored at -20°C and thawed at 37°C before using for experiments.

The formulations were diluted to 10 μg mL^{-1} concentration using milliQ water and the concentration was confirmed using RP-HPLC. Liver homogenate (150 μL) were pipetted in an eppendorf tube and the formulations (15 μL) were spiked in these fluids to give a final concentration of 1 μg mL^{-1} (approx.). This mixture was incubated on water bath set at 37°C with mild shaking (60 rpm). Tubes were withdrawn at specific time points (0, 10, 30, 60, 120 minutes) and were spiked with CUDC-101 internal standard (15 μL, 250 ng mL^{-1}).

The drug from the liver homogenate was then extracted by adding four times the sample volume of ethyl acetate. The vials were then vortexed for 10 minutes, centrifuged at 1500 g for 15 minutes at room temperature and the

supernatant was transferred to a fresh 2 mL eppendorf. This step was repeated twice with the pellet and the clean supernatants from each sample pooled together. The ethyl acetate was then evaporated using a Speedvac (Thermo Fisher Scientific, Waltham, US.) connected to a vacuum pump (Edwards, Sussex, UK) at room temperature. Once the samples are dry, they were dissolved in 0.1% FA in acetonitrile (150 μL) and analysed by LC-MS. Simultaneously, a standard curve was prepared by spiking the standard solutions in liver homogenate and analysed. Results were calculated with reference to the standard curve and if the drug concentrations at other time points were less than the initial, this was interpreted as drug metabolism by liver enzymes. Experiments were done in triplicate.

4.3.2.5 Stability in Plasma

Adult male CD-1 mice (approx. 20 g in wt.) were euthanized and the blood was immediately collected in a vacutainer coated with EDTA, by cardiac puncture method. The collected blood was stored on ice until centrifuging at 2000 g for 10 minutes at 4°C. The supernatant from this step is the plasma, which was carefully collected and stored at -20°C.

The CUDC-101 Captisol formulation (10 mg mL^{-1}) was diluted to 10 μg mL^{-1} concentration using milliQ water and the concentration was confirmed using RP-HPLC. Plasma (150 μL) were pipetted in an eppendorf tube and the Captisol formulation (15 μL) was spiked in the plasma to give a final concentration of 1 μg mL^{-1} (approx.). in a separate experiment, the stability studies were carried out at 37 °C with shaking at 125 rpm. Drug and metabolite standards (15 μL of 1 μg mL^{-1} concentration) were also spiked plasma aliquots (150 μL) to give a final concentration of 100 ng mL^{-1} and the stability studies were carried out in frozen conditions.

Stability at 37°C: The drug-plasma samples (150 μl) were incubated in a water bath set at 37°C with mild shaking (60 rpm). Tubes were withdrawn at specific time points (0, 10, 30, 60, 120 min) and the plasma samples were spiked with the internal standard (15 μL, 250 ng mL^{-1}) and extracted as described below.

Stability on storage at -20°C: The drug-plasma samples (150 μl) were stored at -20°C for a period of seven days and sample tubes were withdrawn at day0, day1, day4 and day7. The samples were spiked with the internal standard (15 μL, 250 ng mL^{-1}) and extracted as described below.

Stability on storage at -80°C: The plasma samples (150 μl) were stored at -80°C for a period of seven days and sample tubes were withdrawn at day0, day1, day4 and day7. The plasma samples were then spiked with the internal standard (15 μL, 250 ng mL^{-1}) and extracted as described below.

Sample extraction: The samples were extracted with thrice the volume of 0.1% FA in ACN. The samples were vortexed for 40 minutes and centrifuged at 10000 g for 10 minutes at room temperature (MSE Microcentaur, UK). The supernatant was carefully collected and analysed by LC-MS. A standard curve was simultaneously prepared by spiking the standards and internal standards in plasma. The standards were then extracted as before and analysed along with the samples. If the concentrations at other time points were different from initial time point, this was interpreted as drug degradation in plasma.

Sample stability after extraction: A plasma standard curve was prepared, extracted and stored on the LC-MS auto sampler for a period of 7 days. The samples were then periodically analysed on days 0, 1, 4 and 7. The peak area ratio of the standards were compared with that of day 0 (control) and a CV value greater than 15% suggests drug degradation on storage after extraction with acetonitrile.

4.3.2.6 Solubility in Aqueous/Non-aqueous solvents:

CUDC 101 (50 mg) was added to amphiphilic/ non-aqueous liquid (1 mL), mixed thoroughly and the resulting suspension probe sonicated for 5 minutes (Soniprep 150, Sanyo, UK) at 25% of its output. The resulting liquid was centrifuged (10,000g X 10 minutes, MSE Microcentaur, UK) to remove insoluble drug and the supernatant sampled (10 μL), diluted with methanol (990 μL) and analysed for drug content by RP-HPLC.

4.3.2.7 Solubility in Simulated Gastric Fluid

SGF/IW (2 mL) were pipetted in an eppendorf tube and labelled appropriately. The CUDC-101 formulations (200 µL) were spiked in these fluids to give a final concentration of 1 mg mL^{-1} (approx.) and were incubated in a water bath set at 37°C with shaking (125 rpm). Samples (150 µL) were withdrawn at specific time points (0, 10, 30, 60, 120 min) and the samples were centrifuged at 1000 g for 10 minutes at room temperature. The supernatant (100 µl) was transferred to a fresh eppendorf tube and extracted as follows.

The samples were extracted with in ACN (900 µl), vortexed for 10 minutes, centrifuged at 10,000 g for 10 minutes at room temperature and the supernatant was analysed by RP-HPLC. A standard curve was simultaneously prepared in SGF/IW and analysed along with the samples. A control sample was also prepared by immediately extracting the sample after spiking with formulation, without the 1000 g centrifugation step. If the drug concentrations at other time points are drastically different from that of control it was interpreted as drug precipitation in the respective fluids.

4.3.3 Methods used for nanoparticle formulation:

4.3.3.1 Encapsulation studies with GCPQ:

Different types of GCPQ (10 mg) with different characteristics (Table 4.7) were placed in a glass vial and CUDC-101 (1 mg) was added to each vials followed by water (1 mL) and the dispersion was probe sonicated for 5 minutes at 25 % of its maximum output. The resulting liquid was centrifuged (1,000 g for 10 minutes) to remove insoluble drug and the supernatant (10 µL), which is the colloidal fraction was diluted with methanol (990 µL) and analysed for drug content by RP-HPLC.

To find the effect of adding a co-surfactant on GCPQ – CUDC-101 nanoparticles, Polysorbate 80 (Tween 80) was added to the mixture of CUDC-101 (1 mg) and GCPQ (10 mg) at different percentages (0% - 10%, v/v in water) and probe sonicated for 5 minutes at a power intensity of 25 %. The resulting liquid was centrifuged (1,000 g for 10 minutes) to remove insoluble drug and the supernatant (10 µL) was diluted with methanol (990 µL) and analysed for drug content by RP-HPLC.

4.3.3.2 Preparation of GCPQ – CUDC-101 formulation 1:

CUDC-101 (40 mg) was dissolved in Cremaphor RH (1 mL) using the probe sonication to get a clear solution. This solution (100 µL) was then added to GCPQ (15 mg, Q48 111111 SR) and the volume was made up to 0.8 mL using HCl (0.1 N) to obtain a clear yellow dispersion.

4.3.3.3 Preparation of GCPQ – CUDC-101 formulation 2:

CUDC 101 (10 mg) was dissolved in sodium hydroxide (0.2 M, 1 mL) containing PVP-K15 (0.16 %) by heating in a shaking water bath at 70°C for 5 minutes. GCPQ (20 mg, Q48 111111 SR) was dispersed in hydrochloric acid (0.2 M, 1 mL) by vortex mixing. To this GCPQ dispersion was added the warm alkaline solution (clear yellow in colour) of CUDC-101 and the resultant colloid suspension was vortexed for 10 seconds. The pH of the resulting formulation was adjusted to a pH 6.8 if necessary.

The GCPQ – CUDC-101 formulation 2 was also developed into a solid dosage form by freeze-drying the formulation. The solid dosage form was packed in to capsules (size 1 and size 9) and enteric coated with Eudragit L100-55 (10% w/v) dissolved in methanol[219]. To coat the capsules with Eudragit, the methanol solution of Eudragit L100-55 was poured in a petridish (10 mL). Capsules containing the formulations were fixed in a specially designed apparatus (Torpac Inc., USA) and dipped for few seconds in the Eudragit solution. The capsules were then left to dry on the apparatus, once dry the capsules are fixed on the opposite end, which is again dipped in Eudragit solution. This process is repeated twice to ensure uniform coated of the capsules.

4.3.3.4 Stability studies of GCPQ formulations:

The pH of the GCPQ – CUDC-101 formulations was adjusted to neutral and the formulations were left undisturbed at room temperature. Samples (100 µL) were withdrawn at specific time points and centrifuged at 1,000 g for 10 minutes and the supernatant was analysed for drug content by RP-HPLC. Stability studies of the formulation were also carried out in SGF and IW by spiking a known concentration of CUDC-101 formulations in SGF or IW (to give 1 mg mL^{-1} concentration of CUDC-101 in SGF/IW) and incubating at 37˚C with shaking at 125 rpm. Samples (100 µL) were withdrawn at specific time points and

centrifuged at 1,000 g for 10 minutes and the supernatant was analysed for drug content by RP-HPLC.

4.3.3.5 pH dependent stability studies:

GCPQ – CUDC-101 formulation 2 (200 µL) was spiked in phosphate buffer (10 mM, 0.8 mL) adjusted to various pH values ranging from 1.2 to 7.2 and incubated at 37˚C with shaking at 125 rpm. Samples (100 µL) were withdrawn at specific time points and centrifuged at 1,000 g for 10 minutes and the supernatant was analysed for drug content by RP-HPLC.

4.3.3.6 Dissolution studies:

The GCPQ – CUDC-101 formulation 2 (1 mL) was freeze-dried and to this dried cake SGF/SIF (5 mL respectively) was added and incubated at 37˚C with shaking at 125 rpm. The samples were withdrawn at predetermined time points and filtered using 0.8um filter and diluted in the methanol and analysed for drug content using RP-HPLC.

4.3.4 Methods used for gastro-retentive dosage form

4.3.4.1 Preparation of PEG-PEO capsules:

PEG 3350 Da (PEG3350) was molten at 70°C and to this liquid PEG (1 mL) CUDC-101 (100 mg) was added and probe sonicated for 10 minutes at 30 % output to get a clear solution. This solution was allowed to cool and form a solid PEG3350 CUDC-101 solution. This solid solution was then ground to get a fine powder and this powder was then mixed with PEO (5,000,000 Da) at different proportions (1:1, 1:1.5, 1:2 w/w ratios) to get a homogeneous mixture. This mixture was then tightly packed in size 0 capsules and used for further experiments.

4.3.4.2 Drug release experiments in SGF:

The PEG3350 – PEO capsules with known amount of CUDC-101 were placed in SGF (50 mL) and placed in a shaking water bath (37°C, 125 rpm). Samples (200 µL) were withdrawn, filtered with 0.8 µm filters and the filtrate was analysed for drug content using RP-HPLC.

4.3.5 TEM imaging

The CUDC-101 formulations were analysed under TEM (Philips 120FEI company, Netherlands). A drop of the formulation was dried on a copper TEM grid (300 mesh- Fomvar/ carbon coated) and stained with a drop of 1% uranyl acetate. Once dried, the samples were analysed under the TEM and the representative images were randomly photographed and documented.

4.3.6 RP-HPLC analysis

CUDC-101 was analyzed using an Agilent 1200 series quaternary pump, equipped with Agilent 1200 series degasser, auto sampler and an UV absorbance detector all supplied by Agilent technologies (Berkshire, UK). Samples were chromatographed over a reverse phase column: Onyx C18 monolith column (100 x 4.6mm, 5μm); a 10mm connector connected two such columns and a guard column (10 x 4.6mm, 5μm), maintained at a constant temperature with an Agilent1200 series column heat exchanger and eluted by a gradient flow with Triflouroacetic acid (0.1% in water): acetonitrile (90:10) mobile phase at a flow rate of 2.0 mL min^{-1} at 35 °C as shown in Table 4.1. The peaks of CUDC-101 and its major metabolite were detected at 254 nm with a retention time of 12.9 min and 14.2 min respectively. The data was analysed using Agilent Chemstation software. Calibration curves for CUDC-101 and its major metabolite (r^2 > 0.99) were obtained using various concentrations of standard solutions ranging from 1-to 200 μg mL^{-1}.

Table 4.1 RP-HPLC method for CUDC-101

Time (min)	0.1% TFA in water (A) (%)	Acetonitrile (B) (%)
0	90	10
3	85	15
10	75	25
20	15	85

Time (min)	0.1% TFA in water (A) (%)	Acetonitrile (B) (%)
20.2	90	10
23.2	90	10

4.3.7 LC-MS/MS analysis

The LC-MS/MS analysis of CUDC-101 was carried out using an Agilent HP 1260 infinity series LC system (Agilent technologies, Berkshire, UK) interfaced directly with a Triple Quad LC/MS 6460 mass spectrometer (Agilent technologies, Berkshire, UK). Samples were separated on a reverse phase C18 Zorbax column (2.1 x 50mm, 5μm) in a gradient mode with 0.1% Formic acid (FA) in water and 0.1% FA in acetonitrile as per **Table 4.2.** The mobile phase flow rate was 0.4 ml min^{-1} and the column was maintained at constant temperature of 25°C. The injection volume was 10 μl and the total run time for each sample was 6 min. The retention time for CUDC-101, its metabolite and the internal standard were 2.3 min, 2.6 min and 3.1 min respectively. The samples were ionized by electrospray ionization (ESI) in a positive ion mode. The electrospray parameters are as follows: electrospray capillary voltage 3.5 kV, source temperature 90°C and desolvation temperature 350°C. Nitrogen was used in the ESI source and the gas flow was 600 L h^{-1}. The collision energy was set for 25 eV and the detection of ions was performed in Multiple Reaction Monitoring (MRM) mode, following the ions as shown in **Table 4.3**.

Table 4.2 LC-MS method for CUDC-101

Time (min)	0.1% FA in water (A) (%)	0.1% FA in Acetonitrile (B) (%)
0.0	95	5

0.2	80	20
4.00	5	95
4.50	95	5
6.00	95	5

Table 4.3 Ions of the analytes monitored in LC-MS/MS

Compound	Molecular weight	Molecular ion	Daughter ion
Drug	434.4	435.4	292.1
Metabolite	419	420.6	292.4
Internal Std	430	431.1	270.2

4.3.8 Oral pharmacokinetic studies in mice

All the experiments were performed under a Home Office license (Animal Scientific Procedures Act 1986, UK). Male CD-1 mice (Harlan, Oxon, UK) or MF-1 mice (Charles River, Harlow, UK) weighing around 20 g at the time of experiment were acclimatized for at least 5 days before the experiment, in the animal housing unit, maintained at an ambient temperature of 22°C, relative humidity of 60% and an equal day-night cycle. The animals were fasted with access only to clean water for 12-16 hours before dosing. The CUDC-101 formulations were dosed orally with the help of an oral gavage needle. The animals were incubated at room temperature and euthanized by CO_2 overdose at specific time points. Blood samples were immediately collected in a vacutainer coated with EDTA by cardiac puncture and plasma was collected as described previously. The plasma collected was stored at -80°C if necessary, but usually extracted immediately as follows. To the plasma (50 µL), CUDC-101 internal standard (IS) was spiked (5 µl, 250 ng mL^{-1}) and extracted with thrice the volume of acetonitrile containing 0.1% FA. The samples were vortexed for 40 minutes and the supernatant was collected after centrifuging at 10,000 g for 10 minutes. The plasma extract was then analysed by LC-MS/MS along with a

standard curve, which was prepared simultaneously in blank plasma. The concentration of CUDC-101 was then calculated from the results and a plasma concentration time curve was constructed.

4.3.9 Oral pharmacokinetic studies in rats:

All the experiments were performed under a Home Office license (Animal Scientific Procedures Act 1986, UK). Male Wistar rats (Charles River, Harlow, UK) weighing around 200 g at the time of experiment were acclimatized for at least 5 days before the experiment, in the animal housing unit, maintained at an ambient temperature of 22°C, relative humidity of 60 % and an equal day-night cycle. The animals were fasted with access only to clean water for 12-16 hours before dosing. The enteric-coated or gastro-retentive capsules (size 9 or size 9 el) containing a known concentration of CUDC-101 were orally given to rats with the help of an oral gavage (Torpac, NJ, USA). The animals were incubated at room temperature and blood samples were collected from tail vein at specific time points. The final blood sample was obtained by a cardiac puncture after killing the animal using a CO_2 overdose. Blood samples were immediately collected in a vacutainer coated with EDTA and plasma was collected as previously described. The plasma collected was stored at -80°C if necessary, but normally extracted immediately as follows. To the plasma (50 µL), CUDC-101 internal standard (IS) was spiked (5 µl, 250 ng mL^{-1}) and extracted with thrice the volume of acetonitrile with 0.1% FA. The samples were vortexed for 40 minutes and the supernatant was collected after centrifuging at 10000 g for 10 minutes. The plasma extract was then analysed by LC-MS/MS along with a standard curve, which was prepared simultaneously in blank plasma. The concentration of CUDC-101 was then calculated from the results and a plasma concentration time curve was constructed.

4.3.10 Statistical analysis

Statistical significance was tested with one-way and two-way analysis of variance (ANOVA) using GraphPad Prism 5 statistical software. For multiple comparisons, Post-Hoc tests such Bonferroni's or Tukey's were used. In some cases, the statistical differences between two populations were compared using the Student's *t* test (Microsoft excel).

4.4 Results

4.4.1 Preliminary studies:

In order to formulate a drug molecule and obtain its pharmacokinetic profile, we need to know the basic parameters such as its solubility in aqueous and non-aqueous media, dissolution and solubility in digestive fluids, stability to endogenous enzymes, baseline oral pharmacokinetic (PK) profile and some information on how to handle the plasma samples obtained during PK experiments. Some of these preliminary experiments were done on CUDC-101 Captisol formulation as supplied by Curis Inc. This section outlines these results and the results informed the design of CUDC-101 formulations.

4.4.1.1 Solubility studies:

The solubility of CUDC-101 in various solvents is given in Table 4.4 and Table 4.5. From the results it can be seen that the water solubility of CUDC-101 is just 0.03 mg mL^{-1}. The drug is readily soluble in N-methyl-2-pyrrolidone (NMP), dimethylsulfoxide (DMSO) and soluble in PEG400. The drug's solubility in these solvents may be improved by heating the samples at 70˚C or by prolonged probe sonication but the drug precipitates upon cooling. Also, too much of heating is detrimental to the drug, as unknown degradation products appear on HPLC chromatogram when samples are probe sonicated for longer duration (Figure 4.1). From thermo gravimetric analysis (Figure 4.2), the degradation point for drug was found to be 160˚C. Care should be taken, not to overheat the drug samples while trying to solubilise the drug. It was possible to achieve a saturated solution of CUDC-101 with the above-mentioned excipients without the degradation. The following table shows the solubility results for CUDC-101 in various solvents.

Table 4.4 Solubility of CUDC-101 in aqueous solvents

Aqueous Medium	**pH**	**CUDC 101 Concentration (mg mL^{-1}, mean ± s.d.)**
HCL (0.01M)	2.02	0.068 ± 0.0166

Aqueous Medium	**pH**	**CUDC 101 Concentration (mg mL^{-1}, mean ± s.d.)**
HCL (0.1 M)	1.07	0.011 ± 0.0010
HCL (1 M)	0.12	< 0.001
Water	6.80	0.03 ± 0.01
Phosphate buffered saline	7.22	< 0.001
NaOH (0.01M)	12.02	0.029 ± 0.002
NaOH (0.1 M)	12.89	6.634 ± 0.490
NaOH (0.2 M)	12.98	50.01 ± 0.849
NaOH (1M)	13.44	0.025 ± 0.002

Table 4.5 Solubility of CUDC-101 in non-aqueous solvents

Amphiphilic/ Non-Aqueous Liquid	**Chemical/ Monograph Description**	**CUDC 101 Solubility (mg mL^{-1}, mean ± s.d.)**	**Comments**
Polysorbate 20	Poly(oxyethylene) sorbitan monooleate	35.01 ± 2.121	Degradation products seen in the chromatogram
Kolliphor RH40	Polyoxyl 40 hydrogenated castor oil	34.46 ± 3.601	Degradation products seen in the chromatogram
PEG 400	Poly(ethylene glycol), molecular weight ~ 400 Da	41.72 ± 0.552	Degradation products seen in the chromatogram (e.g. Figure 1)
PEG 1000	Poly(ethylene glycol), molecular	75.43 ± 6.395	No degradation products seen

Amphiphilic/ Non-Aqueous Liquid	**Chemical/ Monograph Description**	**CUDC 101 Solubility (mg mL^{-1}, mean ± s.d.)**	**Comments**
	weight ~ 1000 Da		
PEG 3350	Poly(ethylene glycol), molecular weight ~ 3350 Da	90.64 ± 7.916	No degradation products seen
Tetraglycol	Poly(ethylene glycol), molecular weight ~ 200 Da	19.1 ± 3.43	No degradation products seen
DMSO	Dimethyl sulfoxide	129.87 ± 5.596	No degradation products seen
NMP	N-methyl-2-pyrrolidone	151.91 ± 4.481	No degradation products seen

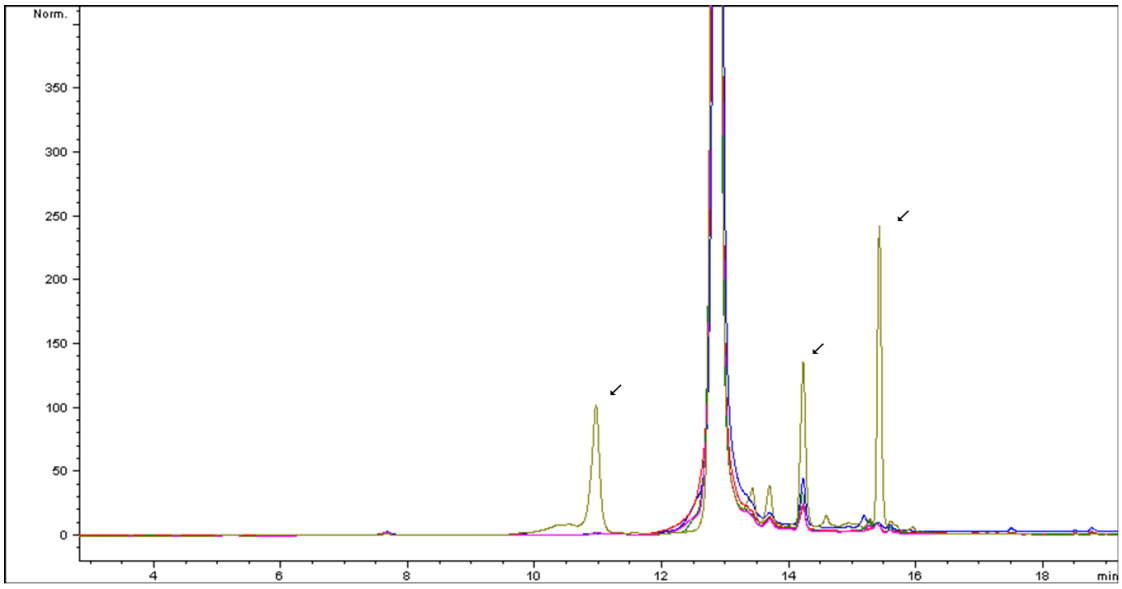

Figure 4.1 HPLC chromatogram of CUDC-101 as PEG400 solution.

A super-saturated solution (50 mg mL^{-1}, green chromatogram) of CUDC-101 in PEG400, showed degradation products (indicated by arrows) of CUDC-101, as the drug is exposed to high temperatures due to excessive probe sonication. At

lower concentration (< 40 mg mL^{-1}, red, blue and pink chromatograms), the drug easily goes into solution and hence doesn't require intense sonication, so no degradation products appear on the chromatogram.

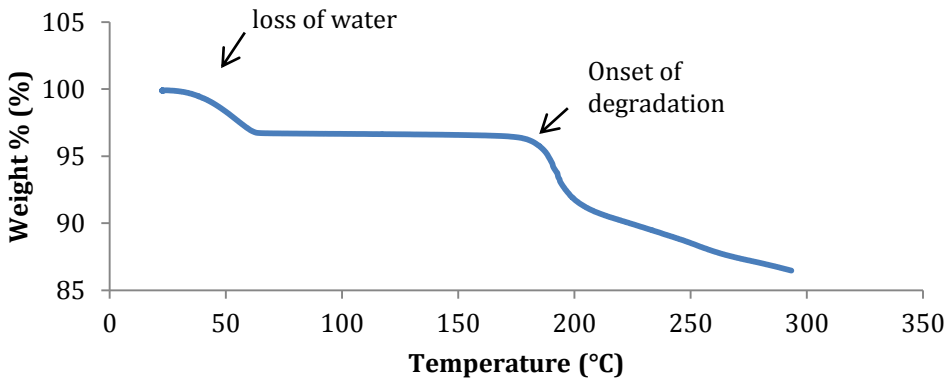

Figure 4.2 TGA analyses on CUDC-101

Thermo gravimetric analysis showing the degradation temperature for CUDC-101.

4.4.1.2 Dissolution and solubility studies in SGF/SIF/IW:

The dissolution of neat CUDC-101 is very poor in both SGF and SIF as shown in Figure 4.3 and Figure 4.4. The dissolution of CUDC-101 as its Captisol formulation was much better in SGF but very poor in SIF. This is due to the fact that the drug has slightly better solubility in acidic pH when compared with neutral pH. This is also further confirmed by the solubility studies in SGF and IW, where a solution of drug (1 mg mL^{-1}) remains as a solution in SGF at pH ~ 2, while it immediately precipitates (concentration drops immediately from 1 mg mL^{-1} to 0.2 mg mL^{-1}) in IW at pH 6.8 (Figure 4.5 and Figure 4.6).

4.4.1.3 Stability in Simulated Gastric Fluid and Intestinal Wash

Stability studies were carried out in different body fluids to check for enzymatic degradation of CUDC-101. The Captisol formulation and PEG400 CUDC-101 solution were both tested for possible degradation in SGF and IW (Figure 4.7 and Figure 4.8). From the graph it is clear that the initial drug level is maintained

throughout the experiment. The level of the drug's major metabolite is also negligible. Thus the question of drug degradation in both stomach and intestinal fluid is ruled out.

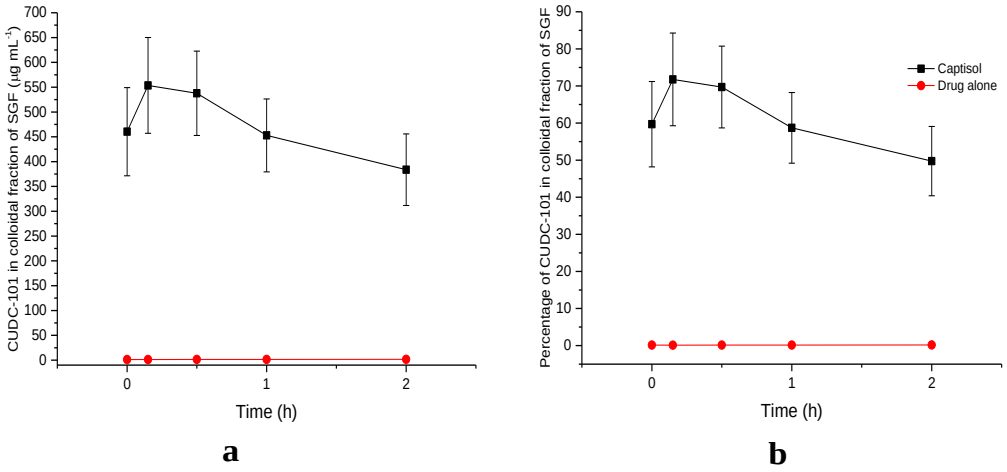

Figure 4.3 Dissolution of CUDC-101 in SGF

a) Expressed as concentration and b) percentage drug in colloidal fraction. Neat drug has very poor dissolution in SGF while the molecular form of drug stays in solution in SGF (n = 3).

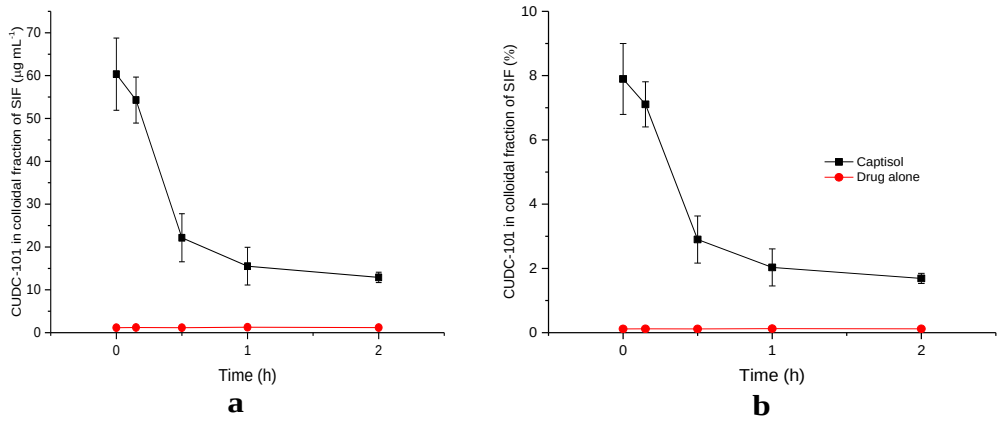

Figure 4.4 Dissolution of CUDC-101 in SIF

a) expressed as concentration and b) percentage drug in colloidal fraction. Neat drug has very poor dissolution in SIF and the molecular form of drug also precipitates as evident from low drug levels (n = 3).

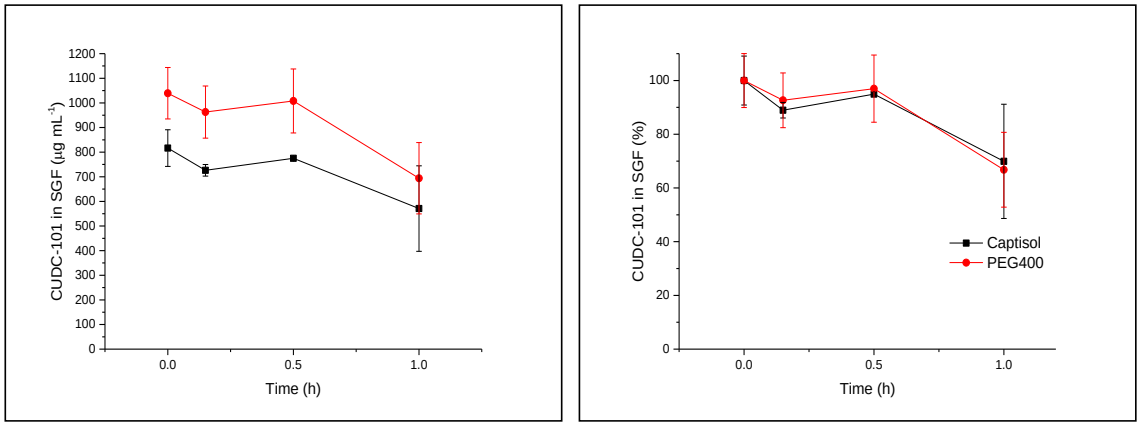

a **b**

Figure 4.5 Solubility of CUDC-101 solution in SGF

a) Expressed as concentration and b) percentage drug in colloidal fraction of SGF. A known concentration of CUDC-101 as either 30 % Captisol or PEG400 solution was spiked in 1 mL of SGF and change in drug concentration was monitored over time. Any change in drug concentration was interpreted as precipitation of drug in SGF (n = 3).

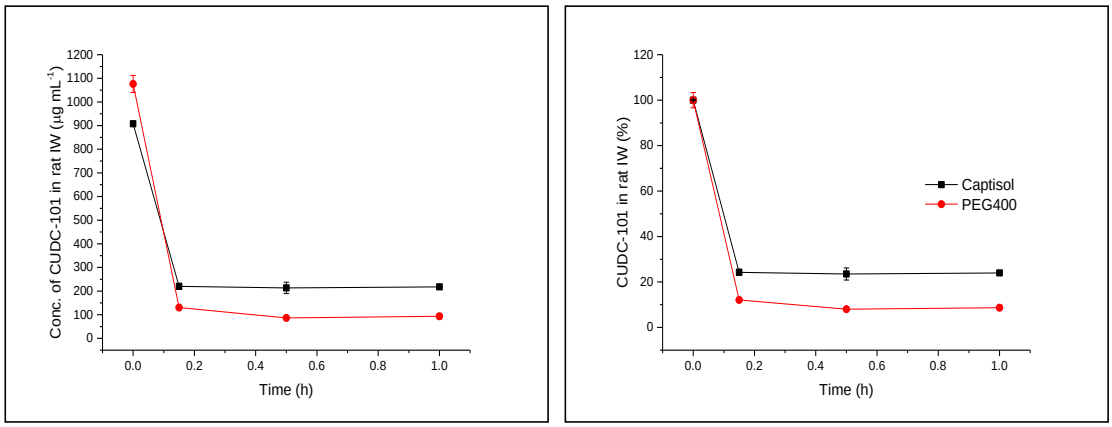

a **b**

Figure 4.6 Precipitation of CUDC-101 solutions in rat intestinal wash

a) Expressed as concentration and b) percentage drug in colloidal fraction of IW. A known concentration of CUDC-101 as either 30 % Captisol or PEG400 solution was spiked in 1 mL of SIF and change in drug concentration was monitored over time. Any change in drug concentration was interpreted as precipitation of drug in IW (n = 3).

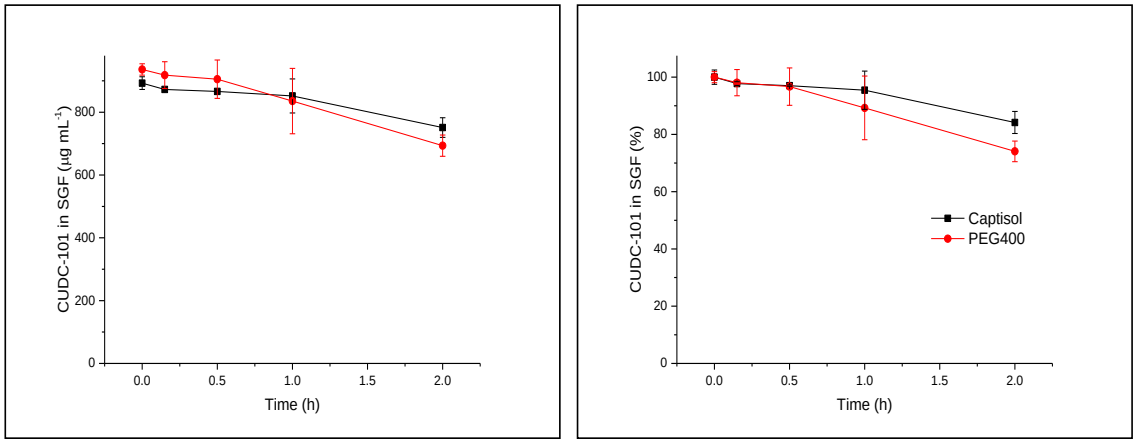

Figure 4.7 Stability of CUDC-101 in SGF

a) Expressed as concentration and b) percentage drug in the whole SGF. A known concentration of CUDC-101 as either 30 % Captisol or PEG400 solution was spiked SGF and change in drug concentration was analysed at particular time point. Any change in drug concentration was interpreted as degradation of the drug SGF. Results indicate that CUDC-101 is not degraded in SGF (n = 3).

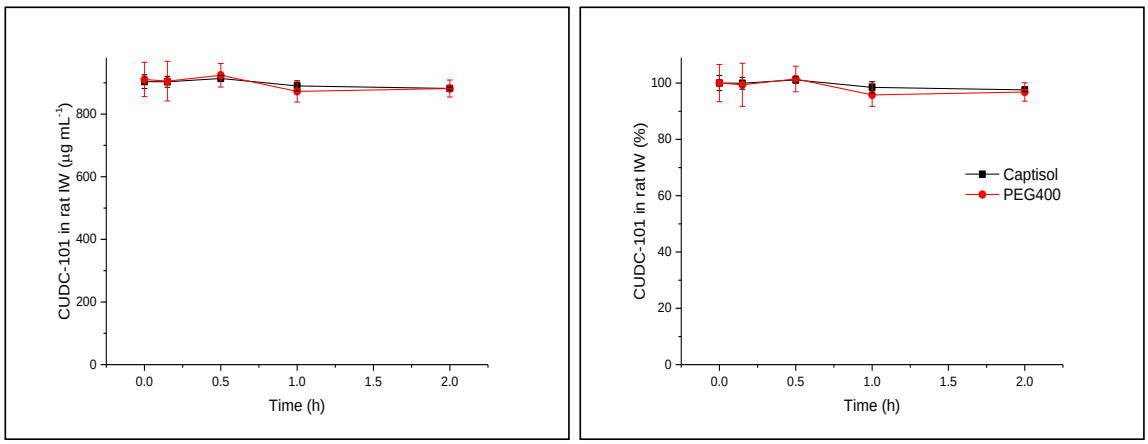

Figure 4.8 Stability of CUDC-101 in rat intestinal wash

a) Expressed as concentration and b) percentage drug in the whole rat intestinal wash. A known concentration of CUDC-101 as either 30 % Captisol or PEG400 solution was spiked SIF and change in drug concentration was analysed at particular time point. Any change in drug concentration was interpreted as degradation of the drug SIF. Results indicate that CUDC-101 is not degraded in SIF (n = 3).

4.4.1.4 Stability in Liver homogenate

The degradation experiments carried out in liver homogenate revealed a significant decrease in drug level of up to 40% in first 30 min and a massive 80% after 4 hours (Figure 4.9). The metabolite level also increases gradually over this 4 hours period, indicating a significant metabolic activity of liver enzymes on the drug. Both the formulations followed exactly the same pattern of degradation. Since CUDC-101 is a P-gp substrate, it is also a substrate for CYP340 family of metabolic enzymes[220], which explains this scale of degradation. The degradation of CUDC-101 in the liver might cause a substantial reduction in the drug's bioavailability.

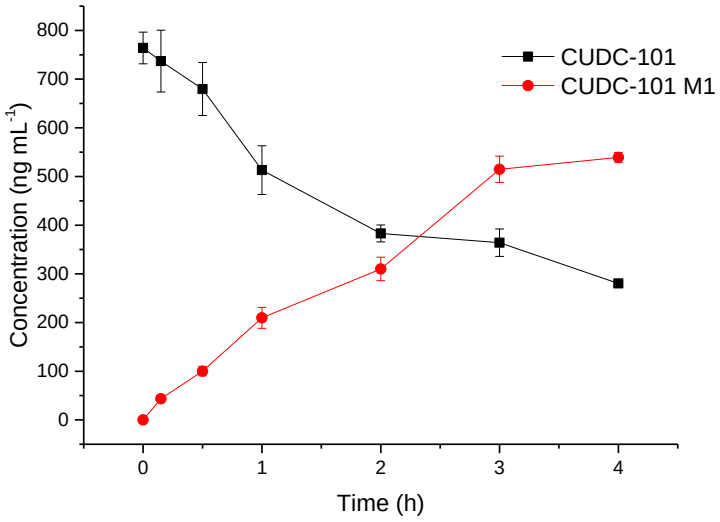

Figure 4.9 Stability of CUDC-101 in rat liver homogenate

A known concentration of CUDC-101 as a solution of DMSO was incubated in rat liver homogenate at 37 °C. Results indicate that the liver enzymes extensively metabolize CUDC-101 as the drug level (■) drops rapidly while the metabolite level (•) increases (n = 3).

4.4.1.5 Stability in Plasma

4.4.1.5.1 Plasma stability at 37°C

The drug was spiked in plasma and incubated at 37°C for a period of 2 hours. The results (Figure 4.10) showed that there is a 15% drop in drug level within an hour and 30% drop in drug level over 2 hours. There was also a substantial

increase in metabolite levels during the course of the experiment. This degradation of drug in plasma might also play an important role in limiting the bioavailability[51].

4.4.1.5.2 Plasma stability on storage at -20°C

The samples were stored at -20°C for a period of 7 days and periodically analysed for drug content (Figure 4.11). There was a clear drop in drug level (80% drop) within a day when the samples were stored at -20°C but the metabolite level remains the same even for seven days. This might be due to non-specific binding of hydrophobic drug to plasma proteins at -20°C.

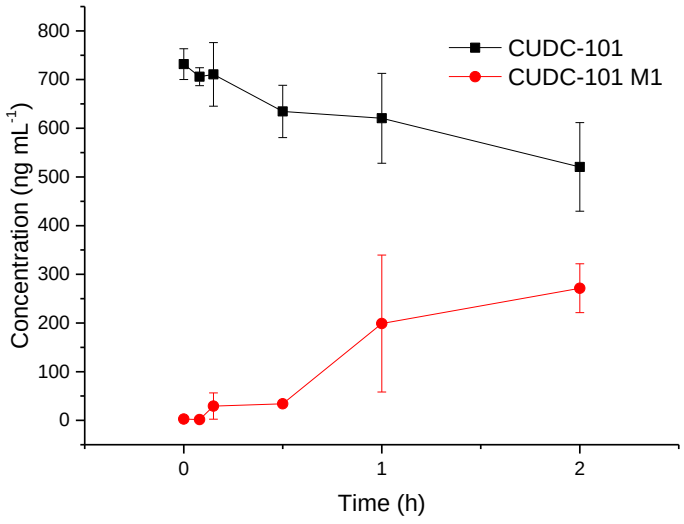

Figure 4.10 Stability of CUDC-101 in plasma

A known concentration of CUDC-101 as a solution of DMSO was incubated in neat plasma at 37 °C. Results indicate that the CUDC-101 is slightly degraded in plasma as the drug level (■) drops gradually while the metabolite level (•) increases slightly (n = 3).

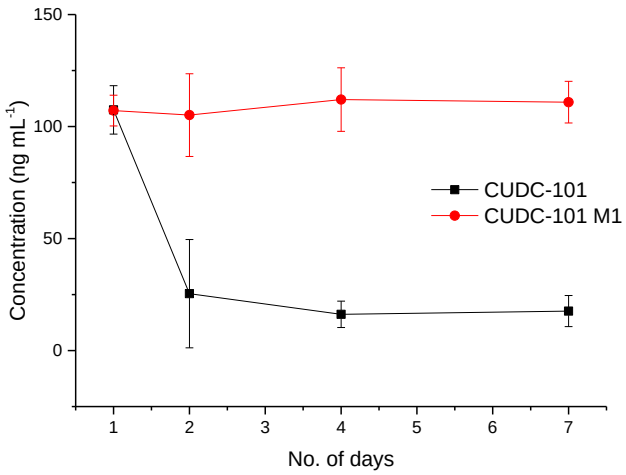

Figure 4.11 Storage stability of CUDC-101 in plasma at -20°C

A known concentration of CUDC-101 and CUDC-101 M1 as DMSO solution was spiked in neat plasma. Changes in the drug and metabolite levels were monitored over a period of time and the drug level dropped significantly within a day while on storage at -20 °C, while the metabolite level remained constant (n = 3).

4.4.1.5.3 Plasma Stability on storage at -80°C

The samples were stored at -80°C for a period of 7 days and periodically analysed for drug content (Figure 4.12). There was no significant change in drug levels during the course of this experiment, suggesting that the drug is stable when stored at -80°C.

4.4.1.5.4 Stability of plasma extracted sample at room temperature

Freshly prepared plasma standards were extracted with ACN and were left at room temperature for 7 days and drug contents were analysed periodically. The CV value calculated from the mean and SD values (Table 4.6) suggests that the drug and metabolite samples were stable for at least 7 days (A CV value less than 20% for lower limit of quantification (LoQ) and 15% for other concentration is considered as stable[221]). According to the data, there was a slight change in drug concentration at 10 ng ml^{-1} standards (CV of 22%) and this is mainly due to the samples run on day 7. This suggests that the plasma samples are stable for at least 4 days when left on the auto sampler, once extracted with ACN, which gives us sufficient time to analyse the samples with LC-MS.

Table 4.6 Storage stability of CUDC-101 plasma extraction samples (n = 3)

Samples ng/ml	Drug peak area ratio			Metabolite peak area ratio		
	Mean	SD	CV %	Mean	SD	CV %
Std 10	0.075	0.017	22.440	0.132	0.010	7.770
Std 20	0.131	0.0184	13.985	0.264	0.017	6.477
Std 40	0.273	0.027	10.156	0.534	0.035	6.565
Std 200	1.498	0.084	5.623	2.463	0.083	3.374
Std 400	2.720	0.348	12.796	4.411	0.382	8.674

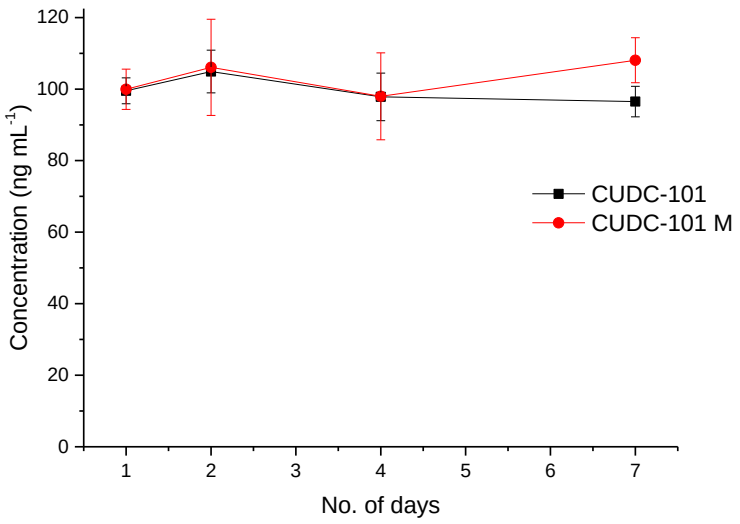

Figure 4.12 Storage stability of CUDC-101 in plasma at -80°C

A known concentration of CUDC-101 and CUDC-101 M1 as DMSO solution was spiked in neat plasma. Changes in the drug and metabolite levels were monitored over a period of time and the both their concentration remained stable on storage at -80 °C for a period of 7 days (n = 3).

From the whole plasma stability experiment, we can infer that the samples collected from PK studies must be extracted with ACN immediately. If at all the samples must be stored due to unavoidable situations, they should be stored at -80°C. The question of sample degradation on the auto sampler is ruled out (at least for 4 days), giving us a good deal of time to finish the analysis.

4.4.1.6 Oral pharmacokinetic studies

The oral pharmacokinetic (PK) profile of CUDC-101 Captisol formulation and PEG400 solution is shown in Figure 4.13. Drug absorption is seen only at the early time point (T_{max} 0.25h) and drug levels drop to negligible amounts at subsequent time points. This might be due to the fact that the drug is poorly soluble at intestinal pH as demonstrated by the *in vitro* experiments. High drug levels only at early time point also suggests that the drug is absorbed from the gastric epithelium[222], where the drug is in solution.

The metabolite level also followed the same trend as that of the drug level - high at early point (T_{max}) and negligible after 2 hours - implying there was no drug available for the liver to metabolise. The metabolite to drug ratio was 0.52 and 1.14 at the initial time point for Captisol and PEG400 formulation respectively, demonstrating high hepatic metabolism as predicted from the *in vitro* results. From the preliminary PK experiment, it is inferred that, the precipitation of drug at intestinal pH might be a major reason for poor oral absorption of CUDC-101. Our formulation strategy was then focused on stabilising the drug against precipitation at the pH of 6.8.

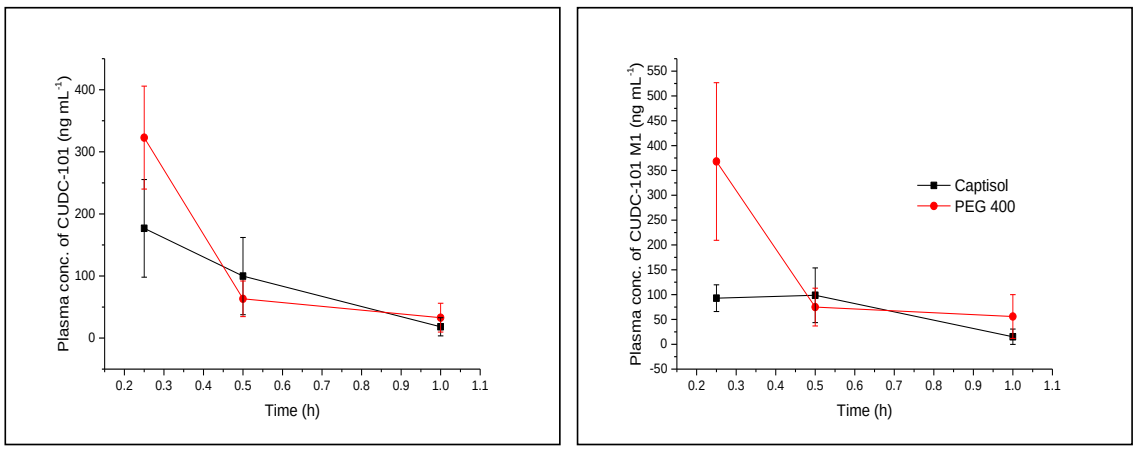

Figure 4.13 Preliminary oral pharmacokinetic experiment of CUDC-101

Mice plasma levels of; a) CUDC-101 and b) CUDC-101 M1 following the oral administration of CUDC-101 as 30 % Captisol and PEG400 solutions. Drug absorption happens only for initial 30 minutes. (Dose – 100 mg kg^{-1}; n = 4).

Since CUDC-101 is also a P-gp substrate (Curis own data), oral absorption studies were also conducted in mice in the presence of a P-gp inhibitor Verapamil. Verapamil prevents the P-gp efflux of other drugs due to its strong affinity to P-gp[48] as a P-gp substrate. So in the presence of verapamil, the absorption of CUDC-101 should be increased. This is confirmed by our results (Figure 4.14 and Figure 4.15), where at initial time points we do see some increase in CUDC-101 uptake but at later time points (2 hours) the drug levels were below the limit of detection. This is again due to the fact that the drug precipitates at intestinal pH and is therefore unavailable for absorption. Paclitaxel (formulated as Taxol), a BCS class IV drug was used as a positive control for this experiment, where we can see enhanced absorption of the drug in the presence of verapamil even at later time points (Figure 3.3). This is because unlike CUDC-101, paclitaxel formulated as Taxol has high dissolution and better solubility in both SGF and SIF and thus has a prolonged window of absorption. We also observed that at a higher dose of paclitaxel verapamil made no difference to the drug's absorption, because of dose-dependent saturation of the activity of the P-gp efflux pumps with excess substrate[171].

From these results, we understand that poor solubility of CUDC-101, particularly around neutral pH is the major factor limiting its oral absorption. Extensive metabolism in liver may also affect the drug's overall bioavailability. P-gp efflux is another important factor affecting the drug's absorption but from our experiment with paclitaxel, we learnt that it is possible to saturate the P-gp pumps by a combination of enhanced dissolution and increasing the dosage of the substrate drug. Thus, improving the dissolution at intestinal pH will be the major focus in oral formulation development of CUDC-101.

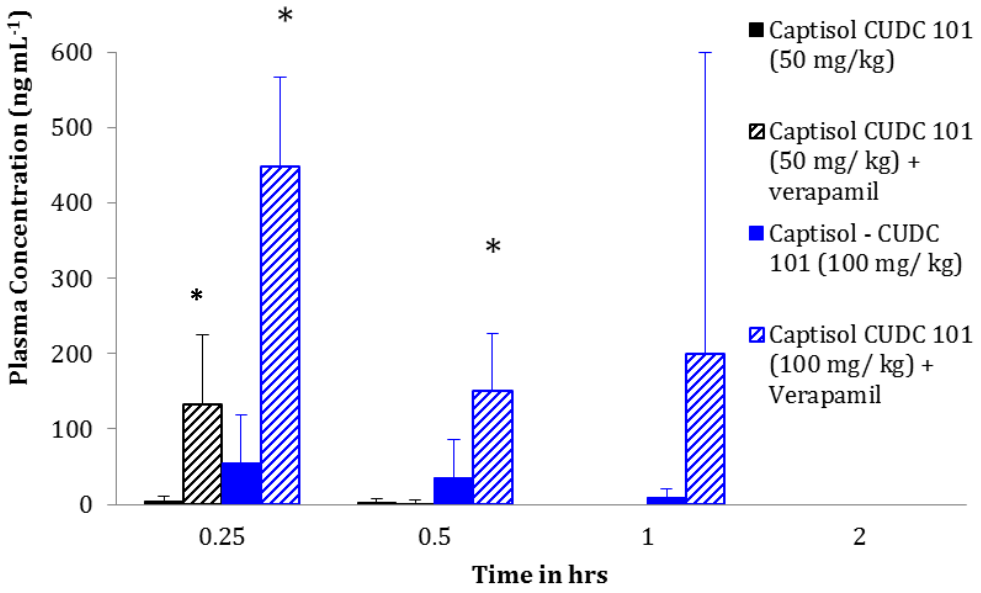

Figure 4.14 Oral absorption of CUDC-101 in the presence of verapamil

Verapamil improves the absorption of CUDC-101 only at initial time points when the drug is in solution. * = $p < 0.05$ and significantly different from Captisol – CUDC 101 without verapamil. (Verapamil dose = 100 mg kg^{-1}; n = 4). Statistics used - Two-way ANOVA with Bonferroni's test.

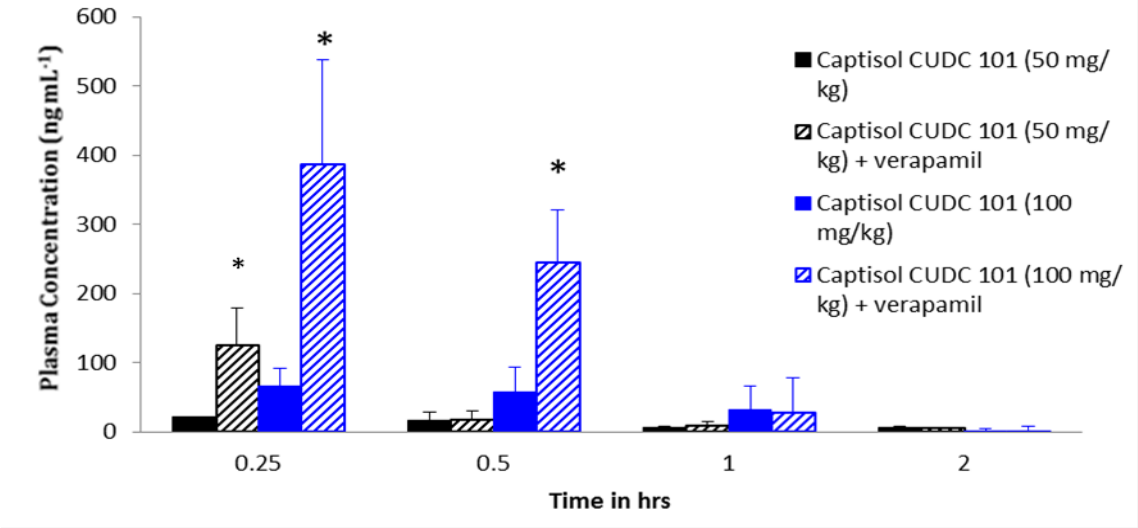

Figure 4.15 Plasma levels of CUDC-101 M1 following the oral administration of CUDC-101 with verapamil

Plasma levels of CUDC-101 M1 follow the same trend as that of the drug level. * = $p < 0.05$ and significantly different from Captisol – CUDC 101 without verapamil. Statistics used - Two-way ANOVA with Bonferroni's test (n = 4).

4.4.1.7 Inferences from preliminary studies

Drug upon ingestion is mixed thoroughly in the stomach (chyme), where it is exposed to harsh acidic conditions alongside with proteolytic enzymes[223]. The maximum residential time for the chyme in stomach is around 2 hours after which it is emptied into the small intestine. Once in the gut, the pH around the drug increases to mild alkaline due to the action of secretions from bile and pancreas[223]. The drug is then absorbed into the blood stream through microvilli and directly transported to liver. While passing through the liver, the drug is metabolised by various classes of liver enzymes and what remains then reaches the systemic circulation. While in the plasma, the drug might get recognized by plasma proteins as a foreign entity, which then binds the drug and transports it to kidney for excretion[223].

For a hydrophobic drug to reach the systemic circulation, it has to remain in solution while in the digestive tract, survive P-gp efflux and liver metabolism. pH variations in the digestive tract and the physiochemical properties of the drug sometimes make the oral absorption of the drug very challenging. Formulation strategies are followed to overcome these challenges and it is very important to identify the key issues limiting the absorption of the drug. Thus, preliminary experiments were carried out on CUDC-101 to identify the key issues, so that a systematic approach to formulation design may be followed.

Through the solubility experiments we have learnt the following: the drug has poor solubility at neutral pH, a solution of the drug is soluble in SGF but immediate precipitation of the drug occurs in SIF. DMSO, NMP, PEG400, PEG1000, PEG3350, 0.2 N NaOH are the possible solvents for CUDC-101. *In vivo* experiments demonstrated that the precipitation of drug at intestinal pH, P-gp efflux and liver metabolism are all reason for poor oral bioavailability of the CUDC-101.

Stability studies in plasma on storage and extraction gave information on storage of samples following the *in vivo* pharmacokinetic experiments. Samples degrade extensively when stored at -20°C and are stable for at least seven

days at -80°C. The samples are stable for at least 4 days, when stored on LC-MS auto sampler (after extraction with ACN).

From our preliminary experiments we found that the absorption of CUDC-101 is very poor after gastric emptying, where pH changes in the small intestine cause the drug to precipitate. From our experiments with Taxol, we also found that increasing the dissolution of the drug and increasing its dose saturates the P-gp pumps. Based on these observations, it was decided that the main formulation strategy would be to prevent the precipitation of CUDC-101 around neutral pH. This in turn will increase the solubility and dissolution of the drug in SIF/IW. The P-gp pumps can then be saturated by increasing the dose of the drug or co-administration with P-gp inhibitors, eventually improving the absorption of CUDC-101. Some CUDC-101 formulations were thus developed, which are discussed in detail in the following segment.

4.4.2 CUDC-101 – GCPQ nanoparticles

4.4.2.1 Encapsulation of CUDC-101 with GCPQ:

CUDC-101 was added to GCPQ with different characteristics, as shown in Table 4.7 and probe sonicated to form GCPQ – CUDC-101 nanoparticles. The encapsulation of CUDC-101 in different variants of GCPQ is given in Figure 4.16. There is an increasing trend in concentration of drug recovered as the molecular weight and palmitoylation of the GCPQ increases. High molecular weight polymer has a longer chain length, which results in complex chain entanglement forming interlinked clusters of micelles. Increase in palmitoylation will increase the hydrophobicity of the polymer, providing more hydrophobic pockets for the drug to solubilise. Moreover, increase in hydrophobicity and molecular weight will also reduce the CMC of the polymer, forming highly stable micelles in the aqueous environment. Thus a polymer with both these characteristics create a perfect mesh for the drug molecules to be trapped and encapsulated. Also, the protonated version of the polymer had slightly more drug encapsulated than the deprotonated version. This might be due to the pH differences between the protonated (pH ~ 3) and deprotonated polymer (pH ~ 6) in water, as CUDC-101 has slightly better solubility in acidic environment.

Table 4.7 Characteristics of GCPQ used for encapsulation studies

	Batch name	Pamitoylation (%)	Quarternisation (%)	M_w (Da)
Polymer 1	Q48 100413 KC*	18	5	10830
Polymer 2	Q48 101111 SR	18	9	9470
Polymer 3	Q24 050213 SR	18	6	16440
Polymer 4	Q2 090313 SR	11	11	48130
Polymer 5	Q2 150909 AL*	21	11	55460
Polymer 6	Q2 220213 SR	19	13	70130

*Deprotonated primary amines

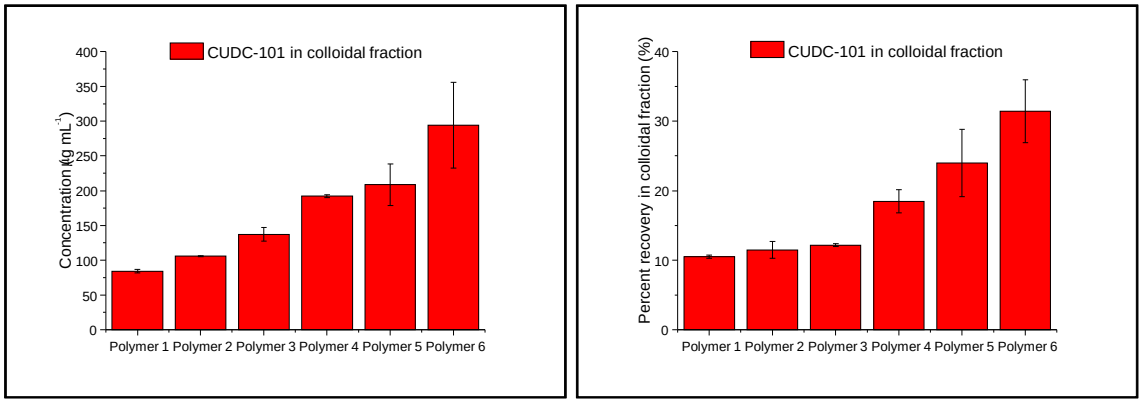

a b

Figure 4.16 CUDC-101 encapsulation by GCPQ

Expressed as concentration of drug (a) and percentage of drug (b) in colloidal fraction. CUDC-101 (1 mg mL^{-1} in water) was probe sonicated with various GCPQ polymers (10 mg mL^{-1}) and drug concentration was measured in colloidal fraction immediately (n = 3).

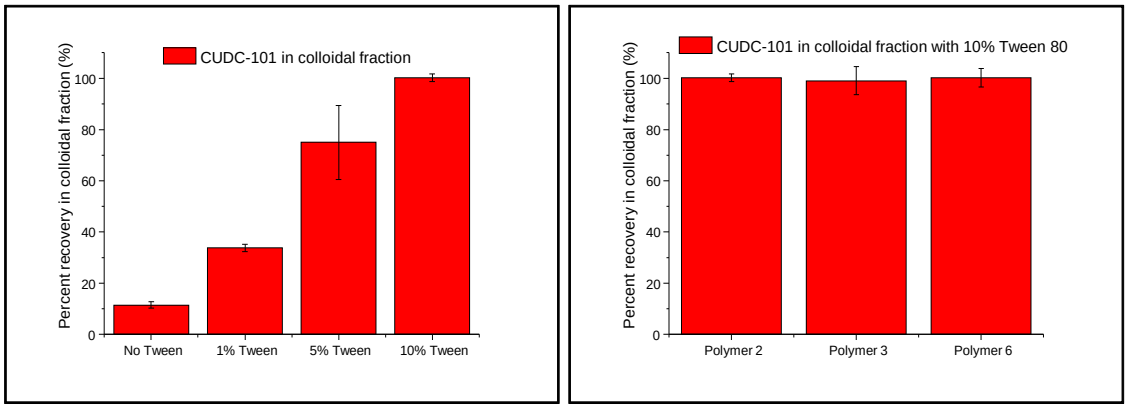

a b

Figure 4.17 CUDC-101 encapsulation by GCPQ in the presence of Tween80

a) Encapsulation of CUDC-101 by GCPQ polymer 2 in the presence of Tween 80. Increasing the concentration of Tween 80 increases the encapsulation efficiency. b) Encapsulation of CUDC-101 by various GCPQ polymers with 10 % Tween 80. Presence of Tween 80 eliminates the variation in encapsulation efficiency caused by differences in characteristics of GCPQ. CUDC-101 concentration 1 mg mL^{-1} in water; GCPQ concentration 10 mg mL^{-1} (n = 3).

There were no differences in the encapsulation of CUDC-101 between the high and low molecular weights of GCPQ when a co-surfactant was added. From Figure 4.17 after adding 10% Polysorbate 80 (Tween 80), the recovery of CUDC-101 in colloidal fraction was 100%. Reducing the concentration of Tween 80 reduced the drug recovery clearly showing a trend. The surfactant might reduce the interfacial tension aiding in encapsulation but it should also be noted that the surfactant is also capable of solubilizing CUDC-101, which in turn will increase the recovery of drug in colloidal fraction. Using Cremaphor RH40 instead of Tween 80 also yielded the same result and thus GCPQ formulation 1 was developed using Cremaphor RH40, as the drug has slightly better solubility in Cremaphor RH40 in comparison with Tween 80. TEM image of this formulation revealed the presence of nanometer sized droplets and micellar structures of GCPQ in the background (Figure 4.18a).

Adding a solution of CUDC-101 (CUDC-101 dissolved in water miscible solvents) to a suspension of GCPQ also resulted in the formation of GCPQ –

CUDC-101 nanoparticles (Figure 4.18b). The CUDC-101 solutions of PEG400, DMSO and 0.2 M NaOH were used for this purpose and all these solution formed nanoparticles with GCPQ but the stability of the nanoparticles with PEG400 and DMSO was very poor, with drug precipitating within 30 minutes of the preparation. Whereas, the nanoparticles formed by mixing 0.2 M NaOH to GCPQ in water had a stability of around 2 hours at pH 6.8. The stability of the nanoparticles was further increase by adding the crystal growth inhibitor polyvinylpyrrolidone (PVP K 15, 0.08% in final volume) and this was eventually developed into GCPQ formulation 2, wherein the 0.2 M NaOH solution of the drug is neutralised by a 0.2 M HCl dispersion of GCPQ. The advantage with this formulation is that it can be easily freeze dried and developed into a solid dosage form, as there are no organic solvents or involatile surfactants involved but disadvantage being salt produced as a by-product might cause side-effects in patients.

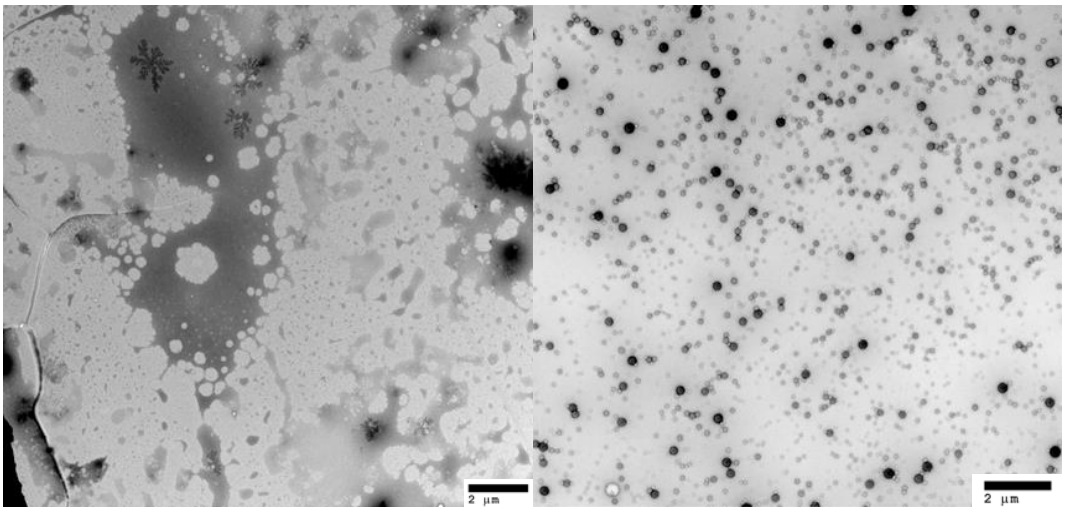

Figure 4.18 TEM images of GCPQ - CUDC-101 formulations

TEM images of a) GCPQ formulation 1 (no vesicular structures visible) and b) GCPQ formulation 2 (GCPQ – CUDC-101 nanoparticles are observed).

4.4.2.2 In vitro results:

The stability of GCPQ formulation 1 and 2 were much better than that of Captisol formulation in IW (Figure 4.19). The GCPQ formulations were stable in IW for at least 4 hours, while Captisol formulation precipitated within 10 minutes

and thus our aim of producing a stable formulation in intestinal fluids was achieved. But the stability of these GCPQ formulations in SGF was poor in comparison with that of Captisol formulation. GCPQ formulation 1 had a better SGF stability than that of GCPQ formulation 2. The presence of salt in SGF might cause salting out effect on GCPQ but the effect of pH on the stability of formulation cannot be ignored as shown in Figure 4.20. As seen from the figure the stability of GCPQ formulation 2 gets better with increase in pH and the main reason for this might be the physicochemical property of CUDC-101 under these pH conditions. The poor stability in SGF might be due to protonation of GCPQ at acidic pH, which reduces the hydrophobicity of the polymer, leading to drug precipitation.

Swapping GCPQ with GCPh in formulation 2 also resulted in nanoparticles but did not contribute much to improve the stability of the formulation in SGF, so does increasing the ratio of drug to GCPQ from 1:3 to 1:10 (Figure 4.21). Since GCPQ formulation 2 can be freeze dried, it was proposed to enteric coat this formulation in order to overcome its poor stability in SGF. Figure 4.22 shows the dissolution pattern of enteric-coated GCPQ formulation 2 capsules in SGF and SIF. The enteric-coating was intact in SGF and therefore no drug was released from these capsules. In SIF the enteric-coating of the capsule with GCPQ formulation 2 gets dissolved, thus exposing the formulation to the dissolution medium. The formulation had a desirable release profile in SIF and these enteric-coated GCPQ nanoparticles might have a better *in vivo* pharmacokinetic release profile. Thus one of our criterions for success was achieved, which was to develop a CUDC-101 formulation that is stable under intestinal pH conditions. This would help to stabilise the drug in its molecular form which is essential for absorption.

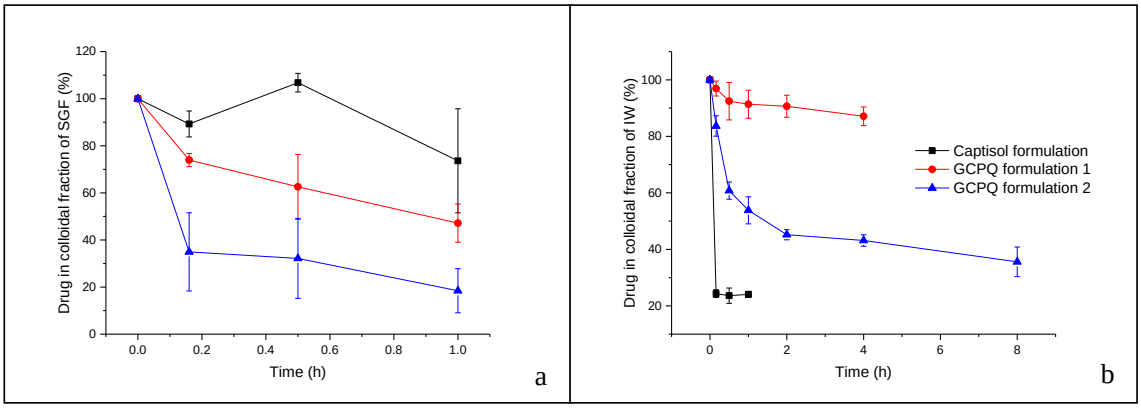

Figure 4.19 Stability of GCPQ - CUDC-101 formulation in dissolution medium

Stability of CUDC-101 formulations in a) SGF and b) IW. The Captisol formulation has better stability in SGF while the GCPQ formulations have better stability in IW. Concentration of CUDC-101 in SGF/IW at the beginning of the study was 1 mg mL^{-1} (n = 3).

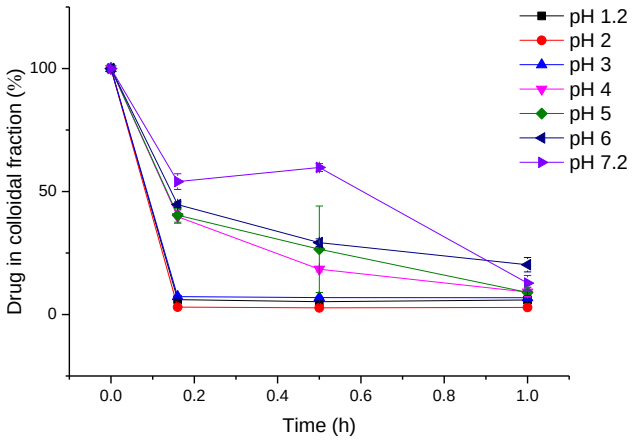

Figure 4.20 Stability of GCPQ formulation 2 at different pH

Freshly made CUDC-101 – GCPQ formulation 2 (200 µL) was spiked in phosphate buffer (10 mM, 800 µL) at different pH conditions. The colloidal stability of the CUDC-101 – GCPQ nanoparticles were monitored at various time points. Results indicate that the formulation has poor stability at low pH conditions, which improves with increase in pH. Final concentration of CUDC-101 = 1 mg mL^{-1}; GCPQ = 2 mg mL^{-1} of phosphate buffer (n = 3).

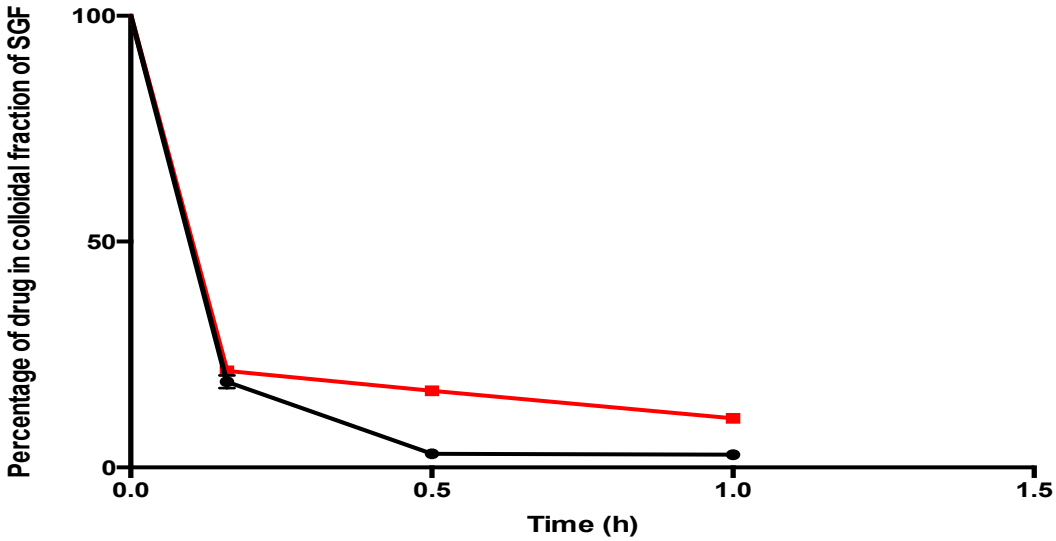

Figure 4.21 Stability of CUDC-101 nanoparticles in SGF with GCPh/GCPQ

Stability of CUDC-101 formulations with GCPh (■) and GCPQ (•) at drug to polymer ratio of 1:5. Increasing the polymer concentration or using GCPh didn't improve the stability of the nanoparticles in SGF. Initial concentration of CUDC-101 = 1 mg mL^{-1} (n = 3).

4.4.2.3 *In vivo* results:

In vivo, the oral absorption of CUDC-101 from both the GCPQ formulations was poor. Though the *in vitro* stability of GCPQ formulation 1 was satisfactory, the formulation's *in vivo* pharmacokinetics was very poor Figure 4.23. CUDC-101 metabolite levels were also very low, indicating that the drug absorption was negligible. Various factors such has the pH differences in the stomach, presence of food, salt etc. could affect the *in vivo* stability of the nanoparticles in the formulation. One or a combination of all these factors could result in drug precipitation, which eventually leads to poor oral absorption.

On the other hand, enteric-coated capsules of GCPQ formulation 2 could not be administered to rats at desired dose, due to practical constraints in oral dosing. Restrictions by the Home Office limit the number of capsules that can be given to rats. Hence, approximately only two-fifth of the desired dose (~ 21 mg kg^{-1}) could be given to each rat but the presence of P-gp pumps and high metabolic activity means that the absorption was very poor (Figure 4.24). A Captisol CUDC-101 control at similar dose (20 mg kg^{-1}) also has poor absorption profile even at initial time points, proving that the dose is not sufficient enough to

overcome the P-gp efflux and liver metabolism. Thus it was not possible to study the pharmacokinetics of GCPQ formulation 2 in rat models due to dosing constraints.

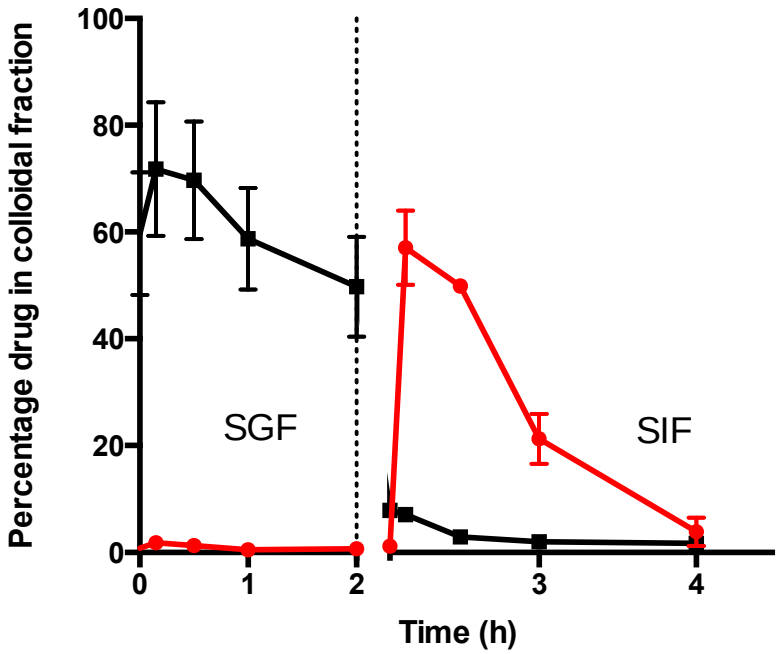

Figure 4.22 Dissolution of enteric-coated GCPQ formulation 2 in SGF and SIF

CUDC-101 – GCPQ formulation 2 (•) was freeze-dried and enteric coated in a capsule. Freeze-dried CUDC-101 Captisol formulation (■) was also packed in a capsule. The capsules were incubated in 5 mL of SGF and the dissolution of CUDC-101 from both these formulations was monitored. After 2 hours, the enteric-coated capsule containing GCPQ formulation 2 and new CUDC-101 Captisol capsules were transferred to 5 mL SIF in separate containers and the dissolution of CUDC-101 was monitored. The release of CUDC-101 from GCPQ formulation 2 was negligible due to the protective enteric coating, while CUDC-101 from Captisol had good dissolution. When transferred to SIF, the GCPQ formulation had good dissolution as the enteric coating fades away but the Captisol formulation had poor dissolution due to the precipitation of CUDC-101 from Captisol around the pH of 6.8. Initial concentration of CUDC-101 = 1 mg mL^{-1} of dissolution medium (n = 3).

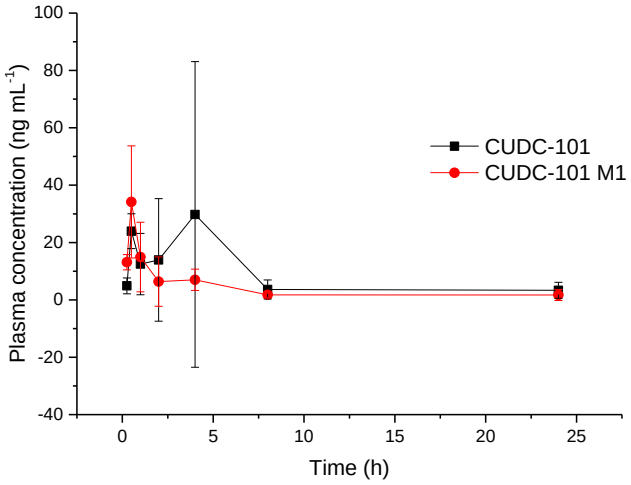

Figure 4.23 Oral PK results of GCPQ formulation 1

Mice plasma levels following the oral delivery of CUDC-101 – GCPQ formulation 1 containing CUDC-101 (5 mg mL^{-1}), GCPQ (19 mg mL^{-1}, Q48 111111 SR), Cremaphor RH (125 µL mL^{-1}). Dose 50 mg kg^{-1}; (n = 5).

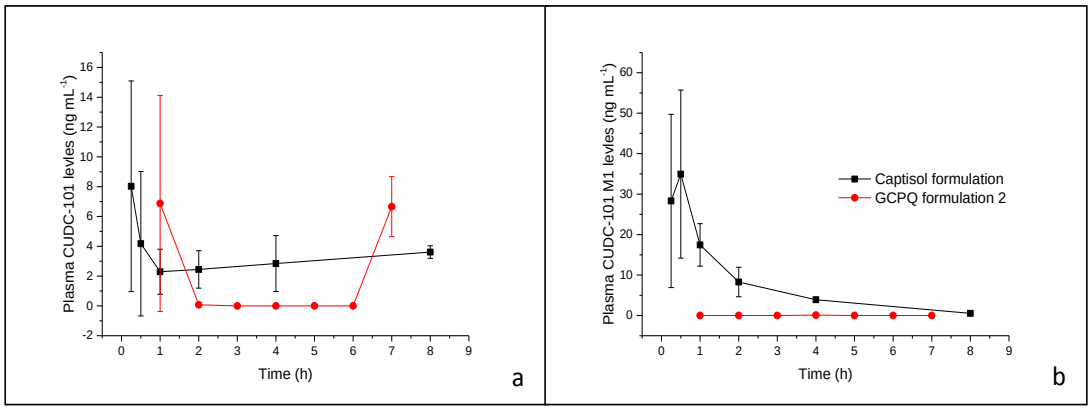

Figure 4.24 Oral PK results of enteric-coated GCPQ formulation 2

Rat plasma levels following the oral administration of capsules containing CUDC-101 – GCPQ formulations 2 and CUDC-101 – Captisol formulation; a) plasma drug levels and b) plasma metabolite levels (Dose of CUDC-101 = 20 mg kg^{-1}; n = 3-4).

4.4.3 Gastro-retentive dosage form:

4.4.3.1 In vitro release testing:

The PEG3350 (PEG) CUDC-101 solution was mixed to PEO5000000 (PEO) in different ratios and the release of CUDC-101 from this formulation was measured in SGF. The release of the drug from these capsules were proportional to the amount of PEO in the formulation, wherein 1:1 (PEG:PEO w/w ratio) mixture gradually released the entire drug load in 4 hours, while 1:1.5 and 1:2 ratios had very slow release profile as shown in Figure 4.25. The formulation without PEO released the entire drug load within 30 minutes demonstrating the importance of PEO in the formulation. The presence of very high molecular weight PEO in the formulation creates a viscous hydrophilic environment, which gelates the outer layer. Inside this gelatinous layer are the trapped PEG3350 and air molecules, which make the dosage form, float. Gradually, the dosage form is completely hydrated and the PEO molecules that are packed inside the gelatinous layer start to swell, creating a porous gelatinous floating matrix. As the outer gelatinous layer erodes, it exposes the trapped PEG3350, which then releases the solubilised CUDC-101 into the surrounding medium. The erosion is faster when there are less PEO molecules and so does the rate of drug release.

While slow and gradual drug release is preferred for most of the therapeutics, it may not be advantageous for CUDC-101 oral uptake due to P-gp efflux. Our aim is to saturate the P-gp pumps with excess drug and a slow release formulation might not serve this purpose. Nevertheless, it might be informative to run a PK experiment so, PEG3350:PEO 1:1 formulation with relatively faster drug release was selected for this purpose.

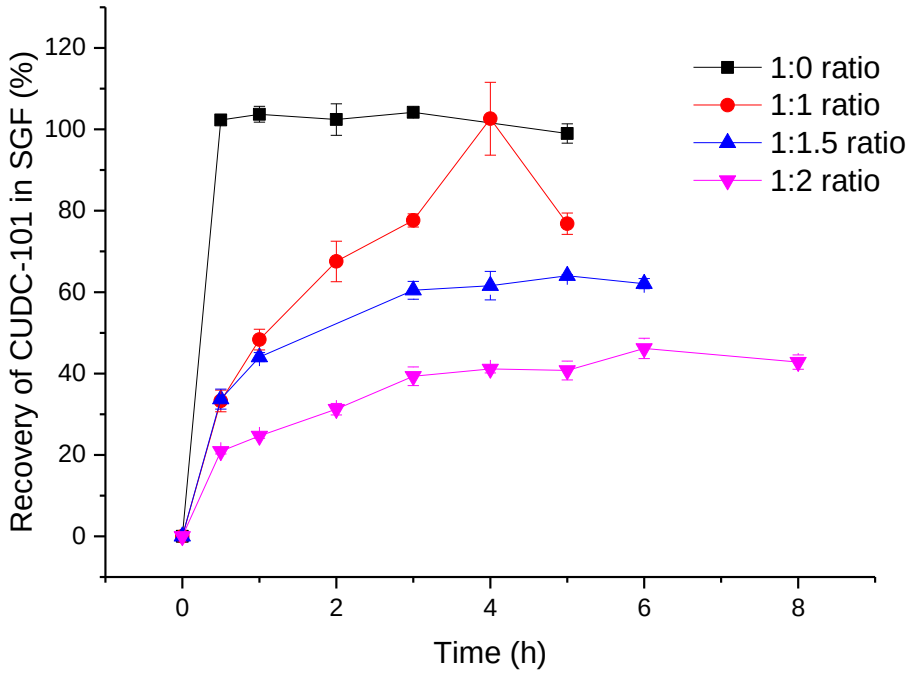

Figure 4.25 *In vitro* drug release profile of gastro-retentive dosage form in SGF

Release of CUDC-101 from PEG:PEO gastro retentive dosage forms at different ratios of PEO to PEG3350 solid solution of CUDC-101. A solid solution of CUDC-101 in PEG3350 (100 mg mL^{-1}) was mixed with PEO at the following PEG3350 to PEO ratios; 1:0, 1:1, 1:1.5 and 1:2. Concentration of CUDC-101 in 10 mg of these formulations was calculated using RP-HPLC and a known volume of this mixture were tightly packed in a size 0 capsule. The capsules (n = 3) were suspended in SGF (50mL) and drug release was monitored over time.

4.4.3.2 *In vivo* studies:

Dosing restrictions by the Home Office means that only 17 mg kg^{-1} against the intended dose of 50 mg kg^{-1} was given to the rats. Low dose and other reasons such has slow release, P-gp efflux and liver metabolism, the concentration of the drug in plasma was negligible at all the time points, except at 4 hours (Figure 4.26). At 4 hours, we observe some drug level, which is similar to that of the Captisol – CUDC-101 formulation at an equivalent dose. The metabolite levels are higher than the drug levels for both these formulations and it follows the similar trend. This demonstrates the extent of CUDC-101 first-pass

metabolism, where low concentrations of the drug are completely metabolised by the liver. The presence of metabolite in plasma at 4 hours is encouraging as this proves that the gastro-retentive dosage forms can prolong the absorption of CUDC-101. The T_{max} for drug and metabolite for the gastro-retentive dosage form is at 4 hours, while the T_{max} for the Captisol formulation is at 30 minutes. This might serve as a proof of concept for our gastro-retention hypothesis but the plasma drug levels are just around 15 ng mL^{-1}, which is close to the limit of quantification. Yet it might help to prove our hypothesis with confidence if this formulation is dosed to large animal models, where we can give the desired dose without any constraints.

Even though we were able to develop stable formulations in both SGF and SIF (success criteria 1), the target plasma concentration of 500 ng mL^{-1} CUDC-101 couldn't be achieved (success criteria 3). This might be due to a combination of factors such as not able to achieve the target dose (success criteria 2), P-gp pump efflux and high first-pass metabolism.

4.5 Discussion:

The oral absorption of CUDC-101 is generally poor and highly variable. The main reason for this poor pharmacokinetics is a combination of poor solubility, P-gp efflux and high first-pass metabolism. Preliminary experiments with the already available Captisol – CUDC-101 formulation yielded valuable information on the drug's oral pharmacokinetic behaviour. Our experiments on P-gp efflux with Paclitaxel (Chapter 3) established a relationship between the drug's *in vivo* dissolution and its P-gp efflux, where enhancing the dissolution of the drug overwhelmed its P-gp efflux. Based on all these information, it was concluded that the solubility/dissolution is the key factor in dictating a drug's absorption and developing a gut soluble formulation is the first step towards enhancing the drug's oral bioavailability. After few preliminary experiments, CUDC-101 formulations were rationally designed with improved dissolution in the form of GCPQ nanoparticles and gastro-retentive dosage form.

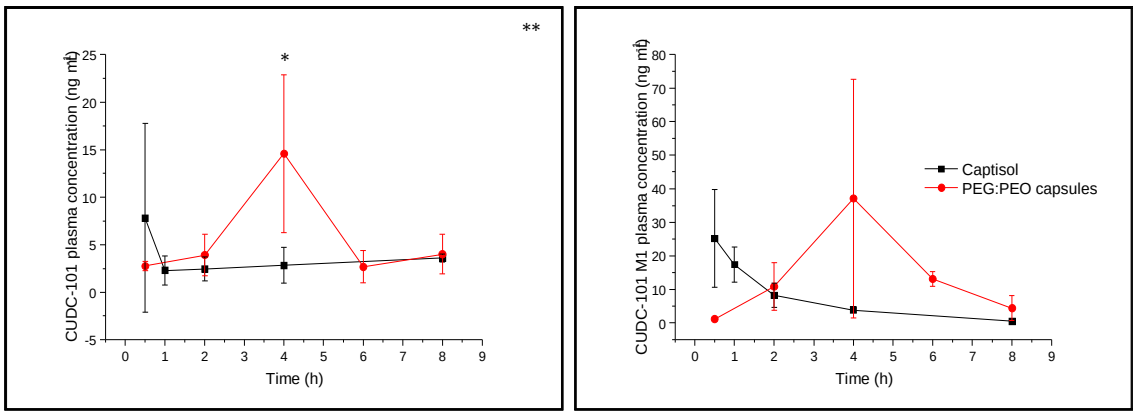

a b

Figure 4.26 PK profile of CUDC-101 gastro-retentive dosage form

Plasma levels of a) CUDC-101 and b) CUDC-101 M1 following the oral administration of CUDC-101 gastro-retentive dosage form (PEG:PEO 1:1 capsules) and liquid CUDC-101 Captisol formulation at 17 mg kg^{-1} (n = 4). ** CUDC-101 plasma levels of PEG:PEO formulation significantly different from that of Captisol formulation. * CUDC-101 plasma levels significantly different at that time point. (Two-way repeated measures ANOVA with Bonferroni's test $p < 0.05$).

GCPQ, a polymeric amphiphile has been previously shown to improve the dissolution and oral bioavailability of hydrophobic drugs[75,177]. Hence, a polymeric nanoparticle formulation for CUDC-101 was developed with GCPQ. The encapsulation of CUDC-101 by GCPQ was dependent on the molecular weight and palmitoylation level of the polymer (Figure 4.16). This is because the hydrophobicity of the polymer increases with increase in palmitoylation. Also high hydrophobicity coupled with longer chain length provides an entangled network of hydrophobic pockets, which provides a thermodynamically favourable environment for the interaction of hydrophobic drugs. Similar results have been noted in other polymeric amphiphiles such as PLGA[155], poly-L-lysine – cholate graft polymer[224], poly(ε-caprolactone)[225] etc, where increasing the hydrophobicity of the polymer improved its encapsulation efficiency. In general the drug loading in polymeric amphiphiles are affected by polymer characteristics[226], compatibility between the hydrophobic drug and polymer's hydrophobic units[227] and also by the physicochemical properties of the drug[228]. Addition of other excipients will also have a profound effect on the

encapsulation of CUDC-101 by GCPQ. When added with Tween80, the encapsulation of CUDC-101 was increased to 100 % irrespective of the polymer characteristics (Figure 4.17). This might be due to the solubilising effect the surfactant might have on CUDC-101 and also due to the surface-active properties of Tween80 that helps better dispersion of the drug in the aqueous environment. Similar results were observed in nimsulide – PLGA nanoparticle, where addition of surfactants such as vitamin E-TPGS and poly(vinyl alcohol) increased the encapsulation efficiency of the PLGA system up to 90 %[229].

The GCPQ – CUDC-101 nanoparticles that were developed was tested for *in vitro* stability in bio relevant mediums. The formulation displayed good stability in SIF, which was indeed a major milestone for CUDC-101 considering its extremely hydrophobic nature. But, the stability of these nanoparticles were poor in SGF, where the drug precipitated up on exposure to low pH conditions. This poor stability affected the *in vivo* absorption of CUDC-101 (Figure 4.23). GCPQ nanoparticles were previously used to enhance the oral uptake of few hydrophobic drugs[75,177]. The C_{max} of cyclosporine A, a BCS Class IV drug, was enhanced 5-folds by using GCPQ nanoparticles when compared to that of the free drug[75]. The enhancement of cyclosporine A uptake was mainly attributed to the increased aqueous dissolution of the drug when formulated as GCPQ nanoparticles along with the mucoadhesive properties of GCPQ[75].

The poor absorption of GCPQ – CUDC-101 nanoparticles were due to poor stability of the formulation in SGF. Hence the nanoparticles were freeze-dried and the solid dosage form was enteric-coated to avoid the release of the nanoparticles in the stomach. Similar studies were done with 5-fluorouracil – chitosan nanoparticles, which were freeze-dried and coated with Eudragit S-100[230]. The enteric coating was done to prevent the degradation of drug in the stomach and also to target the drug release to the large intestine, as the drug is used to treat colorectal cancer[230]. Similar studies are found in the literature with several other polymeric nanoparticles, which were also enteric coated to prevent the release of the drug in the gastric environment[231,232]. The enteric-coated GCPQ – CUDC-101 nanoparticle had the desired *in vitro* stability but failed *in vivo* in rat models due to inadequate drug concentration in the final dosage forms. The freeze-dried nanoparticles were manually filled in size 9

capsules, which were then coated with Eudragit L100-55, thrice. Two such capsules were orally dosed to rats but the maximum dose that was possible to achieve was 20 mg kg^{-1} of CUDC-101, which is not enough to overcome the P-gp efflux or liver metabolism. There are several studies confirming the validity of enteric-coated size 9 capsules[233,234] used in our experiment. But some authors also suggest manually reducing the size of enteric-coated size 9 capsules in order to facilitate gastric emptying[235]. But since we could not find any capsule matter in the stomach after the 'post-mortem' following the oral administration of enteric-coated capsules filled with GCPQ formulation 2, it is safe to assume that the capsules reached the small intestine. Thus the poor oral absorption of CUDC-101 from this formulation is mainly due to very low dose of the active ingredient in the dosage form.

Another strategy to improve the oral absorption of CUDC-101 was to develop a gastro-retentive dosage form. The idea stems from the observation of preliminary results (Figure 4.13), where the drug absorption happens only when the formulation is in the stomach. Thus if we prolong the retention of the formulation in stomach, it will lead to improved absorption of CUDC-101. Hence, a PEG3350:PEO swelling/floating device was designed for the delivery of CUDC-101. The release rate of CUDC-101 from this formulation was dependent on the concentration of PEO in the dosage form (Figure 4.25). Similar observations were made by Prajapati et.al, where the release of domperidone, a hydrophobic drug, was controlled by the amount of PEO in the floating matrix[236]. The drug release in this formulation is mainly due to the erosion of the gelatinous PEO and the PEO also contributes to the swelling and floatation of the formulation. The plasma CUDC-101 levels in rats following the oral administration of PEG3350:PEO formulation was significantly better than that of the Captisol formulation of similar dose. Even though the results are significant, the maximum plasma concentration of CUDC-101 is just under 15 ng mL^{-1}, which is too little to produce a pharmacodynamic effect. This is mainly because CUDC-101 was not dosed at sufficient concentration to overcome the P-gp efflux and liver metabolism. The formulation was packed in 'size 9 extra long capsules', containing just 4 mg of CUDC-101. Only one such capsule can be dosed to a rat due to ethical considerations, which limits the final dose of

CUDC-101 to just 17 mg kg^{-1} per rat (approx. weight 200 g). The C_{max} and AUC of CUDC-101, from the PEG3350:PEO dosage form can be increased if the pharmacokinetic experiments are done in larger animal models, in which the dose of CUDC-101 can be increased due to large stomach volumes.

Gastroretention is a successful strategy for drug delivery if a) the drug's targeted site of action is stomach, b) the drug is specifically absorbed in the upper gastrointestinal tract or c) the drug degrades in the colonic environment[237]. There are several drugs that are marketed as gastroretentive dosage forms such as Valrelease®, Cifran OD®, Topalkan® etc for different disease conditions. When considering an anti-cancer drug, Shishu et.al, developed a floating dosage form for 5-fluorouracil to target stomach papilloma[238]. The floating dosage form of 5-fluorouracil prevented the incidence of tumour by 74 % when compared to that of the conventional tablets (24 %)[238]. Though the concept of gastroretention is not new, this is the first instance to our knowledge where a gastroretentive dosage form for a BCS Class IV anticancer agent was developed. As of now, a satisfactory proof of concept couldn't be established for both the gastro-retentive dosage form and enteric-coated GCPQ – CUDC-101 nanoparticles. But these formulations may perform well when tried at 50 mg kg^{-1} in large animal models such as dogs.

4.6 Conclusion

The oral delivery of CUDC-101 could not be achieved due to its poor solubility, P-gp efflux and extensive liver metabolism. Extensive research is still needed to search for suitable dissolution enhancers, which could potentially aid in the oral absorption of CUDC-101.

5 Subcutaneous delivery of CUDC-101

5.1 Introduction:

CUDC-101 is a clinical stage compound and a potent multi-target tumour growth inhibitor[169]. In the clinical trials the compound is administered intravenously for period of 1 hour, five days a week. This would affect the patient life style and an alternative treatment regime is necessary. Earlier attempts to improve the oral absorption of CUDC-101 were not successful owing to the extremely hydrophobic nature of the drug along with high first-pass metabolism and P-gp efflux (Chapter 4). Thus parenteral delivery options for CUDC-101 were considered as it will eliminate the first-pass effect and the gut solubility issues associated with the oral route. Of all the parenteral routes, the subcutaneous route of drug administration is attractive, as it requires less skill for drug administration in comparison with the intravenous route. There are fewer barriers for subcutaneous absorption unlike the oral route and thus it is easier to achieve a better bioavailability. Hence, it might be informative to try the GCPQ – CUDC-101 nanoparticles developed so far via the subcutaneous route.

But the GCPQ – CUDC-101 nanoparticles developed for oral delivery should be optimized for certain parameters to be given subcutaneously. The most important parameter is that the formulation should include the active ingredient at a therapeutically effective dose. The recommend dose for CUDC-101 in the clinic is 500 mg per day and the maximum volume for subcutaneous injection according to FDA is just 2 mL but 5 mL injections can be given if co-administered with the enzyme hyaluronidase[239]. This means the maximum dose that can be given with the current GCPQ – CUDC-101 formulation (5 mg mL^{-1} CUDC-101) is just around 25 mg, which is 20 times less than the recommended dose. Also the subcutaneous injections should be isotonic and thus it might be necessary to adjust the tonicity of the formulation. Hence the current GCPQ – CUDC-101 formulation (used in Chapter 4) should be optimized for subcutaneous injection.

An ideal subcutaneous dosage form should be easy to inject causing less discomfort to the patients, safe, sterile and more importantly should have a

therapeutic effect. GCPQ is an amphiphilic polymer with a good *in vivo* safety profile and preliminary experiments suggested it has ideal viscoelastic properties for subcutaneous injections[240]. The viscosity of the GCPQ suspension is controlled by the molecular weight and the hydrophobicity of the polymer. Thus the GCPQ nanoparticles may be optimized for controlled drug release by modifying the hydrophobicity (palmitoylation) of the polymer, where a hydrophobic polymer would have a strong interaction with the drug and will have a controlled release profile in comparison with a low palmitoylation polymer. This can be tested by formulating CUDC-101 in GCPQ with different levels of palmitoylation and checking for the subcutaneous drug absorption profile in animal models. On the other hand, high levels of palmitoylation and molecular weight of the GCPQ might increase the viscosity of the formulation, which practically may not be feasible for the subcutaneous injection process. Thus it is necessary to find the ideal levels of palmitoylation and molecular weight in GCPQ to make a successful subcutaneous dosage form using GCPQ.

5.1.1 Western blotting:

Western blotting is an analytical technique used to detect the presence of a particular protein from a complex mixture of samples. For example, oncogenesis is often associated with the expression or suppression of certain proteins in the system, which are termed as 'biomarkers'[241]. Detecting these biomarkers in the system might be useful for the diagnosis of cancer or even for assessing the prognosis of a treatment[241]. Western blotting uses a multitude of techniques to detect a protein of interest[242]. Initially, the proteins are separated based on size using gel electrophoresis techniques, then transferred to a solid support (blotting) and finally the blot with the total protein is probed for the presence of a particular protein using antibodies. The antibody detection is similar to ELISA, where a primary antibody, which is specially designed for the target protein, marks the protein of interest. Once the unbound proteins are washed from the blot, a secondary antibody, which is specific for the primary antibody is used to label the protein of interest. The secondary antibody is also labelled with an enzyme, usually horseradish peroxidase (HRP), whose activity can be monitored using a chemiluminescence substrate, which reveals the presence of the protein of interest[242].

5.2 Aim:

The aim of this section is to develop GCPQ – CUDC-101 nanoparticles into a clinically relevant subcutaneous dosage form. The objectives are to

- Determine the rheological properties of GCPQ.
- Optimize the existing GCPQ – CUDC-101 nanoparticles to obtain an isotonic formulation capable of delivering the 500 mg per day dose of CUDC-101
- Test the new formulation for its *in vivo* activity.

The criteria for success for this project was established based on the objectives as follows:

1. To get an aqueous concentration of CUDC-101 at around 50 mg mL^{-1}.
2. To get a CUDC-101 formulation with a shelf life of minimum 3 months.
3. To get a stable plasma exposure of CUDC-101 for at least 6 hours following subcutaneous injection.

5.3 Materials and Methods:

5.3.1 Materials

Chemical	**Comments**	**Supplier**
Bovine hyaluronidase	600 IU mg^{-1}	Sigma Aldrich (Gillingham, UK)
L – glutamine	200 mM solution	Sigma Aldrich (Gillingham, UK)
Sodium Pyruvate	100 mM solution	Sigma Aldrich (Gillingham, UK)
Dulbecco's Modified Eagle's Medium		Sigma Aldrich (Gillingham, UK)
Trypsin - EDTA	0.25 % trypsin – 1 mM EDTA	Sigma Aldrich (Gillingham, UK)

Chemical	**Comments**	**Supplier**
Fetal Bovine Serum	5 %	Sigma Aldrich (Gillingham, UK)
Tissue Protein extraction buffer - TPER		Thermo Fisher Scientific (Loughborough, UK)
Protease/ Phosphatase inhibitor cocktail		Thermo Fisher Scientific (Loughborough, UK)
LDS sample buffer	pH 8.4	Life Technologies (Loughborough, UK)
Dithiothreitol		Life Technologies (Loughborough, UK)
NuPAGE® Novax® bis-tris gels		Thermo Fisher Scientific (Loughborough, UK)
NuPAGE® MOPS SDS running buffer		Thermo Fisher Scientific (Loughborough, UK)
Novex® nitrocellulose membrane		Thermo Fisher Scientific (Loughborough, UK)

5.3.2 Methods:

5.3.2.1 Viscosity measurements

The viscosities of the GCPQ polymer suspension (60 mg mL^{-1} to 90 mg mL^{-1}) in water were measured with a shear rheometer (Bohlin Gemini HR nano, Malvern Instruments Ltd., Worcestershire, U.K.) The cone-plate geometry was used for the measurements (cone diameter = 40 mm and cone angle = 4^{o}).

5.3.2.2 DLS size & zeta potential measurements

The viscous GCPQ formulations were diluted ten times in NaCl (10 mM) before the size or zetapotential measurements were carried out using the Malvern Zetasizer Nano ZS ZEN3600 (Malvern Instruments Ltd, UK). The diluted formulations were dispersed into low volume dispersible cuvettes and the size distribution graphs were recorded using dynamic light scattering technique.

To measure the zetapotential, the formulations were dispersed into a zetacell and the electrical potential difference between the electrodes was measured using the 'Zeta' module in the instrument. Before measuring the samples the calibration of the instrument was tested with standard solutions supplied by the manufacturer.

5.3.2.3 X-ray Diffraction (XRD) analysis

XRD patterns of the freeze-dried GCPQ – CUDC-101 and reference materials were obtained using a Miniflex 600 (Rigaku, Japan). Powdered formulations were filled in to an hollow aluminium sample holder and the X-ray diffraction patterns were recorded in the 2-θ range 4 – 60° at a speed of 5° per min (step = 0.02°).

5.3.2.4 Preparation of formulation:

5.3.2.4.1 Prototype GCPQ subcutaneous formulation 1:

CUDC 101 (50 mg) was dissolved in a solution of polyvinylpyrollidone (1% w/v, PVPK30) in sodium hydroxide (0.2 M, 5 mL) by heating in a shaking water bath at 70°C for 5 minutes. Quaternary ammonium palmitoyl glycol chitosan (GCPQ, 100 mg, Lot Number = GCPQ48070313VL, mole% palmitoyl groups = 14%, mole% quaternary ammonium groups = 26%) was dispersed in hydrochloric acid (0.2 M, 5 mL) by bath sonication. To this GCPQ dispersion was added the warm alkaline solution (clear yellow in colour) of CUDC 101 and the resultant colloid suspension was vortexed for 10 seconds. The pH of the resulting formulation was adjusted to pH = 6.8 by drop wise addition of sodium hydroxide solution (1 M). The freshly prepared formulation was frozen by liquid nitrogen the frozen formulation freeze-dried (over a 24-hour period). The freeze-dried

cake was then reconstituted to 2 mL in volume by the addition of water and bath sonication.

5.3.2.4.2 Prototype GCPQ subcutaneous formulation 2 and 3:

CUDC 101 (50 mg) was dissolved in sodium hydroxide (0.2 M, 5 mL) by heating in a shaking water bath at 70°C for 5 minutes. Quaternary ammonium palmitoyl glycol chitosan (GCPQ, 100 mg (formulation 2) or 50 mg (formulation 3), Lot Number = GCPQ48 240114SR, mole% palmitoyl groups = 5%, mole% quaternary ammonium groups = 5%) was dispersed in water (5 mL) by shaking. To this GCPQ suspension dextran (100 mg, 6000 Da) was added as a cryoprotectant. To this GCPQ dispersion was added the warm alkaline solution (clear yellow in colour) of CUDC 101 and the resultant colloid suspension was vortexed for 10 seconds. The pH of the resulting formulation was adjusted to pH ~ 6.8. The freshly prepared formulation was imaged by transmission electron microscopy, frozen by liquid nitrogen and the frozen formulation freeze-dried (over a 24-hour period). The freeze-dried cake was then reconstituted to 2 mL in volume (in case of GCPQ formulation 2) or 1 mL in volume (in case of GCPQ formulation 3) by the addition of water and shaking.

5.3.2.4.3 Optimized GCPQ subcutaneous formulation 3

CUDC-101 (50 mg) dissolved in NaOH (0.2 M, 1 mL) by heating at 70°C. GCPQ48 240114SR (50 mg) and Dextran (100 mg, 6 kDa) was dispersed in water (9 mL) by shaking and the warm solution of drug is then added to the GCPQ suspension. The pH of the formulation was adjusted to ~7 if necessary and the formulation was freeze-dried. The freeze-dried GCPQ formulation 3 was reconstituted by simply shaking in Bovine hyaluronidase (1 mL, 0.3 mg mL^{-1} in water) to give 50 mg mL^{-1} of CUDC-101.

5.3.2.5 Stability of GCPQ formulations:

The stability of the GCPQ – CUDC-101 nanoparticles were measured in terms of its ability to suspend CUDC-101 in colloidal fraction. The freeze-dried GCPQ formulations were dispersed in water left undisturbed at room temperature. The samples (100 µL) were withdrawn at specific time points and centrifuged at 1000 g for 10 min, the colloidal fraction (supernatant) was collected and analysed for drug content. Storage stability was carried out on GCPQ

formulation 3 to determine the optimum storage temperature for the GCPQ nanoparticles. For this, the freeze-dried formulation was stored at room temperature, 40°C and 4°C for up to 3 months and samples withdrawn at predetermined time points, dispersed in water and the colloidal fraction was analysed as before at different time points for drug content. The nanoparticles were also characterized for changes in size using DLS, morphology using TEM and physical form using powder-XRD.

5.3.2.6 Pharmacokinetic studies:

Male Wistar rats were acclimatized for at least five days before the experiment, in the animal housing unit, maintained at an ambient temperature of 22°C, relative humidity of 60 % and equal day-night cycle. The animals were given free access to food and water throughout the experiment. The CUDC-101 formulation was then injected into the rats (50 mg kg^{-1} dosage), under the subcutaneous layer above the thigh. Blood samples were collected from the rats at predetermined time points through tail-vein bleeding and at the end of the experiment the rats were euthanised and blood was collected through cardiac puncture.

5.3.2.7 Pharmacodynamic studies:

Female athymic nude mice (CD-1 nu/nu) at age 6-8 weeks were obtained from Charles River laboratories. They were housed in the Animal Facility in ventilated micro-isolator cages in a controlled climate, fed irradiated laboratory rodent diet ad libitum and provided sterilized water. All housing and supplies for nude mice were sterilized by autoclaving before use. Mice were inspected daily including weekends/holidays and all animal procedures were performed under sterile conditions within a biosafety cabinet (for injections) or laminar flow hood (for animal husbandry and non-invasive procedures). All the experiments were carried out in accordance with the Home Office regulatory guidelines.

5.3.2.7.1 Tumour implantation

Before initiation of the animal study, A431 (epidermoid carcinoma) cells were obtained from ATCC (American Type Culture Collection). Studies were carried out under biosafety level 2 (BL-2) conditions. Cryopreserved cells were thawed in a 37 °C water bath and cultured in Dulbecco's modified Eagle's medium plus

10 % Fetal Bovine Serum (FBS) supplemented with sodium pyruvate and L-glutamine, in a tissue culture incubator at 5 % CO_2. When the cells in culture reached about 70 – 90 % confluency, they were harvested by treatment with trypsin-EDTA (0.25 % Trypsin, 1 mM EDTA) and washed with phosphate buffer saline (PBS). Finally, the cells were diluted in serum free medium and mixed with an equal volume of Matrigel for implantation. After a seven-day acclimatization period, 5 million A431 cells per animal suspended in 0.1 ml medium were injected subcutaneously in the right hind flank region of the mouse using a syringe with a 26G hypodermic needle, taking care to avoid blood vessels. Successful implantation was indicated by the formation of a round, raised mass under the skin. The implanted mice were monitored for general health and tumour development daily. As the tumour develops, its progress was measured using a Vernier caliper. From the size measurements, the tumour volume was calculated using the formula (length x width^2)/2.

5.3.2.7.2 Study groups

Tumours were detectable about a week following implantation. Tumour size was measured with a caliper. When A431 tumour sizes reached an average of approximately 7±1 mm in diameter, animals with acceptable tumour size and shape were randomly assigned into three groups of 5-6 animals each to either the vehicle control, low dose (60 mg kg^{-1}), medium dose (90 mg kg^{-1}) or high dose (120 mg kg^{-1}) of GCPQ subcutaneous formulation 3.

The formulations were dosed subcutaneously around the scruff region of the animal everyday and the tumour sizes and mouse body weights were monitored every other day. Studies were continued until either a) the predetermined end date indicated in the study design (50 days) or b) the onset of health problems, whichever occurred first. In addition, the following tumor-related parameters warranted provision of euthanasia: (1) tumor size exceeding 12 mm in diameter (2) loss of ≥15 % of starting body weight (3) appearance for necrotic lesions in the tumour.

5.3.2.7.3 Western blotting:

Tumour samples from the control animals and treatment group were excised after euthanasia and frozen in liquid nitrogen and stored at -80 °C until further experiments. The frozen tumours were ground into fine powder (200 mg) and

added the tissue extraction buffer (T-PER, 600 µL) supplemented with protease/phosphatase inhibitor cocktail (6 µL) and EDTA (0.5 M, 6 µL). This mixture was homogenized until a uniform suspension is obtained (~ 1 min, on ice) and then the samples were centrifuged at 13,000 rpm for 10 min at 4 °C. The supernatant was then transferred to a clean vial and the protein content of the samples was estimated using the bicinchoninic acid assay (BCA).

Samples (30 µg) were mixed with LDS sample buffer (5 µL), dithiothreitol (DTT, 2 µL) and water to make up the volume to 20 µL. Denatured samples (20 µL) were loaded onto 4 – 12 % NuPAGE® Novax® bis-tris gels (Life Technologies, UK) and subjected to electrophoresis in NuPAGE® MOPS SDS running buffer in the Novex® Minicell apparatus (Invitrogen, USA), according to the manufacturer's instructions. Protein standards (MagicMark XP Western standard) were included in the gel following the similar method of preparation for samples. Proteins were transferred to Novex® nitrocellulose membrane using the Novex® Xcell II blot module (Invitrogen, USA) for 1.5 h at 30 V.

Western blots were probed for expression of actin (mouse monoclonal), a house keeping protein and Acetylated-Histone 3 (Ac-H3, rabbit polyclonal), all steps being carried out at room temperature, with gentle shaking. After 60 min in blocking buffer (5% BSA in PBS), blots were incubated for 3 h with the following optimal dilutions of primary antibodies in blocking buffer: 1 in 1000 for rabbit anti-human Ac-H3 (Abcam, USA) and 1 in 2000 for rabbit anti-human Actin (Cell Signalling Technologies, USA). After thorough washing in PBS containing 1 % Tween 20 (wash buffer), blots were incubated for 1.5 h in a 1 in 6000 dilution of the second antibody in wash buffer, horseradish peroxidase (HRP)-conjugated anti-rabbit IgG (Cell signaling technologies, USA) for anti-Ac-H3 and HRP-conjugated goat anti-mouse IgG (Life technologies, UK) for anti-actin. Blots were developed by the SuperSignal™ West Pico Chemiluminescent substrate using the method described by the manufacturer (Thermo Scientific, USA).

5.4 Results and discussion:

5.4.1 Viscosity studies:

The viscosity of GCPQ suspensions as a function of shear rate was measured using a rheometer. GCPQ with different characteristics (Table 5.1) was used for this purpose. As the concentration of the GCPQ increases, the viscosity of the suspension increases (Figure 5.1). Hydrophobicity and molecular weight of the polymer also has a bearing on the viscosity, where increase in both these parameters increased the viscosity of the suspension. From the data it is clear that GCPQ forms viscous suspensions, which behave like Newtonian fluids at low concentrations (≤ 70 mg mL^{-1}). A Newtonian fluid is the one in which the viscosity is not affected by the shear rate. However, at higher concentrations (≥ 80 mg mL^{-1}), the viscosity of the GCPQ suspensions decreases as the shear rate increases, which is due to the transient nature of the chain entanglement and the inter-linked networks (Figure 5.1). This phenomenon is called shear thinning, which is advantages for subcutaneous injection, as even high concentrations of GCPQ suspensions can be easily dispensed from the syringe by applying pressure because the viscosity of the suspensions will decrease with increase in pressure.

The effect of palmitoylation and molecular weight of the polymer on viscosity is evident. The polymers were grouped as mildly hydrophobic (mole% palmitoylation 5-15 %), moderately hydrophobic (mole % palmitoylation 15-25 %) and highly hydrophobic (mole % palmitoylation > 25 %) based on the degree of palmitoylation. The polymer molecular weight had a profound effect on viscosity as the increase in M_w increased the viscosity approximately 50 folds at higher polymer concentrations (comparing Figure 5.1 i and ii). This is because; increase in M_w means longer chain length, which forms a more complex micellar network that increases the viscosity. On the other hand, for a similar M_w, viscosity values for moderate and highly hydrophobic polymers were similar (Figure 5.1 i and iii), while the viscosity values for mildly hydrophobic polymer was very low (Figure 5.1 iv). There seems to be a critical hydrophobicity value above which the viscosity of GCPQ micellar dispersion increases and any further increase in hydrophobicity does not affect the viscosity drastically.

Table 5.1 Characteristics of GCPQ used for viscosity measurement

	Palmitoylation %	Quaternization %	M_w (kDa)	M_n (kDa)	M_w/M_n
Q48 111111 SR	18	11	9.47	8.67	1.09
Q24 250414 AI	23	6.3	13.13	11.03	1.19
Q48 080612 SR	31	7	8.63	5.95	1.45
Q48 150812 SR	6	11	9.75	9.2	1.06

5.4.2 Optimization of GCPQ – CUDC-101 nanoparticles

5.4.2.1 Optimize for concentration

As mentioned earlier the recommended dose for CUDC-101 in the clinic is 500 mg per day and it only possible to achieve 25 mg per day with the current GCPQ – CUDC-101 formulation as the concentration of drug in the formulation is just 5 mg mL^{-1}. Thus it is necessary to increase the concentration of CUDC-101 in the formulation to at least 50 mg mL^{-1} so that the 500 mg per day dose can be subcutaneously injected as 5 mL injections of 250 mg active ingredient twice a day.

The easiest way to increase the concentration of the drug in the GCPQ – CUDC-101 formulation is to freeze dry and reconstitute the formulation in less volume of water. But this will also increase the concentration of GCPQ in the formulation, which will increase the viscosity affecting the ease of reconstitution after freeze-drying. From the viscosity studies we know that use of high palmitoylation would increase the viscosity of the GCPQ suspension drastically (Figure 5.1). Hence, prototype GCPQ formulation 2 and 3 were developed with a low palmitoylation GCPQ at different concentrations in an attempt to minimize the viscosity and to ease the reconstitution after freeze-drying in order to obtain a maximum drug concentration in the formulation.

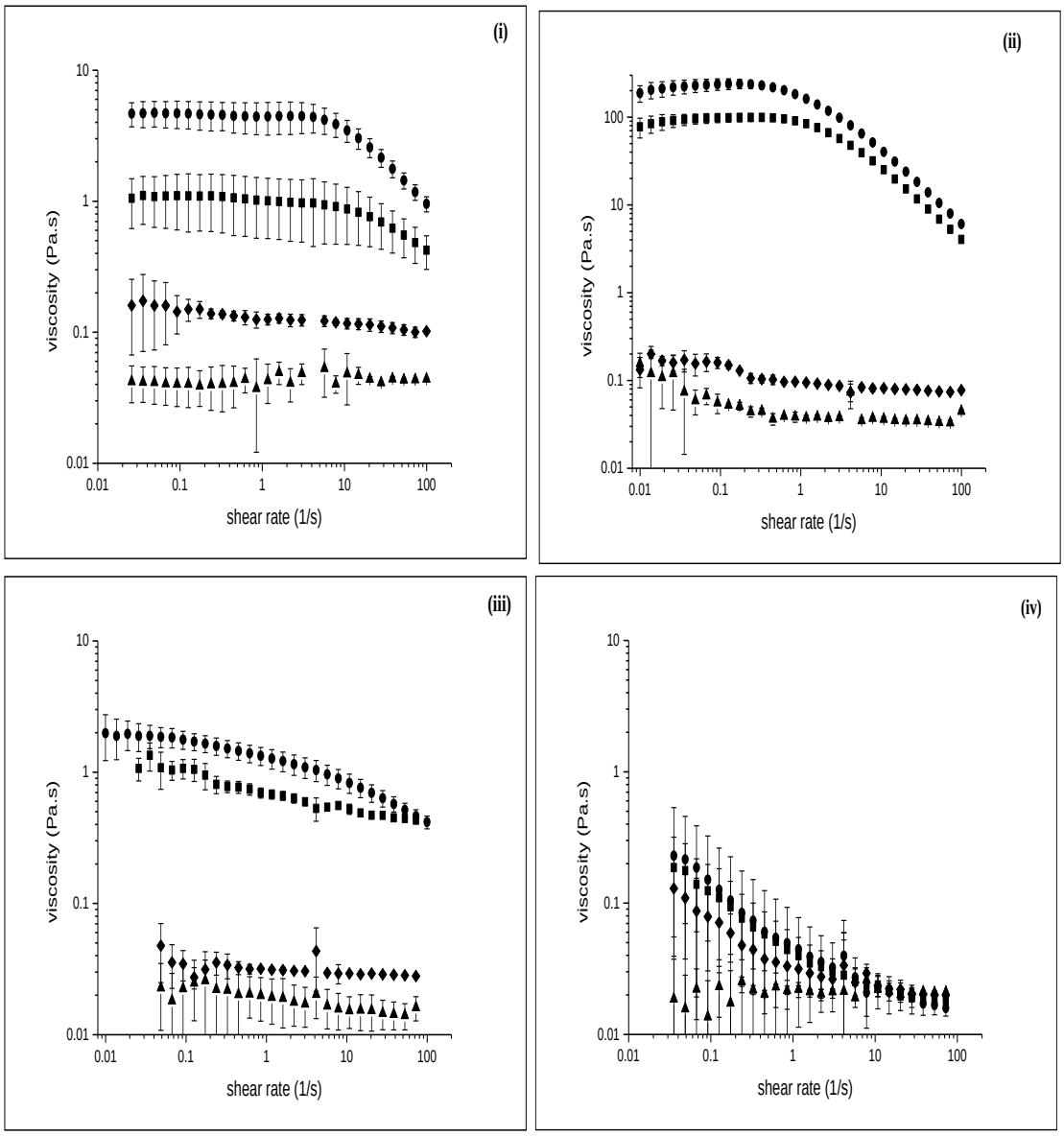

Figure 5.1 Viscosity of GCPQ with different characteristics

Viscosity of GCPQ with different characteristics as a function of shear rate: 0.06 g mL^{-1} (▲), 0.07 g mL^{-1} (◆), 0.08 g mL^{-1} (■) and 0.09 g mL^{-1} (●)]; (i) Q48 111111SR (intermediate hydrophobicity, low M_w); (ii) Q24 250414AI (intermediate viscosity, high M_w) ; (iii) Q48 080612 SR (high hydrophobicity, low M_w); (iv) Q48 150812 SR (low hydrophobicity, low M_w); (n = 3)

Table 5.2 Optimization of GCPQ formulation to increase the concentration

Prototype GCPQ subcutaneous formulation	Before freeze drying		P%	Q%	After freeze drying	
	CUDC-101/mL	GCPQ/mL			CUDC-101/mL	GCPQ/mL
Formulation 1	5 mg	10 mg	14 %	26 %	25 mg	50 mg
Formulation 2	5 mg	10 mg	5 %	5 %	25 mg	50 mg
Formulation 3	5 mg	5 mg	5 %	5 %	50 mg	50 mg

Molecular weight of GCPQ used in all these formulations is 10 kDa.

From the results (Table 5.2) it can be seen that the target concentration of 50 mg mL^{-1} CUDC-101 can be achieved only with GCPQ formulation 3 with low palmitoylation and low concentration of GCPQ. The formulations with high palmitoylation and high concentrations of GCPQ are hard to reconstitute in less volume of water and thus only half the concentration of CUDC-101 could be achieved for formulations 1 and 2 (25 mg mL^{-1}). Dextran (1 %, 6 kDa) was added as a cryo-protectant to the formulations before freeze-drying to ensure that the integrity of the nanoparticles is not broken during the freeze-drying process (Figure 5.2). Dextran (6 kDa) was chosen as a cryo-protectant because it is a non-reducing sugar and high molecular weight means less number of molecules to contribute towards osmotic potential (tonicity).

5.4.2.2 Tonicity adjustment:

With the prototype GCPQ formulations it was possible to improve the concentration of CUDC-101 from 5 mg mL^{-1} to 25 - 50 mg mL^{-1}. But these formulations carry hypertonic concentrations (~ 5 %) of sodium chloride, which is above the FDA permissible limit (FDA limit for subcutaneous suspension is 1.23 %). Thus it is necessary to reduce the salt content of the formulation and this can be achieved by the following approaches; a) use different solvent for the drug instead of NaOH and b) modify the protocol of the original formulation to reduce the salt generated as by-product.

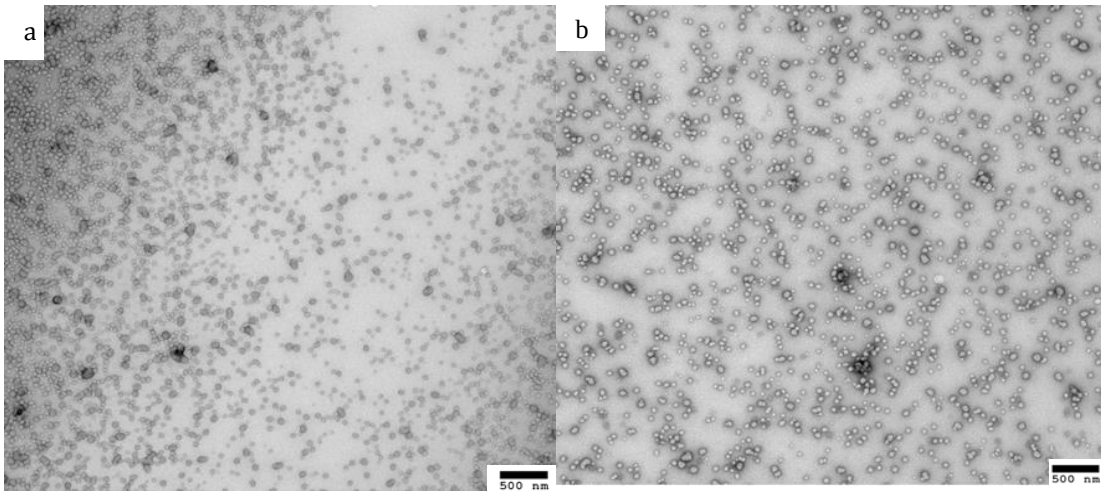

Figure 5.2 TEM images for GCPQ formulation a) before and b) after freeze-drying

The appearances of the nanoparticles are similar before and after freeze-drying suggesting that freeze-drying doesn't affect the structural integrity of the nanoparticles. Although the size of the nanoparticles seem slightly bigger after freeze-drying.

5.4.2.2.1 DMSO as solvent:

During our initial solvent screen for CUDC-101, the only aqueous solvent identified was the concentrated aqueous solutions of sodium hydroxide. PEG, DMSO and NMP were the other non-aqueous solvents identified, which could be potentially used to make GCPQ – CUDC-101 nanoparticles. Out of these formulations, PEG is non-volatile thus cannot be freeze-dried and NMP has low vapour pressure and is toxic, which means only DMSO can be used to make nanoparticles.

Thus it was decided to use DMSO to make GCPQ – CUDC-101 nanoparticles in order to reduce the salt content of the formulation. The GCPQ – CUDC-101 nanoparticles were prepared from DMSO as follows:

CUDC-101 (100 mg) was dissolved in DMSO (1 mL) by heating at 50°C in a water bath. The GCPQ48 240114SR (5 mg, 5% palmitoylation) was dispersed in water (0.9 mL) and to this dispersion the drug DMSO solution (100 µL) was added. The volume of DMSO in the formulation and the concentration of CUDC-101 in DMSO were kept as minimum as possible, because high amounts of both these factors affected the stability of the formulation. The formulation thus

prepared was immediately frozen, as the stability of the formulation was poor (< 30 min). The frozen formulation was then freeze-dried for 48 hours by heating the shelves containing the formulation to 37°C. Once dried, the freeze-dried formulation was then reconstituted in water to give a final concentration of CUDC-101 to be 50 mg mL^{-1}.

The reconstituted formulation was measured for drug content and the results are given in the Table 5.3. The formulation was not reproducible as seen from the high variability in the drug content. This variability might be due to the poor stability of the freshly made nanoparticles and also due to some inconsistencies in the sublimation of DMSO during freeze-drying. The sublimation of DMSO causes the formulation to slightly melt sometimes, which might affect the quality of the final formulation. Thus the idea of using DMSO to prepare GCPQ – CUDC-101 nanoparticles was dropped.

Table 5.3 Concentration of CUDC-101 in DMSO formulation

	Measured concentration (mg mL^{-1})	**Theoretical concentration (mg mL^{-1})**
Trial 1	26.3	50
Trial 2	43.6	
Trial 3	30.92	

5.4.2.2.2 NaOH solvent revaluation:

Another approach to reduce the salt content was to modify the current GCPQ – CUDC-101 nanoparticle, in terms of the volume of NaOH used in the formulation. Initially, the concentration of CUDC-101 in 0.2 M NaOH used to make the nanoparticles was 10 mg mL^{-1}. This was then mixed to an equal volume of GCPQ suspension in 0.2 M HCl, which forms nanoparticles but also produces 0.2 M NaCl as by-product. The concentration NaCl further increases when this formulation is freeze-dried and reconstituted in less volume of water. The possible ways to reduce the salt formation are a) lower the molarity of NaOH solution – it was not feasible as the drug precipitated on any attempts to lower the molarity; b) using a different acid instead of HCl – this will create a different salt as a by-product, for example using acetic acid instead of HCl

would produce sodium acetate, which would still contribute towards osmolality; c) reducing the volume of NaOH used – this would also reduce the concentration of the drug in the final volume, which will in turn increase the dose volume; d) increasing the concentration of CUDC-101 in 0.2 M NaOH – this is possible as the solubility of CUDC-101 in 0.2 M NaOH was found to be increasing upon heating.

The concentration of CUDC-101 in 0.2 M NaOH was increased to 50 mg mL^{-1} by heating at 70°C and 100 µL of this formulation was added to GCPQ suspension to form nanoparticles. This formulation was then freeze-dried and reconstituted in relevant volume of water to get 50 mg mL^{-1} CUDC-101. By this way, the final concentration of NaCl in the formulation was reduced to 1.1%, which is within the FDA limit and close to isotonic (466 mOsm). Thus the new GCPQ – CUDC-101 nanoparticles were made as follows: CUDC-101 (50 mg) dissolved in NaOH (0.2 M, 1 mL) by heating at 70°C. GCPQ48 240114SR (50 mg, 5 % palmitoylation) and Dextran (100 mg, 6 kDa) was dispersed in water (9 mL) by shaking and the warm solution of drug is then added to the GCPQ suspension. The pH of the formulation was adjusted to ~7 if necessary and the formulation was freeze-dried. The freeze-dried powder was then reconstituted in water (1 mL) to give 50 mg mL^{-1} of CUDC-101 in the formulation with reproducible results (Table 5.4).

Table 5.4 Concentration of CUDC-101 in GCPQ formulation

	Measured concentration (mg mL^{-1})	**Theoretical concentration (mg mL^{-1})**
Trial 1	50.52	50
Trial 2	50.94	
Trial 3	49.06	

5.4.2.3 Sterilization of the formulation:

A GCPQ – CUDC-101 nanoparticle developed thus far has an acceptable amount of tonicity and the formulation has 50 mg mL^{-1} of active ingredient. By adding dextran as cryoprotectant, the ease of reconstitution of the formulation has also been improved. Next, the formulation has to be optimized for a

sterilization protocol. Autoclaving is the cheap and cost effective way of sterilization in the pharmaceutical industry and thus the GCPQ – CUDC-101 nanoparticles were autoclaved for 20 minutes. Unfortunately, the formulation caramelized after autoclaving and it was impossible to reconstitute the caramelized solid in water (Figure 5.3). Thus autoclaving is not a feasible method of sterilization for this formulation. The other cost effective way for sterilization is filtration. Filtration with 0.22 µm pore sized filters has been proven effective against most of the microorganisms and through our previous experiments, it is known that a GCPQ suspension can be effectively filtered without any loss of the polymer to the 0.22 µm filter membranes (internal report generated by Charles River).

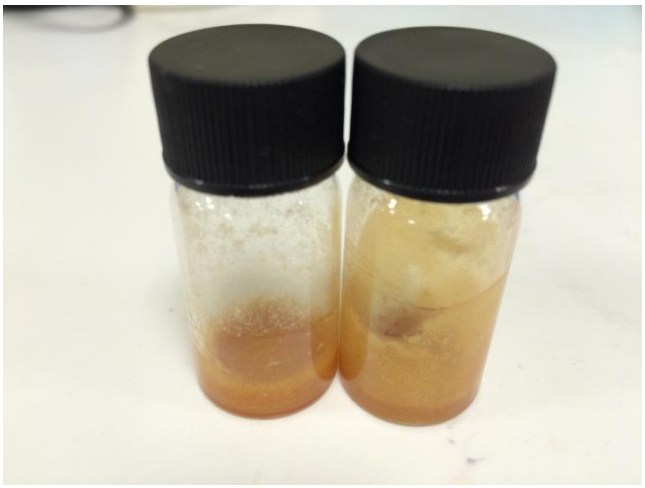

Figure 5.3 Appearance of GCPQ formulation after sterilization by the autoclave

The GCPQ formulation appears caramelized after autoclaving and hence alternative method for sterilization is necessary for GCPQ formulation.

But the solution of 50 mg mL^{-1} CUDC-101 in 0.2 M NaOH is stable only for a short while as the drug precipitates upon cooling. Thus experiments were conducted to check if it was possible to recover the whole concentration of CUDC-101 from 0.2 M NaOH solution after filtration using 0.22 µm pore sized filters. For this, a 50 mg mL^{-1} solution of drug in NaOH was freshly prepared and the drug content was measured before and after filtration using 0.22 µm syringe filters. The remaining unfiltered solution was left on the bench for up to 1 hour and drug content measured after filtration using RP-HPLC.

From the results (Table 5.5), it can be seen that some drug was lost after 1 hour, which means the drug solution should be filtered as soon as possible to make the nanoparticles. More importantly, sterile conditions should be maintained throughout the manufacturing processes once the nanoparticles are made.

Table 5.5 CUDC-101 concentration after filtration

Time (h)	**Filtration** (n = 3)	**Concentration (mg mL^{-1})**
0	Before	50.01 ± 0.85
	After	51.37 ± 1.77
1	After	41.70 ± 17.57

5.4.3 Colloidal stability studies:

The colloidal stability of the three GCPQ – CUDC-101 subcutaneous formulations were assessed before freeze-drying and the results are given in (Figure 5.4a). From the results it is clear that the colloidal stability is affected by the characteristics of GCPQ used in the formulation, where the GCPQ formulation 1 (14 % palmitoylation) had better stability in comparison with GCPQ formulation 2 (5 % palmitoylation). Similarly lowering the concentration of GCPQ also affected the colloidal stability, wherein GCPQ formulation 2 (1:2 drug:GCPQ ratio) had better stability than GCPQ formulation 3 (1:1 drug:GCPQ ratio). So, GCPQ formulation 3, which is more clinically relevant, has poor colloidal stability.

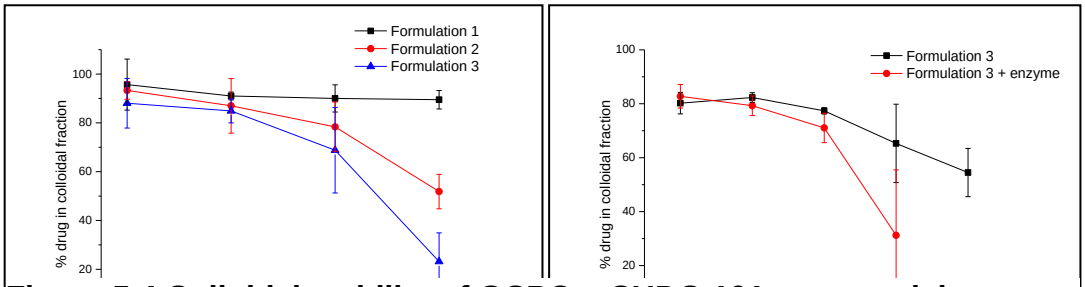

Figure 5.4 Colloidal stability of GCPQ – CUDC-101 nanoparticles

Colloidal stability of a) GCPQ formulation with different characteristics; b) GCPQ formulation 3 with the enzyme hyaluronidase. The stability of the formulation decreases with decrease in both the concentration and palmitoylation of GCPQ. The colloidal stability of the formulation also decreases in the presence of hyaluronidase (n = 3).

The colloidal stability of the GCPQ formulation 3 was also assessed in the presence of the enzyme hyaluronidase. The freeze-dried formulation 3 was reconstituted with water (to get 50 mg mL^{-1} of CUDC-101) containing hyaluronidase (0.3 mg mL^{-1}), mixed by gentle shaking and left at room temperature to assess the colloidal stability. Presence of the enzyme affected the stability of the nanoparticles, where GCPQ formulation 3 without the enzyme was stable for six hours while the one with enzyme was stable for just 4 hours (Figure 5.4b). The difference in stability might be due to interactions between the enzyme and the GCPQ nanoparticles. The hyaluronidase enzyme is made up of number of amino acids and it might be possible that the negatively charged amino acids might interact with the positively charged quaternary ammonium group of GCPQ. The GCPQ – CUDC-101 nanoparticles in the presence of hyaluronidase appear dark under the TEM while the formulation without the enzyme is pale (Figure 5.5). This suggests that the GCPQ nanoparticles are coated with hyaluronidase, as hydrophilic surfaces appear dark under negative staining of TEM.

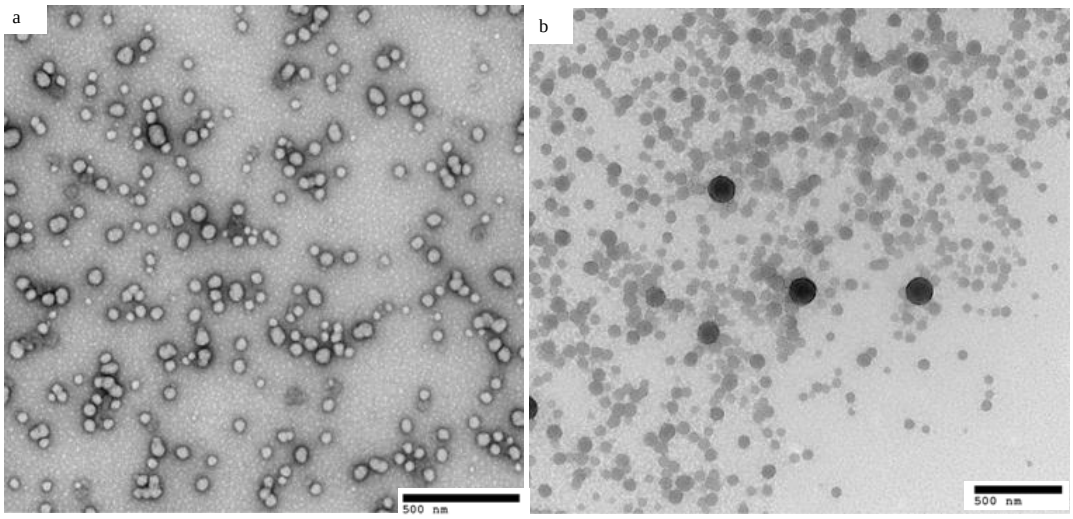

Figure 5.5 TEM images of GCPQ formulation a) without and b) with hyaluronidase

The surfaces of the nanoparticles appear dark in the presence of the enzyme suggesting that surface coating of nanoparticles in possible.

To further confirm that the nanoparticles are surface coated, the zeta potential of the formulation was measured in the presence and absence of the enzyme hyaluronidase. Zeta potential results further confirm that the GCPQ nanoparticles are surface coated as the zeta potential of the formulation with the enzyme drops to 0 mV, while the zeta potential of the formulation without the enzyme is +18 mV (Table 5.6). The charge distribution graph (Figure 5.6) reveals that only one charge population group is present in the formulations, which provides solid evidence that the GCPQ nanoparticles are surface coated with the enzyme hyaluronidase. Thus, novel surface coated GCPQ nanoparticles are developed for the delivery of CUDC-101.

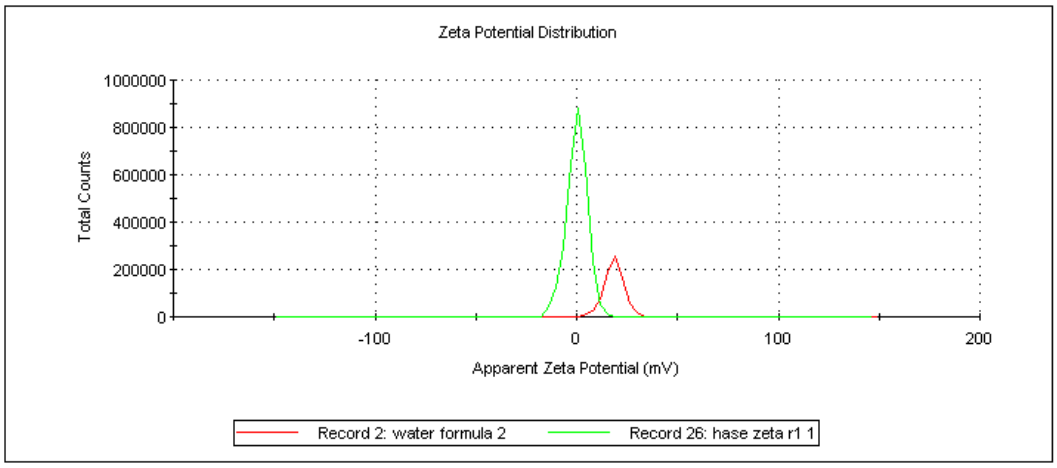

Figure 5.6 Zeta potential distribution of GCPQ nanoparticles

The charge distribution graph shows a single sharp peak for the formulation with hyaluronidase (green peak) and also for the formulation without the enzyme (red peak).

Table 5.6 Zeta potential of the GCPQ formulations (n = 3)

	Size (nm)	Polydispersity	Zeta (mV)
Formulation 3	194.6 ± 6.02	0.143 ± 0.02	18.4 ± 1.53
Formulation 3 + hyaluronidase	175.9 ± 4.56	0.155 ± 0.01	-0.15 ± 0.19

5.4.4 Long-term stability studies:

The preliminary stability studies on the freeze-dried prototype GCPQ formulation 2 were carried out at three different temperatures (room

temperature, 4°C and 40°C). The freeze-dried formulations stored at different temperatures were reconstituted at the concentration of 5 mg mL^{-1} CUDC-101 and the colloidal stability was assessed at room temperature. Based on the preliminary results, storage stability of the freeze-dried optimized formulation 3 was carried out at room temperature after reconstituting the formulation at a working concentration of 50 mg mL^{-1} CUDC-101.

From the preliminary stability data, the formulations stored at room temperature was stable for up to two months, while the stability of the formulations stored at 4°C gradually decreases after a month (Figure 5.7). The formulation stored at 40°C caked completely after a week and was very hard to reconstitute in water and hence withdrawn from the study. The poor stability of the formulation at 40°C is mainly due to the presence of moisture, which partially wets the nanoparticle and might cause drug precipitation. Similar reasons might account for poor stability of formulations stored at 4°C, as there is chance for condensation of water vapour at such low temperatures, which might gradually disrupt the colloidal stability of the particles. Apart from that there were no differences in the morphology or size of the nanoparticles stored at RT and 4°C (Figure 5.8). Thus from this preliminary storage experiment, it can be concluded that it is safer to store the freeze-dried nanoparticles at room temperature devoid of moisture.

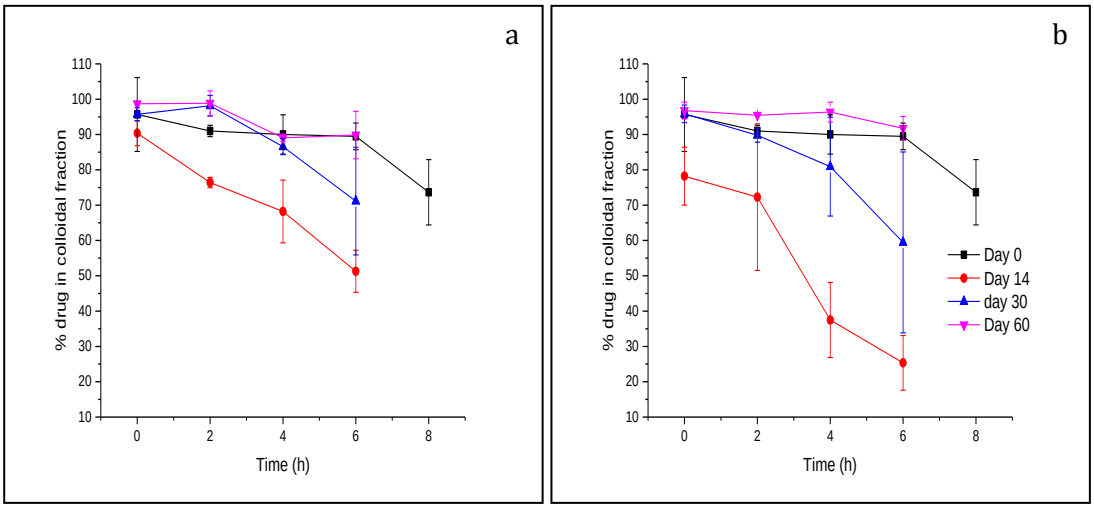

Figure 5.7 Colloidal stability of Freeze-dried CUDC-101 GCPQ nanoparticles

Freeze-dried CUDC-101 – GCPQ formulation 2 stored at a) room temperature

and b) 4°C, containing CUDC 101 (5 mg mL^{-1}), GCPQ (10 mg mL^{-1}), (n = 3).

Based on the observations from the preliminary stability studies, the freeze-dried GCPQ subcutaneous formulation 3 was stored only at room temperature and 3 month long stability experiment was carried out at 50 mg mL^{-1} CUDC-101 concentration. The colloidal stability of the formulation was similar for over a 3-month period (Figure 5.9).

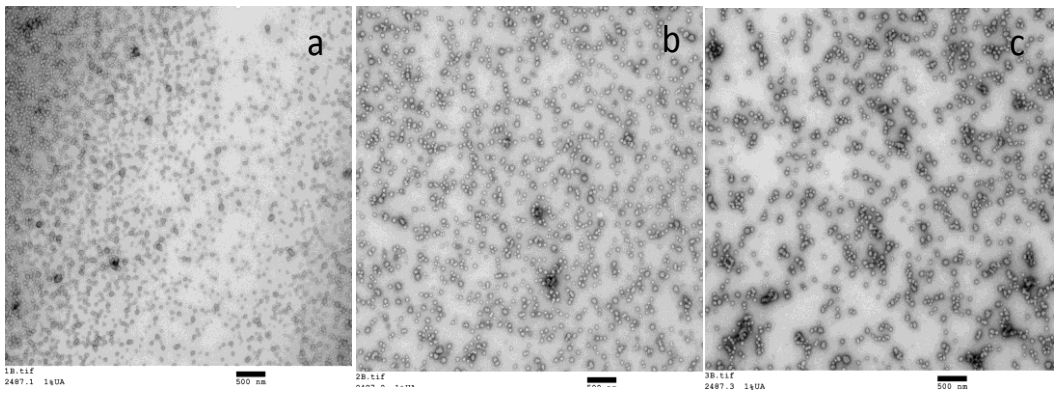

Figure 5.8 TEM images of CUDC-101 - GCPQ nanoparticles stored at different temperatures

Transmission electron micrographs of CUDC 101 – GCPQ Formulation 3: a) freshly prepared CUDC 101 – GCPQ containing CUDC 101 (5 mg mL^{-1}), GCPQ (10 mg mL^{-1}), b) Freeze dried and reconstituted CUDC 101 – GCPQ stored at room temperature for 4 weeks and reconstituted to contain CUDC 101 (5 mg mL^{-1}), GCPQ (10 mg mL^{-1}), c) Freeze dried and reconstituted CUDC 101 – GCPQ stored at 4˚C for 4 weeks and reconstituted to contain CUDC 101 (5 mg mL^{-1}), GCPQ (10 mg mL^{-1}). Size bars = 500 nm.

The size distribution using the DLS also suggests that the size of the reconstituted nanoparticles remains similar for a period of 90 days (Table 5.7). The crystal structure of CUDC-101 in GCPQ formulation can be deduced using powder-XRD (Figure 5.10). CUDC-101 on its own has sharp crystalline peaks, while the physical mixture of the drug and GCPQ still shows some crystalline peaks. But diffraction pattern of the GCPQ – CUDC-101 formulation 3 shows a halo, suggesting that CUDC-101 is in amorphous form when formulated as GCPQ nanoparticles. This might be advantageous as amorphous form of the drug has better solubility when compared with the crystal forms and thus might have better absorption. The physical form of the formulation doesn't change for a period of 3 months, suggesting that the GCPQ – CUDC-101 formulation 3 is stable for at least 3 months when stored at room temperature.

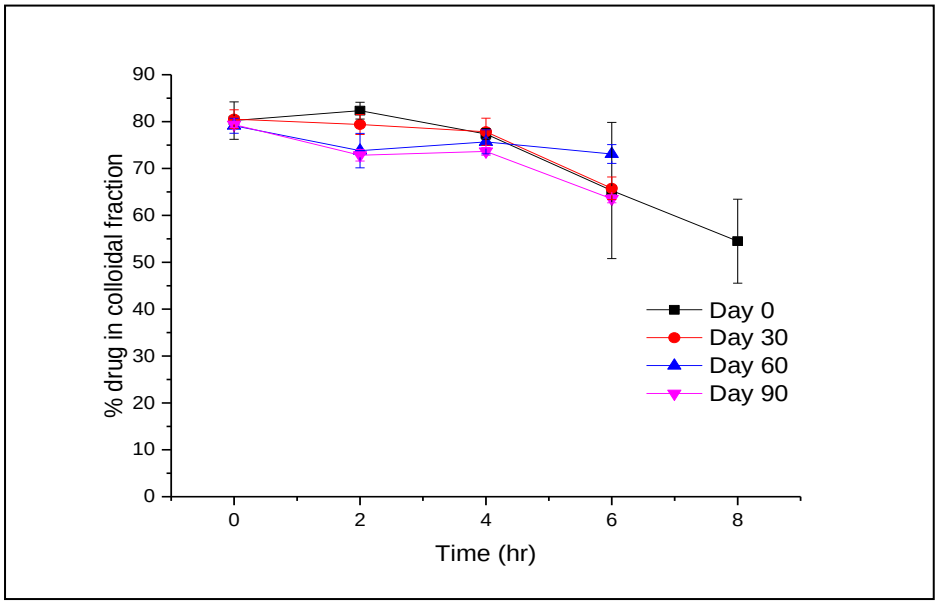

Figure 5.9 Long-term storage stability of CUDC-101 - GCPQ formulation 3

Colloidal stability of CUDC 101 – GCPQ Formulation 3 containing CUDC 101 (50 mg mL^{-1}), GCPQ (50 mg mL^{-1}) stored at room temperature. No hyaluronidase enzyme added (n = 3).

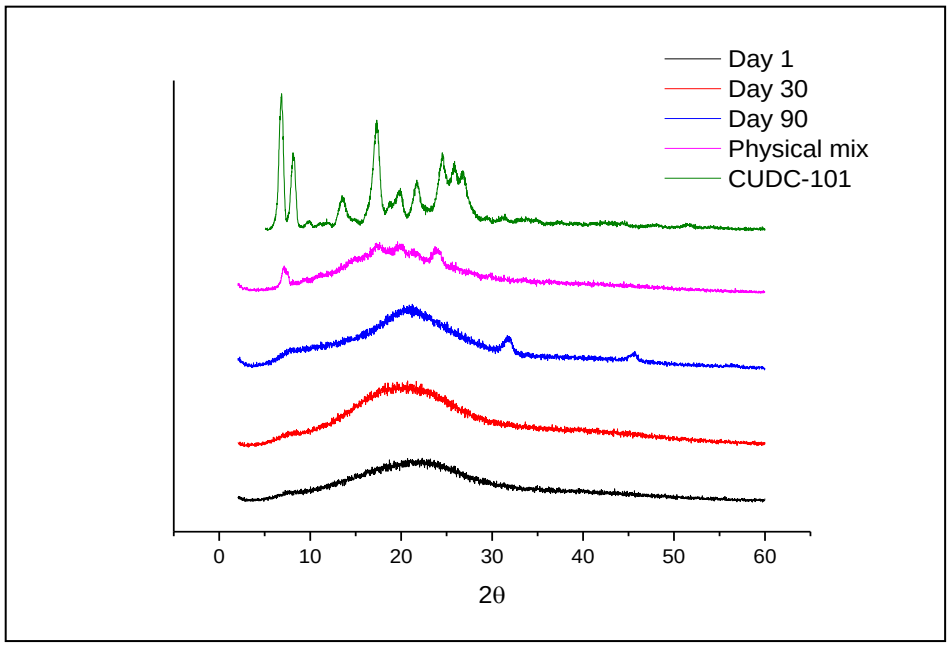

Figure 5.10 Long-term storage stability - XRD spectrum

The freeze-dried CUDC-101 – GCPQ formulation 3 remains in amorphous form for at least 90 days when stored at room temperature. The peaks around 32° and 46° in Day 90 samples corresponds to that of sodium chloride crystals formed as by-product.

Table 5.7 Long-term storage stability for CUDC-101 – GCPQ formulation 3 - DLS size measurements

	Size (nm)		**PD**	
	Mean (n = 3)	**S.D**	**Mean** (n = 3)	**SD**
Month 0	124.2	6.039	0.075	0.022
Month 1	103.1	6.403	0.135	0.063
Month 2	102	2.136	0.133	0.044
Month 3	101.1	2.127	0.091	0.011

5.4.5 *In vivo* studies:

5.4.5.1 Pharmacokinetic (PK) studies:

The *in vivo* subcutaneous drug absorption profiles of the three GCPQ formulations are given in

Figure 5.11. The absorption of CUDC-101 from GCPQ formulation 1 is very stable; with approximately 200 ng mL^{-1} drug plasma level maintained for the at

least 8 hours. The drug absorption from GCPQ formulation 2 and 3 are lower than GCPQ formulation 1 and Table 5.8 clearly shows the difference in the AUC value of all the three GCPQ formulations. The drug plasma AUC of GCPQ formulation 1 was twice better than that of GCPQ formulation 2, which was in turn twice better than GCPQ formulation 3. The PK profile shows very good correlation with the *in vitro* colloidal stability results, where poor colloidal stability translates into poor drug absorption and vice versa. The colloidal stability in turn is dependent on the concentration and hydrophobicity of the GCPQ used in the formulation. Thus it can be inferred that the concentration and palmitoylation of the GCPQ plays an important role in improving the subcutaneous absorption of CUDC-101.

GCPQ formulation 3 was also co-administered with the enzyme hyaluronidase and the AUC of CUDC-101 form the GCPQ formulation 3 with hyaluronidase is twice better than that of GCPQ formulation 3 without the enzyme (AUC similar to GCPQ formulation 2). This is because the enzyme hyaluronidase breaks down the hyaluron barrier in the subcutaneous layer [239], which speeds up the absorption of GCPQ – CUDC-101 nanoparticles improving the plasma AUC.

Another important effect of subcutaneous administration of CUDC-101 is that the metabolite levels are very low (Figure 5.12). The metabolite levels are much lower when compared to that of oral PK results, which is mainly because the subcutaneous route avoids the first-pass metabolism by the liver. The GCPQ – CUDC-101 nanoparticles that failed to improve the oral drug absorption was successful through subcutaneous route for three reasons; mainly, better stability of the nanoparticles around the subcutaneous pH, absence of intense P-gp efflux and finally the evasion of first-pass metabolism. Thus, the optimized GCPQ – CUDC-101 nanoparticles can be potentially used as subcutaneous injections for cancer treatment.

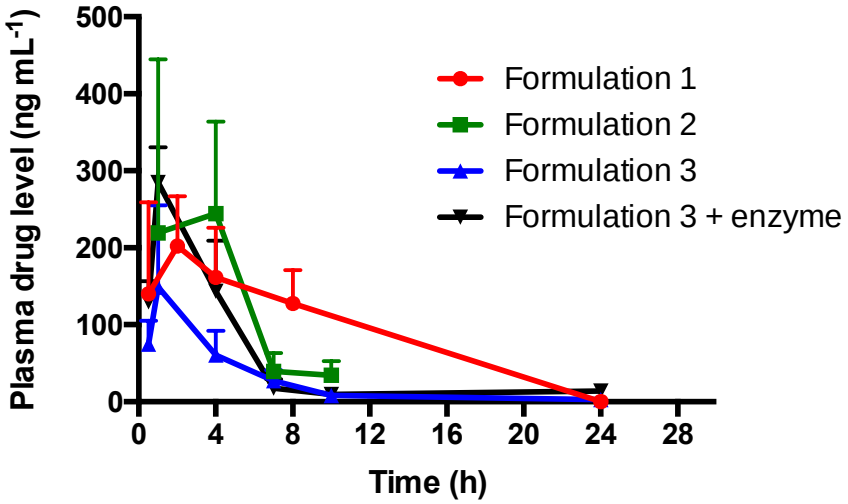

Figure 5.11 Pharmacokinetics of CUDC-101 - GCPQ formulations – drug levels

Plasma drug levels following the subcutaneous administration of CUDC-101 – GCPQ formulations (n = 4).

Table 5.8 Pharmacokinetics of CUDC-101 - GCPQ formulations - drug AUC

	Palmitoylation level	**$AUC_{0\text{-}24\ h}$ (ng h mL^{-1})**	**Duration of drug release (h) (final plasma conc.)**	**Conc.of GCPQ**
Formulation 1	Medium	2441 ± 660*	8 (127 ng mL^{-1})	High
Formulation 2	Low	1232 ± 167*	7 (40 ng mL^{-1})	
Formulation 3		667 ± 322*	4 (60 ng mL^{-1})	Low
Formulation 3 + enzyme		1259 ± 287**	4 (143 ng mL^{-1})	

* = p < 0.005, significantly different from other formulations using One-way ANOVA with Tukey's test. ** = p < 0.05 significantly different from formulation 3 using un-paired T-test (n = 4).

5.4.5.2 Pharmacodynamic (PD) results:

From the PK studies, it was observed that the GCPQ – CUDC-101 nanoparticles had desirable subcutaneous absorption profile. Though the absorption of CUDC-101 from GCPQ formulation 1 was better than the other formulations, it is GCPQ formulation 3 that is clinically relevant, so the PD studies were carried on GCPQ formulation 3 coated with hyaluronidase. Athymic nude mice were implanted with human A431 tumour xenograft, dosed regularly with GCPQ formulation 3 with hyaluronidase at different doses and monitored for tumour size and animal weight changes. Based on this information, tumour survival curve was constructed (Figure 5.13) and from the results it is clear that the lifespan of the animals that receive the treatment is significantly higher (p < 0.001) than the control group. While all the control group animals had to be euthanized by 15 days, three mice from the treatment group survived for at least 50 days after the treatment had commenced.

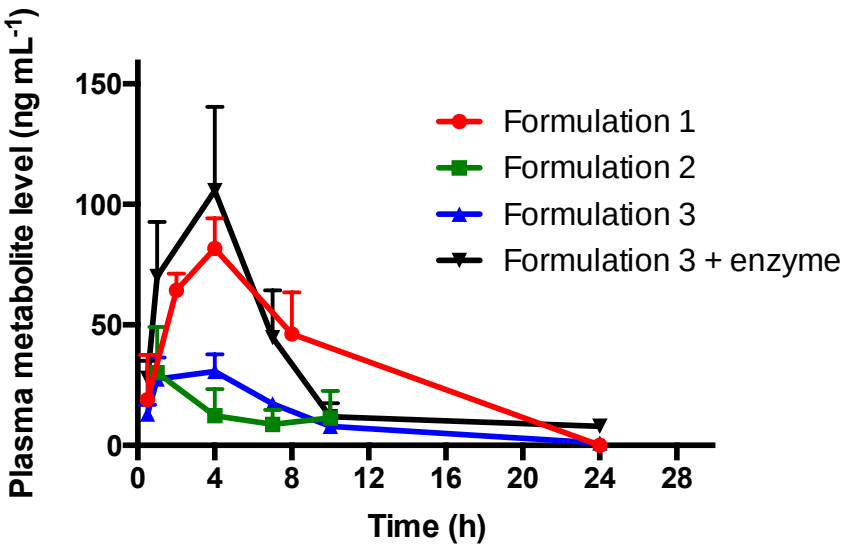

Figure 5.12 Pharmacokinetics of CUDC-101 - GCPQ formulations – metabolite levels

Plasma CUDC-101 metabolite levels following the subcutaneous administration of CUDC-101 – GCPQ formulations (n = 4).

Also there are differences among the treatment group receiving different doses, where survival of the mice that received the lowest dose (60 mg kg^{-1}) was lesser than the animals that received higher doses. On the other hand, the body weight of the mice that received the highest dose (120 mg kg^{-1}) dropped below the permissible limit (body weight change ≥ 15 %), which is a sign for dose limited toxicity. The animals that were treated with the medium dose (90 mg kg^{-1}) had high median survival rate (43 days).

Table 5.9 Median survival determined from Figure 5.13

Treatment	Control	60 mg kg^{-1}	90 mg kg^{-1}	120 mg kg^{-1}
Median survival (days)	15	18.5	43	24

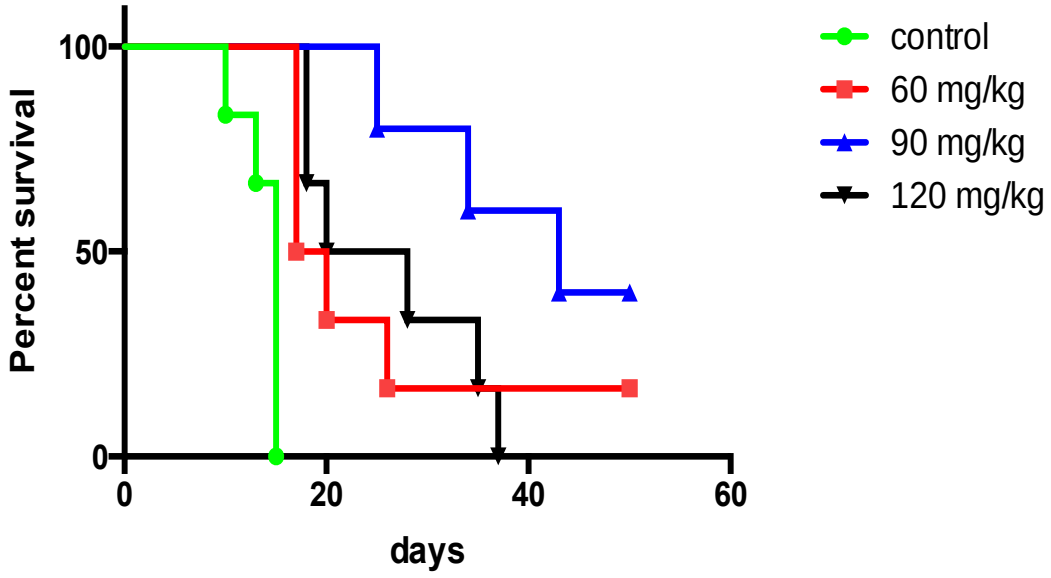

Figure 5.13 Tumour bearing mice survival plot following the daily injection of GCPQ formulation 3 with hyaluronidase.

Statistics used – Mantel-Cox test; Survival curves are significant from one another; ($p < 0.0001$); ($n = 5 – 6$).

The prolonged survival rate of for the 90 mg kg^{-1} treatment group may also be due to the relatively small tumour size at the beginning of the treatment. There is a high likelihood that the effect of 90 mg kg^{-1} treatment is at least in part due to the relatively smaller tumour volume at the beginning of the treatment.

CUDC-101 is a multi-target tumour growth inhibitor, inhibiting human epidermal growth factor (EGFR) receptor kinases and histone deacetlyases (HDAC) [168,169]. Due to its HDAC inhibition activity, the molecule increases the production of acetylated histone protein 3 (Ac-H3), which plays an important role in regulating cellular functions. This HDAC inhibition activity of CUDC-101 in GCPQ formulation 3 + hyaluronidase was monitored in tumour bearing mice using western blotting (Figure 5.15). From the results it can be seen that even the lowest dose of the formulation (60 mg kg^{-1}) inhibits the HDACs and increases the concentration of Ac-H3 within the tumour cells whereas in the control mice, which received just the vehicle there was no expression of Ac-H3. The up regulation of Ac-H3 (along with the inhibition of EGFR receptor kinases) slows down the tumour growth, which eventually prolongs the life span of the tumour bearing mice.

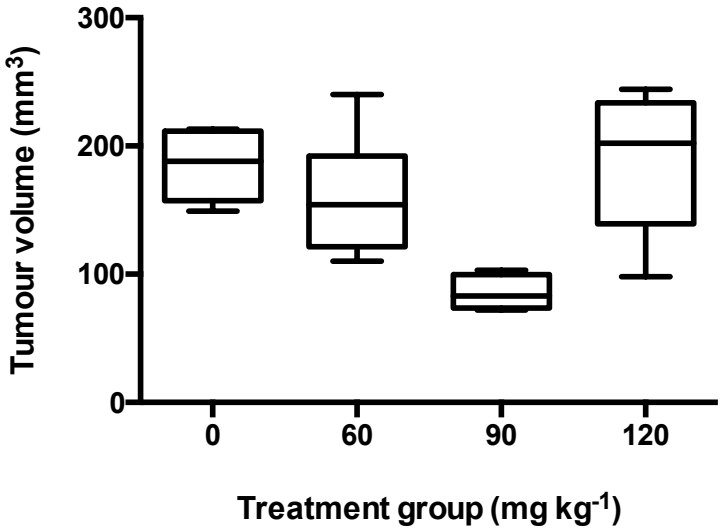

Figure 5.14 Starting tumour volume of the mice on the day of first injection.

The starting tumour volume of 90 mg kg^{-1} treatment group is much smaller than the other treatment group ($p < 0.05$), which might be contributing to the effect of the treatment ($n = 5 – 6$).

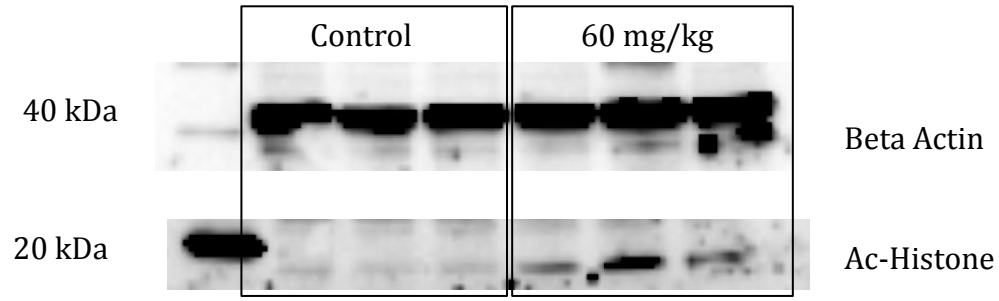

Figure 5.15 Western blot of tumour samples treated with the optimized GCPQ formulation 3.

Levels of acetylated Histone H3 is elevated following the treatment with GCPQ – CUDC-101 nanoparticles at 60 mg kg dose in comparison with the control.

5.5 Discussion:

Subcutaneous administration of nanoparticles are previously reported in the literature on a number of occasions[243–247]. In a recently published article, PLGA – polyvinyl alcohol nanoparticles were used to encapsulate heparin, an anti-coagulant[243]. When injected subcutaneously these nanoparticles prolonged the release of heparin for up to 10 days, while a solution of heparin was absorbed within 24 hours. When it comes to subcutaneous delivery of anti-cancer agents, there are already nine drugs in the market[248]. Thus neither the concept of subcutaneous nanoparticle injections nor subcutaneous cancer therapy is new. But this project has explored a new avenue for GCPQ to prolong the drug release following subcutaneous injections. More importantly this project also aims to develop a clinically relevant subcutaneous dosage form for CUDC-101, which might open up new treatment options for cancer patients.

GCPQ nanoparticles were previously shown to enhance the absorption of hydrophobic drugs through oral and ocular routes[75,176,177]. Here we have shown that GCPQ nanoparticles are capable of improving the absorption of a hydrophobic drug when given subcutaneously. The duration of subcutaneous absorption was directly proportional to the stability of GCPQ-CUDC-101 nanoparticles, which in turn was dependent on the hydrophobicity and concentration of the polymer.

The stability of the drug-polymer complex depends on the hydrophobic interactions between the drug and the polymer's hydrophobic core. Stronger the hydrophobic interaction, longer the colloidal stability and vice versa. High palmitoylation percentages in GCPQ as well as high concentrations of GCPQ itself would give rise to strong hydrophobic interactions with the drug. Hence the colloidal stability of Formulation 1 was much better than that of other formulations, which had high palmitoylation percentage as well as high polymer content, providing more sites for hydrophobic interactions with the drug. The colloidal stability also depends on the concentration of the nanoparticles, as the colloidal particles undergo collision due to Brownian motion, which increases the chances of drug interactions and leads to precipitation.

While the freshly made GCPQ – CUDC-101 nanoparticles are stable for just a period of 8 hours, GCPQ nanoparticles with CyclosporinA (CsA) were stable for a period of 6 months[75]. This difference is mainly due to the intrinsic nature of the drug forming the nanoparticle complexes and also structural differences in a molecule can cause stearic hindrance which might affect the interaction between the drug and the hydrophobic core of GCPQ[91]. The freeze-dried GCPQ – CUDC-101 nanoparticles were stable for at least 3 months which is similar to what is reported for GCPQ – CsA nanoparticles[75].

The *in vivo* subcutaneous absorption of GCPQ – CUDC-101 formulations follows a pattern similar to that of the *in vitro* colloidal stability data. From the results, it is clear that the polymer hydrophobicity and polymer concentration plays an important role in prolonging the duration of subcutaneous release. Similar observations were made with the copolymer PLGA, where increasing the hydrophobicity of PLGA helped in prolonging the release PLGA-risperidone implants in rats[249]. The presence of surface coated hyaluronidase in Formulation 3 also enhanced the drug uptake. Hyaluronidase was long used in the clinic to break the hyaluronic barrier of the skin and human recombinant hyaluronidase (Hylenex) has been approved by FDA to be used in conjunction with Trastuzumab to enhance the uptake of the antibody subcutaneously[239]. In another study, hyaluronidase immobilized on silica nanoparticles (SiNP) were used as adjuvant to deliver carboplatin to A375 cells[250] and in both these cases hyaluronidase was not coated to the active ingredient. In another study,

hyaluronidase was encapsulated within the matrix of chitosan nanoparticles along with 5-flurouracil to improve the drug uptake through cancer cells[251]. So, to our knowledge this is the first instance of using hyaluronidase coated, drug-loaded nanoparticle for the treatment of cancer via subcutaneous route.

The hyaluronidase coated GCPQ – CUDC-101 nanoparticles also prolonged the life span of human A431 xenograft bearing mice by 28 days when compared with the control at 90 mg kg^{-1} dose. The group that received 120 mg kg^{-1} dose, which is also the MTD for CUDC-101 in mice, showed signs of toxicity and thus had many mice removed from the treatment reducing its median survival days. The differences in the effects of treatment might also be due to relatively small tumour size at the starting of 90 mg kg^{-1} treatment group when compared with other treatment groups. This is particularly true for CUDC-101 as the drug's potential mechanism of action is by inhibition of EGFR and HDAC inhibition[169]. The HDAC inhibition down-regulates HIFα, which has a main role in angiogenesis. But in case of well-established tumours, the blood vessels are already in place and the formation of new blood vessels is limited to the periphery of the tumour. When these tumours are treated with CUDC-101 it interferes with angiogenesis in the periphery of the tumour which may severe the blood supply to the core of the tumour, which leads to the development of necrotic lesions as observed in few mice.

EGFR inhibition is also linked to VEGF expression which plays another important role in angiogenesis[252]. Hence later stage tumours already have minimum angiogenic activity, the use of CUDC-101, an anti-angiogenic anti-proliferative compound is rendered less effective. Thus the new subcutaneous treatment regime for cancer using hyaluronidase coated GCPQ – CUDC-101 nanoparticles will be more effective if the treatment is started during the early stages of tumour development.

5.6 Conclusion:

The aim of this section was to develop a clinically relevant formulation for CUDC-101 using GCPQ. GCPQ is known to form viscous dispersions with hydrophobic drugs and the viscosity of these dispersions depends on the concentration, the hydrophobicity and the molecular weight of the GCPQ.

Based on the viscosity measurement, low molecular weight GCPQ with low – medium palmitoylation percentages were used at the concentration 50 mg mL^{-1} to make nanoparticles with CUDC-101. By making these nanoparticles we were able to achieve the target concentration of 50 mg mL^{-1} CUDC-101, thus meeting our first criterion of success. The nanoparticles made were optimized for subcutaneous injection, where the formulation had desired concentration of drug, acceptable tonicity and a storage stability of at least three months, meeting our second criterion for success.

The colloidal stability of the GCPQ – CUDC-101 nanoparticles depends on the concentration and palmitoylation of the GCPQ, where the nanoparticles made with a higher concentration and higher palmitoylation GCPQ had a better colloidal stability. The subcutaneous drug absorption of CUDC-101 from these GCPQ formulations was a reflection of the colloidal stability data, where the formulation with better colloidal stability had better drug absorption and vice versa. The subcutaneous absorption of CUDC-101 was steady and prolonged for duration of more than 6 hours, thus meeting our third criterion for success. The addition of hyaluronidase to the formulation resulted in surface coated nanoparticles, which further enhanced the subcutaneous absorption of the drug.

By meeting all of our three criteria for success, we were able to develop a subcutaneous formulation with a significant pharmacodynamic activity. Tumour treatment with these surface coated GCPQ – CUDC-101 nanoparticles bought in a desirable pharmacodynamic effect, where the life span of human xenograft tumour bearing mice models were prolonged significantly from that of the control. Elevated levels of Ac-H3 in the tumours of the treatment group was documented from Western blotting, which further demonstrates that the GCPQ subcutaneous formulations are pharmacodynamically active.

The optimized GCPQ formulation 3 with hyaluronidase aims to deliver CUDC-101 as twice a day doses of 5 mL each, thereby achieving the current clinical dose of 500 mg active ingredient per day. The formulation is clinically relevant for the following reasons; has desired concentration of active ingredient in the final dosage form, has a long shelf life, easy to administer, has desired tonicity, can be mass produced and manufactured under sterile conditions and more importantly has desired pharmacokinetic and pharmacodynamics profiles. Thus,

a clinically relevant CUDC-101 formulation was developed for subcutaneous injection using GCPQ, which might be therapeutically beneficial to the patients in the clinic.

6 Conclusion and future work:

6.1 Conclusion:

The discovery of hydrophobic new chemical entities has been escalated in recent years due to advancements in combinatorial chemistry and high throughput screening. The oral bioavailability of these NCEs is severely affected by their poor water solubility and sometimes due to the P-gp efflux. Parenteral route of drug delivery overcomes most of the physicochemical and biological barriers but results in poor patient compliance. New technologies are needed to improve the oral absorption of hydrophobic drugs in order to bring new drugs to the market or to increase the treatment options for a marketed drug.

Polymeric amphiphiles are used in drug delivery, because they are capable of improving the absorption and also deliver hydrophobic drugs to a specified target[253]. These amphiphiles are made from natural or synthetic sources but are usually engineered to be biocompatible or biodegradable. Ample publications have been made on use of the polymeric amphiphiles in drug delivery[155,191,240] but more and more such amphiphiles are needed due to the diversity of therapeutic compounds that are hard to formulate[74].

In this project, a new amphiphile was synthesized by conjugating pendant phenoxy acetic acid ring to glycol chitosan (GCPh). This polymer self-assembled at extremely low concentrations (CMC ~ 0.3 μM) and enhanced the oral uptake of paclitaxel through a variety of mechanisms, such as; a) improving the aqueous dissolution by forming nanoparticles with the drug b) mucoadhesion of drug loaded paclitaxel-GCPh nanoparticles and c) the absorption of paclitaxel was P-gp independent due to the uptake of paclitaxel-GCPh nanoparticles through the enterocytes. Thus this new polymer maybe used to improve the absorption of other hydrophobic drugs.

Another important finding of this project is that, an important link between drug dissolution and P-gp efflux was established using paclitaxel formulated as Taxol®. It was found that improving the dissolution of the formulation saturated the activity of the P-gp efflux pumps. This might mean that future formulation strategies to improve the oral delivery of BCS Class IV drugs can be directed

towards improving their rate of dissolution rather than adding excipients to inhibit the P-gp efflux pumps.

Oral delivery of CUDC-101, a BCS Class IV anti-cancer agent was attempted in the form of GCPQ nanoparticles or gastro-retentive dosage forms. But the pre-clinical proof of concept for these formulations could not be achieved through my experiments. Hence attempts were made to deliver the GCPQ nanoparticles through the subcutaneous route. For this purpose a pre-clinical formulation containing hyaluronidase enzyme coated GCPQ – CUDC-101 nanoparticles were developed, which increased the life span of tumour bearing mice by 28 days.

This the first instance were nanoparticles were surface coated with hyaluronidase enzymes and the advantage of this coating is that it increases the chances of intact nanoparticles to be absorbed and reach the tumour. The formulation was optimised for further clinical trials and in future, a self-administrable subcutaneous dosage form could be potentially tested at the clinical level for the GCPQ – CUDC-101 nanoparticles.

6.2 Future work:

The new polymer GCPh should be evaluated for its safety profile. Hemocompatability studies and toxicity studies could be carried out to determine the maximum tolerable dose for GCPh. Additionally, the polymer should be tested for its role in promoting transcellular transport and mechanistic studies should be carried out to determine if the drug loaded nanoparticles are taken up through phagocytosis. Also, the paclitaxel-loaded GCPh nanoparticles could be tested for its *in vivo* anti-tumour activity in human xenograft mice models. Our experiment with ex vivo confocal microscopy suggested that GCPh nanoparticles might be reaching the systemic circulation intact. This needs to be further probed and the mechanism by which this occurs requires in-depth understanding. If this is true then the drug-loaded nanoparticles might specifically get trapped in the tumour tissue due to EPR effect, which might result in improved therapeutic index. The distribution of these nanoparticles in different organs could also be studied, which would lead to better understanding on the fate of GCPh nanoparticles upon ingestion.

To improve the oral absorption of CUDC-101, other formulation strategies such as liposomes or other micellar systems could be experimented. The choice of formulation strategies for CUDC-101 is limited by its extremely poor solubility not just in aqueous environment but also in organic solvents. CUDC-101 – GCPQ nanoparticles showed acceptable stability at neutral pH conditions. Thus enteric-coated capsules containing the dried CUDC-101 – GCPQ nanoparticles should be tested in larger animal models such as dogs, in which high drug doses are possible when compared to rats. Similar studies in higher mammals could also be done for the gastro-retentive dosage form, as the desired dosage for CUDC-101 could not be achieved in the experiments using rats.

The subcutaneous dosage form for CUDC-101 offers an alternative delivery option to the oral delivery of the drug. Studies could be carried out on this formulation to determine if the CUDC-101 – GCPQ nanoparticles are taken up via the lymphatic route, as this could be useful to treat tumour metastasis. Also, studies should be carried out to assess the distribution GCPQ nanoparticles in the tissues such as liver, spleen, kidneys and tumour, so as to understand the toxicity, bio distribution and elimination of the CUDC-101 – GCPQ nanoparticles.

Bibliography

1. Sastry S.V. *et al.* Recent technological advances in oral drug delivery – a review. *Pharm. Sci. Technolo. Today* **3,** 138–145 (2000).
2. Ranade, V. V. Drug delivery systems 5A. Oral drug delivery. *J. Clin. Pharmacol.* **31,** 2–16 (1991).
3. Lipinski, C. A. *et al.* Experimental and computational approaches to estimate solubility and permeability in drug discovery and development settings. *Adv. Drug Deliv. Rev.* **64,** 4–17 (2012).
4. Lipinski, C. A. *et al.* Experimental and computational approaches to estimate solubility and permeability in drug discovery and development settings. *Adv. Drug Deliv. Rev.* **23,** 3–25 (1997).
5. Lipinski, C. A. *et al.* Experimental and computational approaches to estimate solubility and permeability in drug discovery and development settings. *Adv. Drug Deliv. Rev.* **46,** 3–26 (2001).
6. Gallop, M. A. *et al.* Applications of Combinatorial Technologies to Drug Discovery. 1. Background and Peptide Combinatorial Libraries. *J. Med. Chem.* **37,** (1994).
7. Watt, A. & Morrison, D. Strategic and technical challenges for drug discovery. *Drug Discov. Today* **6,** 290–292 (2001).
8. Chaudhary, A. *et al.* Enhancement of solubilization and bioavailability of poorly soluble drugs by physical and chemical modifications: A recent review. *J. Adv. Pharm. Educ. Res.* **2,** 32–67 (2012).
9. Maddineni, S. *et al.* Dissolution Research- A predictive tool for Conventional and Novel Dosage Forms. *Asian J. Pharm. Life Sci.* **2,** 119–134 (2012).
10. Dokoumetzidis, A. & Macheras, P. A century of dissolution research: from Noyes and Whitney to the biopharmaceutics classification system. *Int J Pharm* **321,** 1–11 (2006).
11. Hörter, D. & Dressman, J. . Influence of physicochemical properties on dissolution of drugs in the gastrointestinal tract. *Adv. Drug Deliv. Rev.* **46,** 75–87 (2001).
12. Takaya, T. *et al.* Importance of dissolution process on systemic availability of drugs delivered by colon delivery system. *J. Control. Release* **50,** 111–22 (1998).
13. Kirkpatrick, P. ADME: Pressures in the pipeline. *Nat. Rev. Drug Discov.* **2,** 337–337 (2003).
14. Sun, J. *et al.* Effect of particle size on solubility, dissolution rate, and oral bioavailability: evaluation using coenzyme Q10 as naked nanocrystals. *Int J Nanomedicine* **7,** 5733–5744 (2012).
15. Chillistone, S. & Hardman, J. Factors affecting drug absorption and distribution. *Anaesth. Intensive Care Med.* **9,** 167–171 (2008).
16. Henderson, J. Concerning the relationship between the strength of acids and their capacity to preserve neutrality. *Am. J. Physiol.* **18,** 250–255 (1907).
17. Kokate, A. *et al.* Effect of drug lipophilicity and ionization on permeability across the buccal mucosa: a technical note. *AAPS PharmSciTech* **9,** 501–4 (2008).
18. Pade, V. & Stavchansky, S. Link between drug absorption solubility and

permeability measurements in Caco-2 cells. *J. Pharm. Sci.* **87,** 1604–7 (1998).
19. Masaoka, Y. *et al.* Site of drug absorption after oral administration: assessment of membrane permeability and luminal concentration of drugs in each segment of gastrointestinal tract. *Eur. J. Pharm. Sci.* **29,** 240–50 (2006).
20. Skolnik, S. *et al.* Towards Prediction of In Vivo Intestinal Absorption Using a 96-Well Caco-2 Assay. *J. Pharm. Sci.* **99,** 3246–3265 (2010).
21. Lipinski, C. A. Drug-like properties and the causes of poor solubility and poor permeability. *J. Pharmacol. Toxicol. Methods* **44,** 235–249 (2000).
22. Rodríguez-Spong, B. *et al.* General principles of pharmaceutical solid polymorphism: a supramolecular perspective. *Adv. Drug Deliv. Rev.* **56,** 241–74 (2004).
23. Salzmann, C. G. *et al.* The polymorphism of ice: five unresolved questions. *Phys. Chem. Chem. Phys.* **13,** 18468–80 (2011).
24. Yu, L. Amorphous pharmaceutical solids: preparation, characterization and stabilization. *Adv. Drug Deliv. Rev.* **48,** 27–42 (2001).
25. Lindfors, L. *et al.* Amorphous Drug Nanosuspensions. 3. Particle Dissolution and Crystal Growth. *Langmuir* **23,** 9866–9874 (2007).
26. Harmoinen, J. *et al.* Enzymic degradation of a beta-lactam antibiotic, ampicillin, in the gut: a novel treatment modality. *J. Antimicrob. Chemother.* **51,** 361–5 (2003).
27. Holt, S. *et al.* Measurement of gastric emptying rate in humans by real-time ultrasound. *Gastroenterology* **90,** 918–23 (1986).
28. Bushra, R. *et al.* Food-drug interactions. *Oman Med. J.* **26,** 77–83 (2011).
29. Charman, W. N. *et al.* Physiochemical and physiological mechanisms for the effects of food on drug absorption: the role of lipids and pH. *J. Pharm. Sci.* **86,** 269–82 (1997).
30. Won, C. S. *et al.* Influence of dietary substances on intestinal drug metabolism and transport. *Curr. Drug Metab.* **11,** 778–92 (2010).
31. Leyden, J. J. Absorption of minocycline hydrochloride and tetracycline hydrochloride. Effect of food, milk, and iron. *J. Am. Acad. Dermatol.* **12,** 308–12 (1985).
32. Custodio, J. M. *et al.* Predicting drug disposition, absorption/elimination/transporter interplay and the role of food on drug absorption. *Adv. Drug Deliv. Rev.* **60,** 717–33 (2008).
33. Bakatselou, V. Solubilization and Wetting effects of Bile Salts on the Dissolution of Steroids. *Pharm. Res.* **8,** (1991).
34. Galetin, A. & Houston, J. B. Intestinal and Hepatic Metabolic Activity of Five Cytochrome P450 Enzymes : Impact on Prediction of First-Pass Metabolism. *Pharmacol. Exp. Ther.* **318,** 1220–1229 (2006).
35. Hosea, N. A. *et al.* Elucidation of Distinct Ligand Binding Sites for Cytochrome P450 3A4 †. *Biochemistry* **39,** 5929–5939 (2000).
36. Tracy, T. S. *et al.* Cytochrome P450 isoforms involved in metabolism of the enantiomers of verapamil and norverapamil. *Br. J. Clin. Pharmacol.* **47,** 545–52 (1999).
37. Benet, L. Z. *et al.* Intestinal drug metabolism and antitransport processes: A potential paradigm shift in oral drug delivery. *J. Control. Release* **39,** 139–143 (1996).
38. Tolle-Sander, S. *et al.* Midazolam exhibits characteristics of a highly

permeable P-glycoprotein substrate. *Pharm. Res.* **20,** 757–64 (2003).
39. Williams, M. T. Cytochrome P450. Mechanisms of action and clinical implications. *J. Fla. Med. Assoc.* **79,** 405–8 (1992).
40. Bhat, P. The limiting role of mucus in drug absorption: Drug permeation through mucus solution. *Int. J. Pharm.* **126,** 179–187 (1995).
41. Khanvilkar, K. Drug transfer through mucus. *Adv. Drug Deliv. Rev.* **48,** 173–193 (2001).
42. Qin, X. *et al.* Hydrophobicity of mucosal surface and its relationship to gut barrier function. *Shock* **29,** 372–6 (2008).
43. Chiou, W. L. Effect of 'unstirred' water layer in the intestine on the rate and extent of absorption after oral administration. *Biopharm. Drug Dispos.* **15,** 709–17 (1994).
44. Levitt, M. D. *et al.* Physiological measurements of luminal stirring in the dog and human small bowel. *J. Clin. Invest.* **86,** 1540–7 (1990).
45. Loftsson, T. & Brewster, M. E. Physicochemical properties of water and its effect on drug delivery. A commentary. *Int. J. Pharm.* **354,** 248–54 (2008).
46. Salama, N. N. *et al.* Tight junction modulation and its relationship to drug delivery. *Adv. Drug Deliv. Rev.* **58,** 15–28 (2006).
47. Hunter, J. *et al.* Drug absorption limited by P-glycoprotein-mediated secretory drug transport in human intestinal epithelial Caco-2 cell layers. *Pharm. Res.* **10,** 743–9 (1993).
48. Hunter, J. & Hirst, B. H. Intestinal secretion of drugs. The role of P-glycoprotein and related drug efflux systems in limiting oral drug absorption. *Adv. Drug Deliv. Rev.* **25,** 129–157 (1997).
49. Klyashchitsky, B. A. & Owen, A. J. Drug delivery systems for cyclosporine: achievements and complications. *J. Drug Target.* **5,** 443–58 (1998).
50. Kwan, K. C. Oral bioavailability and first-pass effects. *Drug Metab. Dispos.* **25,** 1329–1336 (1997).
51. Pond, S. M. & Tozer, T. N. First-pass elimination. Basic concepts and clinical consequences. *Clin. Pharmacokinet.* **9,** 1–25
52. Shiffman, M. L. *et al.* Hepatic lidocaine metabolism and liver histology in patients with chronic hepatitis and cirrhosis. *Hepatology* **19,** 933–40 (1994).
53. Borg, K. O. *et al.* Metabolism of alprenolol in liver microsomes, perfused liver and conscious rat. *Acta Pharmacol. Toxicol. (Copenh).* **35,** 169–79 (1974).
54. Tegeder, I. *et al.* Pharmacokinetics of opioids in liver disease. *Clin. Pharmacokinet.* **37,** 17–40 (1999).
55. Fasinu, P. *et al.* Diverse approaches for the enhancement of oral drug bioavailability. *Biopharm. Drug Dispos.* **32,** 185–209 (2011).
56. Shinde, A. J. Solubilization of Poorly Soluble Drugs: A Review |. Available at: http://www.pharmainfo.net/reviews/solubilization-poorly-soluble-drugs-review. (Accessed: 5th February 2013)
57. Stegemann, S. *et al.* When poor solubility becomes an issue: from early stage to proof of concept. *Eur. J. Pharm. Sci.* **31,** 249–61 (2007).
58. Robert O. Williams III. *Formulating poorly water soluble drugs*. (AAPS Press, 2012). doi:10.1007/978-1-4614-1144-4
59. Nelson, E. Comparative dissolution rates of weak acids and their sodium

salts. *J Am Pharm Assoc Am Pharm Assoc* **47,** 297–299 (1958).
60. Serajuddin, A. T. M. Salt formation to improve drug solubility. *Adv. Drug Deliv. Rev.* **59,** 603–616 (2007).
61. Nelson, E. *et al.* Influence of the absorption rate of tolbutamide on the rate of decline of blood sugar levels in normal humans. *J Pharm Sci* **51,** 509–514 (1962).
62. Choi, J. S. & Jo, B. W. Enhanced paclitaxel bioavailability after oral administration of pegylated paclitaxel prodrug for oral delivery in rats. *Int J Pharm* **280,** 221–227 (2004).
63. Zhao, H. *et al.* Antibacterial activities of amorphous cefuroxime axetil ultrafine particles prepared by high gravity antisolvent precipitation (HGAP). *Pharm Dev Technol* **14,** 485–491 (2009).
64. Adrjanowicz, K. *et al.* Effect of cryogrinding on chemical stability of the sparingly water-soluble drug furosemide. *Pharm. Res.* **28,** 3220–36 (2011).
65. Farinha, A. *et al.* Improved Bioavailability of a Micronized Megestrol Acetate Tablet Formulation in Humans. *Drug Dev. Ind. Pharm.* **26,** 567–570 (2000).
66. Strickley, R. Solubilizing Excipients in Oral and Injectable Formulations. *Pharm. Res.* **21,** 201–230 (2004).
67. Vater, W. *et al.* Pharmacology of 4-(2'-nitrophenyl)-2,6-dimethyl-1,4-dihydropyridine-3,5-dicarboxylic acid dimethyl ester (Nifedipine, BAY a 1040). *Arzneimittelforschung.* **22,** 1–14 (1972).
68. RASHEED, A. *et al.* Cyclodextrins as Drug Carrier Molecule: A Review. *Sci Pharm.* **76,** 567–598 (2008).
69. Leroylechat, F. *et al.* Evaluation of the Cytotoxicity of Cyclodextrins and Hydroxypropylated Derivatives. *Int J Pharm* **101,** 97–103 (1994).
70. Gould, S. & Scott, R. C. 2-Hydroxypropyl-beta-cyclodextrin (HP-beta-CD): a toxicology review. *Food Chem Toxicol* **43,** 1451–1459 (2005).
71. Wong, J. W. *et al.* Therapeutic equivalence of a low dose artemisinin formulation in falciparum malaria patients. *J Pharm Pharmacol* **55,** 193–198 (2003).
72. Sachs-Barrable, K. *et al.* Enhancing drug absorption using lipids: a case study presenting the development and pharmacological evaluation of a novel lipid-based oral amphotericin B formulation for the treatment of systemic fungal infections. *Adv Drug Deliv Rev* **60,** 692–701 (2008).
73. T G Mason K Meleson, C B Chang and S M Graves, J. N. W. Nanoemulsions: formation, structure, and physical properties. *J. Phys. Condens. Matter* **18,** 635–666 (2006).
74. De Jong, W. H. & Borm, P. J. a. Drug delivery and nanoparticles:applications and hazards. *Int. J. Nanomedicine* **3,** 133–49 (2008).
75. Siew, A. *et al.* Enhanced oral absorption of hydrophobic and hydrophilic drugs using quaternary ammonium palmitoyl glycol chitosan nanoparticles. *Mol. Pharm.* **9,** 14–28 (2012).
76. Hussain, A. & Rytting, J. H. Prodrug approach to enhancement of rate of dissolution of allopurinol. *J. Pharm. Sci.* **63,** 798–799 (1974).
77. Huttunen, K. M. & Rautio, J. Prodrugs - an efficient way to breach delivery and targeting barriers. *Curr. Top. Med. Chem.* **11,** 2265–87 (2011).
78. Van den Mooter, G. *et al.* Physical stabilisation of amorphous

ketoconazole in solid dispersions with polyvinylpyrrolidone K25. *Eur. J. Pharm. Sci.* **12,** 261–9 (2001).
79. Yoshioka, M. *et al.* Crystallization of indomethacin from the amorphous state below and above its glass transition temperature. *J Pharm Sci* **83,** 1700–1705 (1994).
80. Kesisoglou, F. *et al.* Nanosizing--oral formulation development and biopharmaceutical evaluation. *Adv. Drug Deliv. Rev.* **59,** 631–44 (2007).
81. Jens-Uwe A H Junghanns, R. H. M. Nanocrystal technology, drug delivery and clinical applications. *Int. J. Nanomedicine* **3,** 295–310 (2008).
82. Takatsuka, S. *et al.* Enhancement of intestinal absorption of poorly absorbed hydrophilic compounds by simultaneous use of mucolytic agent and non-ionic surfactant. *Eur. J. Pharm. Biopharm.* **62,** 52–58 (2006).
83. Dimitrijevic, D. *et al.* Effects of some non-ionic surfactants on transepithelial permeability in Caco-2 cells. *J. Pharm. Pharmacol.* **52,** 157–62 (2000).
84. Sajeesh, S. & Sharma, C. P. Cyclodextrin–insulin complex encapsulated polymethacrylic acid based nanoparticles for oral insulin delivery. *Int. J. Pharm.* **325,** 147–154 (2006).
85. Stella, V. J. & He, Q. Cyclodextrins. *Toxicol. Pathol.* **36,** 30–42 (2008).
86. Veiga, F. *et al.* Oral bioavailability and hypoglycaemic activity of tolbutamide/cyclodextrin inclusion complexes. *Int J Pharm* **202,** 165–171 (2000).
87. Francis, M. F. *et al.* Polymeric micelles for oral drug delivery: Why and how. *Pure Appl. Chem.* **76,** 1321–1335 (2004).
88. Blume, G. & Cevc, G. Liposomes for the sustained drug release in vivo. *Biochim. Biophys. Acta* **1029,** 91–7 (1990).
89. Gros, B. L. *et al.* Polymeric Antitumor Agents on a Molecular and on a Cellular Level. *Angew. Chemie Int. Ed.* **20,** 305–325 (1981).
90. Sharma, A. & Sharma, U. S. Liposomes in drug delivery: Progress and limitations. *Int. J. Pharm.* **154,** 123–140 (1997).
91. Narang, A. S. *et al.* Stable drug encapsulation in micelles and microemulsions. *Int. J. Pharm.* **345,** 9–25 (2007).
92. Erez, R. *et al.* Bioorganic & Medicinal Chemistry Enhanced cytotoxicity of a polymer – drug conjugate with triple payload of paclitaxel. *Bioorg. Med. Chem.* **17,** 4327–4335 (2009).
93. Torchilin, V. P. Recent advances with liposomes as pharmaceutical carriers. *Nat. Rev. Drug Discov.* **4,** 145–60 (2005).
94. Chen, Y. *et al.* Enhanced bioavailability of the poorly water-soluble drug fenofibrate by using liposomes containing a bile salt. *Int. J. Pharm.* **376,** 153–160 (2009).
95. Patel, N. & Panda, S. Liposome Drug delivery system : a Critic Review. *J. Pharm. Sci. Biosci. Res.* **2,** 169–175 (2012).
96. Allen, T. M. & Cullis, P. R. Liposomal drug delivery systems: from concept to clinical applications. *Adv. Drug Deliv. Rev.* **65,** 36–48 (2013).
97. Miller, T. *et al.* Drug loading of polymeric micelles. *Pharm. Res.* **30,** 584–95 (2013).
98. Dufès, C. *et al.* Dendrimers in gene delivery. *Adv. Drug Deliv. Rev.* **57,** 2177–2202 (2005).
99. Pillai, O. & Panchagnula, R. Polymers in drug delivery. *Curr. Opin. Chem. Biol.* **5,** 447–451 (2001).

100. Uchegbu, I. F. *et al.* Quaternary ammonium palmitoyl glycol chitosan--a new polysoap for drug delivery. *Int. J. Pharm.* **224,** 185–99 (2001).
101. Neslihan Gursoy, R. & Benita, S. Self-emulsifying drug delivery systems (SEDDS) for improved oral delivery of lipophilic drugs. *Biomed. & Pharmacother.* **58,** 173–182 (2004).
102. Bauer, K. H. & Dortunc, B. Non-aqueous emulsions as a vehicle for capsule fillings. *Drug Dev. Ind. Pharm.* **10,** 699–712 (1984).
103. Suitthimeathegorn, O. *et al.* Intramuscular absorption and biodistribution of dexamethasone from non-aqueous emulsions in the rat. *Int. J. Pharm.* **331,** 204–210 (2007).
104. Voigt, M. Biodegradable Non-aqueous in situ Forming Microparticle Drug Delivery Systems. (Der Freien Universität Berlin, 2011).
105. Shiau, Y. F. Mechanisms of intestinal fat absorption. *Am. J. Physiol.* **240,** (1981).
106. Porter, C. J. H. *et al.* Enhancing intestinal drug solubilisation using lipid-based delivery systems. *Adv. Drug Deliv. Rev.* **60,** 673–691 (2008).
107. Wasan, E. K. *et al.* Development and characterization of oral lipid-based amphotericin B formulations with enhanced drug solubility, stability and antifungal activity in rats infected with Aspergillus fumigatus or Candida albicans. *Int. J. Pharm.* **372,** 76–84 (2009).
108. Streubel, A. *et al.* Gastroretentive drug delivery systems. *Expert Opin. Drug Deliv.* **3,** 217–33 (2006).
109. Arora, S. *et al.* Floating Drug Delivery Systems : A Review. **6,** 372–390 (2005).
110. Khan, F. N. & Dehghan, M. H. G. Enhanced bioavailability of atorvastatin calcium from stabilized gastric resident formulation. *AAPS PharmSciTech* **12,** 1077–86 (2011).
111. Narang, N. An updated review on: Floating drug delivery system (FDDS). *Int. J. Appl. Pharm.* **3,** 1–7 (2011).
112. Prohotsky, D. L. & Zhao, F. A survey of top 200 drugs--inconsistent practice of drug strength expression for drugs containing salt forms. *J. Pharm. Sci.* **101,** 1–6 (2012).
113. Paulekuhn, G. S. *et al.* Trends in active pharmaceutical ingredient salt selection based on analysis of the Orange Book database. *J. Med. Chem.* **50,** 6665–72 (2007).
114. Stephenson, A. G. *et al.* Physical Stability of Salts of Weak Bases in the Solid-State. *J. Pharm. Sci.* **100,** 1607–1617 (2011).
115. Sonje, V. M. *et al.* Effect of counterions on the properties of amorphous atorvastatin salts. *Eur. J. Pharm. Sci.* **44,** 462–70 (2011).
116. Pridgen, E. M. *et al.* Polymeric nanoparticle drug delivery technologies for oral delivery applications. *Expert Opin. Drug Deliv.* **5247,** 1–15 (2015).
117. Ensign, L. M. *et al.* Oral drug delivery with polymeric nanoparticles: the gastrointestinal mucus barriers. *Adv Drug Deliv Rev* **64,** 557–570 (2012).
118. Uchegbu, I. F. & Schatzlein, A. *Polymers in Drug Delivery*. (CRC Press, 2006).
119. Liechty, W. B. *et al.* Polymers for Drug Delivery Systems. *Annu. Rev. Chem. Biomol. Eng.* **1,** 149–173 (2010).
120. Lammers, T. SMART drug delivery systems: Back to the future vs. clinical reality. *Int. J. Pharm.* **454,** 527–529 (2013).
121. Sripriyalakshmi, S. *et al.* Recent trends in drug delivery system using

protein nanoparticles. *Cell Biochem. Biophys.* **70,** 17–26 (2014).
122. Leite, D. M. *et al.* Peptide Self-Assemblies for Drug Delivery. (2015).
123. Uchegbu, I. F. *et al.* Chitosan amphiphiles provide new drug delivery opportunities. *Polym. Int.* **63,** 1145–1153 (2014).
124. Duncan, R. The dawning era of polymer therapeutics. *Nat. Rev. Drug Discov.* **2,** 347–60 (2003).
125. Gulati, N. & Gupta, H. Parenteral drug delivery: a review. *Recent Pat. Drug Deliv. Formul.* **5,** 133–45 (2011).
126. Stoner, K. L. *et al.* Intravenous versus Subcutaneous Drug Administration. Which Do Patients Prefer? A Systematic Review. *Patient* **8,** 145 – 153 (2015).
127. Richter, W. F. *et al.* Mechanistic Determinants of Biotherapeutics Absorption Following SC Administration. *AAPS J.* **14,** 559–570 (2012).
128. Swartz, M. The physiology of the lymphatic system. *Adv. Drug Deliv. Rev.* **50,** 3–20 (2001).
129. Levick, J. R. Flow through interstitium and other fibrous matrices. *Q. J. Exp. Physiol.* **72,** 409–437 (1987).
130. Wiig, H. & Swartz, M. a. Interstitial Fluid and Lymph Formation and Transport: Physiological Regulation and Roles in Inflammation and Cancer. *Physiol. Rev.* **92,** 1005–1060 (2012).
131. McLennan, D. N. *et al.* Subcutaneous drug delivery and the role of the lymphatics. *Drug Discov. Today Technol.* **2,** 89–96 (2005).
132. Porter, C. J. H. *et al.* Lymphatic transport of proteins after subcutaneous administration. *J. Control. Release* **8,** 427–440 (2012).
133. ter Braak, E. W. *et al.* Injection site effects on the pharmacokinetics and glucodynamics of insulin lispro and regular insulin. *Diabetes Care* **19,** 1437–40 (1996).
134. Beshyah, S. A. *et al.* The effect of subcutaneous injection site on absorption of human growth hormone: abdomen versus thigh. *Clin. Endocrinol. (Oxf).* **35,** 409–12 (1991).
135. Mrsny, R. J. & Daugherty, A. *Metabolic Processes at Injection Sites Affecting Pharmacokinetics, Pharmacodynamics and Metabolism of Protein and Peptide Therapeutics*. *Proteins and Peptides: Pharmacokinteic, Pharmacodynamic and Metabolic outcomes* (2009).
136. Kuerzel, G. U. *et al.* Biotransformation of insulin glargine after subcutaneous injection in healthy subjects. *Curr. Med. Res. Opin.* **19,** 34–40 (2003).
137. Charman, S. A. *et al.* Systemic availability and lymphatic transport of human growth hormone administered by subcutaneous injection. *J. Pharm. Sci.* **89,** 168–77 (2000).
138. Wang, W. *et al.* Lymphatic transport and catabolism of therapeutic proteins after subcutaneous administration to rats and dogs. *Drug Metab. Dispos.* **40,** 952–62 (2012).
139. Pajouhesh, H. & Lenz, G. R. Medicinal chemical properties of successful central nervous system drugs. *NeuroRx* **2,** 541–53 (2005).
140. Banks, W. A. Characteristics of compounds that cross the blood-brain barrier. *BMC Neurol.* **9 Suppl 1,** S3 (2009).
141. Supersaxo, A. *et al.* Effect of molecular weight on the lymphatic absorption of water-soluble compounds following subcutaneous administration. *Pharm. Res.* **7,** 167–9 (1990).

142. Oussoren, C. & Storm, G. Liposomes to target the lymphatics by subcutaneous administration. *Adv. Drug Deliv. Rev.* **50,** 143–156 (2001).
143. Oussoren, C. *et al.* Lymphatic uptake and biodistribution of liposomes after subcutaneous injection. *Biochim. Biophys. Acta - Biomembr.* **1328,** 261–272 (1997).
144. Allen, T. M. *et al.* Subcutaneous administration of liposomes: a comparison with the intravenous and intraperitoneal routes of injection. *Biochim. Biophys. Acta* **1150,** 9–16 (1993).
145. Tümer, A. *et al.* Fate of cholesterol-rich liposomes after subcutaneous injection into rats. *Biochim. Biophys. Acta* **760,** 119–25 (1983).
146. Hawley, A. E. *et al.* Targeting of colloids to lymph nodes: influence of lymphatic physiology and colloidal characteristics. *Adv. Drug Deliv. Rev.* **17,** 129–148 (1995).
147. Patel, H. M. *et al.* Assessment of the potential uses of liposomes for lymphoscintigraphy and lymphatic drug delivery failure of 99m-technetium marker to represent intact liposomes in lymph nodes. *Biochim. Biophys. Acta - Gen. Subj.* **801,** 76–86 (1984).
148. Mangat, S. & Patel, H. M. Lymph node localization of non-specific antibody-coated liposomes. *Life Sci.* **36,** 1917–25 (1985).
149. Kaur, C. D. *et al.* Lymphatic targeting of zidovudine using surface-engineered liposomes. *J. Drug Target.* **16,** 798–805 (2008).
150. Kaledin, V. I. *et al.* Subcutaneously injected radiolabeled liposomes: transport to the lymph nodes in mice. *J. Natl. Cancer Inst.* **69,** 67–71 (1982).
151. Hirenkumar, M. K. & Siegel, S. J. Poly Lactic-co-Glycolic Acid (PLGA) as Biodegradable Controlled Drug Delivery Carrier. *Polym.* **3,** 1377–1397 (2011).
152. Zhang, N. *et al.* Polysaccharide-based micelles for drug delivery. *Pharmaceutics* **5,** 329–352 (2013).
153. Samad, A. *et al.* Liposomal drug delivery systems: an update review. *Curr. Drug Deliv.* **4,** 297–305 (2007).
154. Yu, D. *et al.* Hydroxyapatite cement based drug delivery systems: drug release in vitro. *J. Formos. Med. Assoc.* **90,** 953–7 (1991).
155. Namita M, T. *et al.* PLGA/PLA Microparticulate system: A boon for hydrophobic drug delivery. *Int. J. Appl. Biol. P...* **3,** 121–132 (2012).
156. Cai, Y. *et al.* Long-acting preparations of exenatide. *Drug Des. Devel. Ther.* **7,** 963–70 (2013).
157. Lin, X. *et al.* Thermosensitive in situ hydrogel of paclitaxel conjugated poly(ε-caprolactone)-poly(ethylene glycol)-poly(ε-caprolactone). *Soft Matter* **8,** 3470 (2012).
158. Bikram, M. *et al.* Temperature-sensitive hydrogels with SiO2-Au nanoshells for controlled drug delivery. *J. Control. Release* **123,** 219–227 (2007).
159. Swartz, M. A. & Skobe, M. Lymphatic function, lymphangiogenesis, and cancer metastasis. *Microsc. Res. Tech.* **55,** 92–9 (2001).
160. Yan, Z. *et al.* LyP-1-conjugated PEGylated liposomes: a carrier system for targeted therapy of lymphatic metastatic tumor. *J. Control. Release* **157,** 118–25 (2012).
161. Frost, G. I. Recombinant human hyaluronidase (rHuPH20): an enabling platform for subcutaneous drug and fluid administration. *Expert Opin.*

Drug Deliv. **4,** 427–40 (2007).
162. Bookbinder, L. H. *et al.* A recombinant human enzyme for enhanced interstitial transport of therapeutics. *J. Control. Release* **114,** 230–241 (2006).
163. Priya James, H. *et al.* Smart polymers for the controlled delivery of drugs – a concise overview. *Acta Pharm. Sin. B* **4,** 120–127 (2014).
164. Cabane, E. *et al.* Stimuli-responsive polymers and their applications in nanomedicine. *Biointerphases* **7,** 9 (2012).
165. Wu, Z. *et al.* Self-propelled polymer-based multilayer nanorockets for transportation and drug release. *Angew. Chemie Int. Ed.* **52,** 7000–3 (2013).
166. Peng, F. *et al.* Self-Guided Supramolecular Cargo-Loaded Nanomotors with Chemotactic Behavior towards Cells. *Angew. Chemie* **127,** 11828–11831 (2015).
167. Stuart, M. A. C. *et al.* Emerging applications of stimuli-responsive polymer materials. *Nat. Mater.* **9,** 101–13 (2010).
168. Cai, X. *et al.* Discovery of 7-(4-(3-Ethynylphenylamino)-7-methoxyquinazolin-6-yloxy)-N-hydroxyheptanamide (CUDC-101) as a Potent Multi-Acting HDAC , EGFR , and HER2 Inhibitor for the Treatment of Cancer. *Jounral Med. Chem.* **53,** 2000–2009 (2010).
169. Lai, C. *et al.* CUDC-101 , a Multitargeted Inhibitor of Histone Deacetylase , Epidermal Growth Factor Receptor , and Human Epidermal Growth Factor Receptor 2 , Exerts Potent Anticancer Activity. *Cancer Res.* **70,** 3647–3656 (2010).
170. Slichenmyer, W. J. & Von Hoff, D. D. Taxol: a new and effective anti-cancer drug. *Anticancer. Drugs* **2,** 519–30 (1991).
171. Jang, S. H. *et al.* Kinetics of P-glycoprotein-mediated efflux of paclitaxel. *J. Pharmacol. Exp. Ther.* **298,** 1236–42 (2001).
172. Uchegbu, I. F. *et al. Fundamentals of Pharmaceutical Nanoscience (Part 1 - Low molecular weight micelles)*. **23,** (Springer Science & Business Media, 2013).
173. Chan, J. M. *et al.* Polymeric nanoparticles for drug delivery. *Methods Mol Biol* **624,** 163–175 (2010).
174. Uchegbu, I. F. *et al.* Quaternary ammonium palmitoyl glycol chitosan—a new polysoap for drug delivery. *Int. J. Pharm.* **224,** 185–199 (2001).
175. Lalatsa, a *et al.* Delivery of peptides to the blood and brain after oral uptake of quaternary ammonium palmitoyl glycol chitosan nanoparticles. *Mol. Pharm.* **9,** 1764–74 (2012).
176. Qu, X. *et al.* Carbohydrate-based micelle clusters which enhance hydrophobic drug bioavailability by up to 1 order of magnitude. *Biomacromolecules* **7,** 3452–9 (2006).
177. Serrano, D. R. *et al.* Oral Particle Uptake and Organ Targeting Drives the Activity of Amphotericin B Nanoparticles. *Mol. Pharm.* **12,** 420–431 (2015).
178. Chandler, D. Interfaces and the driving force of hydrophobic assembly. *Nature* **437,** 640–7 (2005).
179. Hunter, C. A. *et al.* Aromatic interactions. *J. Chem. Soc. Perkin Trans. 2* 651–669 (2001). doi:10.1039/b008495f
180. Williams, D. & Fleming, I. *Spectroscopic Methods in Organic Chemistry*. (McGraw-Hill Education, 2007).

181. Claridge, T. D. W. *High-Resolution NMR Techniques in Organic Chemistry*. *Tetrahedron Organic Chemistry Series* (Elsevier, 2009).
182. Williams, T. Gel permeation chromatography: A review. *J. Mater. Sci.* **5,** 811–820 (1970).
183. Wyatt. *ASTRA user guide for DAWN DSP and miniDAWN Light Scattering Instruments*. **4,** (2008).
184. Wyatt. *Light Scattering with the massess: Dn / dc with an Optilab*. (1999).
185. Chooi, K. W. *et al.* The Molecular Shape of Poly(propylenimine) Dendrimer Amphiphiles Has a Profound Effect on Their Self Assembly. *Langmuir* **26,** 2301–2316 (2010).
186. Chooi, K. W. *et al.* Claw amphiphiles with a dendrimer core: nanoparticle stability and drug encapsulation are directly proportional to the number of digits. *Langmuir* **29,** 4214–24 (2013).
187. Sogias, I. a *et al.* Why is chitosan mucoadhesive? *Biomacromolecules* **9,** 1837–42 (2008).
188. Saboktakin, M. R. *et al.* Synthesis and characterization of pH-dependent glycol chitosan and dextran sulfate nanoparticles for effective brain cancer treatment. *Int. J. Biol. Macromol.* **49,** 747–51 (2011).
189. Cunha, A. G. & Gandini, A. Turning polysaccharides into hydrophobic materials: a critical review. Part 2. Hemicelluloses, chitin/chitosan, starch, pectin and alginates. *Cellulose* **17,** 1045–1065 (2010).
190. Fray, M. El *et al.* Chemical modification of Chitosan with Fatty acids. *Prog. Chem. Appl. Chitin its Deriv.* **XVII,** 29–36 (2012).
191. Mo, R. *et al.* The mechanism of enhancement on oral absorption of paclitaxel by N-octyl-O-sulfate chitosan micelles. *Biomaterials* **32,** 4609–20 (2011).
192. Zhang, C. *et al.* Biological evaluation of N-octyl-O-sulfate chitosan as a new nano-carrier of intravenous drugs. *Eur. J. Pharm. Sci.* **33,** 415–423 (2008).
193. Lee, S. J. *et al.* Tumor-homing photosensitizer-conjugated glycol chitosan nanoparticles for synchronous photodynamic imaging and therapy based on cellular on/off system. *Biomaterials* **32,** 4021–4029 (2011).
194. Zhu, A. *et al.* The aggregation behavior of O-carboxymethylchitosan in dilute aqueous solution. *Colloids Surfaces B Biointerfaces* **43,** 143–149 (2005).
195. Shelma, R. *et al.* Development and characterization of self-aggregated nanoparticles from anacardoylated chitosan as a carrier for insulin. *Carbohydr. Polym.* **80,** 285–290 (2010).
196. Wang, F. *et al.* Preparation and characterizations of a novel deoxycholic acid–O-carboxymethylated chitosan–folic acid conjugates and self-aggregates. *Carbohydr. Polym.* **84,** 1192–1200 (2011).
197. Li, H. *et al.* Enhanced oral absorption of Paclitaxel in N-Deoxycholic Acid-N, O-Hydroxyethyl Chitosan Micellar System. *J. Pharm. Sci.* **99,** 4543–4553 (2010).
198. Termsarasab, U. *et al.* Chitosan oligosaccharide–arachidic acid-based nanoparticles for anti-cancer drug delivery. *Int. J. Pharm.* **441,** 373–380 (2013).
199. Oh, N. M. *et al.* A self-organized 3-diethylaminopropyl-bearing glycol chitosan nanogel for tumor acidic pH targeting: In vitro evaluation. *Colloids Surfaces B Biointerfaces* **78,** 120–126 (2010).

200. Shelma, R. & Sharma, C. P. Development of lauroyl sulfated chitosan for enhancing hemocompatibility of chitosan. *Colloids Surfaces B Biointerfaces* **84,** 561–570 (2011).
201. Huo, M. *et al.* Synthesis and characterization of low-toxic amphiphilic chitosan derivatives and their application as micelle carrier for antitumor drug. *Int. J. Pharm.* **394,** 162–173 (2010).
202. Li, Y.-Y. *et al.* Aggregation of hydrophobically modified chitosan in solution and at the air–water interface. *J. Appl. Polym. Sci.* **102,** 1968–1973 (2006).
203. Liu, C. G. *et al.* Linolenic acid-modified chitosan for formation of self-assembled nanoparticles. *J. Agric. Food Chem.* **53,** 437–441 (2005).
204. Kwon, S. *et al.* Physicochemical Characteristics of Self-Assembled Nanoparticles Based on Glycol Chitosan Bearing 5β-Cholanic Acid. *Langmuir* **19,** 10188–10193 (2003).
205. Lee, K. Y. *et al.* Physicochemical Characteristics of Self-Aggregates of Hydrophobically Modified Chitosans. *Langmuir* **14,** 2329–2332 (1998).
206. Du, Y.-Z. *et al.* Stearic acid grafted chitosan oligosaccharide micelle as a promising vector for gene delivery system: Factors affecting the complexation. *Int. J. Pharm.* **391,** 260–266 (2010).
207. Xiangyang, X. *et al.* Preparation and characterization of N-succinyl-N′-octyl chitosan micelles as doxorubicin carriers for effective anti-tumor activity. *Colloids Surfaces B Biointerfaces* **55,** 222–228 (2007).
208. Hu, F.-Q. *et al.* Shell cross-linked stearic acid grafted chitosan oligosaccharide self-aggregated micelles for controlled release of paclitaxel. *Colloids Surf. B. Biointerfaces* **50,** 97–103 (2006).
209. Bardelmeijer, H. A. *et al.* Increased Oral Bioavailability of Paclitaxel by GF120918 in Mice through Selective Modulation of P-glycoprotein. *Clin. Exp. Pharmacol. Physiol.* **6,** 4416–4421 (2000).
210. Goodhew, P. J. & Humphreys, F. J. *Electron Microscopy and Analysis*. (Taylor & Francis, 1988).
211. Harris, J. R. The future of transmission electron microscopy (TEM) in biology and medicine. *Micron* **31,** 1–3 (2000).
212. Amersham bioscience. *Reversed Phase Chromatography Principles and Methods*.
213. Gerber, F. *et al.* Practical aspects of fast reversed-phase high-performance liquid chromatography using 3μm particle packed columns and monolithic columns in pharmaceutical development and production working under current good manufacturing practice. *J. Chromatogr. A* **1036,** 127–133 (2004).
214. Hunter, J. *et al.* Functional Expression of P-glycoprotein in Apical Membranes of Human Intestinal Caco-2 Cells. **268,** 14991–14997 (1993).
215. Lin, J. H. & Yamazaki, M. Role of P-glycoprotein in pharmacokinetics: Clinical implications. *Clin. Pharmacokinet.* **42,** 59–98 (2003).
216. Fang, J. *et al.* The EPR effect: Unique features of tumor blood vessels for drug delivery, factors involved, and limitations and augmentation of the effect. *Adv. Drug Deliv. Rev.* **63,** 136–151 (2011).
217. Garrett, N. L. *et al.* Exploring uptake mechanisms of oral nanomedicines using multimodal nonlinear optical microscopy. *J. Biophotonics* **5,** 458–68 (2012).
218. Vauthier, C. & Bouchemal, K. Methods for the Preparation and

Manufacture of Polymeric Nanoparticles. *Pharm. Res.* **26,** 1025–1058 (2009).
219. Swain, S. *et al.* Design and characterization of enteric-coated controlled release mucoadhesive microcapsules of Rabeprazole sodium. *Drug Dev. Ind. Pharm.* **39,** 1–13 (2012).
220. Yasuda, K. *et al.* Interaction of cytochrome P450 3A inhibitors with P-glycoprotein. *J. Pharmacol. Exp. Ther.* **303,** 323–332 (2002).
221. FDA. *Guidance for Industry Bioanalytical Method Validation Guidance for Industry Bioanalytical Method Validation*. (2001).
222. Adrian, C. & Brodie, B. Absorption of drugs from the stomach. II. The Human. *J. Pharmacol. Exp. Ther.* **120,** 540–545 (1957).
223. Tortora, G. J. & Derrickson, B. *Introduction to the human body : the essentials of anatomy and physiology*. (J. Wiley & Sons, 2007).
224. Gu, J. *et al.* Nano self-assemblies based on cholate grafted poly-L-lysine enhanced the solubility of sterol-like drugs. *J. Microencapsul. Micro Nano Carriers* **28,** 752–762 (2011).
225. Qiu, L. Y. & Bae, Y. H. Self-assembled polyethylenimine-graft-poly(epsilon-caprolactone) micelles as potential dual carriers of genes and anticancer drugs. *Biomaterials* **28,** 4132–42 (2007).
226. Gaucher, G. *et al.* Block copolymer micelles: preparation, characterization and application in drug delivery. *J. Control. Release* **109,** 169–88 (2005).
227. Vassiliou, A. A. *et al.* Facile synthesis of polyester-PEG triblock copolymers and preparation of amphiphilic nanoparticles as drug carriers. *J. Control. Release* **148,** 388–95 (2010).
228. Kataoka, K. *et al.* Doxorubicin-loaded poly(ethylene glycol)–poly(β-benzyl-l-aspartate) copolymer micelles: their pharmaceutical characteristics and biological significance. *J. Control. Release* **64,** 143–153 (2000).
229. Turk, C. T. S. *et al.* Formulation and optimization of nonionic surfactants emulsified nimesulide-loaded PLGA-based nanoparticles by design of experiments. *AAPS PharmSciTech* **15,** 161–76 (2014).
230. Tummala, S. *et al.* Formulation and characterization of 5-Fluorouracil enteric coated nanoparticles for sustained and localized release in treating colorectal cancer. *Saudi Pharm. J.* **23,** 308–314 (2015).
231. Hao, S. *et al.* Enteric-coated sustained-release nanoparticles by coaxial electrospray: preparation, characterization, and in vitro evaluation. *J. Nanoparticle Res.* **16,** 2204 (2014).
232. Sun, H. *et al.* Preparation and in vitro/in vivo characterization of enteric-coated nanoparticles loaded with the antihypertensive peptide VLPVPR. *Int. J. Nanomedicine* **9,** 1709–16 (2014).
233. Reix, N. *et al.* Duodenum-specific drug delivery: in vivo assessment of a pharmaceutically developed enteric-coated capsule for a broad applicability in rat studies. *Int. J. Pharm.* **422,** 338–40 (2012).
234. Sonaje, K. *et al.* Enteric-coated capsules filled with freeze-dried chitosan/poly(gamma-glutamic acid) nanoparticles for oral insulin delivery. *Biomaterials* **31,** 3384–94 (2010).
235. Saphier, S. *et al.* Gastro intestinal tracking and gastric emptying of solid dosage forms in rats using X-ray imaging. *Int. J. Pharm.* **388,** 190–5 (2010).
236. Prajapati, S. *et al.* Floating matrix tablets of domperidone formulation and

optimization using simplex lattice design. *Iran. J. Pharm. Res. IJPR* **10,** 447–55 (2011).
237. Nayak, A. K. *et al.* Gastroretentive drug delivery systems: A review. *Asian J. Pharm. Clin. Res.* **3,** 2–10 (2010).
238. Shishu *et al.* Stomach-specific drug delivery of 5-fluorouracil using floating alginate beads. *AAPS PharmSciTech* **8,** Article 48 (2007).
239. Dunn, A. L. *et al.* Hyaluronidase: a review of approved formulations, indications and off-label use in chronic pain management. *Expert Opin. Biol. Ther.* **10,** 127–131 (2010).
240. Chooi, K. W. *et al.* Physical Characterisation and Long-Term Stability Studies on Quaternary Ammonium Palmitoyl Glycol Chitosan (GCPQ)-A New Drug Delivery Polymer. *J. Pharm. Sci.* **103,** 2296–2306 (2014).
241. Henry, N. L. & Hayes, D. F. Cancer biomarkers. *Mol. Oncol.* **6,** 140–6 (2012).
242. Mahmood, T. & Yang, P. Western Blot Technique Theory, and Trouble Shooting. *N. Am. J. Med. Sci.* **4,** 429–434 (2012).
243. Jogala, S. *et al.* Development of subcutaneous sustained release nanoparticles encapsulating low molecular weight heparin. *J. Adv. Pharm. Technol. Res.* **6,** 58–64 (2015).
244. Pandey, R. & Khuller, G. K. Subcutaneous nanoparticle-based antitubercular chemotherapy in an experimental model. *J. Antimicrob. Chemother.* **54,** 266–268 (2004).
245. Kreuter, J. *et al.* Distribution and elimination of poly(methyl methacrylate) nanoparticles after subcutaneous administration to rats. *J. Pharm. Sci.* **72,** 1146–9 (1983).
246. Gautier, J. C. *et al.* Biodegradable nanoparticles for subcutaneous administration of growth hormone releasing factor (hGRF). *J. Control. Release* **20,** 67–77 (1992).
247. Xu, X. *et al.* Formulation and pharmacokinetic evaluation of tetracycline-loaded solid lipid nanoparticles for subcutaneous injection in mice. *Chem. Pharm. Bull. (Tokyo).* **59,** 260–5 (2011).
248. Leveque, D. Subcutaneous administration of anticancer agents. *Anticancer Res.* **34,** 1579–86 (2014).
249. Amann, L. C. *et al.* In vitro-in vivo correlations of scalable plga-risperidone implants for the treatment of schizophrenia. *Pharm. Res.* **27,** 1730–1737 (2010).
250. Scodeller, P. *et al.* Hyaluronan degrading silica nanoparticles for skin cancer therapy. *Nanoscale* **5,** 9690–8 (2013).
251. Rajan, M. *et al.* Hyaluronidase enzyme core-5-fluorouracil-loaded chitosan-PEG-gelatin polymer nanocomposites as targeted and controlled drug delivery vehicles. *Int. J. Pharm.* **453,** 514–522 (2013).
252. van Cruijsen, H. *et al.* Epidermal growth factor receptor and angiogenesis: Opportunities for combined anticancer strategies. *Int. J. Cancer* **117,** 883–8 (2005).
253. Cheng, C. J. *et al.* A holistic approach to targeting disease with polymeric nanoparticles. *Nat. Rev. Drug Discov.* **14,** 239–247 (2015).